

TAILINGS CONFERENCE 2026 - WHERE TO NOW?

ECSA and SACNASP Validated CPD
ActivityCredits = 0.1 per hour attended

Supported by SAIEG

In partnership with MMMA and SAICE

SAIMM
THE SOUTHERN AFRICAN INSTITUTE
OF MINING AND METALLURGY

Proceedings Book

3-4 MARCH 2026 – CONFERENCE | 5 MARCH 2026 – TECHNICAL VISIT
Indaba Hotel, Spa and Conference Centre, Fourways

THE SOUTHERN AFRICAN INSTITUTE OF MINING AND METALLURGY
JOHANNESBURG 2026

TAILINGS CONFERENCE 2026 – WHERE TO NOW?

3-4 MARCH 2026
INDABA HOTEL, SPA AND CONFERENCE CENTRE, FOURWAYS

SAIMM PUBLICATIONS

THE MONOGRAPH SERIES

Ml **Lognormal-De Wijsian Geostatistics for Ore Evaluation**
(2nd ed 1981) D.G. Krige

M2 **An Introduction to Geostatistical Methods of Mineral Evaluation**
(2nd ed 1981) J.-M.M. Rendu

M3 **Principles of Flotation**
(1982) (3rd imp. 1986) Edited by R.P. King

M4 **Increased Underground Extraction of Coal**
(1982) Edited by C.J. Fauconnier and R.W.O. Kersten

M5 **Rock Mechanics in Mining Practice**
(1983) (3rd imp. 1986) Edited by S. Budavari

M6 **Assay and Analytical Practice in the South African Mining Industry**
(1986) W.C. Lenahan and R. de L. Murray-Smith

M7 **The Extractive Metallurgy of Gold in South Africa,**
2 volumes (1987) Edited by G.G Stanley

M8 **Mineral and Metal Extraction — An Overview**
(1994) L.C. Woollacott and R.H. Eric

M9 **Rock Fracture and Rockbursts—an illustrative study**
(1997) Edited by W.D. Ortlepp

THE SPECIAL PUBLICATIONS SERIES

SPI **Proceedings, Underground Transport Symposium**
(1986) Edited by R.C.R. Edgar

SP2 **Backfill in South African Mines (1988)**

SP3 **Treatment and Re-use of Water in the Minerals Industry (1989)**

SP4 **COREX Symposium 1990**
(1990) Edited by H.M.W. Delport and P.J. Holaschke

SP5 **Measurement, Control, and Optimization in Mineral Processing**
(1994) Edited by H.W. Glen

SP6 **Handbook on Hard-rock Strata Control**
(1994) A.J.S. Spearing

SP7 **Rock Engineering for underground coal mining**
(2002) J. Nielen van der Merwe and Bernard J. Madden

SP8 **Second Edition: Rock Engineering for underground coal mining**
(2010) J. Nielen van der Merwe and Bernard J. Madden

SP9 **Theoretical Rock Mechanics for Professional Practice**
(2016) M. Handley

SP10 **Johannesburg and its Holey Mining Heritage 2021**
(2021) T.R. Stacey

SP11 **Mineral and Metal Extraction — An Overview**
(2021) L.C. Woollacott and R.H. Eric

SP12 **The Fall of a Giant: The story of the disintegration of the South African Mining Industry**
(2022/2023) Dr I. Robinsoin

SP13 **COMRO's Legacy: Research and Development of Stoping Mining Machinery and Technologies**
(2023) B. Protheroe

SUPPLEMENT TO THE SAIMM JOURNAL

The Metals and Minerals Industry in South Africa - Part 1 (1989)
Edited by H.W. Glen

THE SYMPOSIUM SERIES

S1 **Mathematical Statistics and Computer Applications in Ore Valuation (1966)**

S2 **Planning Open Pit Mines** (1970) (4th imp.)
Edited by P.W.J. van Rensburg

S3 **Application of Computer Methods in the Mineral Industry** (APCOM 1973) Edited by M.D.G. Salamon

S4 **Infacon 1974** Edited by H.W. Glen

S5 **Proceedings of the 12TH CMMI Congress** 2 volumes (1982)
Edited by H.W. Glen

S6 **Rockbursts and Seismicity in Mines** (1984)
Edited by N.C. Gay and E.H. Wainwright

S7 **The Planning and Operation of Open Pit and Strip Mines** (1986) Edited by J.P. Deetlefs

S8 **GOLD 100: Proceedings of the International Conference on Gold (1986)**
Volume 1: Gold Mining Technology
Edited by H. Wagner and R.P. King
Volume 2: Extractive Metallurgy of Gold
Edited by C.E. Fivaz and R.P. King
Volume 3: Industrial Uses of Gold
Edited by G. Gafner and R.P. King

S9 **APCOM 87: Proceedings of the Twentieth International Symposium on the Application of Computers and Mathematics in the Mineral Industries (1987)**
Volume 1: Mining
Edited by L. Wade, R.W.O. Kersten and J.R. Cutland
Volume 2: Metallurgy
Edited by R.P. King and I.J. Barker
Volume 3: Geostatistics
Edited by I.C. Lemmer, H. Schaum and F.A.G.M. Camisani-Calzolari

S10 **International Deep Mining Conference (1990)**
Volume 1: Innovations in Metallurgical Plant
Edited by G.A. Brown and P. Smith
Application of Materials Engineering in the Mining Industry Edited by B. Metcalfe
Volume 2: Technical Challenges in Deep Level Mining
Edited by D.A.J. Ross-Watt and P.D.K. Robinson

S11 **Infacon 6 (Incorporating Incsac) (1992)**
Edited by H.W. Glen

S12 **Massmin 92**
Edited by H.W. Glen (out of print)

S13 **Minefill 93**
Edited by H.W. Glen

S14 **XVTH CMMI Congress Publications (1994)**
Volume 1: Mining
Edited by H.W. Glen
Volume 2: Metals Technology and Extractive Metallurgy (1994) Edited by H.W. Glen

S15 **Surface Mining 1996**
Edited by H.W. Glen

S16 **Hidden Wealth (1996)**
Edited by H.W. Glen

S17 **Heavy Minerals 1997**
Edited by R.E. Robinson

S18 **The 8TH International Platinum Symposium (1998)**

S19 **Mining in Africa '98**

S20 **Extraction Metallurgy Africa '98**

S21 **Sixth International Symposium for Rock Fragmentation by Blasting (1999)**

S22 **Metallurgy Africa '99**

S23 **Heavy Minerals 1999**
Edited by R.G. Stimson

S24 **Tunnels under Pressure**
Technical Editor T.R. Stacey

S25 **Mine Hoisting 2000**

S26 **Coal–The Future (2000)**

S27 **The Fifth International Symposium on Rockburst and Seismicity in Mines (RaSim 5) (2001)**

S28 **6TH International Symposium on Mine Mechanization and Automation (2001)**

S29 **XIV International Coal Preparation Congress and Exhibition**

S30 **Surface Mining 2002—Modern Developments for the New Millennium**

S31 **IFSA 2002, Industrial Fluidization South Africa**

S31a **APCOM 2003—Application of Computers and Operations Research in the Minerals Industries**

S32 **ISSA/Chamber of Mines Conference—Mines and Quarries: Prevention of Occupational Injury and Disease**

S33 **ISRM—Technology Roadmap for Rock Mechanics**

S34 **Heavy Minerals Conference 2003**

S35 **Safety in Mines Research Institutes (2003)**

S36 **VII International Conference on Molten Slags, Fluxes & Salts (2004)**
Tenth International Ferroalloys Congress INFACONX 2004

S37 **Deep and high stress mining 2004**

S38 **'Platinum adding value' 2004**

S39 **Base Metals—Southern Africa's response to changing global base metals market dynamics 2005**

S40 **Strategic *versus* Tactical approaches in mining 2005**

S41 **Best practices in rock engineering SARES 2005**

S42 **IFSA 2005, Industrial Fluidization South Africa**

S43 **Southern African Pyrometallurgy 2006 International Conference**

S44 **Stability of rock slopes in open pit mining and civil engineering situations**

S45 **'Platinum Surges Ahead' 2006**

S46 **Hydraulic Transport of Solids - Hydrotransport 17 (2007)**

S47 **Fourth Southern African Base Metals Conference 'Africa's base metals resurgence'**

S48 **Heavy Minerals Conference, 2007**

S49 **Cave Mining Conference, 2007**

S50 **International Symposium on Lead and Zinc processing – Lead & Zinc 2008**

S51 **Surface Mining 2008**

S52 **Platinum in transformation 2008**

S53 **IFSA 2008, Industrial Fluidization South Africa**

S54 **Hydrometallurgy Conference 2009**

S55 **Shotcrete for Africa 2009**

S56 **Base Metals Conference 2009**

S57 **Heavy Minerals Conference, 2009**

S58 **Hard Rock Safe—Safety Conference 2009**

S59 **Sampling and Blending 2009**

S60 **World Gold 2009 Conference**

S61 **Physical Beneficiation Conference 2010**

S62 **Second Hardrock Safe—Safety Conference 2010**

S63 **Platinum in Transition 'Boom or Bust' 2010**

S64 **South African Pyrometallurgy 2011 International Conference**

S65 **Minefill 2011 (10TH International Symposium on Mining with Backfill)**

S66 **Base Metals Conference 2011**

S67 **MineSafe 2011 Conference**

S68 **Iron Ore and Manganese Ore Metallurgy 2011**

S69 **Percolation leaching: The status globally and in Southern Africa 2011**

S70 **IFSA 2011, Industrial Fluidization South Africa**

S71 **Southern Hemisphere International Rock Michanics Symposium 2012**

S72 **Platinum Conference 'A catalyst for change' 2012**

S73 **Ferrous 2012—Ferrous and Base Metals Development Network Conference**

S74 **Diamonds - Source to use 2013**

S75 **Sampling and analysis: Best-practice in African mining 2013**

S76 **Base Metals Conference 2013**

S77 **Precious Metals 2013 Conference—The Precious Metals Development Network (PMDN)**

S78 **Physical Beneficiation 2013 Conference**

S79 **21st Century challenges to the southern African coal sector 2014**

S80 **Furnace Tapping Conference 2014**

S81 **Platinum Conference 'Platinum—Metal for the Future' 2014**

S82 **IFSA 2014, Industrial Fluidization South Africa**

S83 **Copper Cobalt Africa 2015**

S84 **The Danie Krige Geostatistical Conference 2015 - Vol. 1**

The Danie Krige Geostatistical Conference 2015 - Vol. 2

S85 **World Gold Conference 2015**

S86 **Slope Stability 2015**

S87 **2nd Annual Young Professionals Conference 2015**

S88 **AMI–Nuclear Materials Development Network 2015**

S89 **MPES–23rd International Symposium on Mine Planning & Equipment Selection 2015**

S90 **Diamonds still Sparkling Conference 2016**

S91 **The SAMREC/SAMVAL Companion Volume Conference 2016**

S92 **New Technology and Innovation in the Minerals Industry Colloquium 2016**

S93 **Theoretical Rock Mechanics for Professional Practice** (Special Publications Series 9) by M. Handley - 2016

S94 **Hydrometallurgy Conference 2016**

S95 **10TH Heavy Minerals Conference 2016**

S96 **MineSafe Conference 2016**

S97 **AMI-Ferrous and Base Metals Development Conference 2016**

S98 **3rd Young Professionals Conference 2017**

S99 **Proximity Detection and Collosion Avoidance Systems in Mining Colloquium 2017**

S100 **6TH Sulphur and Sulphuric Acid Conference 2017**

S101 **Mine Planning Colloquium 2017**

S102 **Chrome Colloquium 2017**

S103 **4TH Mineral Project Valuation Colloquium 2017**

S104 **Water Conference 2017**

S105 **Rapid Underground Mine and Civil Access Engineering 2017**

S106 **MineSafe Conference 2017**

S107 **Uranium 2017 International Conference 2017**

S108 **IFSA 2017–Industrial Fluidization Conference 2017**

S109 **AfriRock 2017–ISRM International Symposium 2017**

S110 **AMI Precious Metals 2017–The Precious Metals Development Network (PMDN) Symposium**

S111 **7TH International Platinum Conference 2017**

S112 **Infacon XV: International Ferro-Alloys Conrgress 2018**

S113 **SOMP–Society of Mining Professors 6TH Regional Conference 2018**

S114 **Digitalization in Mining Conference 2018**

S115 **Diamonds – Source to Use 2018 Conference 2018**

S116 **The 9TH Southern African Base Metals Conference 2018**

S117 **Geometallurgy Conference 2018**

S118 **Mine Safe Technical Conference and Industry Day 2018**

S119 **ASM Conference 2018**

S120 **4TH Young Professionals Conference 2018**

S121 **Furnace Tapping 2018 Conference 2018**

S122 **7TH Sulphur and Sulphuric Acid Conference 2019**

S123 **Mine Planner's Colloquium 2019**

S124 **9TH International Conference on Deep & High Stress Mining 2019**

S125 **New Technology Conference and Trade Show 2019**

S126 **Smart Mining Smart Environment Smart Society Conference 2019**

S127 **The Eleventh International Heavy Minerals Conference 2019**

S128 **Surface Mining Masterclass 2019**

S129 **International Mine Health and Safety Conference 2019**

S130 **Tailings Storage Conference 2020**

S131 **IMPC2020 XXX International Mineral Processing Congress**

S132 **Johannesburg and its Holey Mining Heritage**
(Special Publications Series 10) by T.R. Stacey - 2021

S133 **Mineral and Metal Extraction — An Overview**
(Special Publications Series 11) by L.C. Woollacott and R.H. Eric - 2021

S134 **Diamonds - Source to Use - 2021 Online Conference 2021**

S135 **WorldGold Online Conference 2021**

S136 **APCOM 2021 Minerals Industry4.0-The next digital transformation in mining**

S137 **5TH Young Professionals Online Conference 2021**

S138 **Southern African Rare Earths International Online Conference 2021**

S139 **SAMCODES Conference 2021**

S140 **Global Tailings Standards and Opportunities`For the Mine of the Future Conference 2022**

S141 **The Fall of a Giant: The story of the disintegration of the South African Mining Industry**
(Special Publications Series 12) by I. Robinson - 2022/2023

S142 **Battery Materials Conference 2022**

S143 **32ND SOMP Annual Meeting and Conference 2022**

S144 **SDIMI (Sustainable Development in the Minerals Industry) 10TH International Conference 2022**

S145 **THANOS International Conference 2022**

S146 **Mine Impacted Water Online Conference 2022 (Abstract Book Only)**

S147 **8TH International PGM Conference 2022**

S148 **SANCOT Symposium 2022**

S149 **8TH Sulphur and Sulphuric Acid Conference 2023**

S150 **Southern African Hydrogen and Fuel Cell Conference 2023**

S151 **COMRO's Legacy: Research and Development of Stoping Mining Machinery and Technologies**
(Special Publications Series 13) by B. Protheroe - 2023

S152 **Copper Cobalt Africa in Association with The 10TH Southern African Base Metals Conferenc 2023**

S153 **Digital Transformation in Mining Conference 2023**

S154 **Diamonds Source to Use 2023 Online Conference**

S155 **12TH International Heavy Minerals Conference 2023**

S156 **Geometallurgy Conference 2023**

S157 **Next Generation Tailings Opportunitiy or Risk? Conference 2023**

S158 **6TH Young Professionals Conference 2023**

S159 **Southern African Pyrometallurgy 2024 International Conference**

S160 **The 11TH World Conference of Sampling and Blending 2024**

S161 **SANIRE Symposium 2024**
Technical Applications in Rock Engineering

S162 **2ND International Conference 2024 Southern African Rare Earths**

S163 **2ND Battery Materials Conference 2024**

S164 **Hydrometallurgy Conference 2024**

S165 **Environmental Social Governance Sustainability Conference 2024**

S166 **MineSafe Mine Health and Safety Conference 2024**

S167 **Mintek@90 Conference 2024**

S168 **Mine Closure Conference 2025**

S169 **2ND Southern African Hydrogen and Fuel Cell Conference 2025**

S170 **9TH Sulphur and Sulphuric Acid Conference 2025**

S171 **4TH Digital Transformation in Mining Conference 2025**

S172 **AfriRock 2025 Pioneering Progress Conference**

S173 **Thirteen International Heavy Minerals Conference 2025**

S174 **International Mineral Asset Valuation Conference 2025**

S175 **Geometallurgy Conference 2025**

S176 **9TH International PGM Conference 2025**

S177 **MineSafe Conference 2025**

Published by The Southern African Institute of Mining and Metallurgy
Minerals Council South Africa, 7th Floor, Rosebank Towers, 19 Biermann Avenue, Rosebank, 2196
Republic of South Africa

© The Southern African Institute of Mining and Metallurgy, 2026

ISBN 978-0-6398820-7-9

The papers in this volume have been for the most part prepared from Word documents supplied by the authors, with additional typesetting and formatting by The Southern African Institute of Mining and Metallurgy.

Organising Committee

L. Spies, Conference Chairperson

A. Bovim
A. Coetzee
R. Cooper
L. de Koning
G.C. Howell
E. Kleinhans
K. Morton
S. Maharaj
A. Savvas
L. Spies
A. Strauss

The Organising Committee would like to thank the reviewers listed below for the efforts in the reviewing process

A. Bovin
A. Coetzee
R. Cooper
T. Da silva Burke
L. de Koning
J. Dutchman
G. Heymann
G.C. Howell
I. Hammnond
S.W. Jacobsz
E. Kleinhans
J. Lake
C. MacRobert
S. Maharaj
E. Matinde
H. Meintjes
N. Mincione
K. Morton
Y. Narainsamy
K. O'Brien
A. Savvas
L. Spies
A. Strauss

Desktop prepared by Camera Press, Johannesburg

FOREWORD

It is a privilege for me to introduce the Southern African Institute of Mining and Metallurgy (SAIMM)'s fourth Tailings Conference. Having been involved in the conference organisation since the inaugural event in 2020, I have seen it grow from strength to strength and become a well-established fixture on the SAIMM calendar. The conference continues to provide a platform which encourages collaboration between the various role players in the Southern African tailings industry, and I hope you use this year's conference to do just that.

Since the introduction of the Global Industry Standard on Tailings Management (GISTM) in 2020, the tailings landscape has changed for everyone involved. As we look to the future, the 2026 conference asks: Where to now?

In a world of new standards, evolving expectations, and emerging possibilities, what opportunities lie ahead? What residual risks still need addressing? How can we further reduce, reclaim or reuse tailings? How can we accelerate the adoption of new technologies and set new benchmarks for the industry? Which impacts, once considered acceptable, are no longer tolerable, and how can we best manage them?

The presentations and discussions over the next two days will cover a wide range of topics relevant to the future of tailings storage facilities, including both theoretical papers and practical examples from leading practitioners. Our speakers deserve a round of applause for their time and effort in preparing their presentations and papers and for being willing to share their experiences.

On behalf of the organising committee, I would like to thank our sponsors for their valued contributions which have helped make this event a success, and also to thank the SAIMM secretariat for their dedicated organisational support.

L. Spies
Chairperson: Organising Committee

Contents

Page No

The challenge of GISTM adherence for smaller mining operations in remote parts of the world and the case for a GISTM-Light process
G.V. Price 1

Reliable design with limited data: Characteristic strength selection for slope stability assessment
H.A. Brandao, L. Kirsten, R. Duque, P. Delport, T. Jibiki, A. Fourie 13

Clay-soil a history of theoretical approaches to strength and the way forward
A. Smith, C.J. MacRobert 23

Geochemical characterisation of re-mined copper tailings in Democratic Republic of Congo - best practices that can be adopted in South Africa
M.G. Dube, S. Hareeparsad 37

TSF-specific water balance as a standard practice
A. Scholtz, K. Uderstadt, L. de Villiers, G. Howell 53

Adapting to change: Filtered tailings and the future of tailings management
K. Naidoo, V. Balakistan 65

Assessment of causeway-induced loading on penstock towers
S.C.T. Luis, T. Armstrong 81

Evaluating mine tailings reuse potential through geotextile dewatering
N. Budhai, G.W. Rathod 91

Assessment and mitigation of slope stability risks for TSF closure
P. Sharma, M. Govender 103

State-dependent undrained strength envelopes for gold tailings from NorSand simulations
J. Swanepoel 113

Cross-calibrated in-situ shear strength of gold tailings from CPTU, Vane Shear, and NorSand modeling
J. Swanepoel 127

Undrained shear strength selection within a critical state framework
L.H. Kirsten, H.A. Brandão, F.D. Walsh, L. Murray 141

Installation of an advanced monitoring network for a Tailings Storage Facility
A. Hertenberger, E.C. Lukombo, K.L. Morton, M. Msitsini, T.M. Namane 155

The application of remote sensing techniques in mapping abandoned tailings storage facilities in the West Rand, Gauteng South Africa
L. Nqasha, M. Mpanza 163

Combining real-time and scheduled monitoring of upstream raised TSFs and a filter stack – why both are required
D. Johns, J. Olivier 177

The organisers of the conference thanks the following sponsors for their support

PREMIUM SPONSORS

ecoz ENVIRONMENTAL & ENGINEERING

FRASER ALEXANDER

KAYTECH ENGINEERED FABRICS

Klohn Crippen Berger

Knight Piésold CONSULTING

truco Est. 1892
Leaders in fluid and material handling solutions

CORPORATE SPONSORS

ENPROTEC

HATCH

Metso

The organisers of the conference thanks the following sponsors for their support

EXHIBITORS

AGREENCO

AQUASENS™ Tailings Dam Sensors

COLETANCHE® BITUMINOUS GEOMEMBRANE

DNA BLAST Group

Fibertex NONWOVENS

filtaquip GLOBAL mineral processing solutions sustainability - dewatering - environmental - recovery

HEXAGON

Leica GEOSYSTEMS

MATEC INDUSTRIES

ORICA Digital Solutions

Paterson & Cooke KNOWLEDGE | EXPERIENCE | PASSION

SkyGeo

TECWISE DIGITAL INNOVATION

TH

TRE ALTAMIRA

TSF RISK SOLUTIONS

USK AIR SOIL WATER

The organisers of the conference thanks the following sponsors for their support

BANNER SPONSORS

Pegon
Trusted. Connected. Engineered

srk consulting

LANYARDS SPONSOR

Klohn Crippen Berger

PENS AND NOTEPADS SPONSOR

Civilab
Civil Engineering Testing Laboratories

PROMOTIONAL INSERTS SPONSORS

Civilab
Civil Engineering Testing Laboratories

IMPLATS
EXCELLENCE IN PGMs

TeMa
SOUTH AFRICA

The challenge of GISTM adherence for smaller mining operations in remote parts of the world and the case for a GISTM-Light process

G.V. Price

Klohn Crippen Berger Australia, Australia

This paper, with special reference to Air Upas and Sandai Mines in western Kalimantan Indonesia, describes the problems facing smaller mining operations in remote parts of the globe in acquiescing to the Global Industry Standard on Tailings Management (GISTM). The GISTM as published in 2020, references six topic areas namely Communities, Integrated Knowledge Base, Design Construction and Operation, Management and Governance, Emergency Response, and Disclosure. Each of these encompass 15 Principles in turn incorporating 77 Requirements and 219 Criteria. Tailings storage facilities are audited against these and though well-meaning and a very necessary requirement, are often difficult to adhere to in remote areas where flight access is arduous or impossible, road access is over long distances often along muddy tracks with deep rutting, satellite communications at times non-existent, specialised equipment necessary for geotechnical field testing unavailable or only accessed through difficult and costly establishment, senior geotechnical staff unwilling to locate to remote sites; these to mention but a few of the problems faced. The paper describes where adherence is possible as measured against the main GISTM topic requirements and principles, and perhaps more importantly – where not. These issues of compliance and non-compliance are integrated and presented in tabular format. The paper makes recommendations on how the most difficult adherence requirements can be overcome and concludes with suggestions of how GISTM audit requirements and processes can be softened in a 'GISTM-Light' process, where smaller remote operations can be audited against more appropriate and equitable targets, and so secure their aspirations to stay within the GISTM fold.

Keywords: GISTM, TSF, remote, compliance versus non-compliance, GISTM-Light.

INTRODUCTION

This paper, with special reference to mining operations at Air Upas and Sandai Mines in West Kalimantan, Indonesia, describes the problems facing smaller mining operations in remote parts of the globe in meeting Global Industry Standard on Tailings Management (GISTM) requirements. GISTM (2020), as co-convened by the International Council of Mining and Metals (ICMM), the United Nations Environment Programme (UNDP) and Principles for Responsible Investment (PRI) is structured around six Topic Areas, namely:

- Communities
- Integrated Knowledge Base
- Design Construction and Operation
- Management and Governance
- Emergency Response, and
- Disclosure.

These six Topic Areas encompass 15 Principles, which in turn include 77 Requirements and more than 219 Criteria. Separate from this, the ICMM has developed Conformance Protocols, which are mapped to the 77 Requirements (GISTM, 2021). The ICMM has also produced a Tailings Management Good Practice Guide (ICMM, 2021, 2025). The Conformance Protocols aim to assist members in fulfilling their commitment to the GISTM implementation at tailings storage facilities (TSF) facilities, with a GISTM Classification of 'Very High' to 'Extreme' needing to conform to the standard by 5 August 2023 which date has since passed. All other tailings facilities operated by members not yet in a state of safe closure would have needed to conform by 5 August 2025. Time has run out.

TSF all over the world are audited against all of the GISTM requirements, and though well-meaning and necessary, one must question whether they are really applicable in difficult to access remote areas where operations are small, and environmental concerns often minor. Here a watered-down version of GISTM, namely 'GISTM-Light' may be more applicable as outlined in this paper.

REMOTE OPERATIONS IN INDONESIA AS A CASE STUDY

GISTM audits were undertaken for Air Upas and Sandai Mines in West Kalimantan, Indonesia as published in December 2023 (KCB, 2023). These mines are very remote. It takes two days of travel from major centres such as Singapore and Australia, and even nearby Jakarta requires a full day's travel there, and another back. Exacerbating the problem are time-consuming visa requirements, flights required to bigger cities remote from these sites, and in many parts – Kalimantan included – many hours of 4X4 travel through jungle single-tracks, barely passable, at times flooded and sometimes inaccessible for long periods. Paved access is equally unappetising with many hours of driving across narrow undulating and busy road networks. Figure 1 provides the location of the two Kalimantan mines.

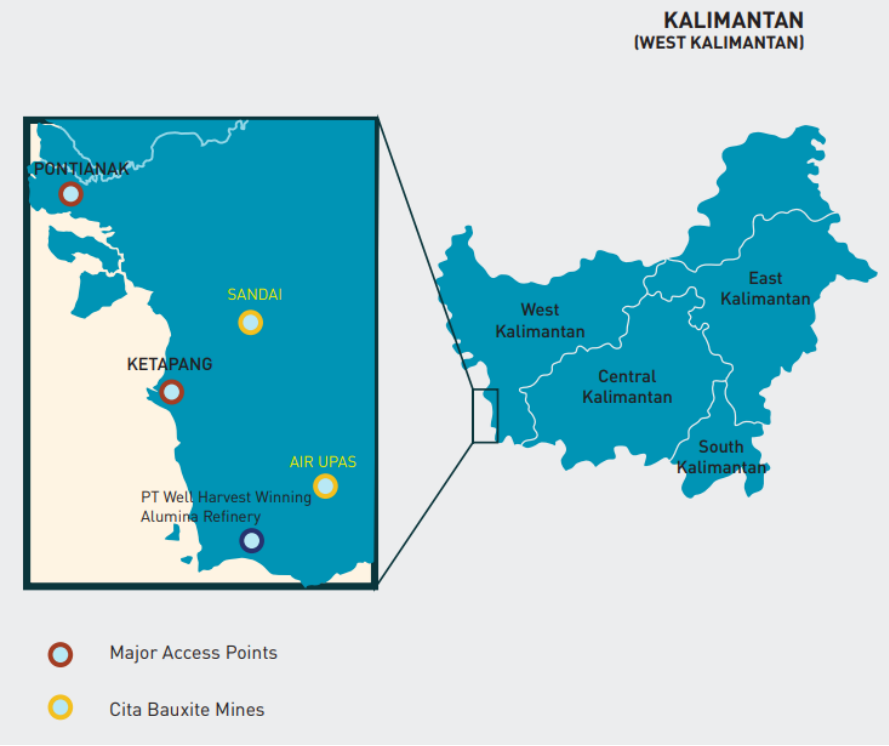


Figure 1. Locality Plan – Air Upas and Sandai Mines.

At both Sandai and Air Upas, bauxite-rich soil from near-surface mining is transported to nearby TSF washing stations where the bauxite-rich ore is separated from soil fines via rotating drum screens in a

washing process, and the residue flushed out as tailings. Flushed residue draining from the washing process is treated with a flocculant before streaming into a primary trench and the thickened residue then excavated and further thickened in secondary, tertiary and quaternary sumps excavated for that purpose. The thickened tailings are eventually loaded onto trucks and transported to residue landfills. The remaining tailings is clarified through progressive overflow across a series of purpose-built residue tailings dams. Clear water from this process is then pumped back for re-use at the washing stations. Mining operations at these two facilities have been in existence for over three decades. The Metallurgical Grade Bauxite washed and concentrated product is trucked from on-site stockpiles to a coastal refinery where it is used as raw material at the refinery plant to produce smelter grade alumina.

The non-dumped tailings are captured in a series of relatively small in height (generally <15 m) TSF dams. The tailings are free from any added chemicals. These mine areas have few inhabitants given their low-lying swamp or jungle locations, and even should over-topping or breaching occur, downstream areas are mostly devoid of people with no habitation as per mining requirements. Being flat-lying also means that any over-topped or breached tailings would have a limited flood footprint that would be mostly confined to the zone abutting the TSF facility. The rhetorical question begs then whether, under these circumstances, is it still necessary to conform to the full omnibus version of stringent GISTM requirements?

AIR UPAS AND SANDAI AUDIT RESULTS

A summary assessment of the conformance levels of the 77 audit GISTM requirements for these two sites is provided in Table I. The table shows the number of requirements that align with each level of conformance.

Table I: Air Upas and Sandai GISTM audit results

Topic Area	Principle	Compliant	Substantially Compliant	Partially Compliant	Not Compliant	Not Applicable
Communities	Principle 1 - Rights of project-affected people with meaningful engagement	2	2			
Integrated Knowledge Base	Principle 2 - Maintenance of a knowledge base to support a safe tailings management lifecycle plus closure	1	2	1		
	Principle 3 - Use of all knowledge base elements – social, environmental, economic, technical – to support TSF lifecycle	1		2		1
Design, Construction and Operation	Principle 4 - Develop plans and design to minimise all risk in all phases of the lifecycle, including closure		3	1	3	1
	Principle 5 – Provide robust design that integrates knowledge base and minimises risk through all lifecycle phases	3	2	1		2
	Principle 6 – Plan, build and operate the TSF to manage risk through all life cycle phases		3	1	1	1
	Principle 7 – Design, implement and operate monitoring systems to manage TSF facilities throughout a lifecycle	1	1	3		
Management and Governance	Principle 8 – Establish policies, systems and accountabilities to support TSF lifecycle safety and integrity		1	2	2	2
	Principle 9 – Appointment and empowerment of an Engineer of Record			1	4	
	Principle 10 – Establishment and implementation of review levels to provide strong quality and manage risk for all phases		2	2	2	1

Topic Area	Principle	Compliant	Substantially Compliant	Partially Compliant	Not Compliant	Not Applicable
	Principle 11 – Develop an organisational structure that promotes learning, communication & early problem recognition	2	2	1		
	Principle 12 – Establish a process for reporting, addressing concerns and protecting whistleblowers	2				
Emergency Response	Principle 13 – Preparation of an emergency response to tailings failures		2			2
	Principle 14 – Preparations for long term recovery in the event of catastrophic failure	1				4
Disclosure	Principle 15 – Publicly disclose and provide access to information in supporting public accountability		2	1		

ICMM (2020) proposes four tabulated levels of conformance as described in Table II. We have included a 5th level of compliance for this Indonesian study, namely 'Substantially Compliant' in order to distinguish between substantial compliance and mere partial compliance. Broadening descriptions also allows accounting for situations where only minor organisational adjustments are needed to be 'Partially Compliant' rather than distinctly 'Not Compliant'.

Table II: Air Upas and Sandai GISTM audit results

Identifier	Conformance Level	Description of Outcome & Corrective actions
	Compliant 90% - 100%	Systems and/or practices related to the Requirement have been implemented and there is sufficient evidence to demonstrate that the Requirement is being met. No action required or only minor refinements.
	Substantially Compliant 75% - 90%	Systems and requirement implementation generally satisfy the Requirement but there is a minor finding, or findings, that need/s to be corrected. Actions required for full compliance.
	Partially Compliant 50% - 75%	The asset has systems and/or practices that relate to the Requirement but do not directly address the Requirement or the asset. There is evidence of existing action plans to comply with the requirement. Corrective actions required.
	Not Compliant 0% - 50%	Systems and/or practices required to support implementation of the Requirement are not in place, or are not being implemented, or cannot be evidenced. There are major findings requiring correction. Major corrective actions required.
	Not Applicable	The specific Requirement is not applicable to the context of the system or asset.

Table I outcomes, using the compliance requirements of Table II, indicate that the mine is achieving 45% compliance in the top two compliance levels, and 79% overall compliance effort if 'Partially Compliant' numbers are added. This is a good outcome when measured against the relatively low 15% 'Not Compliant' category. Especially so – given the remoteness of these sites and lack of sophisticated access to geotechnical testing mechanisms, monitoring, or very experienced geotechnical staff.

Does this result make this mine GISTM-compliant? Unfortunately, 'no' because a number of fundamental prerequisites of the 77 Requirements are not being met as described in the section following. This exposes the Achilles heel of the GISTM since many of these fundamental requirements are almost impossible to fulfill for small and remote mining operations. It also probably means these operations would be lost from the GISTM family which is something GISTM definitely does not want and is the reason for this paper.

We wish to make it absolutely clear that this is not an indictment of the GISTM system which has proved inordinately successful. But we also need to keep small players in the GISTM fold, and to ensure this we may have to offer some restructuring to provide the necessary incentive.

COMPLIANCE VERSUS NON-COMPLIANCE

This section provides a brief overview of GISTM compliance vs non-compliance items for these Indonesian mine sites. Specifically, reasons why some of the six main Topic Areas are compliant and more importantly, those Topic Areas that are not compliant since it is they that determine whether or not the GISTM standard has been met. A broad overview of compliance vs non-compliance in the main six Topic Areas of GISTM follows.

Compliant Topic Areas

Communities

Communities surrounding the TSF areas of these West Kalimantan mines, as well as all local public authorities, are fully engaged as part of the mining process, and mines are therefore compliant with this Topic requirement. The partially compliant items too could be quickly upgraded by evidencing policy statements; minutes of meetings; records of discussions with communities – even ad hoc discussions.

Integrated Knowledge Base

There is robust compliance with this Topic Area. With additional review and regular updating of tailings characterisation, climate change resilience, and environmental/social knowledgebase data partial and substantial, compliance can be upgraded to full compliance. It is concluded that a shift in presentation with respect to dam breach analyses and international best practice would enhance overall GISTM output.

Design Construction and Operation

This is one of the Topic Areas where non-compliance is prevalent. These as discussed in the next section of the paper. But there are also several areas of full compliance as indicated in Table 1, and where our KCB GISTM audit revealed dams orderly and neat with stable slopes; fully compliant freeboard requirements, and with good quality comprehensive TSF management and operation, design, risk management and monitoring. All these items are fully understood and implemented by Air Upas and Sandai mine management. Detailed design has been delivered by geotechnical consultants Tura (2020) who have provided sound geotechnical principles for the TSF sites. There is also robust daily monitoring via a team of inspectors on motorbikes who, from at times remote stations, monitor the facility daily with immediate notification of any issues such as seepage from the dams, overtopping, bulging, erosion, tension cracking, or any other signs of slope instability. Their enthusiasm knows no bounds.

Management and Governance
There is some compliance to this Topic Area but it is nonetheless the second Topic Area where non-compliance is prevalent. Non-compliance items here, as will be shown, are major markers in preventing GISTM compliance. They are described in greater detail in the section following.

Emergency Response
Emergency Response requirements at Air Upas and Sadai elicit good response and governance. GISTM emphasises the necessity of collaborating with first responders and proximate enforcement personnel, and here the mining company CITA has proved adept in drawing from hands-on experience in handling localised flooding, fires, and occasionally problematic tailings dam slopes through concise and swift reaction in emergencies. Their expertise especially shines post-incident when managing individuals, protecting assets, and safeguarding the environment.

Disclosure
Annual reports highlight the company's commitment to embrace innovative approach including strategies to adapt to climate change. These demonstrate CITA's determination to achieve global transparency, especially concerning the safety of mining operations, personnel and communities. Whistle-blowers are in all cases encouraged and always protected.

These West Kalimantan tailings facilities were previously monitored for general tailings deposition compliance by KCB (2019) and therefore in a period before GISTM. Results were acceptable but perhaps on the average side. Even better then, was a second audit in 2023 which provided ample evidence of efforts towards GISTM compliance, including a marked general improvement in management and monitoring of tailings at these facilities. Mine management and staff are keen to ascribe to GISTM requirements, and it is this enthusiasm, as in other remote parts of the world, that must be encouraged and nurtured. It is also one of the prime reasons why smaller remote operations should be drawn into, and remain, within the GISTM fold, and not allow losing them from the GISTM system through targets that are difficult to achieve, if at all.

Non-compliant Topic Areas
The two Topic Areas at Air Upas and Sandai that provide all the non-compliant items are the Design, Construction and Operation, and the Management and Governance Topics (KCB, 2023). These non-compliance item descriptions follow.

Design, Construction and Operation Topic
Non-compliance for this topic relates mainly to personnel, or rather a lack thereof, and reporting that would normally emit from their appointments. The main areas of non-compliance are:

- No appointed Accountable Executive (AE)
- Limited geotechnical instrumentation or field geotechnical input
- No standalone Design Basis Report (DBR), and
- No detailed Tailings Management System (TMS) register or report.

The common thread here is that if the mine had senior personnel these systems and reporting would all be in place. Annexure 1 of the GISTM (2020) defines the requirements of an Accountable Executive to be 'accountable for the safety of tailings facilities' and further someone who 'may delegate responsibilities but not accountability'. This definition describes a very senior company position and is for someone who needs to be continuously in touch with day-to-day mine operations. To all intents and purposes virtually resident on site where even having a remote AE with some delegated authority on the ground would attract major costs. Can small distant and remote operations, as those described, afford such a senior person, and are there senior personnel willing to live/work at these relatively low-key operations? Probably not. There must therefore be a different way to provide such responsibility: perhaps a lower level of authority being one. This lack of a senior Accountable Executive and Engineer of Record (section following) as geotechnical council, means that fulfillment of other GISTM requirements and reports such as DBR and TMS, normally falling to these personnel, are not being completed. And without such senior input will probably not be done. There has to be a different way.

Management and Governance
At Air Upas and Sandai non-compliance for the Management and Governance topic area includes:

- No appointed Accountable Executive (AE) (again)
- No appointed Engineer of Record (EoR)
- No designated Responsible Tailings Facility Engineer (RTFE)
- No documented evidence of internal audits
- No existing Closure Report or related documentation.

These non-compliance items, as for the Design, Construction and Operation Topic Area, all point to the biggest hurdle being a lack of senior executive and engineering personnel necessary for GISTM compliance. These persons are mostly unavailable, or unwilling, to fill these senior posts in small and remote operations. The EoR role, as per the earlier AE description, also requires the GISTM responsibility (GISTM, 2020) of "confirming that the tailings facility is designed, constructed, and decommissioned with appropriate concern for integrity of the facility, and that it aligns with and meets applicable regulations, statutes, guidelines, codes and standards". Repeated is the requirement for full 'accountability'. These stringent GISTM requirements, especially the senior executive and engineering appointments, while well-meaning and mandatory for larger mining operations, are very difficult to conform to for small remote mining operations. The cost is high, and these people just don't want to work in these areas. There has to be another way that GISTM can be implemented satisfactorily to address this impasse.

We, as the GISTM community, need to keep all mining operations in the GISTM fold and if problems with senior executive and engineering appointments are preventing this then we need to investigate alternative ways to set this right. If we don't these small and distant operations will be lost to the GISTM family for good, and with it the international compliance we all so desperately need.

The sections following attempt to address this gridlock.

THE CASE FOR 'GISTM-LIGHT'

General
There looks to be sound argument for development of a 'GISTM-Light' category that will still comply with international GISTM requirements, but that will specifically cater for the TSF management and monitoring needs of smaller remote mining operations. First consider reasons why GISTM in its full compliance requirement is difficult to acquiesce to in mining operations that are small and remotely located.

Primary Reason
Senior executive staff, such as AE and EoR appointments, are invariably too costly to justify for small remote operations, whether on site or even remote with delegated authority. Not only is it prohibitively expensive, it's also virtually impossible to entice these senior personnel to small and therefore relatively insignificant sites. AE and EoR personnel are probably unwilling, justifiably so, to undertake these low-key roles: especially when considering that these are unattractive opportunities in the fight for core skills in a labour market that is already constrained.

GISTM demands these personnel skills since these are the people that compile and produce the documentation and reporting necessary, and mandatory, for mine development, governance and audit fulfillment.

Secondary Reasons
There is further sound reasoning why the omnibus version of GISTM does not meet small remote mining operations. Not only here, but for similar sites worldwide:

- Mining operations are distant, requiring difficult, time-consuming and costly logistics in terms of access. Access remains difficult for both people and machines.

- Sophisticated investigation and monitoring techniques, which would be considered normal for large TSF sites, are difficult to implement because of the logistical obstacles in getting equipment on site, and the relatively exorbitant cost this would attract. These include:
    - Borehole drilling equipment for site investigation and ongoing monitoring
    - Seismic Cone Penetration testing equipment
    - Vibrating Wire Piezometer (VWP) installations with telemetry
    - Inclinometer installations: made even more difficult and costly when considering SAA Shape Array and Inplace Inclinometers type inclinometers.
- The site investigation campaigns associated with the above techniques also require qualified and experienced geotechnical staff, further inflating costs, which taken together with machine establishment, raise expenses by a significant order of magnitude. Offset this against marginal profits and this then becomes a significant deterrent for full GISTM compliance.
- Electricity is often not available in remote areas, and neither is WiFi connectivity.

There is, notwithstanding the above, still every reason to encourage GISTM policies and adherence in even the remotest areas of the world. Even if partially so. GISTM compliance must at all times be encouraged. It is recommended, for this reason alone and in order to provide GISTM continuity, that a GISTM-Light category be considered as part of the broader set of GISTM requirements.

A POSSIBLE GISTM-LIGHT PATHWAY

General

It is generally possible for most TSF sites, even those distant, small and remote to adhere to the following four Topic Areas:

- Communities
- Integrated knowledge base
- Emergency Response
- Disclosure

But it is in the remote and distant sites where the Design, Construction and Operation Topic, and the Management and Governance Topic compliance become very difficult for all the reasons mentioned. Here a GISTM-Light pathway might keep smaller remote mining operations within the GISTM ambit.

It is suggested, and an opinion open for discussion, that such a GISTM-Light pathway might consider:

- Simplification of the Design Construction Operation and Management Governance Topic Areas
- Be confined to within certain minimum physical requirements
- Be determined by dam failure consequence classification, and
- Have minimum engineering requirements.

These items are considered in greater detail in the section following and summarised in Table III.

GISTM-Light Design: Construction Operation and Management/Governance Topics

Design Construction and Operation

First and foremost requirement is the mandatory appointment of a Responsible Tailings Facility Engineer (RTFE) who must reside on site and operate in a full-time capacity to cater for the daily geotechnical TSF requirements including technical execution, management and monitoring. The RTFE will fulfill the EoR and AE responsibility of a standard GISTM.

In addition:

- Sophisticated investigation and monitoring techniques could be substituted for more cost-efficient 'older' techniques such as Casagrande Standpipe Piezometers monitored with a dipmeter rather than VWPs with telemetry; daily land surveying of prism targets in areas possibly prone to slope movements, satellite monitoring procedures, and continued daily TSF

dam inspections and monitoring by motorbike personnel: with immediate reporting of any potential dam safety issues.

Actively encourage local geotechnical self-governance and on-site problem solving. The Air Upas and Sandai sites use, for example, a system of cantilever piles where upturned tree stumps cleared of their branches are knocked vertically into the ground using an excavator. Each rough timber pole is embedded two-thirds of its length close to another. This to provide lateral support to areas showing any slight outward or downward mass movement creep. In so doing they prevent major breach, buying time for the installation of additional geotechnical intervention such as slope flattening, surface drainage and/or internal pore water pressure reduction – say with sub-horizontal drainage. These tree cantilevers are an example of a simple, cost-effective solution using cheap locally available products.

- Undertake TSF rehabilitation measures simultaneously with ongoing, or new, tailings operations or closure. Large fallow dam areas, filled to capacity with tailings, can be partially dried and planted with timber or fruit trees. Such operations are currently being actively undertaken at the Kalimantan mines where residue-filled dams are being planted with fruit trees. Here rehabilitation of open mined-out areas already show excellent tree regrowth (CITA, 2022), all within a short period of a few years.

Management and Governance
Consideration could be given to annual compilation of an internal geotechnical audit with concomitant reporting by the RTFE. This could then be made available to a mine-appointed geotechnical engineering consultancy for checking of potential geotechnical gaps and acceptance of on-site geotechnical systems. A GISTM-Light audit would follow after acceptance by the review consultant. Such RTFE audit, geotechnical firm peer review, and GISTM-Light audit would all be mandatory requirements.

This will provide clear delineation of responsibility and unambiguous accountability to ensure GISTM-Light stands up to scrutiny via independent audit.

The GISTM-Light biannual audit would need to be conducted by an independent consultant familiar with GISTM audit requirements and nous.

Mine accountability would reside with the RTFE as a GISTM-Light replacement of EoR and AE.

Minimum physical GISTM-Light TSF attributes
Operation
All small, remote, isolated and distant mining operations

TSF Wall Height
Average wall height <18 m: open to consideration and discussion

TSF Reservoir Capacity
<180 000 m^3: open to consideration and discussion

Tailing Residue Quality
Treated water free of deleterious chemicals.

Dam Failure Consequence classification requirements (GISTM 2020)
GISTM Dam Failure Consequence Classification
Low.

Potential population at risk
None.

Potential loss of life
None expected.

Environment
Minimal effects and disruption of business and livelihoods. No measurable effect on human health. No disruption of heritage, recreation, community or cultural assets.

Infrastructure and Economics
Low economic losses. Area contains limited infrastructure or services. <US$1M.

Minimum engineering requirements
These could entail:

- Robust TSF design with mandatory peer review and proof of design acceptance by an independent geotechnical consulting firm
- Proof of containment design, such as berm surrounds, to confine breached run-off
- Compliance with all GISTM safety requirements and protocols.

Table III provides a summary of proposed minimum GISTM-Light requirements. It assumes, as per the preceding text, that the Communities, Integrated Knowledge Base, Emergency Response and Disclosure topics areas can all be mostly accounted for by the mining company.

Table III: Summary of proposed minimum GISTM-Light qualification and requirements

GISTM-Light Qualification Requirements	
Physical	• Small, distant, isolated & remote • <18m height [*1] • <180 000 m^3 impoundment • Nil, or isolated, or diluted deleterious chemicals
Minimum GISTM Consequence Classification requirements	• Dam failure classification – Low • Population at risk – None • Loss of life - None expected • Environment – Minimal disruption • Economic loss - <1M US$
Minimum Engineering Requirements	• Robust TSF design required by RTFE • Peer review and proof of design acceptance • Proof of containment design • Independent review by outside geotechnical firm • Compliance with GISTM safety protocols
GISTM-Light Topic Area Compliance Requirements	
Design Construction and Operations Topic	• Permanent RTFE presence on mine site • RTFE replaces AE • RTFE required to derive DBR & TMS • Allow less sophisticated monitoring methods • Accept innovation (e.g., tree stump cantilever piles) • Concurrent closure and operation of all site TSFs
Management and Governance Topic	• RTFE replaces EoR • Ensure mine produced internal audits & closure report • Annual TSF audit report as required by RTFE • Arrange gap review by external geotechnical firm

GISTM-Light Qualification Requirements	
	• Mandatory annual GISTM-Light audit by independent geotechnical firm • Ensure clear RTFE authority and accountability

**1 Heights and volumes for discussion purposes only*

INTERNATIONAL GISTM-LIGHT CONSIDERATION

There can be no consideration of change to a GISTM-Light format without input of the GISTM international body.

Members of this group are therefore encouraged to:

- Consider formulation of a GISTM-Light template and set of rules for small remote mining operations of the world
- Recognition that this is not criticism of the current highly effective GISTM audit system but rather a refinement necessary to keeping even the smallest mining operations in the greater GISTM fold
- A GISTM-Light audit process would need to be compiled with precise details of all geotechnical requirements as determined by the international GISTM group, including clear description to differentiate between GISTM-Light and standard GISTM
- The jump from GISTM-Light to full GISTM compliance, as would be required when a mine outgrows its 'light' status, could see the GISTM-Light studies and audits included in the new omnibus GISTM as an Annexure: thereby exhibiting early fulfilment of GISTM requirements
- GISTM-Light would require clear descriptions to demonstrate precise delineation of responsibility and accountability, and with measurable assurance that the system can stand up to external audit scrutiny.

It is early days but a start, nonetheless.

CONCLUSIONS

The full suite of GISTM TSF audit requirements is difficult, time-consuming and costly to implement, which makes its use in remote small mining operations at times untenable. Geotechnical site investigation campaigns are also costly and difficult to undertake, and senior AEs and EoRs difficult to come by, expensive and hard to entice to smaller remote operations. At the same time the enthusiasm and attempts at compliance by staff in these remote mining operations needs to be lauded and encouraged. It is recommended therefore, in efforts to ensure this, that a GISTM-Light system be considered for use in remote small mining TSF operations. A GSTIM-Light system, as presented in this paper, could be included in the GISTM omnibus version as an Annexure, with protocols and direction as determined by the international GISTM body.

ACKNOWLEDGEMENTS

The author wishes to thank KCB Australia (Pty) Ltd for allowing publication of this paper and CITA Indonesia for inclusion of GISTM data.

REFERENCES

GISTM. (2020). Global Industry Standard on Tailings Management, Co-convened by International Council of Mining & Metals (ICMM), United Nations Environment Programme, and Principles for Responsible Investment (PRI).

GISTM Conformance Protocols. (2021). ICMM Publication. pp 1-110.

ICMM. (2021). Tailings Management Good Practice Guide. pp 1-142.

ICMM. (2025). Tailings Management Good Practice Guide. pp 1-148.

KCB. (2019). Geotechnical Review. KCB Preliminary Review Comments Report.

KCB. (2023). CITA Indonesia, Global Industry Standard for Tailings Management Audit & Gap Assessment. pp 1 – 38.

Laporan pelaksanaan rencana penelolaan permantauan & lingkuncan hidup. (2022). Semester 2 Tahun. (*CITA report on operations, planning, monitoring and environmental considerations)*.

PT Cita Mineral Investindo Tbk. (2022). Sustainability Efforts for Regenerative Future Report.

PT Cita Mineral Investindo Tbk. (2022). Annual Report. Improving Performance as the Leading Bauxite and Alumina Producer in Indonesia.

Regulations of the Government of the Republic of Indonesia, Number 37 of 2010. (2010). Government regulations concerning dams. (*Article 51 – 62 (emergency action), 129 (closure), 155 (community) – 156)*.

Standar operasional prosedur kesiapsiagaan dan tanggap darurat. (2022). SOP-01-HSE-005. (*Standard operating procedures for emergency preparedness and response).*

TURA Consulting Indonesia. (2020). Final Report - Geotechnical Investigation, Hydrology – Hydrogeology and Embankment Design Bauxite Residue Storage Facility, PT Cita Mineral Investindo, Tbk. Sadai Site and Upas Site. Ketapang Regency. West Kalimantan.



Gordon Vivian ("GV") Price

Senior Staff Consultant
Klohn Crippen Berger

Dr. Gordon Vivian "GV" Price is a geotechnical engineering specialist with more than 47 years of international experience managing complex projects and leading multidisciplinary technical teams. Over the course of his career, he has directed four consulting practices in southern Africa, including two that he founded. GV holds both an MSc and a PhD in Engineering Geology from the University of Pretoria, where his doctoral research focused on rockmass characterization for tunnelling applications. His expertise spans a wide range of engineering geological and geotechnical disciplines, including open-pit rock mechanics, tailings dam engineering, GISTM conformance assessments, rock slope evaluation and stabilization, water and hydropower dam investigations, construction materials engineering, and geotechnical input for major road, rail, and mega-bridge infrastructure projects.
He has delivered projects across Africa, Australia, Ireland, Afghanistan, and Indonesia, bringing extensive insight into diverse geological and operational environments. In recognition of his outstanding contributions to the field of engineering geology, GV received the SAIEG Gold Medal in 2020. GV is currently a Senior Staff Consultant at Klohn Crippen Berger in Australia and resides in Brisbane with his family.

Reliable design with limited data: Characteristic strength selection for slope stability assessment

H.A. Brandao[1], L. Kirsten[1], R. Duque[1], P. Delport[1], T. Jibiki[2], A. Fourie[3]

[1]Klohn Crippen Berger, Australia
[2]Rio Tinto, Australia
[3]University of Western Australia, Australia

The selection of characteristic shear strength values for slope stability assessments of tailings storage facilities (TSFs) requires careful consideration of uncertainties in material properties, arising from both spatial variability and the inherently limited scope of site investigations. When sample size and layer geometry are not explicitly considered, the resulting design values may not reliably represent in-situ conditions. This paper demonstrates an approach to deriving characteristic shear strength values that incorporates sample size and layer geometry in accordance with Eurocode 7 (EN 1997). A case study is presented using twelve monotonic simple shear tests on a TSF foundation soil. From this data, a design value for the undrained shear strength ratio (s_u/σ'_v) is obtained by both conventional means and through a procedure guided by the 2nd Generation EN 1997. Comparisons between the two approaches highlight the sensitivity of strength selection and emphasise the importance of appropriate statistical treatment when defining characteristic values. The influence of each approach is further demonstrated through its impact on the stability of a simplified slope. The findings illustrate a structured method for selecting characteristic s_u/σ'_v values that balances limited data with explicit uncertainty treatment, supporting more reliable and defensible design decisions in TSF stability assessment.

INTRODUCTION

The selection of representative values (X_{rep}), taken as the design parameter, for the peak (yield) undrained shear strength ratio (s_u/σ'_v) is a challenging process due to the spatial variability, inherent uncertainties and the inhomogeneous nature of soils. These values have a direct influence on the assessment of the limit state of tailings storage facilities (TSF) during design. Typically, X_{rep} is defined based on ground investigations that comprise both laboratory and field tests; however, the scope and quantity of these investigations are usually limited by economic constraints.

Given these limitations, the selection of the X_{rep} values has traditionally relied on geotechnical judgment and limited data, with the X_{rep} being taken as a nominal value (X_{nom}), without further statistical assessment and consideration of spatial variability and soil uncertainty. The 2nd Generation of the Eurocode 7 1997 (EN 1997) presents a methodology for a data-driven approach to select X_{rep} based on the characteristic value (X_k), defined as values of a soil property associated with a probability of being attained and accounts for the effects of spatial variability.

This paper presents a case study demonstrating the application of the 2nd Generation EN 1997 methodology on the selection of X_{rep} for a foundation material of a TSF based on X_k. The database comprises twelve monotonic simple shear (MSS) tests conducted in a NATA certified geotechnical laboratory. These values were utilised in slope stability assessments to illustrate the influence on the factor of safety (FoS) of a TSF embankment.

The 2nd Generation EN 1997 methodology applies to both field and laboratory test data; however, in this paper, the authors elected to illustrate its application using MSS tests.

2nd Generation EN 1997 – Representative value selection

EN 1997 refers to the Eurocode 7: Geotechnical design, which is part of the ten European Standards that specify how structural design should be conducted. The 1st generation of Eurocodes was released between 1990 and 1999, and the 2nd Generation EN 1997 is under development and is expected to be released in the 1st quarter of 2026.

According to 2nd Generation EN 1997, X_{rep} is defined as the X_{nom} or X_k value of a soil property utilised in ultimate and serviceability limit state verifications. Both X_{nom} and X_k values are defined based on desk studies, site inspection, preliminary and design investigations, and monitoring of the ground and structures, which are converted to derived values (X_{derv}) based on theory, correlation and empiricism or back-analysis (Orr *et al*., 2025).

Once the derived values are defined, the 2nd Generation EN 1997 sets two potential paths to determine X_{rep}:

- Path 1 – Nominal value path, in which the designer applies judgment and experience in the selection of X_{nom}, defined as "*value fixed on a non-statistical basis; for instance, on acquired experience or on physical conditions*", due to the absence of reliable and representative data. (*Orr et al*., 2025).

- Path 2 – Characteristic value path, in which the designer applies statistical procedures to define the X_k, defined as "*value of a material or product property having a prescribed probability of not being attained in a hypothetical unlimited test series*". X_k corresponds to a fractile value of an assumed probability distribution function.

If Path 1 is chosen, X_{rep} equals X_{nom}; for Path 2, X_{rep} equals X_k. A conversion factor (h) can be adopted when appropriate, if correction for scale, moisture, temperature, ageing of materials, anisotropy, stress path or stress level may be required. Figure 1 presents the full path from ground investigation to selection of X_{rep} (Orr *et al*., 2025).

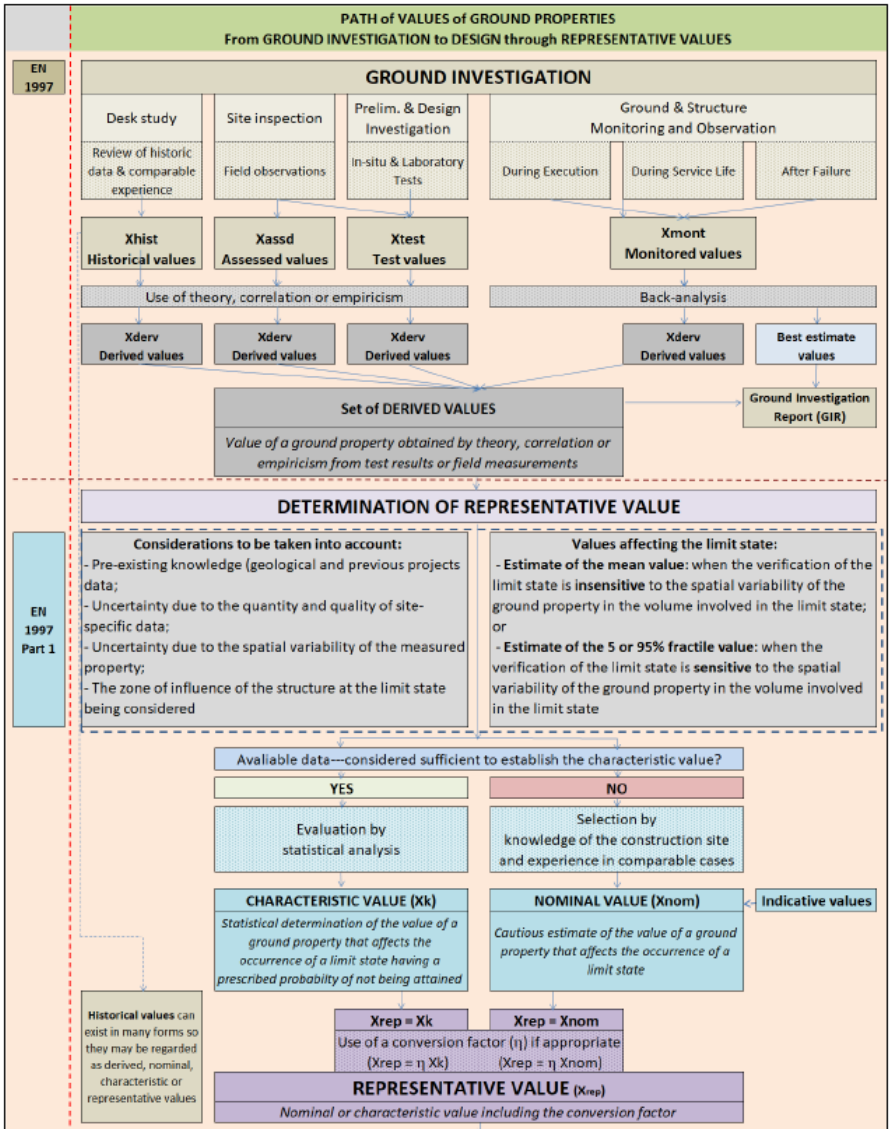


Figure 1. Process for determining the representative value (Orr et al.*, 2025).*

When selecting between Path 1 and Path 2, the designer should account for pre-existing knowledge, uncertainties due to the quantity and quality of the available data, uncertainties due to the spatial variability of the measured property, and the zone of influence of the soil layer in the structure limit state (Orr *et al.*, 2025).

Pre-existing knowledge refers to historical data from previous projects or comparable experience. The quantity and quality of the available data should be assessed, considering the uncertainties associated with the derived values. Regarding the spatial variability and extent of the zone of influence, the 2nd Generation EN 1997 recommends a design approach based on the zone of influence (L), which can be defined as the extent of the failure mechanism, and the scale of fluctuation (q), which represents the spatial variability of the soil property in the horizontal and vertical axes (Orr *et al.*, 2025). The guideline defines three (3) base cases (A, B, and C) for assessment based on the L and q relationship, as presented in Table I. Furthermore, the 2nd Generation EN 1997 also provides recommendations on the minimum number of samples for each type of assessment; however, this is not addressed in this paper (Orr *et al.*, 2025).

This case study focuses on the derivation of X_{nom} and X_k, illustrating the influence of this choice on FoS.

For illustrative purposes, this paper follows both paths to demonstrate the influence of each path on the FoS. Base cases A and B of the L and θ relationship were considered.

Table I: Types of estimates of representative values according to EN 1997 (adapted from Orr et al., 2025)

Type	Definition	L v θ	Representative value	
			Value	Estimate of
A	"If the limit state is insensitive to spatial variability of the ground, the representative value of the ground property shall be determined as an average value."	L >> θ	Nominal (cautious)	Average value
				or
			Characteristic (statistical)	Mean value
B	"If the limit state is sensitive to spatial variability of the ground, the representative value of the ground property shall be determined as an inferior or superior value."	L < θ	Nominal (cautious)	Inferior (unfavourable) or superior (favourable) value
				or
			Characteristic (statistical)	5% (unfavourable) or 95% (favourable) fractile
C	If the limit state is sensitive to the spatial variability of the ground, but not to the extent corresponding to the bounds given by the average and the inferior or superior values. The representative value is between the average/mean and the inferior or superior value. Type C is an intermediate case type between types A and B.	L > θ	Nominal (cautious)	Average value and inferior (unfavourable) or superior (favourable) value
				or
			Characteristic (statistical)	Mean value and 5% (unfavourable) or 95% (favourable) fractile

Characteristic value (X_k) selection

The X_k value is determined based on a prescribed representative statistical distribution, usually normal or log normal. When characterising a soil unit, it is important to distinguish between the sample and the population. A sample represents a subset of measurements (e.g., MSS tests, cone penetration tests, etc), while a population refers to the complete set of all possible values. In geotechnical engineering, we often work with samples with limited measurements to derive X_{rep} of a soil unit, as characterising a soil unit as a population is often impossible due to spatial variability and associated cost.

If enough data is available, X_k can be defined based on prescribed probabilistic distribution functions such as normal or log normal. If data is limited, the 2nd Generation EN 1997 recommends the use of equation 1 that accounts for the sample size (n), where:

- X_{mean} is the mean value of the n samples.
- V_x is the coefficient of variation applicable to the soil unit (population).
- k_n is the coefficient associated with 'n' and the level of knowledge regarding V_x.

The equation denotes ± as it can be utilised to obtain the inferior and superior limits (Orr *et al.,* 2025). This is only applicable to cases where the assessed property does not vary with depth (e.g., increase with depth), as in the case of s_u/s'_v – the focus of this paper.

$$X_k = X_{mean}[1 \pm k_n V_x] \quad [1]$$

There are three cases for establishing the V_x values, which also influence the k_n value:

- Case 1 – V_x is known from prior knowledge.
- Case 2 – V_x is unknown, in which case it should be calculated based on the available sample set.
- Case 3 – V_x is assumed by the designer based on available literature.

Table II presents the equations for determining k_n based on the combination of cases and types, where N_{95} is a factor, equal to 1.64 for all values of 'n', that evaluates X_k for a normal distribution with 95% confidence level, $t_{95,n-1}$ is the t-critical value associated with a t-distribution with a 95% confidence level and n-1 degrees of freedom, and Γ^2 is the ratio between L and θ.

Table II: Characteristic value for different combinations of estimate types and cases (adapted from Orr et al., 2025)

Cases with different knowledge concerning Vx	**Type of estimate of the characteristic value**		
	A: Estimate of the mean value $\Gamma^2 = 0$	**B: Estimate of the inferior (5%) or superior (95%) fractile value** $\Gamma^2 = 1$	**C: Estimate of the intermediate value** $\Gamma^2 = \theta/L$
Case 1: (V_x known) and Case 3: (V_x assumed)	$N_{95}\sqrt{\frac{1}{n}}$	$N_{95}\sqrt{1+\frac{1}{n}}$	$N_{95}\sqrt{\Gamma^2+\frac{1}{n}}$
Case 2: (V_x unknown)	$t_{95,n-1}\sqrt{\frac{1}{n}}$	$t_{95,n-1}\sqrt{1+\frac{1}{n}}$	$t_{95,n-1}\sqrt{\Gamma^2+\frac{1}{n}}$

METHODOLOGY

This paper presents a case study where the 2nd Generation EN 1997 representative value selection methodology was applied to show how to select a representative value for s_u/σ'_v for an alluvial foundation soil unit and how this selection may affect slope stability assessment. The s_u/σ'_v derivation process is not described in this paper.

Three different scenarios were considered as presented in Table III. Case 2 (V_x unknown) from Table II is considered for all scenarios as the population coefficient of variation for the alluvial deposit could not be established.

Table III: Case study scenarios

Scenario	**Type**	**Design consideration**	**Representative value (X_{rep})**
N	-	No consideration of the sample number or the influence of spatial variability	X_{nom} = sample mean
K2A	A	Spatial variability does not influence the limit state	X_k = mean value with 95% confidence level based on t-distribution
K2B	B	Spatial variability influences the limit state	X_k = 5% fractile based on t-distribution

Slope stability assessments were conducted to illustrate how variations in s_u/σ'_v for the alluvium unit influences the FoS under different assessment types. All other material parameters and pore pressures,

derived from steady-state flow simulations, were kept constant. Analyses were performed using the GeoStudio 2025 package, applying the Morgenstern-Price method to calculate FoS. Figure 2 shows the section geometry, and Table IV lists the assigned material strength parameters.
The section represents the upstream configuration of a tailings facility embankment, founded on alluvial deposits, residual soil, extremely weathered (XW) soil, and bedrock. The alluvial layer thickness decreases from approximately 6 m on the downstream side to about 1 m beneath the embankment and upstream. It was adjusted to illustrate the methodology and does not represent an actual condition.

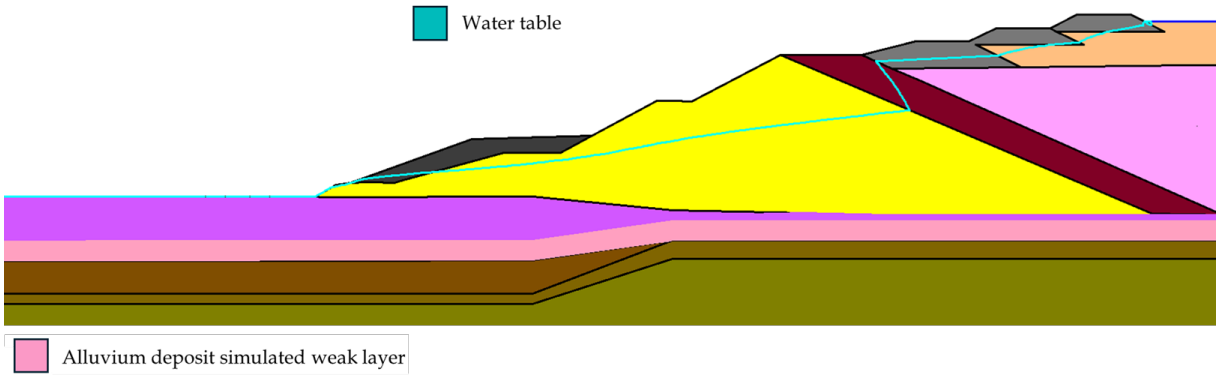


Figure 2. Adopted embankment geometry.

DATABASE

The alluvial deposit is classified as a silty sand-sized material with significant variability in its particle size distribution. The specific gravity ranges from 2.66 to 2.71, with a mean value of 2.68, as expected for natural soils. Based on the consistency limits, it ranges from non-plastic to medium plasticity. All cone penetration tests indicated drained dilative behaviour according to the soil behaviour type classification. These results were accordingly disregarded for derivation of the representative s_u/σ'_v values, as the penetration response is fully drained and does not represent an undrained loading condition.

Test summary
Twelve MSS tests were conducted on soil specimens obtained from the alluvial deposit forming the foundation unit of the TSF. Sampling was performed via boreholes using push tubes to minimise disturbance and preserve in situ structure as much as possible to enhance the reliability of strength measurements. Specimens were collected from multiple depths and locations along the embankment to capture spatial variability within the target deposit.

The MSS tests were carried out under undrained conditions, with consolidation pressures ranging from 150 kPa to 600 kPa to simulate stress states anticipated throughout the life of the facility. This range was selected to ensure the results reflected predominantly normally consolidated behaviour. Shearing was performed at a constant rate of 0.1 mm/min, continuing to a maximum strain of 30%. Key details from the MSS testing program are shown in Table V.

Table V: Summary statistics for MSS tests

Number of tests (n)	X_{mean} (s_u/σ'_v)	Standard deviation (σ)	Coefficient of variation (%)
12	0.46 (0.40 – 0.53)	0.11	24%

CHARACTERISTIC VALUE SELECTION

This section presents the obtained characteristic values considered in this case study. Due to limited data, Case 2 was considered as V_x for the s_u/σ'_v distribution is unknown for the alluvium. Thus, the sample coefficient of variation (24% - refer to Table V) was adopted as V_x to calculate X_k. The estimate of the mean value with 95% confidence level (Type A) and 5% fractile (Type B) was performed as proposed by the 2nd Generation EN 1997 methodology.

Table VI presents all the inputs to equation 1, including the resulting characteristic values. X_{mean} was taken as 0.46, as presented in Table V, which corresponds to the sample mean. k_n values were established based on sample size (n = 12) for both Type A, which is equal to 0.51 and Type B, which is equal to 1.86. V_x equal to 24% was adopted, which corresponds to the sample coefficient of variation. The resulting characteristic values based on equation 1 are 0.40 for scenario K2A and 0.25 for scenario K2B.

Table VI: Input parameters used for deriving characteristic strength values

Scenario	Type	X_{mean}	k_n	V_x	Characteristic value (X_k)
K2A	A	0.46 (refer to Table IV)	0.51	24%	0.40
K2B	B	0.46 (refer to Table IV)	1.86	24%	0.25

REPRESENTATIVE VALUE SELECTION

Table VII presents the derived strength parameters for the alluvial deposit under each scenario. Scenario N does not explicitly consider the influence of spatial variability and sample size in the definition of s_u/σ'_v, whereas scenarios K2A and K2B incorporate both, as reflected in the differences in the s_u/σ'_v values. The mean with a 95% confidence level deviates from the sample mean by 13%, while the 5% fractile differs by 46%. The observed difference between values highlights the importance of considering spatial variability and sample size when estimating s_u/σ'_v, as neglecting these factors might lead to unconservative design assumptions. Slope stability assessments were performed to illustrate the impact of the different representative values on the FoS.

Table VII: Case study scenarios: strength parameters

Scenario	Type	Design consideration	Representative value (X_{rep})
N	-	No consideration of the sample number or the influence of spatial variability	X_{nom} = 0.46
K2A	A	Spatial variability does not influence the limit state	X_k = 0.40
K2B	B	Spatial variability influences the limit state	X_k = 0.25

SLOPE STABILITY ASSESSMENT

Figure 3 illustrates the slip surfaces and associated FoS for the proposed theoretical scenarios N, K2A, and K2B. The slip surfaces exhibit similar shapes and share a common origin and endpoints. Their lower segments (bottom chord) generally follow the contact between the alluvial deposit and residual soil.

Scenario N, with s_u/σ'_v equal to the sample average (0.46), simulates a condition in which spatial variability and sample size are implicitly treated and yields an FoS of 1.50. By considering the sample average, the sample's representativeness of the entire population, or in this case, the soil unit, is assessed as being true.

Scenario K2A, where s_u/σ'_v equals the mean value at a 95% confidence level (0.40), represents a condition where spatial variability has no influence over the limit state ($L > \theta$); however, sample size is now explicitly considered when defining the X_{rep}. This scenario produces an FoS of 1.47. The s_u/σ'_v value of 0.40 differs from the sample mean (0.46) by 13%, resulting in a 3% reduction in FoS. In this specific assessment, the difference between the FoS in Scenarios K2A and N is not considerable, given the associated uncertainties. This is probably due to the low variability in the sample and the number of tests that compose the s_u/σ'_v dataset.

Scenario K2B simulates a condition where spatial variability has a significant influence on the limit state ($L < \theta$). If the 5% fractile value is adopted for s_u/σ'_v (0.25), the FoS is 1.21, which is 21% lower than the value obtained for Scenario N.

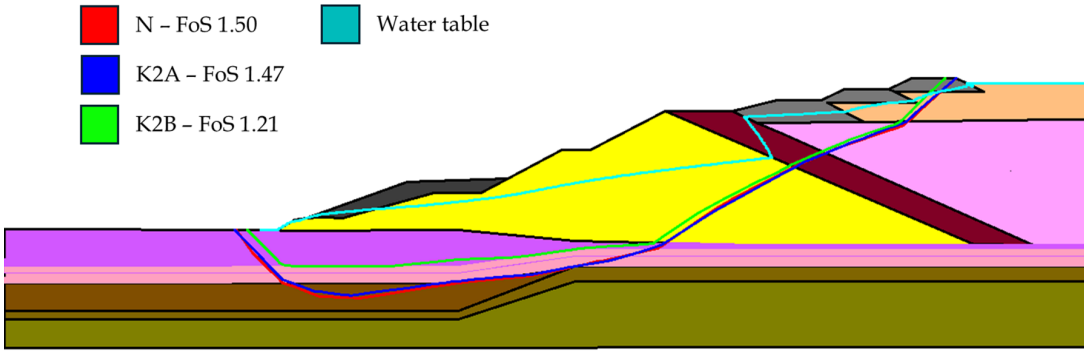


Figure 3. Slip failure surfaces for scenarios N, K2A and K2B.

Table VIII: Case study scenarios results

Scenario	Type	Design consideration	s_u/σ'_v – characteristic value (X_k)	FoS
N	-	No consideration of spatial variability or sample size	0.46 – mean value	1.50
K2A	A	$L >> \theta$	0.40 – mean value with 95% confidence level	1.47
K2B	B	$L < \theta$	0.25 – 5% fractile	1.21

The FoS results highlight the impact of explicitly accounting for spatial variability and sample number when defining X_{rep} for s_u/σ'_v. When these factors are implicitly considered based on judgment, the limit state fully complies with the minimum FoS of 1.5 recommended for normal operational conditions by most guidelines (Scenario N). However, when spatial variability and sample size are explicitly considered, the design condition is only marginally compliant (Scenario K2A) if the limit state is not influenced by spatial variability, and non-compliant (Scenario K2B) if it is. The reduction of the FoS under Scenarios K2A and K2B reflects the direct consideration of spatial variation, through the scale of fluctuation, and of sample size and representativeness with respect to the population. It underscores the importance of probabilistic approaches in geotechnical design, especially where data is limited. Incorporating spatial variability and sample size can reveal vulnerabilities and limitations that deterministic methods may overlook.

CONCLUSION

This case study highlights the importance of reliability-based parameter selection methodology in geotechnical design, particularly within the framework of 2nd Generation EN 1997-2. It demonstrates how spatial variability and sample size impact the derivation of s_u/σ'_v. While deterministic approaches (Scenario N) based on engineering judgment may suggest compliance with stability (FoS) requirements, reliability-based methods can reveal non-compliance. Scenarios K2A and K2B, following the 2nd Generation EN 1992 methodology, indicate reductions in FoS of 3% and 21%, respectively, when spatial variability and sample size are accounted for.

Importantly, the findings reinforce that X_k values should not be selected without further consideration of the geotechnical context, considering spatial variability and sample number. By employing Eurocode-derived values as alternative inputs, it is possible to explore a range of stability outcomes and thereby assess the robustness of design decisions under different assumptions about soil variability.

ACKNOWLEDGEMENTS

The authors gratefully acknowledge KCB for its continued support.

SYMBOLS AND DEFINITIONS

X_{rep} – representative values: nominal or characteristic value, including the conversion factor
X_{nom} – nominal value: value fixed on a non-statistical basis; for instance, on acquired experience or on physical conditions
X_k – characteristic values: defined as values of a soil property associated with a probability of being attained, and account for the effects of spatial variability and sample number
X_{derv} - derived values based on theory, correlation and empiricism or back-analysis
h - conversion factor for scale, moisture, temperature, ageing of materials, anisotropic, stress path or stress level
L – zone of influence for design approach
q - Scale fluctuation, which represents the spatial variability of the soil property in the horizontal and vertical axes
x_{mean} – mean value of the n samples
V_x – coefficient of variation of the soil unit (population)
k_n – is the coefficient associated with 'n' and the level of knowledge regarding V_x
s_u/σ'_v – undrained shear strength ratio
γ_b – Bulk unit weight of material in kN/m3
s_u – Peak undrained shear strength in kPa
φ' – effective friction angle in degrees
c' – cohesion in kPa
σ – Sample population standard deviation

REFERENCES

Orr, T., Sorgatz, T., Estaire, J., Prästings, J., D'Ignazio, M., Andries, J., Ene, A., & Polo Lopez, C. S. (2025). Determination of representative values from derived values for verification with limit states with EN 1997 - Guidelines for the application of the 2nd generation of Eurocode 7: Geotechnical design. Joint Research Centre. https://doi.org/10.2760/0980105.



Hugo Assis Brandao

Senior Geotechnical Engineer
Klohn Crippen Berger

Hugo Brandão is a geotechnical engineer focused on tailings dams and dry stack design; integrating geological and geotechnical data to deliver safe, resilient solutions. As a team leader, Hugo values collaboration and mentoring, helping professionals grow with confidence. He is passionate about how data science, AI, and data-driven design are reshaping geotechnical engineering—unlocking deeper insights, improving reliability-based design, and enabling smarter decisions throughout project lifecycles. Hugo sees these tools as catalysts for innovation and sustainability in the field. Excited about the future, he welcomes opportunities to connect with others who share curiosity and a commitment to advancing geotechnical practice.

Clay soil – A history of theoretical approaches to strength and the way forward

A. Smith, C.J. MacRobert

Stellenbosch University, South Africa

Structural failures on clay soils date back to antiquity, with tailings storage facilities (TSFs) being particularly vulnerable due to their frequent foundation on clay. Clay's shrink-swell behaviour, low strength, high compressibility, and settlement issues pose significant challenges. Between 1910 and 2018, 17.3% of over 300 TSF failures were attributed to foundation failure, highlighting its importance. For structures on clay, including TSFs, accurate strength parameters are critical throughout the project lifecycle. Site investigations using in situ and laboratory testing remain the preferred approach for determining design parameters, while empirical correlations assist in preliminary assessments and validation. Literature over the past three centuries reflects substantial work on clay shear strength and empirical correlations, yet notable gaps persist. A reliability assessment of key correlations, informed by documented failure case studies, is recommended. This research aims to enhance TSF design by improving long-term performance, resilience, and cost-effectiveness, ultimately reducing risk for critical infrastructure.

Keywords: Clay soils, Drained, Effective stress, Shear strength, Tailings storage facility, Total stress, Undrained

INTRODUCTION

Site-specific geotechnical data is essential for civil engineering design. For tailings storage facilities (TSFs), stability assessments are a fundamental requirement. However, during early design phases, such as pre-feasibility and feasibility, geotechnical data is often limited, while accurate cost estimates are needed for budgeting. Where clay soils occur, representative shear strength data is critical to achieve a cost-effective, low-risk design. In the absence of detailed data, empirical shear strength correlations based on Atterberg limits (consistency limits) can support TSF design on clay foundations. The reliability of these correlations directly influences project cost and risk. Once detailed site data becomes available, typically during the detailed design phase, empirical correlations can also serve as a validation tool.

The development of clay strength theories spans over three centuries, beginning with early soil mechanics concepts in the 1800s (Skempton, 1985a). Coulomb (1776) introduced a formula for drained shear strength, while Collin (1846) examined deep slips in clay slopes and embankments. Terzaghi's effective stress principle in the early 20th century revolutionised geotechnical analysis, earning him recognition as the 'father of geotechnical engineering'. Casagrande (1936) later advanced methods for determining pre-consolidation pressure and soil consistency. Skempton (1953) and Skempton (1957) enhanced empirical modelling by linking undrained shear strength to plasticity index (PI) and effective stress, and introduced the concept of activity to relate plasticity to clay mineralogy. Bjerrum and Simons (1960) demonstrated that higher plasticity reduces the angle of shearing resistance in normally consolidated clays.

Mitchell (1976) explored critical state friction angles, while Kulhawy and Mayne (1990) addressed correlations for undisturbed and remoulded clays. Recent contributions by Sorensen and Okkels (2013), Ishibashi and Hazarika (2015), and Carter and Bentley (2016), refined these models and highlighted limitations. Due to its complex behaviour, clay remains a key focus in geotechnical engineering research.

Tailings storage facilities

TSFs, also known as tailings or slimes dams, rank among the largest engineered structures globally. A TSF encompasses dams, tailings discharge systems, water reclaim and treatment systems, and associated infrastructure (CIGB, 2025). Tailings typically consist of silty or clayey particles produced during mineral processing. TSF implementation, including initial construction, often spans more than 50 years, depending on the life of mine, followed by closure. The *Global Tailings Portal* (2025) lists 2144 TSFs worldwide, including 233 in South Africa, comprising active, inactive, and closed facilities. TSFs are founded on diverse soil types, frequently including clay. Site selection is often constrained by existing mine infrastructure, which may necessitate foundations on clay soils. Additionally, starter walls may incorporate clay, depending on the design and material availability.

Globally, numerous TSF failures have resulted in catastrophic consequences, including fatalities, severe environmental damage, and long-term soil and water contamination. Cumulative fatality rates are estimated at six deaths per failure and 0.1–0.3 death per constructed TSF as of 2020. Bowker and Chambers (2015) report 226 failures between 1917 and 2009, while the *Chronology of major tailings dam failures* (2025) records 177 incidents from 1960 to May 2025. Lyu *et al*., (2019) attribute over 300 failures (1910–2018) to five root causes:

1) Seepage (21.6%),
2) Foundation failure (17.3%),
3) Overtopping (20.6%),
4) Earthquake (17.0%), and
5) Others (23.5%).

These figures confirm foundation failure as a significant contributor to TSF instability.

Clay properties and technical definitions

South Africa is well endowed with a wide range of clay soils (Heckroodt, 1991). There is no standardised definition of soft clay in terms of conventional soil parameters, mineralogy, or geological origin (Jones & Davies, 1985). However, soft clays are associated with shear strength, compressibility, and settlement problems. Clay consists of mineral particles smaller than 0.002 mm (2 μm) and typically exhibits low strength, high compressibility, and significant volumetric changes (Ural, 2018). Compared to silt, sand, and gravel, clay has unique geotechnical properties under the Unified Soil Classification System (USCS). Its Atterberg limits—shrinkage limit (SL), plastic limit (PL), and liquid limit (LL)—reflect its high plasticity. These properties cause clay to adhere when wet, become brittle when dry, and undergo substantial swelling and shrinking with moisture variations. Hogentogler (1937) describes clay as a fine-textured soil forming hard lumps or clods when dry.

Skempton (1953) states that in any clay stratum the ratio of the PI to the clay fraction (CF) content is approximately constant and may be defined as the 'activity' of the clay. Knappett and Craig (2012) state that the degree of plasticity of the clay-size fraction of a soil is expressed by the ratio of the PI to the percentage of clay-sized particles in the soil, this ratio is called the 'activity'. 'Normal' soils have an activity between 0.75 and 1.25. Activity below 0.75 is considered 'inactive', while soils with activity above 1.25 are considered 'active'. Soils of high activity have a greater change in volume when the water content is changed (i.e., greater swelling when wetted and greater shrinkage when drying). Soils of high activity can therefore be particularly damaging to geotechnical works.

Al-Ani and Sarapää (2008) define 'clay minerals' as phyllosilicates and minerals that impart plasticity to clay and harden upon drying or firing. They occur mainly in shales, the most common sedimentary rock. In cool, dry, or temperate climates, clay minerals are stable and form an important soil component. Acting as 'chemical sponges', clay grains have unbalanced electrical charges, with some surfaces

positive and others negative, enabling adsorption of water molecules. Common clay minerals include kaolinite, smectite, illite, chlorite, vermiculite, and palygorskite, each with distinct structures and compositions. These properties underpin clay's unique behaviour in geotechnical engineering.

In geotechnical engineering, clay strength refers to a soil's ability to resist failure, including penetration and load-bearing capacity. Shear strength is a key component, measuring resistance to sliding or shearing failure. Hvorslev (1961) states that soil failure conditions can be expressed as a limiting shear stress or as a function of principal stresses. Shear strength, τ_f, is the shear stress in the failure plane at the point of failure. Resistance to shear failure is defined by drained shear strength (c' and ϕ') for long-term loading and undrained shear strength (s_u) for short-term loading. Drained shear strength, expressed in terms of effective stress, applies under conditions where pore water pressure change is negligible, representing long-term stability unaffected by transient pressures. Undrained shear strength, expressed in terms of total stress, is critical for short-term scenarios such as construction or rapid loading, where excess pore pressures cannot dissipate during that short time frame. It represents the maximum stress a soil can withstand before failure when pore water cannot escape. Understanding both drained and undrained behaviour is essential for safe and effective geotechnical design.

Historical advances in terms of clay strength

Skempton (1985a) divides the period 1700–1927 into four major phases of geotechnical study, each providing foundational insights into clay behaviour and contributing to the evolution of soil mechanics and strength theories:

1) The pre-Classical period (1700–1776) focused on natural slopes, soil unit weights, and semi-empirical earth pressure theories. De Belidor (1729) introduced a soil classification system based on unit weight, while early laboratory tests reported results on a 76 mm retaining wall with sand backfill. Lokkas *et al.*, (2021) state that the first, pre-classical period, was characterized from the studies, which were mainly concentrated on the natural slope of earth and the unit weights for the different kinds of soil, along with semiempirical theories referred to the pressure of earth.
2) The Classical soil mechanics Phase I period (1776–1856) saw major French contributions. Coulomb (1776) applied calculus principles to determine the true sliding surface behind retaining walls, using friction and cohesion laws for solids. Poncelet (1840) introduced the symbol ϕ for soil friction angle and developed the first ultimate bearing-capacity theory for shallow foundations. Collin (1846) detailed deep slips in clay slopes, cuttings, and embankments, theorising that failure occurs when mobilised cohesion exceeds existing cohesion. Rankine (1857) advanced earth pressure theory and equilibrium of earth masses, simplifying Coulomb's work and further progressing soil mechanics. These developments laid critical foundations for modern geotechnical engineering.
3) The Classical soil mechanics Phase II period (1856–1910) marked the start of experimental soil mechanics. Laboratory tests on sand became common, with the Darcy (1856) study on sand filter permeability being a landmark contribution. From these tests, Darcy introduced the coefficient of permeability (hydraulic conductivity), a parameter still widely used. Mohr (1882) advanced stress analysis through Mohr's circle, while Boussinesq (1885) developed the theory of stress distribution beneath loaded areas in a homogeneous, semi-infinite, elastic medium. Darwin (1911) conducted laboratory tests on overturning moments for hinged retaining walls with sand in loose and dense states. These pioneering studies established key principles of soil behaviour, forming the basis for modern geotechnical engineering.
4) The Modern soil mechanics period (1910–1927) saw a shift towards clay soils. Research established fundamental clay properties and parameters. Atterberg (1911) defined clay-size fractions as particles smaller than 2 μm and highlighted their role in soil plasticity. Fellenius (1918) developed stability analysis for saturated clay slopes under $\phi = 0$ conditions, assuming a circular sliding surface. These advances marked a turning point, laying the foundation for modern geotechnical engineering and the scientific understanding of clay behaviour.

The post-1927 period marked significant advances in geotechnical engineering, transitioning from empirical to analytical approaches (Das, 2013). Terzaghi's pioneering research on soil behaviour, clay settlement, and piping failure in sand beneath dams laid the foundation for modern geotechnical

analysis. Skempton (1948) further addressed the $\phi = 0$ concept for clays, while two further milestones between 1948 and 1960 were the Skempton (1954) A and B pore pressure parameters, enabling practical effective stress calculations, and the Bishop and Henkel (1957) influential book 'The Measurement of Soil Properties in the Triaxial Test'. Bishop *et al*., (1960) also provided early guidance on factors controlling the strength of partially saturated cohesive soils, paving the way for unsaturated soil mechanics. Subsequent research expanded understanding of unsaturated soil behaviour, including strength, compressibility, and implications for earth-supported and earth-retaining structures.

Peck (1985) emphasised that the Terzaghi (1925) 'Erdbaumechanik' and his leadership propelled soil mechanics into mainstream civil engineering. Much of modern soil mechanics was already established by 1926–1929. Regarding saturated clays, Peck noted the Terzaghi (1939) contributions to slope stability analysis and highlighted the Hvorslev (1937) work as a major advance. Collectively, these developments refined understanding of drained shear strength (effective stress) and undrained shear strength (total stress), forming the analytical basis for safe and efficient geotechnical design.

Clay strength formulae and empirical correlations

Early clay strength formulae, developed in the late 18th century, addressed drained shear strength only. Formulae for undrained strength emerged in the early 20th century, followed by empirical correlations based on Atterberg limits. These correlations remain practical tools for estimating clay strength and validating laboratory results. Selected literature on drained and undrained shear strength is discussed below.

Drained shear strength

Coulomb (1776) established that shear strength (τ) is depended on normal stress (σ) and friction, proposing equation [1], where ϕ is the angle of internal friction.

$$\tau = \sigma \tan(\phi) \quad [1]$$

Mohr (1882) introduced a graphical method (Mohr's Circle) to represent complex stress states (normal and shear stresses) on any plane. He combined Coulomb's equation with the concept of cohesion (c), a material's inherent stickiness, to create the combined Mohr-Coulomb equation [2].

$$\tau = c + \sigma \tan(\phi) \quad [2]$$

The Mohr-Coulomb failure criterion remains fundamental, relating shear strength to cohesion, normal stress, and friction angle. Primarily addressing drained shear strength, it underpins limit equilibrium methods and introduced the concepts of friction and cohesion in soil mechanics.

Gibson (1953) describes drained shear tests carried out on undisturbed and remoulded clay specimens to examine the validity of the Coulomb-Hvorslev failure criterion. The 'true' cohesion and 'true' angle of internal friction parameters are evaluated from the results of these drained tests. Hvorslev (1937) shows that the strength (τ_f) could be expressed by equation [3], where the 'true' cohesion (c_e) and 'true' angle of internal friction (ϕ_e), were parameters characterising the soil.

$$\tau_f = c_e + \sigma'_n \tan \phi_e \quad [3]$$

He defined 'true' cohesion' (c_e) as the part of the shear strength of a soil that is independent of the applied normal effective stress and is instead a direct function of the void ratio (or water content) at the time of failure. He furthermore defined the 'true' angle of internal friction (ϕ_e or ϕ_{true}) as a fundamental shear strength parameter for saturated clays that represents the frictional resistance component acting on a failure plane. The 'true' angle of friction is a fundamental property that remains nearly constant regardless of the over consolidation ratio (OCR) or void ratio at failure. For drained tests on normally consolidated clay, the strength (τ_f) could be expressed by equation [4], where c_r and ϕ_r implies the residual cohesion and residual angle of internal friction respectively.

$$\tau_f = c_r + \sigma'_n \tan \phi_r \quad [4]$$

Skempton (1964) mainly focuses on drained shear strength, specifically the concept of residual shear strength. He states that long-term stability in cohesive soils is governed by drained conditions and introduces the use of residual shear strength for pre-existing failure surfaces. He indicates that the shear strength (s) of a clay may be represented by the Coulomb-Terzaghi equation [5], where c' is the 'cohesion intercept' and ϕ' is the 'angle of shearing resistance', both parameters being expressed in terms of the

$$s = c' + (\sigma - u) \tan \phi' \quad [5]$$

effective stress $\sigma' = (\sigma - u)$ acting normal to the slip surface. As the clay is strained, so it builds up an increasing resistance. In terms of the shear strength characteristics of an over-consolidated clay, the peak strengths can therefore be expressed by equation [6] and the residual strengths by [7]. The available test results showed almost invariably that c_r' is very small, and probably not significantly different from

$$s_f = c' + \sigma' \tan \phi' \quad [6]$$

$$s_r = c'_r + \sigma' \tan \phi'_r \quad [7]$$

zero. Thus, equation [8] reflects the residual strength. I.e., moving from the peak to the residual, the cohesion intercept c' disappears completely. During the same process the angle of shearing resistance also decreases, in some clays by only 1° or 2°, but in others by as much as 10°.

$$s_r = \sigma' \tan \phi'_r \quad [8]$$

Skempton (1985b) examined drained shear strength, focusing on the residual strength of clays in landslides. He highlighted its importance for long-term slope stability and its link to critical state strength. For slopes with pre-existing shear surfaces, residual drained strength should be used in stability analyses. In over-consolidated clays, post-peak strength reduction occurs in two stages: 1) at small displacements, strength falls to the 'fully softened' or 'critical state' value due to increased water content (dilatancy), and 2) at large displacements, strength drops to the residual value as clay minerals reorient parallel to the shear direction. In normally consolidated clays, reduction is solely due to particle reorientation. Measurements on natural shear surfaces align closely with values from back-analysed reactivated landslides.

Mesri and Abdel-Ghaffar (1993) examined the role of the cohesion intercept in slope stability analysis within the effective stress framework, addressing drained shear strength parameters such as effective cohesion (c'). They emphasised its influence on slip surface location and factor of safety. The cohesion intercept arises from a linear approximation of a nonlinear relationship between shear strength and effective normal stress. According to Mesri and Abdel-Ghaffar (1993), the shear strength mobilised during global instability is typically less than the peak strength measured in laboratory tests, varying based on clay type. They suggest that for stiff clays, mobilised strength can range from residual to peak due to factors like softening and progressive failure, while for soft clays, it ranges from large-strain strength up to peak, reflecting a less drastic reduction from peak. While peak strength governs initial slip surface formation, mobilised strength—equal to or less than peak—is used to calculate safety factors. Effective stress-based stability analyses apply a reduction factor to peak strength to estimate mobilised strength for first-time slides. For over 60 failures in soft and stiff clays, mobilised cohesion values (c'_{mob}) ranged from 0–26 kPa, compared to 1–150 kPa for peak c', highlighting the variability and importance of accurate strength characterisation.

Atkinson (2008) discusses the rules of thumb for both drained and undrained shear strength scenarios. He covers specific correlations and rules related to 1) drained shear strength, 2) undrained shear strength (s_u), and 3) stiffness and strength. He states that if soil is continuously distorted it must reach a state in which stress and water content no longer change. This is the critical state and the parameters ϕ'_c, C_c and e_Γ (as defined by Atkinson (2007)) which define the critical state are material parameters. He furthermore refers to the relationship between ϕ'_c and PI given by Wood (1990). Wood (1990) states that data of angle of friction (plotted as $\sin \phi'$) and PI have been assembled by Mitchell (1976). Mitchell observed that the peak value of ϕ' decreases with increasing PI and activity and can be described by equation [9].

$$\text{Sin } \phi' = 0.35 - 0.1 \ln \text{PI} \quad [9]$$

Knappett and Craig (2012) refer to data of the critical state angle of shearing resistance (ϕ'_{cv}) for 32 undisturbed and 32 remoulded fine-grained soils from triaxial testing collected by Kenney (1959), Parry (1960) and Zhu and Yin (2000). The data are correlated against PI which is also independent of the current soil state (defined by the current water content w). A correlation line, representing a best fit to the undisturbed data, suggests that ϕ'_{cv} reduces as the PI increases. Refer equation [10].

$$\phi'_{cv} = 57\ (I_P)^{-0.21} \quad [10]$$

Residual friction angle (ϕ'_r) - The residual strength of a soil reduces with an increasing proportion of platy particles (e.g., clays) and is therefore correlated with CF and PI. Data of ϕ'_r determined from ring shear (RS) tests was plotted against I_P for 89 clays and tills and 23 shales, collected by Lupini *et al*., (1981), Mesri and Cepeda-Diaz (1986) and Tiwari and Marui (2005). The data appears to follow a power law as per equation [11], where ϕ'_r is in degrees.

$$\phi'_r = 93\ (I_P)^{-0.56} \quad [11]$$

Mayne (2013) states that statistics confirm that there is absolutely no correlation between the ϕ and PI parameters. Several reasons negate the well-worn-out relationship between ϕ' and PI including fabric, structure, and the presence of diatoms and forams in the soil mineralogy (Locat *et al*., 2003). An improvement is to assume ϕ' = 28.6° (mean value) with a standard deviation (SD) = 5.1°.

Duncan *et al*., (2014) discuss the drained shear strength scenario which is a fundamental concept in soil mechanics for slope stability analysis. They state: 1) the shear strength of clays in terms of effective stress can be expressed by the Mohr–Coulomb strength criterion, 2) the strengths that can be mobilised in stiff fissured clays in the field are less than the strength of the same material measured in the laboratory (undisturbed test specimens), 3) the normally-consolidated peak strength, also called the fully softened strength (FSS), corresponds to strengths back calculated from first-time slides, 4) once a failure has occurred and a continuous slickensided failure surface has developed, only the residual shear strength is available to resist sliding, 5) tests to measure fully softened and residual drained strengths of stiff clays can be performed on remoulded test specimens, and 6) RS tests are preferable for measuring residual shear strengths, because unlimited shear displacement is possible through continuous rotation.

Stark and Fernandez (2018) examined FSS, a drained shear strength parameter used for slope stability analysis in stiff fine-grained soils. Using the torsional RS apparatus, they developed correlations to estimate FSS from soil index properties. Key findings include: 1) FSS applies to shallow cut slopes and compacted embankments, representing strength after over-consolidation, compaction, and weathering effects diminish, 2) first-time slides in natural slopes and embankments involve shear behaviour closer to consolidated-drained (CD) triaxial compression than RS or direct shear (DS) tests, 3) slope-specific LL and CF values should be used for FSS estimation, and 4) Castellanos (2014) and Castellanos *et al*., (2016) correlations are unreliable and should not be applied.

Stark and Fernandez (2020) provide updated correlations and recommendations for estimating drained shear strength. Recent empirical efforts to estimate FSS from soil index properties include Eid and Rabie (2017), defining a general linear relationship for PI values between 3 and 247. Five main correlations exist, including: 1) Mesri and Shahien (2003), 2) Wright (2005), 3) Tiwari and Ajmera (2011), 4) Gamez and Stark (2014), and 5) Stark and Fernandez (2020). Except for Tiwari and Ajmera (2011), all conclude that the FSS envelope is stress-dependent, first noted by Stark and Eid (1997). Stark and Fernandez recommended using at least two RS-based correlations—such as Stark and Eid (1997), Mesri and Shahien (2003), Wright (2005), Eid and Rabie (2017), or their own—to verify laboratory data. Tiwari and Ajmera (2011) provide valuable insight into mineralogical effects on shear strength; however, without mineralogy data, their correlation produces conservative, non-stress-dependent envelopes. These findings reinforce the need for careful selection and validation of FSS correlations in geotechnical design.

Undrained shear strength

Skempton and Golder (1948) address the '$\phi = 0$ analysis' for saturated clays under undrained conditions, where water content remains constant, including relevant case studies. This approach treats soil as purely cohesive, with zero friction angle, and evaluates stability using undrained shear strength (c_u or s_u) and was originally proposed by Fellenius (1927).

Skempton (1954) introduced pore-pressure coefficients (A and B parameters) to predict changes in pore pressure under undrained conditions, a key factor in analysing undrained shear strength, particularly in clays. This work is fundamental for understanding soil behaviour when water cannot drain, critical for stability in earth dams and similar structures.

Skempton (1957) examined undrained shear strength during the Hong Kong Airport geotechnical investigation, focusing on vane shear tests (VST) for soft clays. Initial laboratory samples indicated very low strengths, prompting VST to confirm values. He observed that in normally consolidated clays, shear strength (c) at any depth is proportional to effective overburden pressure (p'), with the ratio c_u/p' correlating closely with PI. Equation [12] expresses this relationship, providing a practical method for checking strength in normally consolidated clays and validating laboratory results.

$$c_u / p' = 0.11 + 0.0037\ (PI) \qquad [12]$$

Kenney (1959) states that the ratio of the undrained shear strength of a clay and the vertical effective stress under which a soil was consolidated in the field, was a constant. This ratio has since been denoted by c_u / p'.

Wroth (1984) explored interpreted in-situ tests, such as the pressuremeter test, for determining undrained shear strength of clays using critical state soil mechanics. He stressed the importance of selecting appropriate properties for correlations and proposed the undrained strength ratio (s_u / σ_{v0}') as a function of friction angle and OCR. The in-situ vertical effective stress is denoted by σ'_{v0}. In his Rankine Lecture, Wroth compared results from various tests by expressing them in terms of this ratio and applied the Matsuoka and Nakai (1982) failure criterion. He recommended adopting equation [13] as a practical engineering compromise, defining s_u / σ'_{v0} as the undrained strength ratio.

$$s_u / \sigma'_{v0} = f\ (\phi, OCR) \qquad [13]$$

Ladd (1991) emphasised that undrained shear strength analysis (USA) is the most realistic approach for staged construction on soft cohesive soils, rather than traditional drained analysis. USA evaluates strength variations during construction, using field vane test (FVT) data for preliminary design (±25% with the Bjerrum (1972) correction). Data should reflect stress history and be assessed via log-log plots of undrained strength ratio versus OCR, applying equation [14]. The effective overburden stress is denoted by $\sigma'_{v0.}$ S_{fv} denotes the undrained shear strength ratio measured from a field vane (FV) test, and m denotes the strength rebound exponent. Since parameters such as S_{fv} and m vary with soil type, accurate estimates of σ'_p (preconsolidation pressure) require site-specific correlations, ensuring reliable stability predictions for staged construction projects.

$$s_u\ (FVT)/\sigma'_{v0} = S_{fv}\ (OCR)^m \qquad [14]$$

Kayabali and Tufenkci (2010) investigated undrained shear strength (s_u) of remoulded soils at the PL and LL, using reverse extrusion tests and proposing a prediction method based solely on consistency limits. Undrained strength of remoulded soils is critical in geotechnical engineering, including offshore investigations, glacial soils, and pile design. Casagrande (1939) reported an average shear strength of 2.65 kN/m² at the LL, noting variability due to test apparatus. Sharma and Bora (2003) summarised key literature and cited Skempton and Northey (1953) to conclude that shear strength at the PL is approximately 100 times that at the LL, highlighting the significance of index properties in strength estimation.

Knappett and Craig (2012) address undrained shear strength (c_u) and sensitivity (S_t). S_t is a measure of the loss in strength of a soil (specifically clays) because of disturbance or remoulding. It describes how brittle a clay is and how much of its structure is destroyed when deformed, such as during construction activities like pile driving or excavation. The undrained strength of a fine-grained soil is not an intrinsic material property but is dependent on the state of the soil (as defined by w, the water content) and the stress level. The undrained shear strength should therefore be correlated to a state-dependent index parameter, namely liquid index (IL). Sensitivity is also correlated to IL as indicated by equation [15].

$$S_t \approx 100^{(0.43\,IL)} \quad [15]$$

Mayne (2013) focuses on both drained and undrained shear strength by discussing an integrated approach to site characterisation that includes in-situ, laboratory, and geophysical testing. Unfortunately, the geotechnical community tends to rely on several old empirical correlations that were derived from small and early data sets that are not at all applicable to the situations for which they are now applied. He indicates that equations [16] and [17] are used in estimating the undrained shear strength (S) of soft normally consolidated (NC) clays.

$$S = s_u/\sigma'_{voNC} = 0.11 + 0.0037\ PI\ (\%) \quad [16]$$

$$S = s_u/\sigma'_{voNC} = \phi'/100 \quad [17]$$

These two equations are incompatible with one another. The first was developed by Skempton (1957) based on raw (uncorrected) FV shear data on 19 soft clays, while the second represents an approximation to laboratory triaxial compression tests based on critical-state soil mechanics, Wroth (1984). These two modes are completely different from one another, so an inevitable inconsistency will be found should the geotechnical engineer go forth and use them both. Note: the earlier c/p' ratio has been replaced by equation [18] (Ladd, 1991).

$$S = (s_u\ /\ \sigma'_{vo})_{NC} \quad [18]$$

Duncan *et al*., (2014) discuss undrained shear strength which is a fundamental concept in soil mechanics for slope stability analysis. They state: 1) the shear strength of clays in terms of total stress can be expressed as $s = c + \sigma \tan \phi$, 2) for saturated clays, ϕ equals zero, 3) samples used to measure undrained strengths of normally-consolidated and moderately over-consolidated clay should be as nearly undisturbed as possible, and 4) undrained strengths of compacted clays vary with compaction water content and density and can be measured using unconsolidated undrained (UU) triaxial tests performed on specimens at their as-compacted water contents and densities.

Mohammed (2024) investigates undrained shear strength (s_u) in high-plasticity clays (CH), exploring its correlation with index properties such as LL, PL, PI, moisture content (MC), and dry density (γ_d). CH soils exhibit unique behaviour, making accurate prediction of s_u and compression index (C_c) essential for slope stability and foundation design. S_u is not a fundamental property but depends on soil condition and composition. Over 1000 data points from literature were analysed, and nonlinear multiple regression models were developed (see equation [19]) to estimate s_u using easily measurable properties. Findings show strong correlations between s_u, C_c, and index properties, enabling practical prediction without extensive laboratory testing. This approach supports cost-effective geotechnical design for CH soils, particularly in applications such as embankments, foundations, and slope stability assessments.

$$s_u = 26.3 * (LL)^{0.5} * (PI)^{-0.3} * (MC)^{-0.2} * (\gamma_d)^{1.9} \quad [19]$$

Over- or underestimation of clay strength

The literature review indicates that empirical correlations for clay strength often over- or underestimate actual conditions due to variations in soil structure, mineralogy, and stress history. Common correlations, such as those based on PI or LL, frequently fail to capture the nuances of heavily OC or sensitive clays. Notable gaps are summarised below.

Drained strength correlations

1) Stark and Eid (1994) residual strength correlation: While widely used, these can under- or overestimate residual friction angles if the soil possesses significant diagenetic bonding, often found in heavily OC clays/shales. Such bonding survives standard, remoulded, or slow-rate testing, leading to incorrect estimation of the fully softened or residual state.
2) ϕ' versus PI correlation: Generally, as clay mineral content increases, the drained friction angle decreases. However, direct correlations often show significant scatter, sometimes overestimating the available frictional resistance in soils with high percentages of active, platy clay minerals.
3) Linear Mohr-Coulomb at high pressure: Assuming a linear, constant ϕ' (linear envelope) for drained, high-pressure, or highly OC clays, typically overestimate the shear strength at lower pressures (below the pre-consolidation pressure).

Undrained strength correlations

1) Unconfined compression strength ($q_u/2$): Often underestimates in situ undrained strength in saturated clays. This is primarily due to sample disturbance, fissures/discontinuities, and the presence of sand partings, which reduce the measured strength in laboratory tests.
2) FVT (S_u): While considered reliable, standard FV tests can overestimate the undrained strength in highly sensitive or quick clays if not corrected for plasticity.
3) S_u versus PI correlations (e.g., Henkel and Skempton (1955)): Often overestimate S_u in low-plasticity clays, and often underestimate S_u in high-plasticity clays.
4) SPT N-value correlation ($S_u \approx f_1 \cdot N$): Studies have shown that standard correlations (e.g., Stroud (1974)) can be notably unconservative (overestimate strength) when applied to specific regional clays, such as Turkish clays, and are generally less reliable than site-specific correlations. Note that the SPT N-value is the number of hammer blows (63.5 kg hammer falling 760 mm) required to drive a standard split-spoon sampler 300 mm into soil.
5) CPTu cone factor (N_k): The assumption of a unique N_k factor can cause significant variability. Relying on generalised N_k values frequently leads to inaccurate estimates, as N_k is heavily dependent on soil structure, which varies site-to-site. N_k (or often N_{kt}) represents an empirical cone factor or cone bearing factor used to estimate the undrained shear strength (s_u or c_u) of cohesive soils (clays) from Cone Penetration Test data.

CONCLUSIONS

The literature review confirms that understanding clay strength has evolved over three centuries, progressing from empirical observations to rigorous scientific analysis. While empirical correlations offer a quick, cost-effective means of estimating shear strength parameters, they must be applied cautiously and validated through site-specific investigations and sound engineering judgement. Many correlations are based on limited datasets or assume linear relationships, despite soil properties often being non-linear. Geological variability and spatial heterogeneity further limit their reliability, and some correlations have been shown to significantly over- or underestimate strength. Common causes for errors include sample disturbance, anisotropy and rate effects, diagenetic bonding, and sensitivity. Authors differ on which correlations are dependable, with several recommending that certain methods should not be used. Designs relying solely on these correlations risk neglecting geological weaknesses, particularly for complex loading conditions or less common clay types.

To address these limitations, a reliability assessment of key empirical correlations estimating clay shear strength from index properties such as Atterberg limits and particle size distribution is recommended. These correlations should be evaluated against documented failure case studies of TSFs and embankments founded on clay soils to determine predictive accuracy. Back-analyses for drained and undrained conditions should be included, considering both normally- and over-consolidated clays to capture variations in consolidation state and index properties. This comparative approach will identify correlations that provide consistent and conservative estimates and highlight those prone to error. The outcome will guide appropriate use of empirical methods where laboratory data is limited, contributing to safer, more reliable TSF design and improved long-term performance.

REFERENCES

Al-Ani, T., & Sarapää, O. (2008). *Clay and clay mineralogy* (M19/3232/2008/41). (Physical-chemical properties and industrial uses, Issue.

Atkinson, J. H. (2007). Peak strength of overconsolidated clays. *Géotechnique*, *57*(2), 127–135. https://doi.org/10.1680/geot.2007.57.2.127

Atkinson, J. H. (2008). Rules of thumb in geotechnical engineering. *Soil-Structure Interaction*, *1*, 9.

Atterberg, A. M. (1911). Uber die physikalische Bodenuntersuchung, und über die Plastizität de Tone. *International Mitteilungen für Bodenkunde*, *1*, 10–43.

Bishop, A. W., Alpan, I., Blight, G., & Donald, I. (1960). Factors controlling the strength of partly saturated cohesive soils.

Bishop, A. W., & Henkel, D. J. (1957). *The measurement of soil properties in the triaxial test*. E. Arnold.

Bjerrum, L. (1972). Embankments on soft ground, State of the Art Report. Proc. Spec. Conf. on Performance of Earth and Earth-Supported Structures, Purdue Univ., ASCE.

Bjerrum, L., & Simons, N. E. (1960). Comparison of shear strength characteristics of normally consolidated clays. *Norwegian Geotechnical Institute. Publication*, *35*, 13–22.

Boussinesq, J. V. (1885). *Application dès potentiels a l'étude de l'équilibre et du mouvement des solides élastiques*. Gauthier-Villars. https://doi.org/OL20553862M

Bowker, L. N., & Chambers, D. M. (2015). The risk, public liability, & economics of tailings storage facility failures. *Earthwork Act*, *24*, 1–56.

Carter, M., & Bentley, S. P. (2016). *Soil properties and their correlations*. John Wiley & Sons. https://doi.org/10.1002/9781119130888

Casagrande, A. (1936). *The determination of the pre-consolidation load and its practical significance* International Conference on SMFE, Cambridge, MA.

Casagrande, A. (1939). Soil Mechanics in Action. *Journal of the Boston Society of Civil Engineers*, *26*(3), 227–256.

Castellanos, B. (2014). *Use and measurement of fully softened shear strength.*

Castellanos, B., Brandon, T., & VandenBerge, D. (2016). Correlations for fully softened shear strength parameters. *Geotechnical Testing Journal*, *39*(4), 568–581. https://doi.org/10.1520/GTJ20150184

Chronology of major tailings dam failures. (2025). https://www.wise-uranium.org

CIGB, I. (2025). Tailings Dam Safety/Sécurité des Barrages de Stériles. https://doi.org/10.1201/9781003544067

Collin, A. (1846). *Recherches experimentales sur les glissements spontanes des terrains argileux, accompagnees de considerations sur quelques principes de la mecanique terrestre par Alexandre Collin*. Carilian-Goeury.

Coulomb, C. A. (1776). ESSAI Sur une application des regles de Maximis & Minimis a quelques Problemes de Statique, relatifs a lArchitecture. *7*, 343–387.

Darcy, H. P. G. (1856). *Les fontaines publiques de la ville de Dijon: Exposition et application des principes à suivre et des formules à employer dans les questions de distribution d'eau: Ouvrage terminé par un appendice relatif aux fournitures d'eau de plusieurs villes, au filtrage des eaux et à la fabrication des tuyaux de fonte, de plomb, de tôle et de bitume* (Vol. 2). Victor Dalmont, éditeur.

Darwin, G. H. (1911). *Periodic orbits and miscellaneous papers. 1911* (Vol. 4). University Press. https://doi.org/10.1017/CBO9780511703508

Das, B. M. (2013). *Principles of Geotechnical Engineering* (4th Edition ed.). Cengage.

De Belidor, B. F. (1729). *La Science des Ingenieurs dans la Conduite des Travaux de Fortification et D'Architecture Civil*. Jombert.

Duncan, J. M., Wright, S. G., & Brandon, T. L. (2014). *Soil strength and slope stability*. John Wiley & Sons.

Eid, H. T., & Rabie, K. H. (2017). Fully softened shear strength for soil slope stability analyses. *International Journal of Geomechanics*, *17*(1), 04016023. https://doi.org/10.1061/(ASCE)GM.1943-5622.0001038

Fellenius, W. (1918). Kaj-och jordraset i Goteborg. *Teknisk Tidsskrift*, *48*, 17–19.

Fellenius, W. (1927). *Jordstatiska berakningar, med friktion och kohesion (adhesion) och under antagande av cirkularcylindriska glidytor*.

Gamez, J. A., & Stark, T. D. (2014). Fully softened shear strength at low stresses for levee and embankment design. *Journal of Geotechnical and Geoenvironmental Engineering*, *140*(9), 06014010. https://doi.org/10.1061/(ASCE)GT.1943-5606.0001151

Gibson, R. E. (1953). Experimental determination of the true cohesion and true angle of internal friction in clays.

Global Tailings Portal. (2025). https://tailing.grida.no

Heckroodt, R. (1991). Clay and clay materials in South Africa. *Journal of the Southern African Institute of Mining and Metallurgy*, *91*(10), 343–363. https://doi.org/10.10520/AJA0038223X_2070

Henkel, D., & Skempton, A. (1955). A landslide at Jackfield, Shropshire, in a heavily over-consolidated clay. *Géotechnique*, *5*(2), 131–137. https://doi.org/10.1680/geot.1955.5.2.131

Hogentogler, C. A. (1937). Engineering Properties of Soil.

Hvorslev, M. J. (1937). *Physical Properties of Remolded Cohesive Soils (Über die Festigkeitseigenschaften gestörter bindiger Böden)* (Publication Number Ingeniørvidenskabelige Skrifter A-Nr. 45).

Hvorslev, M. J. (1961). *Physical components of the shear strength of saturated clays* (1-361).

Ishibashi, I., & Hazarika, H. (2015). *Soil mechanics fundamentals and applications*. CRC Press. https://doi.org/10.1201/b18236

Jones, G. A., & Davies, P. (1985). Soft clays: problem soils in South Africa-state of the art. *Civil Engineering*, *27*(7), 355–365.

Kayabali, K., & Tufenkci, O. O. (2010). Shear strength of remolded soils at consistency limits. *Canadian Geotechnical Journal*, *47*(3), 259–266. https://doi.org/10.1139/T09-095

Kenney, T. C. (1959). Discussion of "geotechnical properties of glacial Lake clays". *Journal of the Soil Mechanics and Foundations Division*, *85*(3), 67–79.

Knappett, J. A., & Craig, R. F. (2012). *Craig's soil mechanics* (8th ed.). Spon Press. https://doi.org/10.1201/b12841

Kulhawy, F. H., & Mayne, P. W. (1990). *Manual on estimating soil properties for foundation design*.

Ladd, C. C. (1991). Stability Evaluation during Staged Construction. *Journal of Geotechnical Engineering*, *117*(4), 540–615. https://doi.org/10.1061/(asce)0733-9410(1991)117:4(540)

Locat, J., Tanaka, H., Tan, T., Dasari, G., & Lee, H. (2003). Natural soils: geotechnical behavior and geological knowledge. 3–28.

Lokkas, P., Chouliaras, I., Chrisanidis, T., Christodoulou, D., Papadimitriou, E., & Paschalis, E. (2021). Historical background and evolution of Soil Mechanics. *Wseas Transactions On Advances In Engineering Education*, *18*, 96–113. https://doi.org/10.37394/232010.2021.18.10

Lupini, J., Skinner, A., & Vaughan, P. (1981). The drained residual strength of cohesive soils. *Géotechnique*, *31*(2), 181–213. https://doi.org/10.1680/geot.1981.31.2.181

Lyu, Z., Chai, J., Xu, Z., Qin, Y., & Cao, J. (2019). A comprehensive review on reasons for tailings dam failures based on case history. *Advances in Civil Engineering*, *2019*(1), 4159306. https://doi.org/10.1155/2019/4159306

Matsuoka, H., & Nakai, T. (1982). A new failure criterion for soils in three-dimensional stresses.

Mayne, P. W. (2013). *Updating our geotechnical curricula via a balanced approach of in-situ, laboratory, and geophysical testing of soil* 61st Annual Geotechnical Conference.

Mesri, G., & Abdel-Ghaffar, M. E. M. (1993). Cohesion intercept in effective stress-stability analysis. *Journal of Geotechnical Engineering*, *119*(8), 1229–1249. https://doi.org/10.1061/(ASCE)0733-9410(1993)119:8(1229)

Mesri, G., & Cepeda-Diaz, A. (1986). Residual shear strength of clays and shales. *Géotechnique*, *36*(2), 269–274. https://doi.org/10.1680/geot.1986.36.2.269

Mesri, G., & Shahien, M. (2003). Residual Shear Strength Mobilized in First-Time Slope Failures. *Journal of Geotechnical and Geoenvironmental Engineering*, *129*(1), 12–31. https://doi.org/10.1061/(asce)1090-0241(2003)129:1(12)

Mitchell, J. (1976). Fabric, structure, and proterty relationships. *Fundamentals of soil behavior*, 222–252.

Mohammed, A. (2024). Property correlations and statistical variations in the geotechnical properties of (CH) clay soils. *Geotechnical and Geological Engineering*, *42*(1), 843–858. https://doi.org/10.1007/s10706-017-0418-2

Mohr, C. O. (1882). Über die Darstellung des Spannungszustandes und des Deformationszustandes eines Körperelementes und über die Anwendung derselben in der Festigkeitslehre. *Der Civilingenieur*, *28*(2), 113–156.

Parry, R. H. G. (1960). Triaxial compression and extension tests on remoulded saturated clay. *Géotechnique*, *10*(4), 166–180. https://doi.org/10.1680/geot.1960.10.4.166

Peck, R. B. (1985). The last sixty years. *11th International conferene on soil mechanics and foundation engineering*, 123–133.

Poncelet, J.-V. (1840). *Mémoire sur la stabilité des revêtements et de leurs fondations*. Imprimerie et Librairie de Bachelier.

Rankine, W. J. M. (1857). On the stability of loose earth. *Philosophical transactions of the Royal Society of London*(147), 9–27. https://doi.org/10.1098/rstl.1857.0003

Sharma, B., & Bora, P. K. (2003). Plastic limit, liquid limit and undrained shear strength of soil—reappraisal. *Journal of Geotechnical and Geoenvironmental Engineering*, *129*(8), 774–777. https://doi.org/10.1061/(ASCE)1090-0241(2003)129:8(774)

Skempton, A. W. (1948). The ϕ=0 Analysis of Stability and Its Theoretical Basis. Proceedings.

Skempton, A. W. (1953). The colloidal activity of clays. *Selected papers on soil mechanics*, *1*, 57–61.

Skempton, A. W. (1954). The pore-pressure coefficients A and B. *Géotechnique*, *4*(4), 143–147. https://doi.org/10.1680/GEOT.1954.4.4.143

Skempton, A. W. (1957). Discussion on the Planning and Design of the new Hong Kong Airport. In.

Skempton, A. W. (1964). Long-Term Stability of Clay Slopes. *Géotechnique*, *14*(2), 77–102. https://doi.org/10.1680/geot.1964.14.2.77

Skempton, A. W. (1985a). *A History of Soil Properties, 1717 to 1927*. North Carolina State University, Department of Civil Engineering.

Skempton, A. W. (1985b). Residual strength of clays in landslides, folded strata and the laboratory. *Géotechnique*, *35*(1), 3–18. https://doi.org/10.1680/geot.1985.35.1.3

Skempton, A. W., & Golder, H. Q. (1948). Practical examples of the ϕ=0 analysis of stability of clays. Proc. 2nd Intern. Conf. on Soil Mechanics and Foundation Engineering.

Skempton, A. W., & Northey, R. D. (1953). The sensitivity of clays. *Géotechnique*, *3*(1), 30–53. https://doi.org/10.1680/GEOT.1952.3.1.30

Sorensen, K. K., & Okkels, N. (2013). *Correlation between drained shear strength and plasticity index of undisturbed overconsolidated clays* 18th International Conference on Soil Mechanics and Geotechnical Engineering, Paris.

Stark, T. D., & Eid, H. T. (1994). Drained residual strength of cohesive soils. *Journal of Geotechnical Engineering*, *120*(5), 856–871. https://doi.org/10.1061/(ASCE)0733-9410(1994)120:5(856)

Stark, T. D., & Eid, H. T. (1997). Slope stability analyses in stiff fissured clays. *Journal of Geotechnical and Geoenvironmental Engineering*, *123*(4), 335–343. https://doi.org/10.1061/(ASCE)1090-0241(1997)123:4(335)

Stark, T. D., & Fernandez, R. (2018). Fully Softened Shear Strength Measurement and Empirical Correlations. https://doi.org/10.1520/GTJ20190124

Stark, T. D., & Fernandez, R. (2020). Fully Softened Shear Strength Measurement and Correlations. *Geotechnical Testing Journal*, *43*(5). https://doi.org/10.1520/gtj20190124

Stroud, M. (1974). The standard penetration test in insensitive clays and soft rocks proceedings of the European symposium on penetration testing. *Stockholm, June*, 5–7.

Terzaghi, K. (1925). Erdbaumechanik auf bodemphysikalischer Grundlage.

Terzaghi, K. (1939). 45th James Forest Lecture, 1939. Soil Mechanics - A New Chapter in Engineering Science. *Journal of the Institution of Civil Engineers*, *12*(7), 106–142. https://doi.org/10.1680/ijoti.1939.14534

Tiwari, B., & Ajmera, B. (2011). A new correlation relating the shear strength of reconstituted soil to the proportions of clay minerals and plasticity characteristics. *Applied Clay Science*, *53*(1), 48–57. https://doi.org/10.1016/j.clay.2011.04.021

Tiwari, B., & Marui, H. (2005). A new method for the correlation of residual shear strength of the soil with mineralogical composition. *Journal of Geotechnical and Geoenvironmental Engineering*, *131*(9), 1139–1150. https://doi.org/10.1061/(ASCE)1090-0241(2005)131:9(1139)

Ural, N. (2018). The importance of clay in geotechnical engineering. In: IntechOpen London, UK.

Wood, D. M. (1990). *Soil behaviour and critical state soil mechanics*. Cambridge university press.

Wright, S. (2005). *Evaluation of soil shear strengths for slope and retaining wall stability analyses with emphasis on high plasticity clays.*

Wroth, C. P. (1984). The interpretation of in situ soil tests. *Géotechnique*, *34*(4), 449–489. https://doi.org/10.1680/geot.1984.34.4.449

Zhu, J.-G., & Yin, J.-H. (2000). Strain-rate-dependent stress-strain behavior of overconsolidated Hong Kong marine clay. *Canadian Geotechnical Journal*, *37*(6), 1272–1282. https://doi.org/10.1139/t00-054



Alwyn Smith

Stellenbosch University (SU)

Affiliations - Member, South African Institution of Civil Engineering (SAICE) and Engineering Council of South Africa (ECSA).

Employment - 1994 – 2000 (LTA Construction Limited, Civil and Earthworks Division), 2000 – 2025 (SRK Consulting (Pty) Ltd., Environmental Geotechnics Department), 2025 – present (fulltime research student at SU).

Specialisation - Geotechnical and pavement engineering.

Expertise - Detailed design and monitoring of tailings storage facilities (TSFs), return water dams (RWDs), and associated infrastructure. Dam safety evaluations (DSEs). Soil characterisation. Geotechnical investigations. Slope stability assessments. Risk assessments. Compilation of design reports, operations, maintenance and surveillance manuals, and continuation reports. Preparation of tender documentation and drawings. Tender adjudication, and project management.

Publications – 'South African Road Network Classification Based on the Traffic Loading' (2001), 'An Evaluation of the Adequacy of the Most Commonly used Pro forma Contracts within the South African Mining Construction Industry' (2007), and 'Platinum Tailings – Field and Laboratory Investigation to Evaluate Geotechnical Behaviour' (2018).

Geochemical characterisation of re-mined copper tailings in the Democratic Republic of Congo – best practices that can be adopted in South Africa

M.G. Dube, S. Hareeparsad

WSP Africa Pty Ltd., South Africa

As the demand for minerals increases and technology advances, the remining of waste from historical facilities has become a feasible option. This was exemplified by a specific copper mine in the Democratic Republic of Congo, which sought to enhance metallurgical recoveries to ~95%, thus significantly lowering the residual copper content in the tailings. This remining project will introduce additional water into the tailings storage facility (TSF) through hydro-mining operations. The remining process will also produce secondary tailings (finer) that are representative of future tailings to be generated at the mine, which will be disposed of in the TSF. This paper presents the findings of a comprehensive geochemical assessment, incorporating static, kinetic, and ecotoxicological testing over a 21-week period on metallurgical tailings samples. The integrated approach enabled a robust risk evaluation and provided a practical framework for similar projects in South Africa. Results indicated stable pH and declining sulfate and total dissolved solids concentrations, suggesting a low potential for acid rock drainage under laboratory conditions. However, Toxicity Characteristic Leaching Procedure, Synthetic Precipitation Leaching Procedure, and Australian Standard Leaching Procedure results classified the tailings as leachable mine waste, implying potential metal mobility. Ecotoxicological tests revealed high acute toxicity (Class IV) to aquatic organisms, indicating that undiluted leachate may adversely affect sensitive species. In the absence of geochemical modelling, drainage from the remined tailings should be treated before discharge, using passive or active systems to reduce electrical conductivity and remove elevated iron and copper. These results highlight the importance of early geochemical screening and toxicity assessment in remining projects, particularly when legacy tailings are reused or reprocessed.

The study contributes practical insights into the environmental risks and mitigation requirements associated with re-mined copper tailings and offers a transferable approach for improving environmental outcomes at similar operations in South Africa.

Keywords: Copper mine, acid rock drainage, metal leaching, environmental risks, remining, Democratic Republic of Congo, ecotoxicological tests, static and kinetic tests

INTRODUCTION

The global drive for sustainable development and the rising demand for minerals has stimulated innovation in the mining industry, including the remining of historical tailings. Many legacy facilities, developed with historically less advanced technology, contain residual metal values that remain economically recoverable. Advances in metallurgical processing now enable the extraction of these metals, offering dual benefits: enhanced resource recovery and the reduction of long-term environmental liabilities associated with waste storage facilities.

A notable example is a copper mine in the Democratic Republic of Congo (DRC) that has implemented a remining project to reprocess historical tailings and achieve recoveries of approximately 95%. While this initiative significantly reduces residual copper content, it also introduces environmental complexities.

The remining project evaluated in this study involves the hydraulic re-mobilisation (hydro-mining) of historical copper tailings, whereby pressurised water is used to excavate and slurry previously deposited material for reprocessing. This approach enables enhanced metallurgical recovery but increases the water load within the tailings storage facility (TSF) and generates finer secondary tailings with altered geochemical behaviour through changes in particle size, mineral surface exposure, and water–solid interactions, necessitating a testing framework that captures both short- and long-term environmental responses. In this paper, tailings were characterised using a tiered geochemical assessment comprising static, kinetic, and ecotoxicological test protocols. Static tests, including mineralogical analysis, acid–base accounting, whole-rock chemistry, and leach procedures (TCLP, SPLP, and ASLP), were used to screen acid-generation potential, identify potentially concerning elements, and assess short-term metal mobility under contrasting pH and leaching conditions. Kinetic leach testing was undertaken using a 21-week humidity-cell programme to simulate accelerated weathering and to evaluate time-dependent changes in drainage chemistry associated with sulfide oxidation and neutralisation reactions. In recognition that chemical stability alone may not adequately predict ecological risk, screening-level aquatic toxicity tests were applied to leachates to assess acute biological responses to dissolved constituents. Together, these complementary protocols provide an integrated basis for evaluating both geochemical stability and potential environmental impacts associated with re-mined copper tailings.

The findings provide a practical framework for sustainable remining and environmental management, with direct applicability to similar projects in South Africa.

Methodology

The geochemical assessment was undertaken on metallurgical tailings samples representative of material expected to be produced during the remining process. Sampling was designed to capture the physical and geochemical characteristics of the remined tailings following hydraulic remobilisation, recognising that hydro-mining produces finer materials with increased surface area and altered water–solid interactions. The testing programme was therefore designed to evaluate the potential environmental impacts of the tailings under simulated laboratory conditions through static, kinetic, and ecotoxicological assessments.

Static Geochemical Testing

Static geochemical tests were conducted to provide baseline characterisation and screening-level risk indicators. These tests provided baseline information on particle size distribution, mineralogical composition, acid-generating capacity, buffering potential, and short-term metal mobility. The following are the different static tests that were carried out as part of the study:

Particle Size Distribution

Particle size distribution (PSD) is a critical parameter influencing drainage behaviour and reaction kinetics in tailings materials. Particle size controls the distribution of voids that act as flow pathways and storage zones for porewater and gases within the facility. As reactivity is generally proportional to surface area, finer materials exhibit a greater tendency for geochemical reactions. PSD was determined using standard mechanical sieving to characterise the physical nature of the remined tailings. In this method, a representative dried sample was passed through a stack of sieves with progressively smaller mesh sizes, allowing the mass percentage of material retained on each sieve to be quantified. The results, also depicted in a PSD curve, describe the relative proportions of coarse and fine particles within the tailings and provide a reproducible measure of material texture. Coarser particles tend to form larger, better-connected voids that promote drainage and gas exchange, whereas finer particles create smaller pore spaces that retain porewater and restrict airflow. These conditions influence oxygen availability, moisture retention, and solute transport, all of which directly affect geochemical processes within a TSF.

Particle size also strongly influences reaction kinetics, as mineral reactivity increases with surface area. Finer particles generated during hydro-mining have a higher surface-area-to-volume ratio, which enhance mineral–water contact and accelerate processes such as metal dissolution, carbonate buffering reactions, and sulfide oxidation where present. PSD analysis therefore provides essential context for interpreting acid–base accounting (ABA), leach test results, and kinetic leach behaviour, as variations in particle size help explain differences in reaction rates, buffering persistence, and leachate chemistry.

Mineralogy

Mineralogical analysis was conducted using X-ray diffraction (XRD) to identify and quantify the crystalline mineral phases present in the re-mined tailings. XRD is a non-destructive analytical technique that determines mineralogy by measuring the diffraction patterns produced when X-rays interact with the crystal lattice of minerals in a sample. Representative bulk tailings samples were air-dried, homogenised and finely ground to produce a uniform powder suitable for XRD analysis. Powdered samples were analysed using a laboratory X-ray diffractometer, and diffraction patterns were collected over a range of angles appropriate for identifying minerals. The resulting diffraction patterns were compared with reference mineral databases to identify mineral phases, and relative proportions were estimated based on peak intensities.

The primary purpose of the XRD analysis in this study was to determine the relative proportions of acid-producing sulfide minerals and acid-neutralising carbonate minerals, as mineralogical composition is a fundamental control on acid rock drainage (ARD) potential. Sulfide minerals, such as pyrite, can generate acidity through oxidation reactions, whereas carbonate minerals consume acidity through dissolution and buffering reactions. Identifying the presence or absence of these mineral groups therefore provides direct insight into the balance between acid-generating and neutralising processes within the tailings.

In addition, XRD was used to identify dominant minerals that influence long-term geochemical behaviour, including buffering persistence, weathering rates, and metal release mechanisms. The mineralogical data provide critical context for interpreting ABA, net acid generation (NAG), and leach test results, as mineralogy constrains both the source of acidity and the availability of reactive phases capable of releasing or immobilising metals. As such, XRD forms a foundational component of the multi-line-of-evidence approach used to assess the geochemical stability and environmental risk of the remined copper tailings.

Acid–Base Accounting

ABA, including total sulfur speciation, neutralisation potential, and NAG testing, was undertaken to evaluate the balance between acid-producing and acid-consuming reactions within the tailings and to classify their potential to generate ARD. ABA integrates a suite of complementary measurements that quantify both the sources of acidity and the capacity of the material to neutralise that acidity, providing a screening-level assessment of short-term geochemical stability.

Total sulfur was measured by LECO combustion to quantify the overall sulfur content of the tailings, while sulfur speciation was used to distinguish forms of sulfur. Sulfide sulfur represents the principal source of potential acidity, as oxidation of sulfide minerals can generate sulfuric acid, whereas sulfate sulfur reflects sulfur that has already been oxidised and therefore does not contribute to future acid generation. The sulfide sulfur content was used to calculate the sulfide acid potential (SAP), assuming complete oxidation to sulfuric acid. The neutralisation potential (NP) of the tailings was determined using the modified Sobek method, which measures the capacity of carbonate and other acid-consuming minerals to neutralise acidity. In addition, Total Inorganic Carbon analysis was used to quantify carbonate-derived neutralisation potential (CaNP), providing an independent measure of buffering capacity associated specifically with carbonate minerals. Comparison of NP and SAP allows calculation of net neutralisation indices, which indicate whether acid-consuming reactions are likely to offset potential acid generation.

To complement the static ABA calculations, NAG testing was conducted by oxidising the sample with hydrogen peroxide to simulate accelerated sulfide oxidation. The resulting NAG pH and acidity provide an integrated measure of the balance between acid generation and neutralisation under forced oxidation conditions. NAG testing is particularly useful for confirming ABA classifications and identifying cases where static calculations may be uncertain.

Together, these ABA components provide a multi-parameter, screening-level evaluation of ARD potential by quantifying sulfur content, acidity generation potential, and buffering capacity. The results were used to classify the tailings as potentially acid-generating or non-acid-generating and to guide interpretation of subsequent leach and kinetic test results.

Whole-rock composition
Whole-rock chemical analyses were performed to identify potentially concerning elements and to contextualise subsequent leach and toxicity results. Major and trace elements were analysed to quantify potential constituents of concern (PCOCs).

Leach testing
Standardised short-term leach tests, namely TCLP, Synthetic Precipitation Leaching Procedure (SPLP), and Australian Standard Leaching Procedure (ASLP), were selected to evaluate the potential for metals to be released from the tailings under different, but environmentally relevant, water-chemistry conditions. Each leaching protocol represents a distinct exposure scenario and therefore provides complementary information on metal mobility rather than redundant results. The TCLP (US EPA 1311), with a standard 20:1 L:S ratio, simulates leaching under acidic conditions typical of waste disposal environments influenced by organic acids or industrial landfills. The test uses a weak acetic acid solution and is designed to identify whether metals can be mobilised under low-pH conditions that maximise solubility. TCLP results are commonly used for regulatory classification of waste and to assess worst-case leaching scenarios. SPLP (US EPA 1312) simulates leaching by meteoric water, using a dilute sulfuric–nitric acid solution representative of rainfall. This, modified to a 5:1 liquid-to-solid (L:S) ratio, test provides insight into metal release under conditions more closely aligned with natural infiltration and surface runoff, making it particularly relevant for predicting seepage quality from tailings storage facilities exposed to rainfall. Additionally, ASLP with a standard 20:1 L:S ratio evaluates metal mobility under near-neutral conditions, using water or a mildly buffered solution to represent prolonged contact between tailings and porewater or groundwater. This test is useful for assessing leaching behaviour where strong acidity is absent and buffering reactions dominate.

No single leach test can adequately represent the full range of geochemical conditions that tailings may experience in the field. Acidic, meteoric, and near-neutral environments promote different dissolution, complexation, and adsorption mechanisms, which can significantly influence metal release. The combined application of TCLP, SPLP, and ASLP therefore provides a more robust assessment of short-term leachability, allowing sensitivity of metal mobilisation to pH and solution chemistry to be evaluated and supporting defensible classification of tailings in terms of environmental and regulatory risk. Leachates from each test were analysed for pH, electrical conductivity (EC), total dissolved solids (TDS), major ions, and trace metals.

Radioactivity and toxicity screening
Gross alpha and beta activity, uranium (U) and thorium (Th) isotopes, and screening-level aquatic toxicity tests were undertaken to identify potential radiological or biological risks. Recognising that chemical characterisation alone may not adequately predict ecological impacts, screening-level aquatic toxicity tests were conducted. These bioassays were used to directly evaluate the acute biological response of standard aquatic organisms to dissolved constituents, thereby integrating geochemical results with ecological relevance.

Kinetic Leach Testing
To address longer-term behaviour not captured by static tests, kinetic leach testing was conducted using a 21-week humidity-cell programme. This method simulates accelerated weathering through cyclic

wetting and drying, enabling assessment of time-dependent changes in drainage chemistry associated with sulfide oxidation, carbonate dissolution, and secondary mineral formation (ASTM, 2018a; ASTM, 2018b; MEND, 2009). Weekly leachates were analysed for pH, EC, TDS, alkalinity, major ions, and trace elements, to provide insight into reaction rates, buffering persistence, and trends in contaminant release over time.

This approach aligns with the World Bank Environmental, Health and Safety Guidelines (IFC, 2007), which recommend accelerated weathering tests at feasibility stage to characterise PAG or metal-leaching materials. The results informed seepage quality predictions, recognising that laboratory oxidation rates typically exceed field conditions. Together, the static, kinetic, and ecotoxicological methods were selected to provide a reproducible, multi-line-of-evidence assessment of the environmental behaviour and risk profile of remined copper tailings.

Data Analysis

Geochemical Abundance Index

Total metal and semi-metal concentrations in mining waste materials can be compared to the median crustal abundance for unmineralised soils (Bowen, 1979) and (INAP, 2010). The extent of enrichment is expressed as the Geochemical Abundance Index (GAI), which relates the actual concentration in a sample to the median or average crustal abundance. The GAI was used as a screening tool to place the elemental composition of the tailings in a broader geochemical context by comparing measured concentrations to average crustal abundances. This comparison allows identification of elements that are anomalously enriched as a result of mineralisation and metallurgical processing, rather than natural background levels. In the context of remined tailings, GAI is not intended to predict environmental mobility or toxicity directly, but to flag elements that may warrant further evaluation through leach testing or ecotoxicological assessment. Elements showing elevated GAI values represent potential sources of environmental concern if mobilisation occurs under changing geochemical conditions. The GAI therefore supports interpretation of whole-rock chemistry results by prioritising elements for subsequent leachability and risk assessment, and by linking bulk composition to observed leachate chemistry and toxicity outcomes.

Elemental enrichment relative to crustal averages was evaluated using:

$$GAI = log2\ [Cn/1.5 \times Bn] \quad [1]$$

where Cn is the concentration of the element in the sample and Bn is the median crustal abundance (Bowen 1979 ; INAP 2010). The GAI is expressed in integer increments from 0 through to 6, where a GAI of 0 indicates the element is present at a concentration similar to or less than the crustal abundances; GAI of 3 corresponds to a 12-fold; and so forth, up to a GAI of 6, indicating approximately 100-fold or greater enrichment above the median crustal abundances.

Acid-generation potential

The acid-generation potential of the copper tailings was assessed using widely applied screening criteria derived from Price *et al*., (1997), Soregaroli *et al*., (1997), Morin *et al.* (1997), and the Mine Environment Neutral Drainage (MEND, 2009) guidelines. These frameworks classify mine waste materials based on a combination of paste pH, sulfide sulfur content, and the balance between acid-producing and acid-neutralising components. In general, materials with low sulfide sulfur contents (typically < 0.3 %), circumneutral paste pH values (> 5.5), and a surplus of neutralisation potential relative to calculated sulfide acid potential are considered unlikely to generate acid and are classified as non-PAG. Conversely, materials with elevated sulfide contents, low paste pH, and insufficient neutralisation capacity are classified as PAG, with an intermediate category recognising uncertainty where indicators are contradictory.

Metal-leach assessment

Leachate concentrations from SPLP, TCLP, and ASLP tests were compared against threshold values for PCOCs defined by the World Bank–IFC, DRC Mine Discharge Guideline (2009), WHO Drinking-Water

Guidelines, and the DRC Mining Code (Decrees 038/2003 and 18/024). Materials were classified as low-risk, leachable, or high-risk based on TCLP results relative to Annex VIII and X criteria.

Radioactivity classification
The Ionising Radiation Index (S) was calculated per the International Atomic Energy Agency (IAEA 2012):

$$S = \left(\frac{C1}{A1}\right) + \left(\frac{C2}{A2}\right) + \left(\frac{C3}{A3}\right) + \cdots + \left(\frac{Cn}{An}\right) \quad [2]$$

Where: S = Ionising radiation index (dimensionless), Cn = Measured specific activity of radionuclide n in the waste (kBq/kg), and An = Maximum allowable specific activity of radionuclide n, as per IAEA limits (kBq/kg)

Aquatic toxicity
Acute toxicity of ASLP leachate was evaluated using Daphnia pulex (48 h) and Poecilia reticulata (96 h) bioassays (Tonkes and Baltus, 1997). Toxicity units (TUa = 100 / LC_{50}) were calculated to classify effects as non-toxic, mildly toxic, or acutely toxic. Hazard categories were further defined using the Persoone *et al*. (2003) five-class system, ranging from Class I (no acute hazard) to Class V (very high acute hazard).

Results and discussion
Particle Size Distribution
The PSD results for the remined tailings (Figure 1) indicate a fine-grained material, with 98.8% passing the 75 µm sieve and a dominant fraction below 0.5 mm. Such fine particle sizes imply a high reactive surface area and an increased potential for rapid sulfide oxidation and solute release under kinetic leach conditions. This highlights the need for effective control of oxidation and drainage pathways within the TSF.

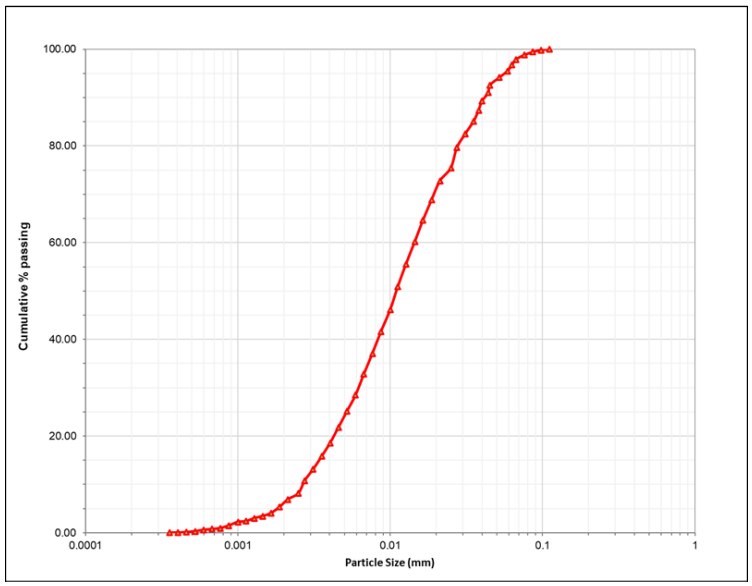


Figure 1. Particle size distribution.

Mineralogy
The mineralogical composition of the tailings is summarised in Table I. XRD analysis identified seven crystalline mineral phases dominated by relatively inert minerals, quartz (45.8 wt.%) and muscovite (35.2 wt.%). Pyrite (FeS_2), the principal sulfide mineral associated with ARD, was not detected. Fast-reacting carbonate minerals, including dolomite [$CaMg(CO_3)_2$], occurred at 4.1 wt.% and contribute to the acid-neutralising capacity. Muscovite, a slow-weathering aluminosilicate, is expected to buffer within the pH range of approximately 2.2–5.1 as it dissolves gradually (Bowell *et al.*, 2000). The presence

of chlorite (9.2 wt.%) together with minor microcline, haematite, and titanite supports a geochemically stable mineral assemblage with moderate to strong buffering capacity.

Overall, the XRD results indicate that the remined tailings contain negligible quantities of acid-generating minerals and consist mainly of silicate and carbonate phases capable of neutralising acidity under prolonged weathering conditions.

Copper in primary ore deposits is commonly hosted in sulfide minerals. However, during prolonged weathering, historical deposition and metallurgical reprocessing, these sulfide phases may be preferentially oxidised and depleted (Jena *et al.*, 2022; Mun, *et al,.* 2021; and Mbuya, *et al.*, 2025). The mineralogical assemblage observed in the re-mined tailings therefore reflects the residual, post-processing material rather than the primary ore mineralogy. The absence of detectable pyrite or other copper-bearing sulfide minerals in the XRD results suggests that sulfide phases originally associated with the ore have either been effectively removed during processing or oxidised over time, leaving behind a mineral assemblage dominated by silicate and oxide phases. Despite the lack of identifiable copper sulfides in the mineralogical data, copper remains enriched in the tailings based on whole-rock chemical analysis detailed below. This indicates that copper is likely present in non-sulfide forms, such as trace substitutions within silicate minerals, adsorption onto secondary iron oxides (e.g., hematite), or incorporation into fine-grained or amorphous phases below the detection limit of XRD.

The dominance of quartz and muscovite, together with chlorite, minor feldspar, hematite, and dolomite, indicates a geochemically stable tailings matrix with limited acid-generation potential but sufficient reactive surfaces to influence metal mobility. Carbonate minerals contribute to buffering capacity, while aluminosilicate and oxide phases provide potential sinks—and sources—for trace metals under changing geochemical conditions. Thus, the mineralogical composition reflects an advanced state of sulfide depletion relative to the original ore, while the bulk chemical enrichment of copper explains its continued environmental relevance in leach and toxicity assessments.

Table I. Mineralogical composition of the tailings and weathering rates of individual minerals

Mineral	**Chemical formula**	**Weathering rate (Bowell *et al.*, 2000)**	**Tailings**
Quartz	SiO_2	Inert	45.8
Muscovite	$KAl_2(Si_3Al)O_{10}(OH)_2$	Very slow weathering	35.2
Chlorite	$(Mg, Fe^{2+}, Fe^{3+}, Mn, Al)_{5-6}(Si_{2-4}Al_{2-0}O_{10})(OH)_8$	Fast weathering	9.2
Dolomite	$CaMg(CO_3)_2$	Dissolving	4.1
Microcline	$KAlSi_3O_8$	Intermediate weathering	3.3
Hematite	Fe_2O_3	Inert	1.9
Titanite	$CaTiSiO_5$	Intermediate weathering	0.5
Total			**100**

Elemental Composition

The elemental composition of the tailings, expressed as the Geochemical Abundance Index (GAI; Equation [1]), is summarised in Table II. Elements showing notable enrichment (GAI ≥ 3) include selenium (Se), tin (Sn), copper (Cu), mercury (Hg), and tellurium (Te). Moderate enrichment (GAI = 2) was observed for molybdenum (Mo), while most other elements exhibited background to minor enrichment levels. A high GAI value indicates the relative concentration of an element compared with average crustal abundance, but it does not necessarily imply environmental mobility or risk. Instead, it highlights potential contaminant sources that require further evaluation through leachate or toxicity

testing (INAP, 2010). The enrichment of Cu, Hg, and Se reflects the metallurgical origin of the tailings and suggests that these elements could contribute to elevated concentrations under certain geochemical conditions.

Table I. Geochemical abundance index for the tailings sample

Material type	**Elements with GAI = 0**	**Elements with GAI = 1**	**Elements with GAI = 2**	**Elements with GAI = 3**	**Elements with GAI = 4**	**Elements with GAI = 5**	**Elements with GAI = 6**
Tailings	Al, Ag, As, B, Ba, Be, Fe, Mg, Mn, Na, Ni, P, Pb, Sr, Si, Tl, U, V, and Zn	K, Li, and Ti	Mo	Se	Sn	Cu	Hg and Te

Acid Base Accounting

Table III summarises the ABA results for the tailings. The material contains low concentrations of total sulfur (0.065%) and sulfide sulfur (0.02%). According to MEND (2009), materials with paste pH values greater than 5.5 and sulfide contents below 0.3% are considered to have a low acid-generating potential, whereas lower pH or higher sulfide values indicate PAG behaviour. The paste pH of 7.7 (Figure 2) and the very low sulfide content confirm that the remined tailings are less likely to generate acid. The calculated SNPR = Bulk NP/SAP; (Figure 3) of 54.4 and the positive SNNP = 33.4 kg $CaCO_3$/t) further support this classification. Based on these indicators, the tailings are classified as non-PAG.

Table II. Summary of acid–base accounting results for the tailings

Paste pH	**Total Sulfur (%)**	**Sulfide-Sulfur**	**sulfate-sulfur**	**[1]Bulk NP**	**[2]CaNP**	**[3]SAP**	**[4]SNNP**	**[5]SNPR**
	(% as S)	(% as S)	(% as S)	(kg $CaCO_3$/ t)	(kg $CaCO_3$/ t)	(kg $CaCO_3$/ t)	(kg $CaCO_3$/ t)	
7.7	0.065	0.020	0.045	34	34.194	0.625	33.375	54.4

Note: [1] Bulk NP measured by the modified Sobek titration and used for the NPR calculation.[2] CaNP – l derived from TIC expressed as $CaCO_3$ equivalent.[3] SAP – calculated from sulfide sulfur content (assuming complete oxidation to H_2SO_4).[4] SNNP – , calculated as Bulk NP –/ SAP.[5] SNPR – calculated as Bulk NP / SAP.

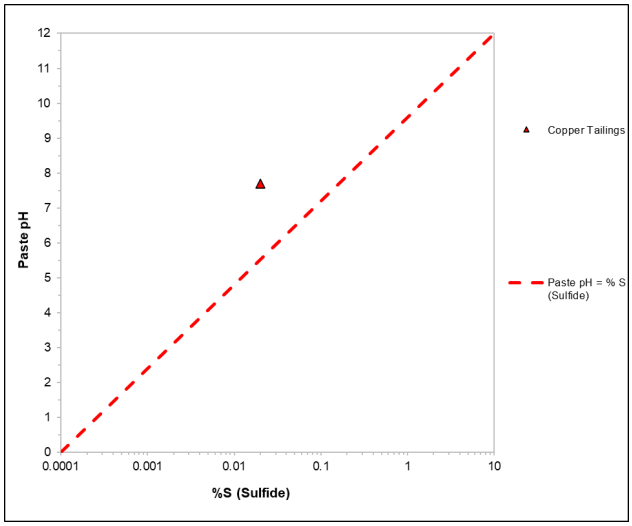


Figure 2. Paste pH vs sulfide-sulfur (%) for the tailings sample.

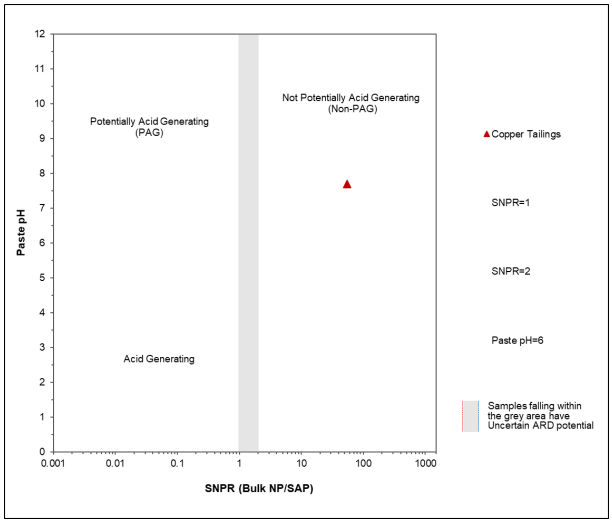


Figure 3. Paste pH vs SNPR (Bulk NP / SAP) for the tailings sample.

Net Acid Generation

A NAG test was performed to confirm the acid-generating potential of the copper tailings, with results at pH 4.5 and pH 7.0 presented in Table IV. A NAG pH threshold of 4.5 is commonly used to identify PAG materials; values above this indicate a low likelihood of acid formation. The tailings recorded a NAG pH of 7.7, consistent with the paste pH, suggesting that pH conditions are expected to remain stable over time. Measured acid generation was less than 0.5 kg H_2SO_4/t at both pH 4.5 and pH 7.0, confirming negligible acid potential. When correlated with the SNPR = Bulk NP / SAP; (Figure 4), the results further confirm that the tailings are non-PAG.

Table IV. Summary of Net Acid Generation results for the Tailings

Sample ID	**NAG pH: (H_2O_2)**	**NAG at pH 4.5**	**NAG at pH 7.0**
Units		kg H_2SO_4/t	kg H_2SO_4/t
Tailings	7.7	<0.5	<0.5

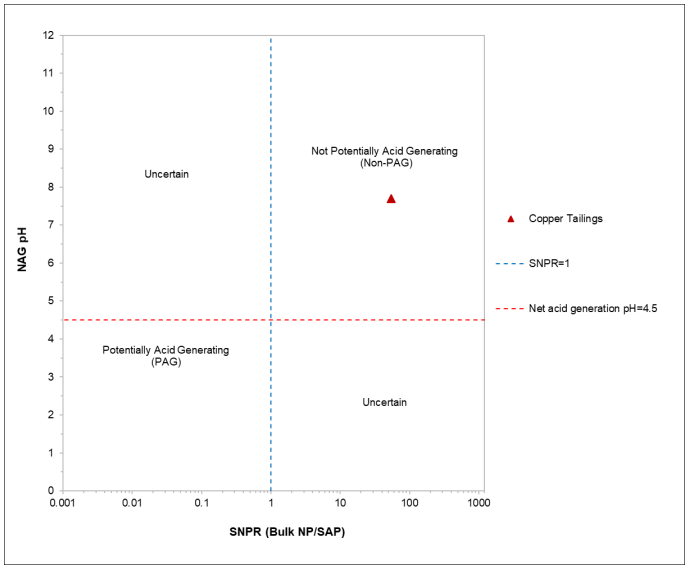


Figure 4. NAG pH vs SNPR (BulkNP/SAP) for the tailings.

Metal Leaching Assessments

Short-term leach results obtained from the TCLP, SPLP, and Australian ASLP are presented in Table V. Results were compared with applicable international and regional water quality standards, including the IFC, WHO, and DRC Mine Discharge Guidelines (Annexure X, 2018).

Toxicity Characteristics Leach Procedure

The TCLP leachate exhibited an acidic pH of 4.3, below the acceptable range (6–9) of reference guidelines. Copper (58 mg/L) and iron (32 mg/L) exceeded the low-risk thresholds defined by DRC regulations. Aluminium and chromium were above WHO guideline values, while manganese marginally exceeded the WHO limit and zinc slightly exceeded the IFC standard. All other PCOCs were within acceptable limits.

Synthetic Precipitation Leach Procedure

The SPLP leachate was slightly alkaline (pH 8.8), within the accepted standards. Concentrations of aluminium (12 mg/L) exceeded both IFC and WHO limits, while copper (0.76 mg/L) and iron (5.1 mg/L) were above all guideline criteria, including DRC low-risk thresholds. These exceedances are consistent with the higher solubility of Al and Fe under near-neutral to slightly alkaline conditions where complexation can occur.

Australian Standard Leaching Procedure

The ASLP leachate displayed a slightly acidic pH (5.5). None of the measured parameters exceeded the DRC low- or high-risk criteria; however, aluminium, arsenic, and manganese exceeded WHO guideline values. Overall, the low metal concentrations reflect minimal mobility of trace elements under short-term leaching conditions.

Collectively, the results indicate that copper, iron, aluminium, and manganese are the principal elements of concern across the three leach protocols. The variability in pH and metal mobility reflects the buffering capacity identified in the ABA and mineralogical assessments, where carbonate and aluminosilicate phases dominate. Although several PCOCs exceeded drinking-water guideline values, the concentrations remain well below those typically associated with acid-generating material. The tailings are therefore classified as leachable but low-risk, consistent with non-PAG behaviour observed in the ABA and NAG results.

Table III. Tailings short-term leach results compared to IFC, DRC water quality limits, WHO, and DRC Regulation guidelines

Sample ID		**Short Term Leach Tests**	**Short Term Leach Tests**	**Short Term Leach Tests**	**Water Quality Standards**			**DRC Regulations (Annexure X, 2018)**	
Parameter	**Units**	**TCLP**	**SPLP**	**ASLP**	**IFC**	**DRC Mine Discharge Guideline**	**WHO**	**Low risk Mine waste[1]**	**High risk Mine waste[2]**
pH	s.u	***4.3***	8.8	***5.5***	**6 – 9**	***6 – 9***	*6 – 8.5*	ng	**ng**
EC	mS/m	250	24	17	**ng**	***ng***	*ng*	ng	**ng**
TDS	mg/L	1800	230	130	**ng**	***ng***	*ng*	ng	**ng**
Total Alkalinity	mg $CaCO_3$/L	900	40	<12	**ng**	***ng***	*ng*	ng	**ng**
Acidity	mg $CaCO_3$/L	-	-	10	**ng**	***ng***	*ng*	ng	**ng**
Chloride	mg/L	2.3	6	22	**ng**	***ng***	*250***	ng	**ng**
Fluoride	mg/L	0.12	0.44	0.15	**ng**	***ng***	*1.5*	ng	**>150**
Nitrate	mg/L	<0.5	0.3	0.49	**ng**	***ng***	*50*	ng	**ng**
Nitrite	mg/L	<0.03	<0.5	<0.5	**ng**	***ng***	*ng*	ng	**ng**
Sulfate	mg/L	14	68	24	**ng**	***ng***	*ng*	ng	**ng**
Aluminium	mg/L	*4.1*	*12*	*0.07*	**ng**	***ng***	*0.1***	ng	**ng**
Antimony	mg/L	<0.02	<0.02	<0.02	**ng**	***ng***	*ng*	ng	**ng**
Arsenic	mg/L	<0.01	<0.01	*0.04*	**0.1**	***0.4***	*0.01 (P)*	<1	**>5**
Barium	mg/L	0.78	0.13	0.023	**ng**	***ng***	*1.3*	ng	**ng**
Beryllium	mg/L	0.004	<0.0001	<0.0001	**ng**	***ng***	*ng*	ng	**ng**
Boron	mg/L	0.012	0.014	0.006	**ng**	***ng***	*ng*	ng	**ng**
Cadmium	mg/L	<0.001	<0.001	0.002	**0.05**	***ng***	*0.003*	<0.1	**>0.5**
Calcium	mg/L	330	27	15	**ng**	***ng***	*ng*	ng	**ng**
Chromium	mg/L	*0.12*	0.035	<0.002	**ng**	***ng***	*0.05 (P)*	<1	**>5**
Cobalt	mg/L	0.2	0.02	0.05	**ng**	***ng***	*ng*	ng	**ng**
Copper	mg/L	***58***	**0.76**	0.06	**0.3**	***1.5***	*2*	<0.3	**ng**
Iron	mg/L	***32***	***5.1***	<0.05	**2**	***6***	*0.3 (C)*	<2	**ng**
Lead	mg/L	0.01	<0.01	<0.01	**0.2**	***0.5***	*0.01 (A, T)*	<0.6	**>5**
Lithium	mg/L	0.013	0.021	0.005	**ng**	***ng***	*ng*	ng	**ng**
Magnesium	mg/L	140	5.6	4.1	**ng**	***ng***	*Ng*	ng	**ng**
Manganese	mg/L	*14*	*0.05*	*0.54*	**ng**	***ng***	*0.1***	ng	**ng**
Mercury	mg/L	<0.001	<0.001	<0.001	**0.002***	***0.002***	*0.006*	<0.002	**>0.01**
Nickel	mg/L	0.049	0.005	0.021	**0.5**	***1***	*0.07*	<0.5	**ng**
Selenium	mg/L	<0.01	<0.01	<0.01	**ng**	***ng***	*0.04 (P)*	ng	**>1**
Uranium	mg/L	<0.01	<0.01	<0.01	**ng**	***ng***	*0.03 (P)*	ng	**>2.0**
Zinc	mg/L	**0.54**	0.02	0.05	**0.5**	***10***	*4*	<1	**ng**

[1] Light grey shading denotes exceedances of low-risk guideline limits. Mining waste is considered low risk if concentrations do not exceed criteria defined in the provincial mineral concentration database or remain below the average mine waste composition at the deposition site.

[2] High-risk mining waste classification applies where leachate exceeds high-risk TCLP concentration criteria, emits ionising radiation > 0.05 Bq/kg, or contains > 5 mg/kg PCBs or PCDFs (Article 8, Annexure XI).

Notes:

Bold = exceeds IFC standard.

Italic = exceeds WHO standard.

Bold italic = exceeds DRC standard.

Underline = exceeds more than one standard.

n/g = no guideline value available.

P = provisional guideline value (limited data on health effects).
T = provisional guideline value (below achievable treatment level).
A = provisional guideline value (below analytical quantification limit).
C = aesthetic consideration only — concentrations at or below this value may affect the appearance, taste, or odour of water.

Radioactivity

The radioactivity results for the tailings are summarised in Table VI. Specific activities of uranium and thorium isotopes were normalised against their respective maximum thresholds defined by the IAEA, (2012). The calculated ionising radiation index (S) for the tailings was 0.01, which is well below the high-risk threshold of 0.05 and far below the classification limit of 1.0 for radioactive waste. Measured gross alpha (375 Bq/kg) and gross beta (1 970 Bq/kg) activities fall within typical background ranges for mineralised materials and therefore pose no radiological concern. These results confirm that the tailings are not classified as radioactive waste under both IAEA (2012) and DRC Mining Code (2018) criteria.

Table VI. Radioactivity results for the copper tailings

Parameter	**Units**	**Activity**	**Uncertainty**	**Maximum Threshold (IAEA, 2012) (Bq/kg)**
U-238	Bq/kg	51.7	2.3	180000
U-234	Bq/kg	52.2	2.4	231000000
U-235	Bq/kg	2.38	0.11	26000000
Th-232	Bq/kg	34.2	1.7	4066
Gross Alpha	Bq/kg	375	-	None
Gross Beta	Bq/kg	1970	50	None
Calculated S		0.01	-	

Notes:
S = Ionising radiation index (dimensionless).

Aquatic Toxicology

The toxicity screening results for the copper tailings leachate are summarised in Table VII. The leachate supernatant had a pH of 8.28, within the acceptable range (6–9) where pH-related stress can be excluded as a primary driver of toxicity (USEPA, 1996). Electrical conductivity (89.9 µS/cm) was relatively low but within the range (25–200 µS/cm) associated with potential reductions in taxa abundance and diversity (Olson and Hawkins, 2017). Such low ionic strength may disrupt osmoregulatory processes in fish and invertebrates, leading to physiological stress. Dissolved oxygen concentration (7.32 mg/L) exceeded the minimum threshold (4 mg/L) required to support aquatic life, and no residual chlorine was detected, confirming that toxicity effects were not artefacts of oxygen limitation or disinfection.

The 48-hour Daphnia pulex bioassay resulted in 100% mortality, while the Poecilia reticulata test indicated 50% mortality under identical conditions. Both assays exceeded the > 50 % acute-effect threshold, confirming acute toxicity. As only single-strength leachate was tested, data were insufficient to calculate LC_{50} and toxicity units (TUa) with confidence. Hazard classification assigned the leachate to Class IV, High acute hazard (see Table VII), reflecting complete mortality in at least one test organism. This indicates that only tolerant taxa are likely to survive direct exposure to undiluted leachate.

These results demonstrate that although the tailings are non-acid-generating, the leachate contains sufficient soluble constituents—primarily Cu and Fe—to induce acute biological stress. This emphasises the importance of integrating ecotoxicological testing with geochemical assessments to ensure comprehensive evaluation of drainage impacts on aquatic ecosystems.

Table IV. Water toxicity results for the copper tailings

Physical and Chemical Data	**Copper Tailings**
pH	8.28
Electrical Conductivity (µS/cm)	89.9
Dissolved Oxygen concentration (mg/L)	7.32
Residual Total Chlorine (present/not present)	Not present
Temperature (C)	20
24-hours Daphnia pulex Acute Toxicity Screening Test (% mortality)	100
48-hour Daphnia pulex Acute Toxicity Screening (% mortality)	100
48-hour Daphnia pulex Acute Toxicity Test, Toxicity Unit (TUa)	UR
96-hour Daphnia pulex Acute Toxicity Screening Test (% mortality)	50
96-hour Daphnia pulex Acute Toxicity Test, Toxicity Unit (TUa)	UR

Notes:
UR = Insufficient toxicity data available from the screening results to determine TUa with certainty.

Table VIII. Acute hazard classification system applied to the copper tailings

	Copper Tailings
Daphnia pulex	3
Poecilia reticulata	2
Weighted Score	2.50
%	83.33
Hazard Class	IV
Hazard	High acute hazard tolerant taxa present
Percentage Effect	The PE_{100} is exceeded in at least one test

Notes:
Hazard classes follow Persoone *et al.* (2003).
Class IV = High acute hazard; PE_{100} exceeded in ≥ 1 test.
TUa = Toxicity unit (100 / LC_{50}).

CONCLUSIONS

The results from the static and kinetic tests provided a comprehensive understanding of the environmental behaviour of the remined copper tailings. The material was found to be predominantly inert, consisting mainly of quartz (45.8 wt.%) and muscovite (35.2 wt.%), with minor dolomite (4.1 wt.%) contributing limited buffering capacity. No pyrite or other acid-generating sulfide minerals were detected, and total and sulfide sulfur concentrations (0.07 % and 0.02 %, respectively) were low. Both paste and NAG pH values (7.7) confirmed that the material is non-acid generating (non-PAG).

Despite the stable pH and neutralising potential, leach testing (TCLP, SPLP, and ASLP) classified the material as leachable mine waste, indicating potential for metal mobility under certain conditions. Localised geochemical variability and interactions with different water chemistries could promote mobilisation of soluble metals, particularly copper and iron. Ecotoxicological testing revealed acute toxicity in standard aquatic bioassays, with the leachate assigned a Class IV hazard classification due to complete mortality in Daphnia pulex. These findings highlight that although the acid generation potential is low, soluble metal toxicity represents a significant environmental risk.

Drainage from the remined tailings should be incorporated into site-wide water management systems and treated prior to environmental release to reduce electrical conductivity and remove dissolved metals. Continued water quality monitoring and the development of site-specific geochemical models are recommended to ensure long-term environmental protection. Overall, the study demonstrates that remining of legacy tailings, although beneficial for resource recovery, does not eliminate ecological risk. The integrated geochemical and ecotoxicological approach applied here provides a transferable framework for sustainable remining and environmental management in both the DRC and other comparable mining contexts.

RECOMMENDATIONS FOR REMINING OPERATIONS IN SOUTH AFRICA

The findings from this DRC-based study offer a robust framework for assessing and managing risks in remining projects, which is highly applicable to South African mining operations. Comprehensive assessment or the multi-faceted approach, combining standard geochemical tests with extended long term kinetic testing and ecotoxicology, proved essential for a thorough risk assessment. Relying solely on ARD potential (stable pH) would have missed the significant ecotoxicological risk posed by the leachable metals. Legacy tailings might be hazardous as this study confirms that even with improved metallurgical recovery, legacy tailings remain a potential source of aquatic environmental contamination. The reprocessing does not eliminate the inherent risks of metal mobility and toxicity.

REFERENCES

American Society for Testing and Materials (ASTM). (2018a). Standard Test Method for Laboratory Weathering of Solid Materials Using a Humidity Cell. ASTM D5744–18a. ASTM International, West Conshohocken, PA.

American Society for Testing and Materials (ASTM). (2018b). Standard Practice for Performing Laboratory Leaching Studies of Contaminants from Solid Materials Using a Column Testing Apparatus. ASTM D4874–18b. ASTM International, West Conshohocken, PA.

Bowell, B.D., Alpers, C.N. and Jambor, J.L. (2000). Mineral weathering rates and environmental geochemistry of mine wastes. Reviews in Economic Geology, 6A, 435–459.

Bowen, H.J.M. (1979). Environmental Chemistry of the Elements. Academic Press, London.

Democratic Republic of Congo (DRC). (2009). Mine Discharge Guidelines (5drc09 (5)). Ministry of Mines, Kinshasa, Democratic Republic of Congo.

Democratic Republic of Congo (DRC). (2018). Mining Code, Decree No. 18/024 of 8 June 2018, amending Decree No. 038/2003 (Annex VIII and Annex X). Government of the Democratic Republic of Congo, Kinshasa.

International Atomic Energy Agency (IAEA). (2012). Radiation Protection and Safety of Radiation Sources: International Basic Safety Standards. General Safety Requirements Part 3, IAEA, Vienna.

International Finance Corporation (IFC). (2007). Environmental, Health and Safety Guidelines: Mining. World Bank Group, Washington DC.

International Network for Acid Prevention (INAP). (2010). Global Acid Rock Drainage Guide (GARD Guide). http://www.gardguide.com

Jena, S. S., Tripathy, S. K., Mandre, N. R., Venugopal, R., & Farrokhpay, S. (2022). Sustainable Use of Copper Resources: Beneficiation of Low-Grade Copper Ores. Minerals, 12(5), 545. https://doi.org/10.3390/min12050545

Mbuya, B., Fosso-Kankeu, E., Bongaerts, J. (2025). Thermodynamic Investigation on the Impact of Oxidized Copper–Cobalt and Copper Sulfide Ores Stream Mixture Toward the Dissolution of Cu and Co. J. Sustain. Metall. 11, 1299–1318 (2025). https://doi.org/10.1007/s40831-025-01041-2

Mine Environment Neutral Drainage (MEND). (2009). Prediction Manual for Drainage Chemistry from Sulphidic Geologic Materials. MEND Report 1.20.1, Natural Resources Canada, Ottawa.

Morin, K.A., Hutt, N.M. and Ferguson, K.D. (1997). A Literature Review of Acid Rock Drainage Prediction Methods. MEND Report 1.12.1, Natural Resources Canada, Ottawa.

Mun, Y., Strmić Palinkaš, S., & Kullerud, K. (2021). The Role of Mineral Assemblages in The Environmental Impact of Cu-Sulfide Deposits: A Case Study from Norway. Minerals, 11(6), 627. https://doi.org/10.3390/min11060627

Olson, J.R. and Hawkins, C.P. (2017). Effects of total dissolved solids on growth and reproduction of stream macroinvertebrates. Environmental Toxicology and Chemistry, 36 (3), 730–744.

Persoone, G., Marsalek, B., Blinova, I., Törökne, A. and Zarina, D. (2003). A practical and user-friendly toxicity classification system with microbiotests for natural waters and wastewaters. Environmental Toxicology, 18 (6), 395–402.

Price, W.A., Morin, K.A. and Hutt, N.M. (1997). Guidelines for the Prediction of Acid Rock Drainage and Metal Leaching for Mines in British Columbia. Ministry of Energy and Mines, British Columbia.

Soregaroli, A., MEND, and Price, W.A. (1997). Development of Acid Rock Drainage Prediction Protocols and Guidelines for British Columbia. MEND Report 1.16.1, Natural Resources Canada, Ottawa.

Tonkes, M. and Baltus, C. (1997). Acute toxicity assessment using toxicity units: A practical evaluation for industrial effluents. Water Science and Technology, 36 (6–7), 275–281.

United States Environmental Protection Agency (USEPA). (1992). Test Methods for Evaluating Solid Waste, Physical/Chemical Methods (SW-846), Method 1311: Toxicity Characteristic Leaching Procedure.

United States Environmental Protection Agency (USEPA). (1992). Test Methods for Evaluating Solid Waste, Physical/Chemical Methods (SW-846), Method 1311: Toxicity Characteristic Leaching Procedure.

United States Environmental Protection Agency (USEPA). (1994). Method 1312: Synthetic Precipitation Leaching Procedure (Revision 0). https://www.epa.gov/sites/default/files/2015-12/documents/1312.pdf.

United States Environmental Protection Agency (USEPA). (1996). Ecological Effects Test Guidelines: OPPTS 850.1010 Aquatic Invertebrate Acute Toxicity Test (Freshwater Daphnids). EPA 712–C–96–114, Office of Prevention, Pesticides and Toxic Substances, Washington DC.

World Health Organization (WHO). (2022). Guidelines for drinking-water quality: fourth edition incorporating the first and second addenda. Geneva: World Health Organization.



Mpule Gloria Dube

Associate
WSP Africa Pty Ltd

Gloria is presently working for WSP Africa Pty Ltd, Associate position and recently promoted to Line Manager. With almost 13 years of experience, she has developed expertise in geo-environmental sciences, focusing specifically on areas affected by mining activities. Her professional background encompasses geochemical characterisation of legacy, operational, and greenfield mines across South Africa and other African countries, as well as geochemical modelling and environmental risk/impact assessments, among others. She is passionate about addressing challenges associated with mining and aims to enhance the geochemical modelling aspect of her career.

TSF-specific water balance as a standard practice

A. Scholtz, K.M. Uderstadt, L. de Villiers, G.C. Howell

SRK Consulting, South Africa

Site-wide water balances provide valuable oversight of mining water management, but the complexity and critical role of Tailings Storage Facilities (TSFs) require a focused, facility-specific approach. TSFs often remain a "black box" in conventional balances, particularly with respect to entrapped and interstitial water. Yet, understanding how much water is stored within a TSF, and how it changes over time, is fundamental to water optimisation, environmental stewardship, and dam safety. This paper highlights the advantages of developing TSF-specific water balances. By explicitly accounting for inflows and outflows, including slurry water, rainfall, evaporation, seepage, recovery processes, and entrapped water, operators can better characterise water dynamics that are typically underestimated in broader site-wide assessments. A case study illustrates how such focused analysis provides clearer insights into water storage and release, supporting improved conservation, regulatory compliance, and enhanced stability of TSFs. Given that TSFs evolve over decades, with changing tailings properties and seepage regimes, a robust water balance informed by up-to-date hydraulic data is essential for long-term management. It is proposed that TSF-specific water balances should be regarded as standard practice in mining. Such an approach not only strengthens operational decision-making but also supports sustainable water use and minimises environmental impacts, ensuring that TSFs continue to perform their essential function without compromising safety or integrity.

INTRODUCTION

Site-wide water balances provide a critical framework for understanding and managing water resources in mining operations. The complexity and significance of Tailings Storage Facilities (TSFs), however, necessitate a tailored, TSF-specific approach to water balance analysis. TSFs play a pivotal role in the overall water management strategy of a mine, yet their unique hydrological dynamics often remain underexplored in broader site-wide evaluations. While general water balances account for incoming flows, evaporation, percolation, and external outflows, the TSF presents distinct challenges. Entrapment of water within the TSF, for instance, is a critical factor that is not always fully quantifiable. Understanding the volume of water retained within the TSF, its spatial distribution, and its variations over time is vital for optimising water use, improving environmental stewardship, and ensuring the stability and safety of the facility.

This paper explores the advantages of developing a TSF-specific water balance, which focuses on the unique inflows, outflows, and internal water dynamics of TSFs. Through a detailed case study analysis, we demonstrate how this approach can provide insights that are often obscured in site-wide assessments. By examining key factors such as evaporation, seepage, recovery processes, interstitial water, and phreatic surface dynamics, mining operations can achieve a more comprehensive understanding of TSF water behaviour. This deeper insight supports the development of more effective water conservation strategies, enhances compliance with regulatory requirements, and promotes the long-term stability of TSFs.

A robust TSF-specific water balance requires the integration of up-to-date hydraulic data and an understanding of the evolving characteristics of tailings over the life of the facility. TSFs, which are constructed incrementally over decades, experience changes in tailings properties, internal seepage regimes, and storage capacities. Anticipating and adapting to these changes is critical for both existing and new facilities. The Global Industry Standard on Tailings Management (GISTM) underscores the importance of integrating design, economic, and environmental considerations into TSF management, further emphasising the need for innovative approaches to water balance modelling.

This study advocates for the adoption of TSF-specific water balances as a standard practice in the mining industry. By addressing the unique challenges and opportunities associated with TSFs, this approach promotes a more sustainable and responsible management of water resources. It ensures that TSFs can fulfil their essential functions without compromising environmental integrity, while also mitigating risks and enhancing operational efficiency. Through the implementation of tailored water management strategies, the mining industry can better align with sustainability goals and regulatory frameworks, safeguarding both operational and environmental outcomes.

Conventional water balances in mining operations

Water balances in mining operations are typically conducted at a site-wide scale, providing a high-level overview of water inputs, outputs, and storage within the mine's operational framework (refer to Figure 1). This site-wide approach provides a broad understanding of the mine's water use efficiency, compliance with regulatory requirements and potential environmental impacts. However, within these overarching water balances, TSFs are often represented as a relatively small and simplified component. The focus on TSFs in conventional water balances is typically limited to what is added to the facility and what comes out.

In most cases, TSFs are treated as a "black box" in site-wide water balances, where the intricate internal dynamics of water movement within the facility are not explicitly modelled or quantified. The focus is primarily on the net water entering and exiting the TSF, with little attention given to the internal storage and redistribution of water within the tailings mass. By treating TSFs as a minor component of the overall water balance, site-wide assessments may fail to capture critical insights into the facility's water behaviour. This can lead to missed opportunities for optimising water recovery, improving TSF stability, and minimising environmental risks. Furthermore, the lack of detailed TSF-specific data may hinder compliance with evolving regulatory standards, such as the GISTM, which emphasises the need for robust water management in TSFs.

Energy balance as a foundation for water balances

Understanding how potential energy converts to kinetic energy provides a useful analogue for water balance development. Just as water stored at elevation possesses potential energy that is released as kinetic energy when it flows, a TSF retains water, the movement and transformation of which must be carefully tracked. The shift between “stored” and “moving” water underpins the risks associated with phreatic surfaces, seepage, and stormwater response. Recognising this dynamic reinforces the need for a staged approach: starting with simple storage checks, progressing to monitored flows, and ultimately building a three-dimensional picture of how water is stored and released within the facility.

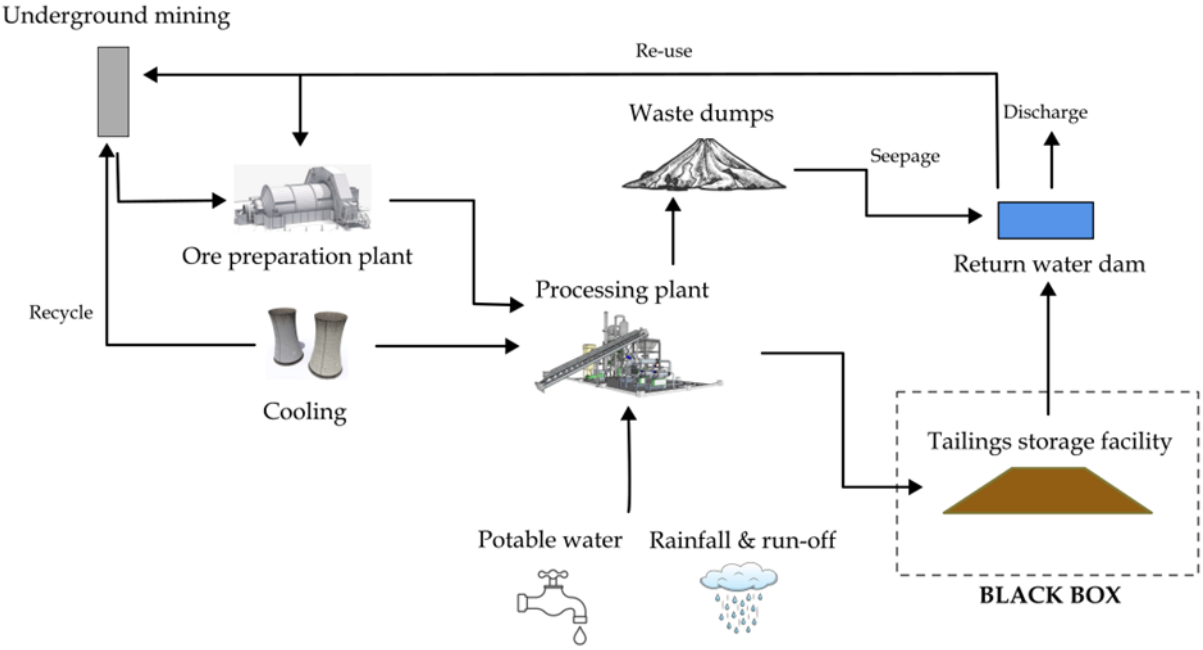


Figure 1. Site-wide mine water balance.

Energy stored in a TSF

When water is stored in a TSF, it possesses gravitational potential energy. This is because it is elevated above the natural ground level. The higher the water level (phreatic surface) and the greater the volume stored, the greater the increase in potential energy. Figure 2 depicts the changes in energy when it is stored in a TSF.

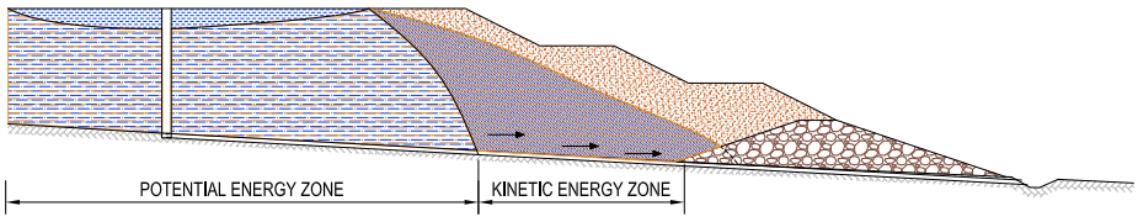


Figure 2. TSF energy zones.

Potential energy is given by:

$$P_E = mgh \quad [2]$$

Where m is the mass of stored water (kg), g is the gravitational acceleration (m/s^2) and h is the height of the water surface above a reference point (usually downstream ground level) (m).

If seepage (piping), overtopping, or a structural breach occurs, this stored potential energy is released and transforms into kinetic energy as water flows downstream. The slurry water then accelerates under gravity, and its energy, K_E is now expressed as motion:

$$K_E = \tfrac{1}{2}mv^2 \quad [3]$$

With v as the velocity (m/s).

This conversion of energy explains why uncontrolled releases from a TSF can be so destructive, namely that stored potential energy is suddenly converted to accelerated moving flows with high erosive and transport capacity.

Potential energy is effectively stored under the pool area. This is called the passive zone. Over time, this volume of tailings increases in density, although it is saturated. From the pool area, a phreatic surface develops and tapers towards the lowest elevation of the dam. This area is where the kinetic energy is developed. This is the active zone. This is where the gravelly tailings material is stored. Void ratio is higher in this area and seepages develop rapidly. Phreatic surfaces can fluctuate significantly in this zone depending on the density and hydraulic conductivity (permeability). Volumetric changes can vary considerably if not controlled effectively. Volumetric change in soils is linked to density changes that can be controlled by managing the deposition plan efficiently (thin lift deposition), rate of flow (% water: solids ratio), and maintaining effective beach slopes. The stored energy is released and converted into kinetic energy, which is the energy of motion. This is when failure starts to occur as typically occurs with piping failures.

In normal TSF operations, the potential energy of stored water is managed by discharge structures such as decant systems, spillways, seepage drains, and solution trenches that control the conversion of potential to kinetic energy in a safe manner. Failure scenarios develop if systems are not controlled and monitored. The rapid conversion of potential to kinetic energy represents a major risk factor which is not clearly understood, and therefore, water balance modelling must consider this when evaluating storage levels and freeboard requirements.

Interconnection between degree of saturation, porosity, and void ratio
Degree of saturation (%), porosity (%), and void ratio are interrelated measures of a soil's void space and water content. Porosity describes the volume of voids with respect to the total volume of the material. Void ratio describes the volume of voids with respect to solids volume. The degree of saturation indicates the fraction of voids filled with water. Together, these factors govern the soil's water storage, density, and flow characteristics.

As the TSF fills with tailings, the material matrix particles become compressed, the degree of saturation increases resulting in a gradual increase in pore water pressure with depth. As water continues to infiltrate, a zone of fully saturated soil develops at the bottom, where all voids are filled with water. The upper surface of this saturated zone is the phreatic surface. The phreatic surface assumes a shape governed by hydraulic gradients, soil permeability, and boundary conditions.

Approach to a TSF-specific water balance
A critical issue in current practices is that water balances often do not explicitly state the current storage volume of water contained within the TSF i.e. the "black box". If this volume cannot be quantified, it cannot be effectively managed. By adopting a three-staged approach, operators can move from simple checks to comprehensive modelling, thereby visualising how water storage changes over time. This progression allows for proactive management, ensuring that boundary conditions such as phreatic surface levels and freeboard requirements are continuously monitored and that trigger actions, such as halting deposition during extreme rainfall events, can be implemented effectively.
A typical water balance follows a fundamental equation given as:

$$\text{Inflows} - \text{Outflows} = \Delta S \qquad [1]$$

Where ΔS is the change in storage volume. Inflows include slurry water, precipitation on the TSF surface, surface runoff entering the TSF and groundwater inflows. Outflows include evaporation from the TSF surface, seepage through the TSF base and walls, recovered water via decant systems and underdrains and entrapped water within the tailings (Barthe et al., 2018). Refer to Figure 3 for the visual presentation.

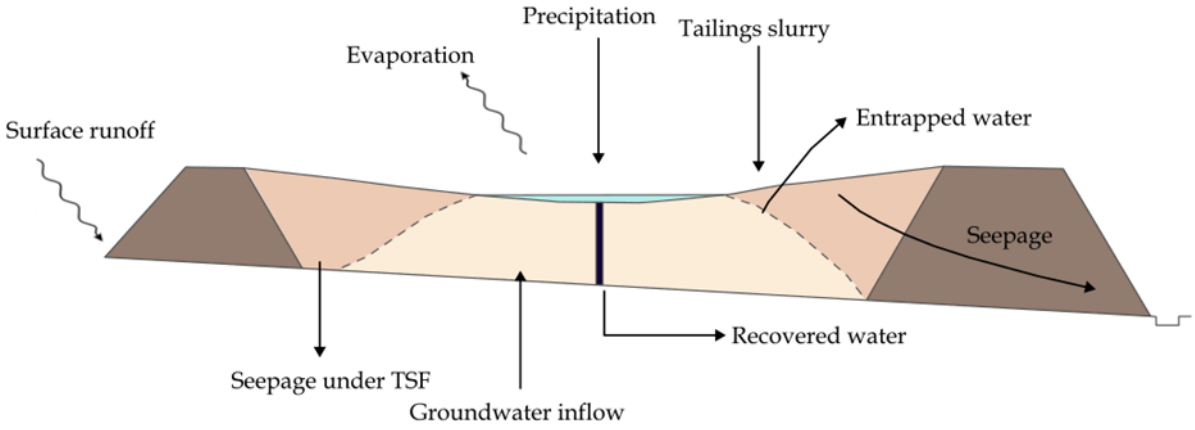


Figure 3. Elements of a water balance of a TSF (after Younger and Wolkersdorfer, 2004).

Staged approach

Fundamentally, TSF design depends on the in-situ ground conditions, and time of construction (given the ever-developing regulations and requirements) and the base treatment (lined or unlined). Furthermore, the choice of TSF will depend on whether it is designed as an upstream, centreline, or downstream construction.

To develop a robust water balance for a TSF, a structured stage system is proposed. This will allow mines to assess the TSF's storage capacity in an effective realistic approach as follows:

- Stage 1: Matchbox approach
  This approach begins with a basic "matchbox" check, where inflows and outflows are compared to estimate changes in storage. This is based on current information at hand.
- Stage 2: Informed approach
  Current data-informed assessment. This incorporates site monitoring information such as slurry flows, rainfall records, evaporation records, pond levels, seepage flows, piezometer measurements and phreatic levels to refine stage one estimates.
- Stage 3: Detailed approach
  Detailed analysis using advanced tools such as three-dimensional modelling, survey data, and geotechnical investigations to capture the spatial and temporal behaviour of water within the facility. It involves a detailed process to acquire spatially distributed hydraulic and geotechnical properties, bathymetry, survey grids and run 3D models and ensembles, all related to the stability of the facility.

By progressing through these stages, shown visually in Figure 4, the water balance development evolves from a simple check to a comprehensive management tool, ensuring that both short-term operations and medium and long-term risks are effectively addressed. However, prior to following these approaches, it is important that key information is gathered about the site and from its position in the regional context.

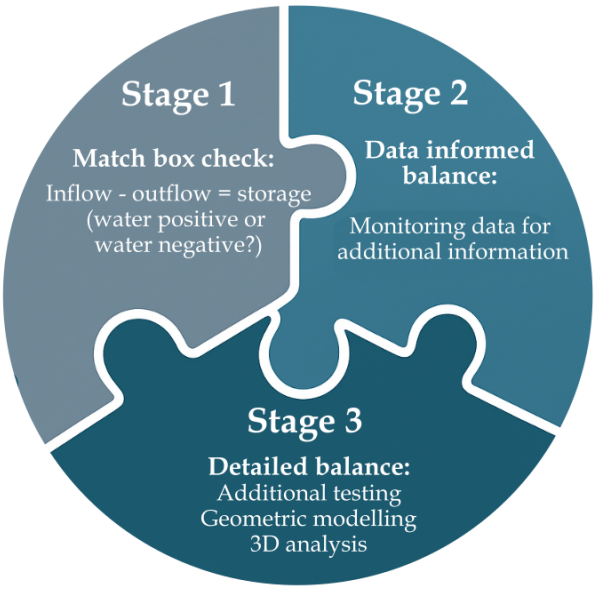


Figure 4. Approach to the TSF-specific water balance.

Basic parameter development & guidance for a three-stage TSF water-balance program
Identifying key parameters controls the focus of the water balance assessment. This will enhance the staged approach to ensure that a robust set of parameters is utilised effectively and realistically. The flow of data development should follow the staged approach described above.

Data gathering
Data is essential at every stage of a water balance model to ensure accuracy and relevance. The data will include typical parameters such as actual type of mine, type of TSF and geometry (pool areas, footprint etc.), climatic inputs (local and regional), rainfall, storm statistics and evaporation/ evapotranspiration rates, seepages (both groundwater into the TSF and seepage from the TSF base), deposition tonnages, slurry volumes and densities, specific gravity, dry density, void ratios, porosity, phreatic surfaces, hydraulic conductivities to name a few. Some of the data will be readily available, others will require detailed investigations and analysis. These parameters and their mechanisms are detailed in Table I.

Table I. Key parameter and data requirements

Category	Examples / Parameters	Relevant Stages
• Climate and Meteorology	Rainfall, evaporation, storm statistics	Stage 1: Basic estimates Stage 2: Linked to weather data Stage 3: Extreme event analysis
• Operational Process Data	Run-of-mine (ROM) production, slurry density, return water rates	Stage 1: ROM tonnage & slurry density Stage 2: Regular operational data Stage 3: Integrated with water use forecasts
• Pond and Geometry	Pond water level, stage-area-volume relationships, beach topography, bathymetric survey	Stage 1: Simple assumptions, pond levels, areas & volumes Stage 2: Monitored pond levels Stage 3: Survey-based, installation of piezometers,

Category	Examples / Parameters	Relevant Stages
		geometry & 3D modelling
• Tailings Properties	Specific gravity, void ratios, degree of saturation, hydraulic conductivity, compressibility/consolidation parameters	Stage 1: Generic values and volumes Stage 2: Existing data Stage 3: Detailed geotechnical investigations, CPTu testing
• Boundary/Drainage Elements	Penstock and seepage drains, liners, permeable horizons, and groundwater levels	Stage 2: Visual inspections & seepage monitoring Stage 3: Hydrogeological modelling
• Instrumentation	Pond gauges, piezometers, flow meters, weather stations, SCADA/telemetry databases	Stage 2: Install and monitor instruments Stage 3: Long-term datasets for calibration
• Monitoring Data	Time-series records, survey updates, operational logs	Stage 2: Short-term data records Stage 3: Continuous datasets for trend analysis

Planning guidelines

Each stage in the water balance development will depend on the availability of data. Typical timelines for mine management to consider are:

- Stage 1: Immediate (days → weeks)
- Stage 2: Near term (weeks → 3 months)
- Stage 3: Long term (3-12 months)

In addition to the above, procurement considerations of at least 3 months can be added to the current timelines.

Recommended practical tolerances

In developing and applying any stage for water balance models for TSFs, it is important to recognise that absolute precision is neither possible nor practical. Instead, tolerances and target levels of accuracy should be defined to guide data collection, model development, and decision-making. These tolerances acknowledge the variability of natural systems (e.g., rainfall, evaporation and seasonal changes), the uncertainty in material properties (e.g., tailings hydraulic conductivity), and the operational challenges of measuring flows and volumes in real time.

Establishing realistic, accurate targets ensures that models remain both credible, flexible and operationally useful, providing sufficient confidence for management decisions to be made without creating unrealistic expectations.

The following should be considered as a guideline:

- Rainfall: ±2–10% (gauge siting and wind effects).
- Evaporation: ±10-15% (seasonal considerations).
- Pond WL: ±0.02-0.05 m (regular surveys).
- Bathymetry depth: ±0.1-0.5 m depending on depth.
- Stage-area-volume relationship: ±5% of volume (depends on survey resolution and frequency).
- Slurry density: ±2-5% (continuous or frequent grab samples).
- Tailings geotechnical parameters: order of magnitude (Stage 1)- initial assumptions, narrowing to ±20% (Stage 3)- based on targeted lab and field-testing refinement.
- Piezometers: ±0.01-0.05 m.
- Hydraulic conductivity (field): reported as range; ensure order-of-magnitude confidence and quantify spatial variability.
- Seepage/drainage flows: ±10-20%.
- Return flow meters: ±2-5% reading.

Uncertainty handling & realistic notes
Uncertainty is unavoidable in water balance modelling due to variable climatic conditions, measurement errors, and limited data. The aim is not to eliminate uncertainty but to manage it transparently, focusing on the largest contributors and refining estimates as new information becomes available. Pragmatic notes help ensure models remain useful for decision-making despite these limitations. The following considerations are provided:

- Stage 1 – Default assumptions: use conservative retention (higher retained porewater) and low recovery to avoid underestimating pond development.
- Stage 2 – Progressive reduction of uncertainty: calibration should reduce key uncertainties (pond geometry, return flows, basic seepage).
- Stage 3 – Additional testing reduces hydraulic/geotechnical uncertainties and 3D modelling.
- Data quality assurance procedures – Daily credibility checks (mass balance), monthly reconciliation, and correction of instrument errors.

Best practice parameters
For illustrative purposes, the following parameter ranges are considered best practice for a typical platinum TSF in South Africa. These values provide a benchmark for design, monitoring, and operational management. They are not absolute but should be refined as site-specific data becomes available. The best practice parameters are summarised in Table II.

Table II. Best practice parameters

Parameter	**Typical Range / Target**	**Notes / Best Practice Considerations**
• Rainfall data resolution	± 600 mm/year	Site-specific gauges: supplement with regional stations.
• Evaporation (pan data)	±1500 mm/year	Cross-check with station or satellite datasets.
• Slurry density (t/m^3)	1.45 – 1.55	Calibrate with plant data: maintain stability.
• Tailings solids SG	2.7 – 3.7	Verify per deposit.
• Tailings void ratio (e)	0.7 – 0.9	Depends on mineralogy and deposition method affects seepage/storage.
• Hydraulic conductivity (m/s)	1×10^{-7} – 1×10^{-8} (fine matrix)	Use lab/field tests, critical for seepage assessments.
• Phreatic surface position	≥ 5 m from downstream crest ≥ 50 m from downstream toe	Monitor via piezometers, trigger action if encroaching.
• Water recovery efficiency (%)	60 – 75%	Improve via decant systems, return pumps, or thickened tailings.
• Seepage collection efficiency (%)	≥ 80%	Design cut-off, toe, blanket, chimney drains, etc.

Worked example

Matchbox check

The first step in developing a water balance is to carry out the simple "matchbox" check as described in the above sections. The purpose of this first stage is not to deliver precise values, but rather to establish whether inflows and outflows are broadly consistent, and to identify any unexplained changes in storage.

This quick diagnostic tool highlights imbalances that indicate seepage losses, measurement gaps, or operational risks. This will enable the analyst to establish whether the TSF is water positive or negative. This foundational step builds confidence and provides a baseline for progressively more detailed assessments in later stages.

Inputs required for the matchbox check

To perform a Stage 1 matchbox check, the following key inputs must be identified. These values are typically available from mine records or can be estimated from site measurements and climatic data. While accuracy at this stage is not critical, using realistic values provides a meaningful first estimate of storage changes. Typical input values for a platinum mine in South Africa include:

- Dry tonnages: 240 kt/month
- Slurry density: 1.5 t/m^3
- Specific gravity (SG): 3.3
- Slurry water: 1.2 m^3 of water per dry tonne of tailings.
- Direct rainfall: 800 mm/ year.
- Evaporation: 1500 mm/year
- Areas: Dam 112 Ha, pool 7 Ha
- Dam volume: 22 400 000 m^3
- Dam void ratio: 0.9
- Other inputs: Catchment runoff onto TSF.
- Return water: Pumped back to the plant i.e. penstock, drainage systems.
- Seepage losses: 10% of inflows (estimate) below seepage drainage system.

These values are then combined to check whether inflows and outflows balance within reasonable limits. Any unexplained difference is treated as a change in storage, which highlights whether the facility is gaining or losing water overall. From the above, the following was calculated:

- Total inflows 486 000 m^3/month
- Total outflows 127 680 m^3/month
- Net Storage 358 920 m^3/month

It is therefore seen that the TSF is retaining water, and this creates a starting point for further development of Stage 2 and 3 investigations and assessments. To put this into perspective, an Olympic-sized swimming pool has a storage volume of 2 500 m^3, this equates to ~ 144 pools being stored in the facility per month.

Development of order of magnitude of water (OMW) factors for water balances

Through the development of a refined water balance, key OMW factors can be derived that can aid both mine management and the engineers to apply during the life cycle of the TSF. In the above example for a Stage 1 estimate, the volume of the TSF divided by the net storage is calculated as 62.4. These factors can then be calculated for each stage of the development of the TSF and ultimately for closure. The industry can then set limits to these factors based on the risk profile of the facility.

Critical water storage levels within a TSF

OMW factors will play a significant role in the strategic development of a water balance. A generic illustration is shown in Figure 5, whereby a frustum (circular TSF) is modelled against different heights versus the positioning of seepage drains i.e. toe and blanket drains. Further, if seepage occurs at a bench, the figure highlights a critical boundary (critical line). The position of seepage drains forms an integral part of the design of TSFs.

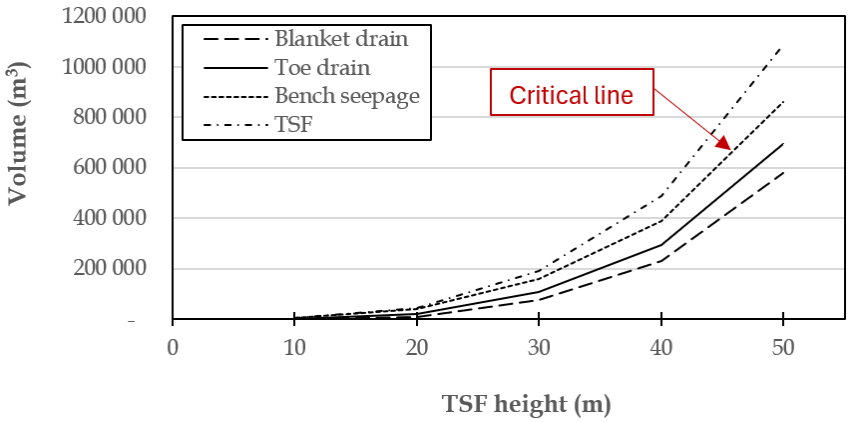


Figure 5. Critical storage zone

With further research, graphs such as nomographs and hydrographs aided by computer programs could form an evolutionary approach to understanding the knowledge base of site-specific TSF water balances.

Compliance regulations

In South Africa, dam safety guidelines are found in the National Water Act (NWA), 1998 (Act No. 36 of 1998) and its regulations regarding the safety of dams. The Act, together with these regulations, stipulate the registration of dams with a safety risk (wall height > 5m, capacity > 50,000m^3). The dams are classified into Categories I, II, or III based on size and hazard potential.

The Act further stipulates that owners must obtain a license for construction or modification, and for dams above a certain risk, a registered professional engineer must be appointed to be approved by the Department of Water and Sanitation, Dam Safety Office Directorate (DWS:DSO) (i.e., Approved Professional Person (APP)) to conduct safety inspections and ensure compliance with the regulations and their own common law duty of care.

For TSFs, merely using the pool storage volume in safety checks is incorrect, as the interstitial and water contained below the phreatic surface should be considered. This could change the classification of the facility and its risk profile. Currently, it is unknown which volumes to use when registering a TSF at the DSO. In the past, only the pool volume was considered, and now, sometimes the whole capacity of the TSF is considered. Most TSFs have a storage capacity larger than 50 000 m^3, but the amount of water inside this structure has not been quantified. This is where the site-specific water balance can fill the gap.

Key findings from a site-specific water balance

Carrying out a site-specific water balance for a TSF is essential for moving beyond assumptions and unknowns. The exercise allows operators to quantify, track, and manage the movement and storage of water, providing several important outcomes:

- Clarity on water storage – It identifies how much water is contained in the facility, which is often poorly understood but is central to both stability and water supply planning.
- Early warning of risks – Discrepancies between inflows and outflows highlight potential seepage, rising phreatic surfaces over time, or unmeasured discharges that may compromise dam safety. Links phreatic surface dynamics to TSF stability and factor of safety.
- Support for decision-making – Provides a structured basis for operational decisions such as assessing energy balance, reducing pond size, adjusting deposition, change of slope angle, enhancing drainage, or preparing for storm events.
- Improved water efficiency – By quantifying return water and losses, it supports process water recovery and reduces reliance on external water sources.
- Foundation for staged improvement – The simple "matchbox" check develops into progressively

more refined monitoring and modelling, creating a path towards continuous improvement.
- Compliance and transparency – Demonstrate responsible management to regulators, communities, and stakeholders by showing that water is being actively monitored and managed.
- Site-specific TSF water balances are to be conducted on a quarterly, biannual or annual basis depending on Life of Mine (LOM) status.
- Storing water on TSFs should always be avoided.

The site-specific water balance transforms the TSF from a "black box" into a measurable system. This shift from uncertainty to quantifiable information is critical for safe operation, sustainable water use, and long-term risk reduction.

CONCLUSION

Water management in mining cannot be fully understood without accounting for the unique role of TSFs. Unlike other site components, TSFs store large and variable volumes of water whose behaviour changes over time. If left unquantified, this storage represents both an operational unknown and a potential safety risk.

The three-stage water balance approach presented here offers a practical pathway to address this challenge. Starting with a simple "matchbox" check of inflows and outflows, operators can establish a baseline understanding of whether the TSF is gaining or losing water. Building on this, Stage 2 incorporates measured data such as pond levels, return water flows, and rainfall, refining the balance into a more reliable monitoring tool. Stage 3 then applies advanced modelling and geotechnical inputs to create a dynamic picture of water storage and movement, enabling predictive management.

The key message is that water balances should not stop at the site scale. By applying a TSF-specific focus, operators gain clearer insight into stored water volumes, improve water recovery, enhance dam safety, and align with international standards such as the GISTM. Ultimately, adopting TSF-specific water balances transforms the facility from a "black box" into a managed system (termed a "blue box"), reducing risks while supporting sustainable and responsible water use.

ACKNOWLEDGEMENTS

The authors would like to thank SRK Consulting participants who assisted with the compilation of this paper.

REFERENCES

Barthe, P., Eder, P., Savin, H. G. M., Orveillon, G. and Garbarino, E. (2018) *Best available techniques (BAT) reference document for the management of waste from extractive industries – In accordance with Directive 2006/21/EC*, Publications Office. https://data.europa.eu/doi/10.2760/35297

International Council on Mining and Metals (ICMM), United Nations Environment Programme (UNEP) & Principles for Responsible Investment (PRI), 2020. Global Industry Standard on Tailings Management. Available at: https://globaltailingsreview.org/global-industry-standard/

National Water Act (NWA), 1998 (Act No. 36 of 1998). Pretoria

Younger, P. and Wolkersdorfer, C. (2004) Mining Impacts on the Fresh Water Environment: Technical and Managerial Guidelines for Catchment Scale Management, *Mine Water and the Environment,* 23, s2-s80. DOI:10.1007/s10230-004-0028-0



Kurt Uderstadt

Principal Engineer
SRK Consulting

Kurt Uderstadt is a Principal Engineer with over 30 years of experience in geotechnical, civil, structural, and environmental engineering. Based in Johannesburg, South Africa, he specialises in the design and project management of complex infrastructure projects, including tailings storage facilities (TSFs), stormwater systems, and structural foundations. Kurt has extensive expertise in geotechnical investigations, stability analysis, hydraulic structures, and environmental rehabilitation.

Adapting to change: Filtered tailings and the future of tailings management

K. Naidoo, V. Balakistan

WSP in Africa, South Africa

In recent years, the mining industry has placed a spotlight on the operation and management of tailings storage facilities (TSFs) due to the devastating repercussions of mismanagement of TSFs. The focus of the experts in the industry has been directed at minimising the risk of failure that is usually associated with traditional slurry/wet deposition. This has led to the development of standards such as the Global Industry Standard for Tailings Management (GISTM).

For this reason and among others, mining companies are turning to alternative forms of deposition that pose less of a risk than conventional slurry deposition. Hence, the rising popularity of a relatively new technology referred to as filtered tailings (FT) deposition.

FT deposition is deemed a safer option primarily because of the low water content of the tailings. However, since the FT stacking method of deposition is a relatively new concept, we find ourselves facing new challenges and hurdles that have not been tackled before when it comes to its design and operation. There are plenty of unknowns and not enough research or case studies to understand how the facilities/materials will behave under certain conditions. There are also a host of different types of risks that arise with FT operations. This paper highlights our personal experiences in overcoming setbacks through innovative ideas and unique ways of thinking. It also delves into various case studies, showcasing the challenges encountered during the design and construction phase of an FT facility.

After all our research and experiences with FT stacking, we are left with a compelling question: Is FT stacking truly a better alternative to traditional slurry deposition? One can argue that the most dangerous risks – slope failure and breaches of liquefied tailings – are almost entirely mitigated with an FT operation. However, certain types of wet TSFs, such as those with engineered embankments (e.g., impoundment TSFs), significantly reduce the risk of slope failure as well. Therefore, a more refined question is: Are the new risks and challenges that come with FT stacking worth the effort, or should the industry continue exploring other methods of tailings storage?

INTRODUCTION

The dangers associated with wet TSFs have been tragically highlighted by several catastrophic failures in recent years. Notable examples include the Jagersfontein disaster in South Africa, the Brumadinho TSF collapse in Brazil and the Fundão TSF failure, also in Brazil. These incidents have not only resulted in devastating environmental and social consequences but have also catalysed a global shift in how tailings are managed. In response, regulatory bodies and industry stakeholders have introduced frameworks such as the Global Industry Standard for Tailings Management (GISTM) and the Consequence Classification System (CCS), placing significant pressure on mining companies to meet the highest safety and environmental standards (ICMM, 2023; Global Tailings Review, 2020).

Compliance with these standards is no longer just an industry requirement — it is a moral imperative.

In light of these developments, the mining industry is increasingly turning to filtered tailings (FT) deposition as a safer alternative to conventional slurry deposition. FT deposition is considered safer primarily due to the lower water content in the dewatered tailings, which significantly reduces the risk of embankment failure caused by elevated pore water pressures. In the event of a slope failure, FT material is more likely to slump rather than liquefy, thereby avoiding the destructive 'mudslide' scenarios often associated with wet facilities. Additional benefits include improved water recovery, reduced environmental impact and smaller facility footprints (McLanahan, 2020; Mining Magazine, 2020).

However, while FT deposition offers promising advantages, it is not without its own set of challenges. The relative novelty of FT stacking means that there is limited empirical data and operational experience to guide design and management practices. Unique risks, such as material variability, compaction behaviour and operational logistics must be carefully considered and addressed (Davies, 2020; Lupo & Hall, 2020). These complexities underscore the need for continued research and innovation in this space.

This paper presents practical insights and lessons learned from recent FT projects, focusing on the challenges encountered during the design and construction phases. Through case studies and personal experiences, it explores how innovative thinking and adaptive strategies have helped overcome setbacks. Ultimately, the paper aims to critically evaluate whether FT stacking is a viable long-term alternative to traditional slurry deposition, or whether the industry should continue exploring other tailings storage and deposition solutions.

FILTERED TAILINGS – NOT A PERFECT SOLUTION

One of the primary challenges with FT or dry stack TSFs (DTSFs) is the stringent criteria that must be met, particularly regarding moisture content (MC). The design and construction of a dry stack facility leave little room for error, as any deviation from the specified criteria can lead to significant operational issues (Davies, 2020). For instance, achieving the correct MC is critical to supporting the stability and compaction of the tailings. This requires meticulous planning and coordination among various stakeholders, including design engineers, construction teams and operational staff.

Case Study 1 serves as a pertinent example of the complexities involved in managing a FT facility or DTSF. Although we will delve deeper into this project in subsequent sections, it is worth noting here that the stringent MC criteria posed significant challenges. This issue is not unique to this project but is a commonality across most dry stack facilities, highlighting the importance of early and thorough planning (Davies, 2020).

In addition to technical constraints, the financial implications of DTSFs are significant. Both capital expenditure (CAPEX) and operational expenditure (OPEX) can be substantial. If the initial planning and design are not executed correctly, the operational costs can escalate dramatically, impacting the overall project budget (Flottmann, Williams & Kazmi, 2019).

It is essential to emphasise that dry stack facilities, while innovative, are still relatively new in the industry. This novelty means that there are less historical data and fewer established best practices compared to wet facilities. As such, it is imperative to approach DTSFs with caution and to recognise that they come with their own set of unique challenges and unknowns (Davies, 2020).

Another significant challenge with DTSFs is their sensitivity to rainfall and water accumulation. Since dry stacks do not have freeboard and were never designed to retain water, even small low spots formed during rain events can lead to ponding, overtopping risks and elevated pore water pressures. This highlights the need for strict operational control and effective stormwater management to rapidly divert runoff off the facility. Unlike slurry facilities, which incorporate engineered water-handling systems

and detailed regulatory guidance, dry stacks lack mature design standards for water management, making them vulnerable to infiltration, softening of compacted layers and potential liquefaction under sustained wet conditions. These concerns are amplified in regions with higher rainfall, as frequent or intense precipitation can diminish the intended stability benefits of filtered deposition. As a result, climate conditions must be a central factor in evaluating the suitability of a dry stack TSF, and wetter regions may require additional engineered controls to ensure safe long-term operation.

Therefore, while dry stack tailings facilities have many benefits, they are not a perfect solution. The stringent design criteria, high CAPEX and OPEX and the need for careful planning and coordination make them a complex and demanding solution. As the industry continues to evolve, it is crucial to remain vigilant and proactive in addressing the unique challenges posed by DTSFs.

CASE STUDY 1

Introduction

There are various case studies that we will reference in this paper. However, we will pay special attention to one specific example of an FT facility where we were involved extensively in the design and construction phase. We will refer to this facility as Facility 1. Facility 1 is located in an arid area that experiences hot, wet summers and dry, mild winters. The tailings are classified as a Type 3 waste, therefore the facility is required to be lined by a Class 3 barrier system according to the National Environmental Management: Waste Act (NEM:WA)(Act no.59 of 2008). Facility 1 is a temporary storage facility specifically designed to hold tailings for a period of less than five years, after which the deposition will commence in another location.

Issues during the design and construction phases underscored the importance of clear communication and collaboration across disciplines. A key lesson was that working in silos or within narrow battery limits hindered progress, whereas coordinated cross-disciplinary effort proved essential. However, the biggest takeaway from working on this project was the importance of ensuring that the design criteria is met on site. This is especially important when it comes to FT operations as we have seen that out-of-spec material can potentially halt production at the mine plant until the desired condition is achieved. This is a major consequence for the mine.

A specific criterion that will be examined in this paper is the moisture content (MC) of the tailings. Facility 1 was designed assuming the tailings to have an MC of between 12-13% in metallurgical terms. This range was chosen as it is close to the optimum moisture content (OMC), meaning that the highest compaction densities can be achieved at this range of MC. During the construction phase, testing completed on the filter press indicated that the actual MC achieved was between 15-20%. Material handling test work indicated that this range exceeds the transportable moisture limit, making the tailings susceptible to liquefaction during transportation. This was a major concern as the effects of the higher MC were not fully understood but it was known that it would have a negative effect on the stability of the FT facility if not handled properly. Therefore, a range of testing was undertaken to determine the effects of MC on the properties and behaviour of material, which is discussed later in the article.

The most obvious solutions to the MC problem would be to:

- Procure a more effective filter press.
- Locate a large enough area for the tailings to dry out atmospherically before being placed onto the Facility 1 footprint.

However, in the case of this site, the biggest constraints were the available capital and time. The mine was not willing to invest in the site because it was a temporary storage facility. Therefore, the solution had to require almost no additional capital. Furthermore, the mine was planning to begin production within a couple of months and therefore the solution had to be identified and implemented immediately. These two constraints were extremely limiting; however, some very innovative solutions

were identified, which will be discussed in the following sections.

The Critical Role of Moisture Content in Dry Stack Tailings Storage Facilities

MC is a critical parameter in the design, construction and operation of DTSF. Case Study 1 serves as a cautionary tale on the profound impact that deviations in MC can have on a mining operation. Facility 1 was originally designed to handle tailings with a low MC, which meant that the drainage layers may not have been equipped to manage the excess water associated with wetter tailings. The operational aspects such as the handling and placement of tailings were also impacted. Additionally, the difficulties in achieving the necessary compaction compromises the structural integrity of the facility. Due to the construction process already nearing completion, no alterations to the design could be made and the solution to the problem had to be implemented prior to the tailings reaching the facility.

The elevated MC essentially halts the mine production until the issue can be resolved. The tailings material is split at the stockpile, with portions transported to both the DTSF and the paste backfill plant. The inability to transport and store tailings safely on the DTSF poses a significant risk to the entire operation. The wetter tailings are prone to liquefaction during transportation by load and haul trucking, making it unsafe to move the material to the DTSF. This not only affects the storage of tailings but also has a knock-on effect on the backfill plant, which requires tailings with a maximum MC of 14%. The higher MC disrupts the backfill operations, further complicating the overall project. In addition, the expected higher MC will lead to a reduction in the lifespan and capacity of the facility. This highlighted the importance of planning for MC variability from the outset, as basing designs on a fixed assumed MC (12%) proved insufficient.

An additional complication was the confusion between the definition of "moisture content" according to metallurgical engineers and geotechnical engineers. The metallurgical definition is the percentage mass of water divided by the total mass of the sample, whereas the geotechnical definition is the percentage mass of water divided by the mass of solids only.

Options Assessment

When it became clear that the MC could not be lowered by the filter press due to capital constraints, we were tasked with identifying solutions for drying the tailings. The options needed to be cost effective and easy to integrate into the existing system and deposition methodology. Furthermore, the solution would have to address multiple aspects of the MC issue such as the transportation, stability of the facility, compressibility, trafficability and also the paste backfill plant requirements. Interestingly enough, another hindrance for the project was that it became difficult to give recommendations as there were very little data and case studies to refer to. There is a notable knowledge gap in the industry regarding the technology of dewatered tailings and FT stacking.

In order to tackle the task, we reached out to internal and external experts to develop a comprehensive list of options. We ended up with 20 solutions altogether ranging from lime addition, Geotubing, in-line flocculation, etc. Many of the options would have been viable and effective but were not implemented due to the abovementioned limitations.

One of the most viable and obvious options would have been to air dry the tailings before placing it onto the facility. The main drawback of this option was the need for potentially lining the air-drying footprint with a class-C barrier, which would be a costly exercise. There were no prior studies that were available or documented for testing the effectiveness of this application. Therefore, we had to undertake our own testing to determine the time and space requirements for atmospheric drying to be an effective and successful solution based on the tailings production schedule provided by the mine.

Laboratory Testing

Laboratory testing was carried out to determine the extent of the effects of MC on the properties and behaviours of the tailings. Unfortunately, the full suite and range of testing that was initially planned was not completed due to project complications. This paper presents the testing results that added value to the project such as:

- Optimum moisture content (OMC) and maximum dry density (MDD)
- California bearing ratio (CBR) tests
- Foundation indicator tests
- Oedometer tests
- Shear vane tests
- Triaxial tests
- Air drying tests

All MC values referred to in this section will be in terms of the metallurgical definition.

OMC and MDD
The dry density-MC curve is developed through these tests and indicates the MC at which the material will reach its peak dry density under compaction. This point is known as the OMC and MDD. It is generally observed that the material behaves most favourably when it's in this state.

This test is conducted by preparing samples to a range of MC levels. Each sample is then compacted into a mould. The final dry density for each sample is then recorded.

Figure 1 indicates that the OMC for the tailings is approximately 10.9% and the corresponding MDD is 2057 kg/m³. A significant drop in dry density as MC increases was observed. At an MC of 12.5%, the dry density decreased to 2036 kg/m³. This highlights that excess moisture negatively impacts compaction and density.

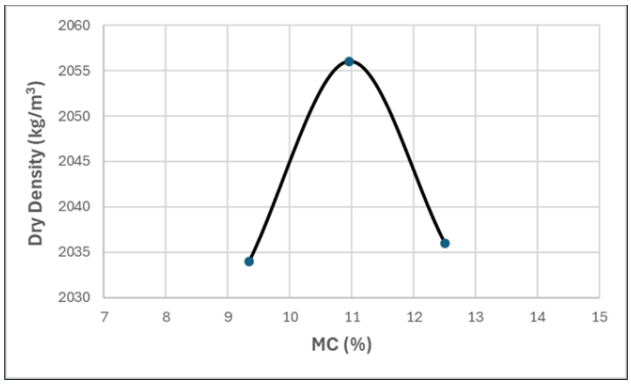


Figure 1: MDD and OMC results.

California Bearing Ratio Tests
The outcome of the CBR test provides an indication of the bearing capacity of the material. The lower the CBR value, the lower the bearing capacity and vice-versa. The purpose of this test was to determine how the MC levels of the tailings would affect the trafficability on the FT facility.

Figure 2 shows the CBR value versus compaction effort for the various samples and illustrates that the higher the MC, the lower the CBR value, indicating that significant trafficability is lost when tailings are placed wet of the OMC. The results also emphasise the importance of achieving the specified compaction effort and densities on site, as the CBR value decreases with a decrease in density achieved.

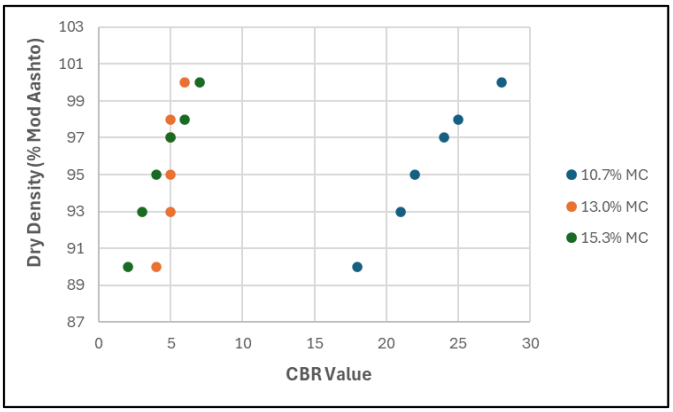


Figure 2: CBR results.

Oedometer Tests

The purpose of this test was to compare the effect that varying MC levels have on the compressibility/ consolidation potential of the tailings and gauge the sensitivity of these parameters.

The results are presented in the form of the effective stress verses void ratio for each sample. The lower the void ratio measured, the more densely the sample can be compressed/consolidated on site and therefore, the higher the stability of the tailings over time and vice-versa.

Figure 3 presents the results of the oedometer tests. The sample prepared to a lower MC achieved a much lower void ratio than the sample prepared to a higher MC. This demonstrates that the sample with a lower MC has the ability of becoming much more densely consolidated when loads are placed on it (i.e., as the Facility 1 is raised) than the higher % MC sample. The denser and more consolidated the tailings become, the higher the strength of the tailings and vice-versa.

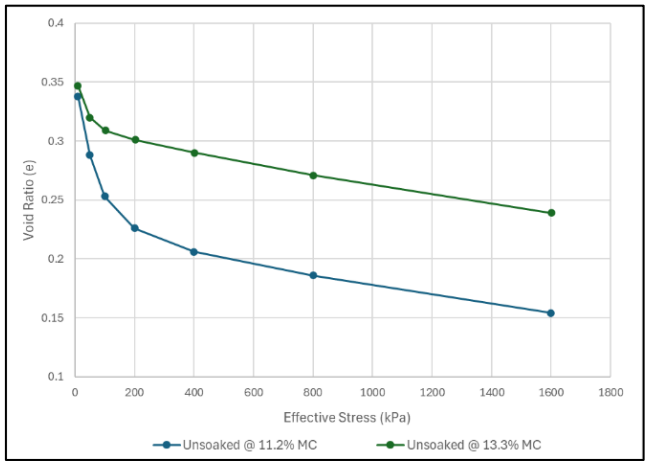


Figure 3: Oedometer results.

Shear Vane Tests

The purpose of performing shear vane testing for this project was to gain an understanding of the sensitivity of the shear strength due to change in MC. Multiple shear vane tests were conducted on remoulded samples with varying MCs, ranging from 10% to 14%, in order to derive a comprehensive comparison of the effect that MC has on the shear strength.

Figure 4 presents graphically the shear strength obtained versus the MC of the sample. The results demonstrate that approximately 20% of the peak shear strength is lost by an increase of MC from 10.7%

to 11.5%. A minimal increase in MC may lead to a drastic loss of shear strength. Therefore, the shear vane testing has provided an indication of the importance of maintaining the MC as low as practical to ensure that the shear strength is not compromised.

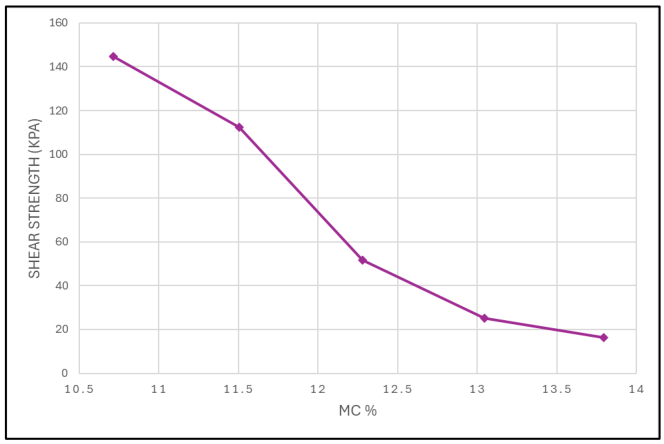


Figure 4: Shear vane results.

Triaxial Testing

Triaxial tests provide an indication of the shear strength parameters of a material. The parameters derived from the triaxial tests are usually applied as inputs into a stability analysis. The idea for conducting triaxial testing for this study was to determine the effect that increasing the MC of the tailings have on the strength parameters of the tailings and in turn the structural stability.

The initial aim was to conduct multiple sets of triaxial tests using samples prepared to various MC levels. Due to project complications, only one set of tests were done with sample prepared to MC of 13.3% and densely remoulded. The results from this test were compared to previous test work done for the same material, which was loosely remoulded and prepared to OMC.

Figure 5 presents the stress paths for the densely remoulded sample at 13.3% MC. Figure 6 presents the stress paths for the loosely remoulded sample at OMC. The 13.3% MC sample (densely compacted) results were more favourable than the sample prepared to OMC, due to the fact that the 13.3% MC sample exhibits dilative behaviour while the OMC (loosely compacted) sample exhibits contractive behaviour. More investigations need to be made into this phenomenon; however, the theory here is that the compaction effort plays a bigger role than MC for the strength of the material.

The comparison of the results, once again, emphasises the need for the specified compaction efforts to be met on site.

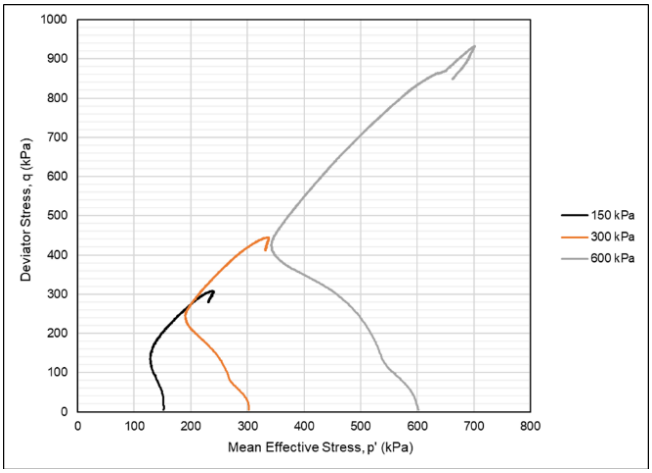


Figure 5: Effective vs deviator stress (13.3% MC densely compacted).

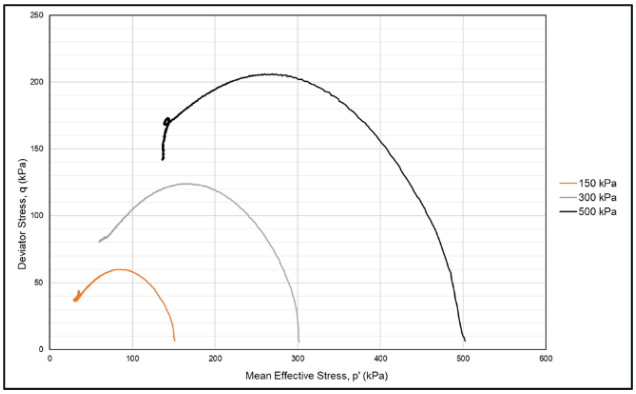


Figure 6: Effective vs deviator stress (OMC loosely remoulded.)

Conclusion

The test work results demonstrate that the optimum MC is around 10.9% and anything higher than this value leads to less favourable conditions such a decline in transportability, operability and structural integrity of the material and facility. Hence, tailings at the expected MC of 15-20% will be extremely difficult to handle and cause short-term operational issues and long-term stability issues.

Furthermore, there is evidence to support that the densities achieved on site will also play a role in the behaviour of the material. Therefore, it is important that the design criteria specified for these parameters are strictly adhered to.

Atmospheric Drying Tests

In the absence of comparable tests within the industry, we embarked on a unique journey to address the critical questions surrounding the air drying of tailings. Standard laboratory tests such as triaxial and CBR tests provided valuable data, but they fell short of answering the most fundamental questions: Could the tailings dry? How long would it take? And what area of space on-site would be required to dry the tailings adequately without causing significant delays in the production schedule and the placement of tailings on the DTSF? The lack of industry data made it essential for us to generate our own drying curves, particularly to understand whether the material could reach its OMC within an operationally acceptable timeframe.

Our testing schedule was carefully planned to simulate natural environmental conditions. We prepared tailing samples with initial MCs of 14.5%, 17.4% and 20%, then we placed them over a drainage layer in containers. These containers were then exposed to sunlight during the day and kept at a constant room

temperature of 30°C in the afternoons. Over a period of five days, we monitored the drying process, measuring MC and water levels at regular intervals. Two test types were completed: a drained test (100 mm lift thickness) and an undrained test (250 mm lift thickness), allowing us to compare the effect of drainage and thickness on drying rates.

By physically handling the tailings in the laboratory, we gained insights into its behaviour that standard tests could not provide. We observed how quickly the tailings settled and how easily they liquefied with minimal disturbance. This hands-on approach revealed that the tailings, at the current moisture limits, were not transportable. Pressing into the tailings caused water to rise, indicating that the material was too wet and sludgy to support vehicle traffic, let alone compaction. These visual observations aligned strongly with MC measurements: the 17.4% and 20% samples released free water shortly after placement, while the 14.5% sample remained moist but structurally stable.

The drying results were particularly insightful. For the drained tests, all three samples (14.5%, 17.4% and 20%) reached approximately the OMC after two days where most of the moisture loss occurred in the first 48 hours. The wetter samples also released 600–700 g of free water into the drainage container. In contrast, the undrained 250 mm sample required six to seven days to reach OMC and only began to dry noticeably after Day 4. This clearly demonstrates the impact of drainage and lift thickness on achievable drying times. Most importantly, these results allowed us to directly answer the operational question: "Is air drying feasible within the required timeframe?" Based on our findings, thin drained lifts (100 mm) can dry to design specifications within two days, whereas thicker undrained lifts (250 mm) may require up to a week. This provides the mine with realistic expectations for drying pad sizing and operational sequencing.

This experience reinforced the value of stepping back, defining objectives clearly and embracing innovative thinking when faced with complex problems. As young engineers, our fresh perspectives proved valuable, and by collaborating across our international team, we were able to develop an effective testing procedure. The air-drying tests not only demonstrated the importance of creativity and resilience but also provided practical insight: atmospheric drying can be effective when tailings are placed in thin lifts with drainage support, allowing MC to reach design criteria in roughly two days, whereas thicker undrained layers require significantly longer drying times.

OTHER CASE STUDIES

Case Study 2: Çöpler Gold Mine Heap Leach Failure

The Çöpler Gold Mine heap leach failure is a significant case study that challenges the perception of DTSFs as inherently safer than wet facilities. This incident, which occurred on 13 February, 2024, resulted in a catastrophic landslide that tragically claimed the lives of nine workers and caused extensive environmental damage (SSR Mining, 2025; Eos, 2024).

It is important to note that the categorisation of the Çöpler heap leach as a 'dry stack' is itself subject to industry debate. The mining industry currently lacks a universally accepted definition or checklist that clearly distinguishes dry stack, filtered tailings, hybrid systems and wet deposition. As a result, classification often depends on operational practice, water content and engineering intent rather than codified standards. Although some industry peers may argue that Çöpler does not meet their personal definition of a dry stack facility, its method of deposition, low initial moisture levels relative to slurry, and stacked configuration justify its inclusion as a relevant case study. More importantly, the failure highlights that structures commonly perceived as 'dry' can still behave like saturated, flow-prone systems under unfavourable conditions—an insight directly aligned with the objectives of this paper.

The heap leach at Çöpler was classified as a dry stack, yet the failure exhibited characteristics more commonly associated with wet facilities. Instead of the expected slumping, the failure was a flowing one, indicating a subcritical state with a high phreatic surface in the basin. The high water content within the heap leach material significantly contributed to the disaster (SSR Mining, 2025).

Several factors led to this failure, including the facility exceeding the height ranges supported by global empirical experience for heap leach and dry-stack-type structures. Reports indicated that the heap leach height reached 257 m, far exceeding the 150 m upper bound typically observed in international case histories and operational practice (SSR Mining, 2025). Additionally, the excessive water content in the heap leach, coupled with its accumulation near blasting points in the production area, exacerbated the situation (SSR Mining, 2025).

The failure at Çöpler highlights the importance of adhering to stringent design standards. The design errors, insufficient monitoring during the operation phase, inadequate warning systems and lack of an effective management system to act upon warning signs of cracks were all influential factors in the occurrence of the incident (SSR Mining, 2025).

Another major factor contributing to the failure was the geographic location and placement of the heap leach. The facility was situated in an elevated valley with a height of 100 m, creating a pyramid of 350 m. The elevated nature of the valley accelerated the movement of soil, aggravating the disaster (Descartes Labs, 2025). Geographic considerations, including weather conditions and the valley's topography, played a crucial role in the failure. The environmental impact of the failure was significant. The release of cyanide into the environment posed a severe risk to local water sources and ecosystems. The incident underscored the need for rigorous environmental monitoring and adherence to safety standards to prevent such disasters (Eos, 2024).

The Çöpler Gold Mine heap leach failure serves as a stark reminder that dry stack facilities, while perceived to be safer, are not without their own set of challenges. This case study highlights the importance of thorough planning, adherence to design standards and continuous monitoring to ensure the safety and stability of tailings facilities. It also emphasises the need for a comprehensive understanding of geographic and environmental factors in the design and placement of such facilities.

Case Study 3: Foundational Issues in Dry Stack Facilities

In our exploration of tailings management, we have identified moisture content as a significant challenge for DTSFs. However, it is essential to recognise that DTSFs are not immune to other issues, such as structural problems. This section introduces a case study from a power station project, highlighting the importance of thorough geotechnical investigations and proper planning.

The power station, commissioned in the mid-1980s, was initially designed with a 40-year operating life and an eight-year contingency period. Due to upgrades and other factors, the operating life has been extended to 60 years, with decommissioning expected by 2058. The initial dry ash dump site, designed to accommodate the station's operational life, is now under full capacity. To address this, an area to the north of the existing facility has been earmarked for additional ash disposal.

Unlike the moisture content challenges faced in Case Study 1, this power station project encountered foundational issues. A major problem arose due to an inadequate geotechnical investigation during the design phases, which failed to identify a section of the proposed facility was to be underlain by clay. During the construction and operation phases, a further geotechnical investigation was undertaken which led to the discovery of the clay. This oversight led a change in the layout and design of the dry stack to avoid constructing on the affected section and ensure the facility's integrity.

Interestingly, the facility is only partially lined. This was driven by South Africa's own legislation, which introduced formal barrier system requirements several years earlier. Under the National Environmental Management Act regulations (Regulations 632, 634, 635 and 636 of 2013), administered by the Department of Water and Sanitation, many mineral residue deposits, including tailings, were already required to include engineered barrier systems such as geomembrane liners (South Africa, 2013; Spies, 2020). Although the facility only began incorporating liners around 2020, coinciding with the release of GISTM, the requirement originated from national legislation. This late introduction resulted in only the newer sections of the facility being lined, complicating environmental authorisation and adding another layer of operational and design complexity.

This case study underscores that both wet and dry facilities can experience similar problems. Despite being classified as a dry stack and having dry tailings, the facility still faced foundational challenges and issues with the barrier system not meeting standards. While dry tailings may reduce the consequences of a failure, the fundamental issues remain the same.

The primary lesson from this case study is the importance of proper planning and thorough geotechnical investigations. If a comprehensive site investigation had been conducted early on, the presence of clay underlying a section of the facility would have been identified, preventing the subsequent changes to design.

Case Study 4: Another Instance of High MC

This case study is based on the information provided in a paper published in the Paste 2023 journal (Copeland, Daigle, & Strauss, 2023). The facility referred to in the paper is a FT deposit located in Namibia. According to the paper, the filtered tailings was transported by conveyor to the deposit. Due to the high mica and clay content, regular blockages occurred at chute transfer points. Two modifications were made to address these issues:

- Increased Moisture Content: Water was added to raise the MC which reduced blockages in the chutes.
- Chute Shape Redesign: The chutes were reshaped from box-like to tube-like (banana-shaped).

While these changes improved the operational efficiency by allowing the tailings to flow more freely and slumping further on the dump, increasing the moisture content by adding more water had several negative impacts:

- Supernatant water began to accumulate in low spots on the dump.
- Excess water infiltrated the groundwater, which was unexpected.
- Due to the high MC, the tailings flowed when deposited at the FT deposit. This led to the need for accelerated containment or sidewall construction using overburden material.

The additional water kept on the FT facility may also have led to structural stability issues. This case study showcases a real-life scenario of the implications of deviating from the design criteria.

NAVIGATING RAPID INDUSTRY CHANGES

The tailings management industry is evolving at an unprecedented pace, presenting significant challenges for engineers tasked with designing and implementing TSFs. Tailings management is a relatively new concept in relation to many other engineering disciplines and the standards governing mine waste design, classification and regulatory compliance are still emerging and being refined. This rapid evolution makes it difficult for engineers to keep up with the latest classifications and standards, which are constantly changing.

One of the issues we face as tailings engineers is ensuring that our designs remain relevant and effective over the long term, despite the industry's dynamic nature. We bear the immense responsibility of creating designs that not only meet current standards but also anticipate future regulatory requirements and industry advancements. This is a daunting task, given the lengthy and complex design and implementation process involved in tailings management.

The process of developing a TSF begins with the tendering phase, followed by kick-off meetings and progresses through several stages of design, including pre-feasibility, feasibility and detailed design for construction. Once the design is finalised, construction documents are prepared and issued before the facility can be built. This entire process can span many years, during which industry standards and regulations may change multiple times. Within this long and complex lifecycle, one of the most critical responsibilities of tailings engineers is planning for closure from the earliest stages. GISTM requires that closure and post-closure considerations be incorporated at project inception, ensuring that long-term stability, environmental rehabilitation and the safe management of residual tailings are all accounted

for in the initial design (GHD, 2024). Integrating closure planning upfront is essential to ensure that the facility can be responsibly decommissioned decades later and that the design remains resilient throughout the full life of mine.

As tailings engineers, we must ensure that our designs are robust enough to withstand these changes and still remain compliant throughout the facility's life of mine. This requires a proactive approach to monitoring industry trends and regulatory updates, as well as a commitment to continuous learning and adaptation. Furthermore, this responsibility places significant risk and accountability on the design engineers and the Engineer of Record (EoR). In the event of any issues, these professionals are often held accountable for ensuring that the designs are compliant and resilient to evolving standards and unforeseen challenges. The stakes are high and the consequences of any oversight can be severe, both in terms of safety and financial impact. Therefore, the role of tailings engineers and EoRs is pivotal in safeguarding the integrity and success of mining projects through to closure and beyond.

CONCLUDING REMARKS

In conclusion, our journey through this project serves as a cautionary tale of the critical impact of moisture content on FT facilities/DTSFs. The importance of planning cannot be overstated. This planning must commence well before the design phase, involving all stakeholders from the outset. It is essential that everyone, from process plant operators to on-site personnel and backfill plant teams, participates in these early discussions to ensure clarity and cohesion throughout the project.

Our experience has shown that while dry stacks offer certain advantages over wet facilities, they are not without their own set of challenges. The stringent criteria, particularly regarding moisture content, demand rigorous attention to detail and coordination. The lessons learned from our airdrying tests underscore the necessity of addressing these issues early on to avoid costly setbacks and operational inefficiencies. Mitigation measures for uncontrollable and changing variables (such as tailings properties, MC, production rates) should be planned for during the design phase.

Knowing what we know now, it is clear that the question of whether dry stacks are inherently better than wet facilities is not straightforward. Both methods have their pros and cons and the ultimate success of either approach hinges on thorough planning and execution. There is no one size fits all solution; the best approach is often site- and project-specific.

As we reflect on our findings, we pose a thought-provoking question to the industry: Are dry stacks truly the better option, or do wet facilities still hold their ground in certain contexts? The answer may not be definitive, but it is a question worth exploring as we continue to innovate and improve tailings management practices.

REFERENCES

Ajayi, S. (2012). Effect of Lime Varioation on the Moisture Contect and Dry Density of Lateritic Soil in Ilorin. *International Journal of Forest, Soil and Erosion, 2(4)*, 165-168.

Alrubaye, A., Hasan, M., & Fattah, M. (2016). Engineering Properties of Clayey Soil Stabilized with Lime. *ARPN Journal of Engineering and Applied Sciences, 11(4)*, 2434-2441.

Cacciuttolo, C., & Atencio, E. (2023). Dry Stacking of Filtered Tailings for Large-Scale Production Rates over 100 000 Metric Tons per Day: Envisioning the Sustainable Future of Mine Tailings Storage Facilities. *Minerals, 2023, 1445*, 1-30.

Copeland, A., Daigle, V., & Strauss, A. (2023). Is Implementation of Dry Stacking for Tailings Storage Facilities Increasing? A Southern African Perspective. *Paste 2023*, 611-619.

Davies, M. (2020) 'Filtered Dry Stacked Tailings – The Fundamentals'. Available at: https://open.library.ubc.ca/media/stream/pdf/59368/1.0107683/1 (Accessed: 19 February 2025).

Flottmann, S., Williams, D. and Kazmi, D. (2019) 'Cost-Effectiveness Of Tailings Dewatering And Stacking'. Australian Geomechanics Society. Available at: https://www.australiangeomechanics.org/papers/cost-effectiveness-of-tailings-dewatering-and-stacking/ (Accessed: 19 February 2025).

GHD (2024) 'Mine closures: planning for a century of maintenance'. Available at: https://www.ghd.com/en-ca/insights/mine-closures---planning-for-a-century-of-maintenance (Accessed: 19 February 2025).

Government of South Africa. (2008). *National Environmental Management: Waste Act 59 of 2008.*

Hudson, A., Hussey, A., Harley, A. and Dyhr, T. M. (2015) 'Simulating the Performance of a Dry Stack Tailings Design for Water Control Permitting'. Available at: https://www.imwa.info/docs/imwa_2015/IMWA2015_Hudson_082.pdf (Accessed: 19 February 2025).

Lara, J., Pornillos, E., & Munoz, H. (2013). Geotechnical- Geochemical and Operational Considerations for the Application of Dry Stacking Tailings Deposits. *Paste 2013*, 249-261.

Little, D. (1999). Evaluation of Structural Properties of Lime Stabilized Soils and Aggregates. *National Lime Association*.

Lupo, J. and Hall, J. (2020) 'Dry Stack Tailings – Design Considerations'. IQPC Corporate. Available at: https://www.iqpc.com/media/6139/588.pdf (Accessed: 19 February 2025).

Matthews, J., Dhadli, N., House, P., & Simms, P. (2011). Field Trials of Thin Lift Deposition of Amended Mature Fine Tailings at the Muskeg River Mine in Northern Alberta. *Paste 2011*, 271-280.

Newman, P., Bruton, M., Burgos, J. and Purrington, J. (2020) 'Innovations in Tailings Management – Hydraulic "Dry" Stacking'. Available at: https://www.angloamerican.com/~/media/Files/A/Anglo-American-Group-v5/PLC/our-stories/innovation-and-technology/innovations-in-tailings-managementhydraulic-Dry-stacking.pdf (Accessed: 19 February 2025).

Ovalle, C., & Le, V. H. (2024). Stability of Filtered Tailings Storage Facilities. *Geo Montreal* . Polytechnique Montreal.

UNDP (n.d.) 'Extracting good practices: Regulations, Feasibility, Development, Institutions, Planning, Exploration, Production, Closure, Post-closure & Licensing & Rule of Law'. Available at: https://www.undp.org/sites/g/files/zskgke326/files/publications/UNDP-MINING%20Step%2007.pdf (Accessed: 19 February 2025).

South Africa (2013) Regulations 632, 634, 635 and 636 under the National Environmental Management Act. Department of Water and Sanitation.

Spies, L.H. (2020) 'Design of a lined platinum tailings storage facility in South Africa', Journal of the Southern African Institute of Mining and Metallurgy, 120(7), pp. 385–396.

SSR Mining (2025) 'SSR review of Çöpler mine incident points to third-party design flaw'. Available at: https://www.mining.com/ssr-review-of-copler-mine-incident-points-to-third-party-design-flaw/ (Accessed: 19 February 2025).

Eos (2024) 'The 13 February 2024 landslide at the Çöpler Mine in Turkey'. Available at: https://eos.org/thelandslideblog/copler-mine-1 (Accessed: 19 February 2025).

Descartes Labs (2025) 'Çöpler Mine Case Study Update'. Available at: https://descarteslabs.com/hubfs/EDA_Copler%20Mine_Case%20Study%20Update_PDAC%202025.pdf?hsLang=en (Accessed: 19 February 2025).



Kiasha Naidoo

Tailings Engineer
WSP Africa

Kiasha Naidoo is a Tailings Engineer at WSP with a strong focus on geotechnical engineering and tailings storage facility (TSF) design. She holds a Bachelor of Science in Civil Engineering from the University of the Witwatersrand and has been actively involved in the mining and infrastructure sector since 2023. Although relatively new to the industry, Kiasha has already contributed meaningfully to several high-impact projects across South Africa, particularly in the field of filtered tailings (FT) and dry stack TSF operations.

Her experience includes serving as an assistant Engineer of Record (EoR) for operational monitoring of TSFs at three mines where she conducted inspections, analysed instrumentation data, and contributed to safety and performance reporting. She also played a key role in the development of a Dry Stack Tailings Storage Facility, where she authored the Operations, Monitoring, and Maintenance Manual. This work involved integrating GISTM-aligned protocols, developing surveillance and emergency response strategies, and addressing the unique challenges of FT stacking in a high-risk environment.

Kiasha has also conducted airspace modelling, geotechnical assessments, and design reviews. Her academic background includes a geotechnical design project focused on landfill slope stability and barrier systems, further reinforcing her technical foundation in critical state soil mechanics and slope performance.

She is proficient in a wide range of engineering software, including GeoStudio, Slide, AutoCAD Civil 3D, and HEC-RAS, and is particularly passionate about fluid mechanics, tailings dam design, and pump and pipeline systems. Her recent work on moisture content optimization for FT deposition reflects her commitment to innovation and problem-solving in the face of evolving industry challenges.

Driven by a deep sense of responsibility for the communities and environments affected by mining operations, Kiasha is passionate about advancing the field of tailings engineering. She is especially interested in improving surveillance, monitoring, and risk mitigation strategies for TSFs, recognizing the devastating consequences of tailings failures. Her work is guided by a strong ethical foundation and a desire to contribute to safer, more sustainable mining practices.

Kiasha is committed to continuous learning and collaboration, and she brings a fresh, enthusiastic perspective to the field. Her goal is to help shape the future of tailings management through thoughtful design, rigorous analysis, and a proactive approach to risk.



Veshania Balakistan

Tailings Engineer
WSP Africa

Veshania is a Tailings Engineer with four and a half years of experience in design, surveillance and monitoring of Tailings Storage Facilities (TSFs). She is currently employed at WSP Africa and is part of the Mine Waste team. Prior to this, she worked in the Tailings Department at Jones and Wagener for nearly three years. Her qualifications consist of a Bachelor of Science degree in Civil Engineering, which she obtained from the University of the Witwatersrand in 2020.

Throughout her career, she has had the opportunity of working on projects for various prominent Mining companies such as Anglo Gold Ashanti, De Beers, Glencore, etc. Her experience and expertise includes surveillance and design of a range of tailings facilities with various deposition and construction methods, namely; traditional upstream slurry deposition, impoundment facilities, dry stacking and filtered tailings facilities.

Assessment of causeway-induced loading on penstock towers

S.C.T. Luis, T. Armstrong

SRK Consulting, South Africa

Tailings storage facilities (TSFs) in South Africa commonly incorporate centrally located concrete penstock towers to facilitate the decanting of the supernatant pond from the TSF surface. During operation, these towers must be progressively raised in accordance with the rising elevation of the tailings. This is typically achieved by stacking prefabricated, interlocking concrete rings, often accompanied by internal grout sleeving to ensure vertical integrity and watertightness. The responsibility for raising the penstock towers lies with the TSF operator and any appointed contractors. To enable ongoing access to the penstock tower, which is located near the centre of the facility where the supernatant pool is managed, a tailings-constructed access structure (commonly referred to as a causeway or pool handle) is typically constructed and progressively raised. A catwalk is generally installed at the end of this structure to permit personnel access across the supernatant pool for inspection, maintenance and operational activities. However, the presence and geometry of this causeway introduces additional geotechnical considerations that are often not considered. If constructed in close proximity to the penstock tower, the causeway can impose unbalanced surcharge loads that may induce pressures which affect the structural integrity of the tower. If not properly accounted for, these loads could lead to tower distress or deformation through soil-structure interaction mechanisms. This paper investigates the interaction between the surcharge loading induced by a tailings causeway. Using analytical methods, the study examines the critical relationship between causeway height, distance from the tower, and the resulting impact on the tower's performance. A key focus of this paper is the determination of the critical causeway height and position, relative to the penstock tower, at which the structural integrity of the penstock tower is at risk of being compromised. The findings of this study aim to support engineers of record (EoR), designers and TSF operators by providing design guidance and operational limitations for causeway construction near penstock towers. By quantifying the critical parameters influencing soil-structure interaction in this context, the study contributes to the development of safer and more robust TSF operating guidelines. The outcomes are also applicable to other scenarios where surcharge loading adjacent to vertically stacked infrastructure in soft or transitional material poses a potential geotechnical risk.

INTRODUCTION

Tailings storage facilities (TSFs) are critical components of mining operations, designed to store fine-grained waste material generated during mineral processing. In South Africa, TSFs commonly feature centrally located concrete penstock towers to facilitate the decanting of supernatant water from the TSF surface. These towers are progressively raised during the operational life of the TSF to accommodate the rising elevation of tailings, typically through the stacking of prefabricated, interlocking concrete rings with internal grout sleeving to ensure structural integrity and watertightness. Access to these towers and supernatant pond control is facilitated by tailings-constructed causeways (also known as pool handles) and wing walls, respectively, which are also progressively raised to maintain functionality. While these structures are essential for inspection, maintenance and operational activities, their construction introduces geotechnical challenges that are often overlooked during design and operational planning.

The proximity and geometry of causeways and wing walls can impose unbalanced surcharge loads on the surrounding tailings, potentially inducing pressures that compromise the structural integrity of penstock towers through soil-structure interaction mechanisms. These risks are particularly concerning given the critical role of penstock towers in maintaining TSF stability and operational efficiency. Industry standards such as the Global Industry Standard on Tailings Management (GISTM), 2020, and the current South African National Standard (SANS) 10286, 1998, emphasise the importance of robust design and operational practices to ensure the safety and stability of TSFs. However, the impact of causeway and wing wall-induced surcharge loading on penstock towers remains an undeveloped area in TSF design and management.

This paper investigates the impact of surcharge loading induced by tailings causeways and wing walls on the magnitude of unbalanced forces exerted onto the concrete penstock towers. Analytical methods are employed to examine the critical relationship between the height of the causeway and wing walls, and their distance from the tower. The study aims to examine the relationship between the causeway and wing wall height and position, relative to the forces exerted onto the penstock tower. Excessive unbalanced horizontal loads on a penstock tower may result in the exceedance of the critical overturning moment, resulting in failure and loss of a key component to the functionality of a TSF. By quantifying one of the parameters influencing soil-structure interaction, this research provides valuable design guidance and operational limitations for causeway and wing wall construction near penstock towers. The findings aim to support engineers of record (EoR), designers and TSF operators in developing safer and more robust TSF operating guidelines, while also contributing to broader geotechnical applications where surcharge loading adjacent to vertically stacked infrastructure poses potential risks.

MATERIAL PARAMETERS AND CONFIGURATIONS

In order to find a generalised solution to the loading induced by a causeway and wing walls on a penstock tower, typical material parameters, structural configurations and construction materials were used during the analysis. The material parameters used are typical of southern African platinum TSFs and specifically relate to the tailings, as no other loading material was considered. The causeway and wing walls are constructed of a coarser fraction of tailings, typically achieved through cycloning or specified deposition strategies.

The penstock tower under consideration is a ringed penstock tower, which is typical of platinum TSFs in this region. The tower was analysed to a depth of 20 m, from the elevation of the tailings to the base of the tower. A maximum design height of approximately 20 m for a ringed penstock tower is considered industry norm (Stuart *et al.*, 2001). The material parameters and strength of the penstock tower was not considered in this study, as the paper focuses on the loading induced by the causeway and wing walls and not the resistance of the tower to failure. Notwithstanding this, the potential influence of unbalanced horizontal loading on a penstock tower is briefly discussed.

A typical configuration of a penstock tower, causeway and wing walls is illustrated in Figure 1. This configuration formed the basis of the analytical calculations discussed in this paper.

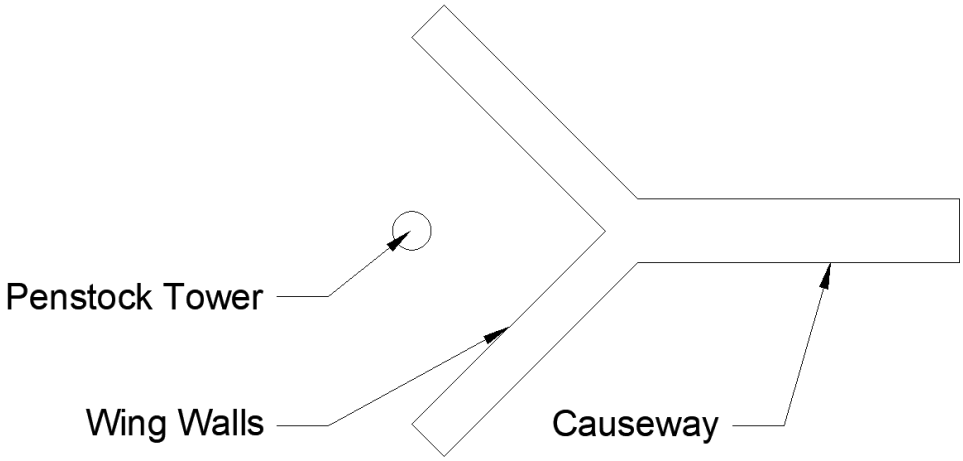


Figure 1. Typical configuration of the penstock tower, causeway and wing walls.

The causeway and wing walls are trapezoidal in cross-section, as is typically required on site. The causeway was analysed as illustrated in Figure 1, but the wing walls were simplified to a semicircle around the penstock tower to minimise computational complexity.

METHODOLOGY

The Boussinesq equation (Boussinesq, 1885) was applied to calculate the vertical stresses induced within the tailings and along the penstock tower as a result of the surcharge loading from the causeway and wing walls. It was assumed that the tailings is a homogenous, isotropic, elastic and semi-infinite medium during these calculations. The Boussinesq equation is given as:

$$\sigma_z = \frac{3Q}{2\pi z^2} \frac{1}{[1+\left(\frac{r}{z}\right)^2]^{\frac{5}{2}}} \quad [1]$$

Where:
Q – The magnitude of the point load acting on the surface
z – The vertical depth below the surface where the stress is being calculate
r – The horizontal radial distance from the point of load application to the point where the stress is calculated

The surface loads imposed by both the wing walls and causeway were calculated as multiple point loads (Q) per metre length from the penstock tower, continuing along the width of the wing wall and length of the causeway (r). The vertical stresses (σ_z) were calculated for each distance (r) at incremental depths of 0.5 m (z) along the height of the penstock tower, extending up to a depth of 20 m below the tailings surface. The vertical stresses calculated for each depth along the penstock tower, and for each distance (r), were converted into horizontal forces, considering the coefficient of lateral earth pressure at rest (K_0). The relationship proposed by Jáky, 1944, was used to calculate K_0 based on the effective internal friction angle (φ′) of the tailings. Jáky's equation is given as:

$$K_0 = 1 - \sin(\phi') \quad [2]$$

Where:
ϕ' - The soil's effective internal friction angle

For the purpose of this assessment, the distance from the penstock tower to the start of the wing wall will be described as x, while the distance between the penstock tower and the point at which the vertical point load has been calculated for use in Boussinesq's equation is described as r. In this analysis the wing walls were assumed to be semicircular with the total length as a function of the distance between the penstock and the start or the wing wall (x). This allowed the distance (x) from the penstock tower to be constant along the whole length of the wing wall. A total horizontal force acting on the penstock tower, induced by the wing walls and causeway, was calculated for each distance (r) as the summation of all forces calculated along the depth of the tower.

Furthermore, the height of the wing wall and causeway were adjusted to evaluate the effect of height on the vertical stresses and horizontal forces experienced at the penstock tower. Three heights of 2 m, 3 m and 4 m were assessed and compared following the same methodology described above for each.

RESULTS

To replicate typical conditions found in practice, the methodology described above was followed for varying positions of the wing walls. The distance of the wing walls relative to the penstock tower varied from 5 m to 40 m, in 5 m increments, and has been demarcated as distance (x). The position of the causeway remained adjacent to the wing walls (Figure 1) in each iteration. The results of varying the distance (x) between the wing walls and penstock tower was assessed for three different causeway and wing wall heights, namely 2 m, 3 m and 4 m. An increase in height corresponds to an increase in the induced surcharge load imposed by the wing wall and causeway structures.

A penstock tower is believed to be in equilibrium in the horizontal direction as the tailings surrounding the tower is homogenous and all-encompassing. The introduction of a load or force on a single side of the tower, such as the forces considered in this study, will result in an unbalanced system in the horizontal direction. This unbalanced system could potentially result in the tower overturning, if the critical moment is exceeded at its base.

The total horizontal force exerted onto the penstock tower for each height increment has been plotted in Figure 2. The distance (x) corresponds to the distance between the penstock tower and the toe of the wing wall.

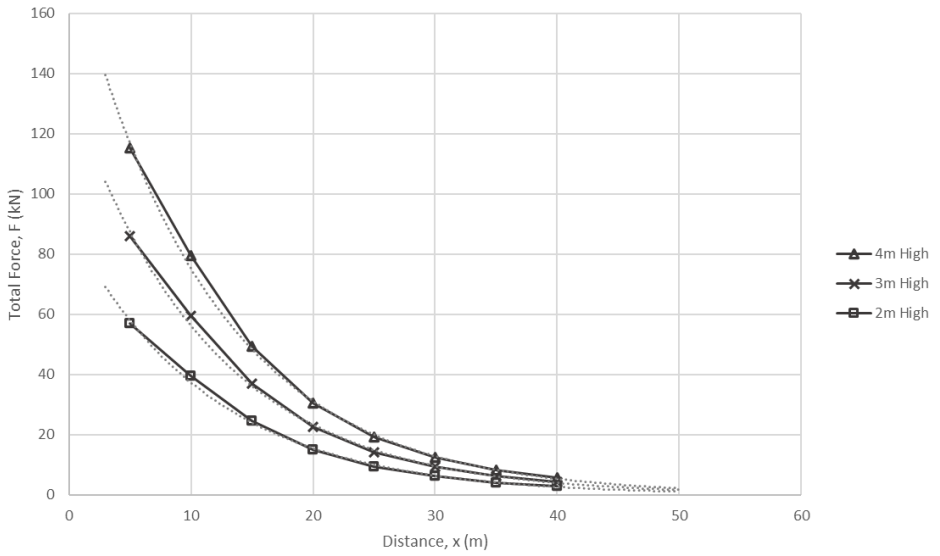


Figure 2. Causeway and wing wall distance vs. total force exerted onto the penstock tower.

It should be noted that the maximum value of r (Equation 1) used in the analysis was 80 m, with the penstock tower at 0 m and the maximum causeway distance at 80 m. Loading induced by a causeway (of typical height and density) was found to be negligible after approximately 80 m.

The equations of the line of best fit for each of the respective curves shown in Figure 2 are presented in Table 1.

Table 1: Line of best fit – distance vs total force

Causeway and wing wall height	Equation for line of best fit
2 m	$F = 181.57\ e^{-0.088x}$
3 m	$F = 135.62\ e^{-0.088x}$
4 m	$F = 90.05\ e^{-0.088x}$

Estimating an equation that can quantify the total force for a distance (x) serves as a means for evaluating the influence that stresses imposed by the causeway and wing walls may have on a penstock tower. It should be noted that the forces imposed by the wing walls are only a small portion of the forces that are imposed on a penstock tower during its operational life. Additional forces will, however, not be considered in this study but include drag down forces, self-weight, external water pressure and external tailings pressure. The total forces induced by the causeway may increase the drag down, external water pressure and external tailings pressure, which should be considered accordingly.

It should be noted that the above analysis was completed for a single penstock tower; however, if more than one penstock tower is present, the same maximum horizontal force will apply to all towers.

DISCUSSION AND ANALYSIS OF RESULTS

From the information presented in the results, it is evident that loading induced by the causeway and wing walls needs to be considered in the design and operation of TSFs that utilise penstock towers to decant supernatant water. The influence of unbalanced horizontal forces induced by a causeway and wing walls may result in the exceedance of the critical overturning moment of the penstock tower. Should the penstock tower lose verticality, and tilt passed the critical level of strain, the tower will be compromised, causing the inflow of fine tailings and interstitial water into the newly opened gap in the tower. Thus adversely affecting the downstream infrastructure and potentially the downstream environment.

Based on the results, the following key findings were noted:

- The total horizontal force exerted on the penstock tower increases, with increasing height of the causeway and wing walls.
- The total forces exerted onto the penstock tower decreases exponentially with increasing distance between the wing walls and the penstock tower.
- Beyond a distance of 40 m from the penstock tower, the loading curves begin to converge to a single line. This is advantageous to know as a change in wing wall or causeway material (example: waste rock), height or density will not affect the tower if constructed a distance greater than or equal to 40 m.
- Beyond a distance of 50 m from the penstock tower the total horizontal force becomes small to negligible. It can, therefore, be said that additional point loads (example, a track-mounted plant) will not have an influence on the vertical stability of the penstock tower at a distance equal to or greater than 50 m.

It was found that the total horizontal force (F) can be determined from the distance (x) between the wing walls and the penstock tower using the following equation:

$$F = a\ e^{bx} \qquad [3]$$

Where:
F – Total horizontal force
a – Exponential coefficient
e – Euler's number
b – Exponent constant
x – Distance between the wing walls and penstock tower

From Equation 3, it should be noted that the coefficient of the exponential function is directly influenced by the weight of the wing walls and causeway, as it is the only variable that changes with the increase in weight. Although, this is not to say that the coefficient is not influenced by distance (r) or depth (z) of Boussinesq's equation.

The exponent of the exponential function, however, is uninfluenced by weight and is only affected by changes to distance (r) and depth (z) of Boussinesq's equation. Therefore, for a causeway and wing wall configuration like the one presented in this paper (including simplifications and assumptions), the exponent of the exponential equation presented in Equation 3 will remain -0.088.

The use of the exponential equation can assist with determining the safe distance in which the wing walls and causeway should be constructed and operated from the penstock towers, such that the stability of the TSF remains within acceptable serviceability and design limits.

IDEALISED APPROACH

For completeness, a simplified version of the analysis is presented in this section. The updated analysis has used conservative material parameters and a generic causeway and wing wall configuration. The analysis aims to present a set of graphs based on the information, equations and outcomes presented earlier in this paper. The graphs may be used to determine if the horizontal loading induced by wing walls and a causeway will exceed the critical overturning moment of a penstock tower.

In order to present graphs that can be used in practice, a simplified causeway and wing wall configuration was used and is illustrated in Figure 3. It should be noted that this configuration is similar to that used earlier in the study to generate the initial results. The wing wall and causeway widths are provided, along with the demarcation of distance variable (x). A conservative tailings bulk unit weight of 22 kN/m^3 and penstock height of 20 m below the tailings level were used in the analysis to increase the probability that the results will be higher than those obtained through normal practical applications.

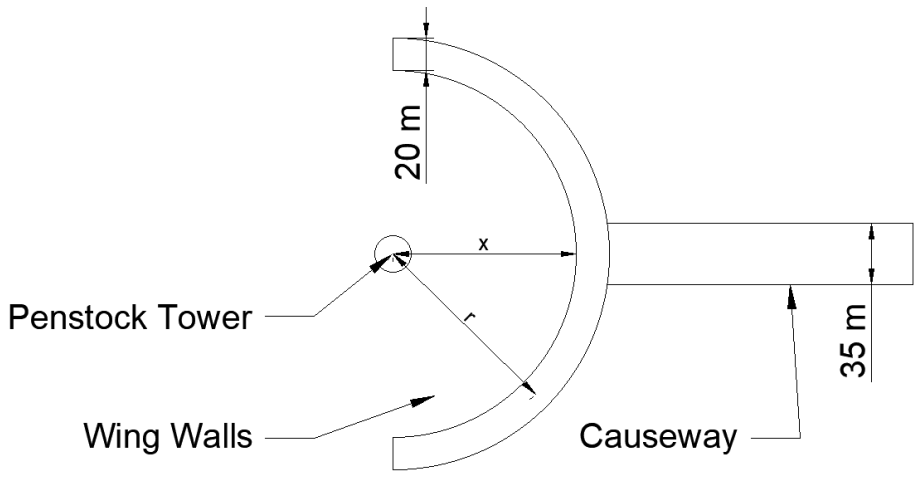


Figure 3. Simplified configuration of the penstock tower, causeway and wing walls.

Four graphs have been presented in Figure 4, presenting the results of four different causeway and wing wall constructed heights. The four heights were chosen by their applicability to typical southern African TSFs. The graphs can be used if the critical overturning moment, and the corresponding critical horizontal load, of a penstock tower is known.

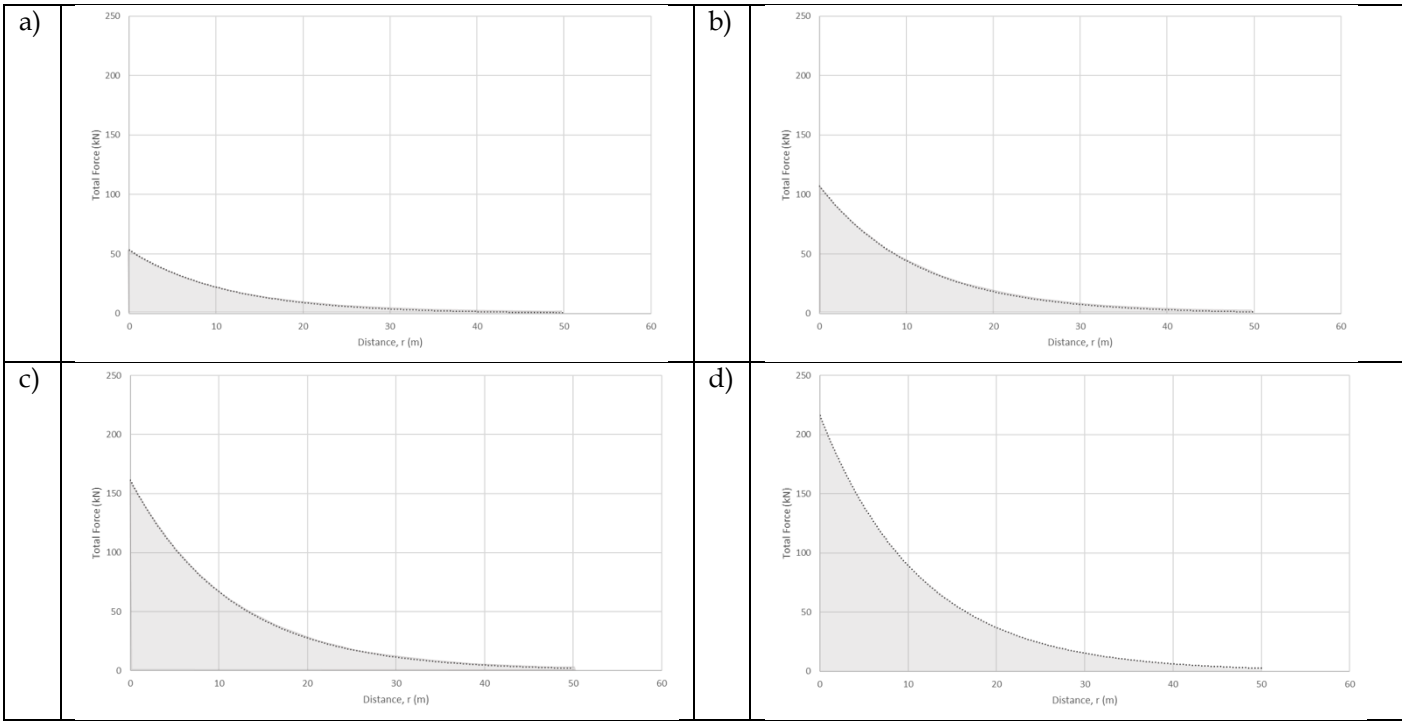


Figure 4. (a) 1 m causeway height. (b) 2 m causeway height. (c) 3 m causeway height. (d) 4 m causeway height.

The graphs presented in Figure 4 contain shaded regions beneath the calculated exponential line for each height. If the pre-determined critical horizontal load plots within this shaded region, the penstock tower is susceptible to failure through the mechanism of overturning.

It should be noted that this is a simplified approach to determine the position and height of wing walls and a causeway. The graphs are unique to the specified configuration and material parameters that were used. Additionally, no partial material factor of safety or partial load factor of safety was used in the determination of the graphs.

CONCLUSION

This study highlights the critical importance of considering surcharge loading induced by tailings causeways and wing walls in the design and operation of TSFs that utilise penstock towers for decanting supernatant water. The findings demonstrate that unbalanced horizontal forces exerted on penstock towers due to these structures can significantly impact their stability, potentially leading to structural failure, compromising the functionality of the TSF.

Key insights from the research include the exponential relationship between the total horizontal force exerted on the penstock tower and the distance between the tower and the wing walls or causeway. It was observed that increasing the height of these structures increases the horizontal forces, while increasing their distance from the penstock tower reduces the forces exponentially. Beyond a distance of 40 m, the loading curves converge, indicating minimal influence on the tower, and at distances greater than 50 m, the forces become negligible. These findings provide valuable guidance for determining safe construction and operational distances for wing walls and causeways to ensure the stability of penstock towers.

The study emphasises the importance of implementing robust design and operational practices that consider soil-structure interaction mechanisms and unbalanced loading conditions. By identifying and quantifying the parameters affecting these interactions, the research provides practical tools, including the derived exponential equation, to assess and address risks associated with surcharge loading near penstock towers.

A set of four idealised graphs were presented as a means of determining the position and height of a causeway and wing walls in relation to the penstock tower.

Ultimately, this research contributes to the development of safer and more resilient TSF operating guidelines, aligning with industry standards such as the GISTM and the SANS 10286. The findings not only support EoRs, designers and TSF operators in optimising TSF designs but also provide broader geotechnical insights into managing surcharge loading adjacent to vertically stacked infrastructure. By addressing these challenges, the study aims to enhance the safety, functionality and environmental governance of TSFs in the mining industry.

REFERENCES

Boussinesq, J.V. (1885). Applications des potentiels à l'étude de l'équilibre et mouvement des solides elastiques.

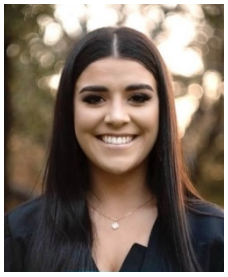
Global Industry Standard on tailings management (2020) Global Tailings Review. Available at: https://globaltailingsreview.org/global-industry-standard.

Jáky, J. (1944). The Coefficient of Earth Pressure at Rest.

Knappett, J. and Craig, R.F. (2012). Craig's soil mechanics. 8th ed. Abingdon, Oxon ; New York: Spon Press.

South African Bureau of Standards. (2025). DRAFT SANS 10286: Code of practice: Mine residue. Pretoria: SABS Standards Division.

Stuart, R.J., Venter, D.J. and Shepherd, P.J. (2001). Tailings dam penstock decants in the South African mining industry, Tailings and Mine Waste 2001. Balkema, Rotterdam.



Simone Luis

Civil Engineer
Company: SRK Consulting (South Africa)

Simone Luis is a Junior Civil Engineer with over two years of experience in structural and geotechnical engineering, with a strong focus on the tailings industry. Her work has involved supporting the design, analysis, and monitoring of tailings storage facilities, contributing to safe and sustainable mining practices. She has contributed to greenfield tailings dam designs, with specific focus on concrete infrastructure such as penstock towers, return water dam intake towers, and silt traps. She has also contributed to penstock pipeline alignment design and on-site QA/QC during construction phases. She brings a practical and detail-oriented approach to projects, drawing on a solid foundation in civil engineering principles and a growing expertise in managing geotechnical challenges in complex environments.



Tyler Armstrong

Senior Geotechnical Engineer
SRK Consulting (South Africa)

Tyler Armstrong is a senior geotechnical engineer and project manager at SRK Consulting, where he has worked for the past five years. With an Honours degree in geotechnical engineering, Tyler Armstrong brings deep technical expertise and a strong project leadership background to the field of tailings engineering.

Throughout his career, Tyler Armstrong has specialised in the design, analysis, and management of tailings storage facilities. His work spans a wide range of critical activities including laboratory testing, numerical modelling, construction QA/QC, dam breach analysis, stability assessments, penstock structural analysis, and critical state soil mechanics. His integrated approach ensures the delivery of robust and resilient tailings solutions in line with evolving industry standards and sustainability objectives.

As a presenter at this conference, Tyler Armstrong shares insights grounded in both technical proficiency and practical experience, contributing to the advancement of geotechnical and tailings engineering practices globally.

Evaluating mine tailings reuse potential through geotextile dewatering

N. Budhai[1,2], G.W. Rathod[2]

[1]WSP Africa
[2]University of Witwatersrand, South Africa

Mine tailings management is commonly based on a linear disposal approach, where fine residues are stored as slurry with limited opportunity for reuse. Circular economy principles offer an alternative by transforming waste materials into reusable resources, with dewatering serving as a key enabling step. This paper presents a structured, qualitative methodology for early-stage assessment of geotextile-based dewatering of fine industrial residues, including fly ash and fine tailings. The paper adopts a conceptual and analytical approach based on published experimental studies, reported field applications, and bench-scale filtration observations. Governing material, process, and outcome parameters are organised into evaluation categories to support early screening rather than detailed design. The results show that dewatering performance cannot be inferred from material classification alone and that systematic early-stage assessment is essential for reducing uncertainty and supporting more sustainable tailings management.

Keywords: Geotextile dewatering, Tailings management, Geosynthetics' Circular Economy

INTRODUCTION

Mine tailings are increasingly recognised as a potential resource, rather than a waste management challenge, provided their physical and hydraulic behaviour can be effectively controlled (Pizarro Barraza *et al.*, 2024). A primary barrier to tailings reuse is excessive water retention, particularly in fine-grained tailings that are difficult to dewater using conventional methods (Wang *et al.*, 2014). Geotextile-based dewatering systems offer a viable pathway for water recovery and solids consolidation (Pirouzi *et al.,* 2024); however, tailings behaviour varies significantly between commodities and mineral processing routes (Liu *et al.,* 2025). This paper presents a structured approach for evaluating tailings reuse potential through geotextile dewatering. Figure 1 provides a conceptual overview of the key factors considered in assessing the reuse potential of dewatered tailings.

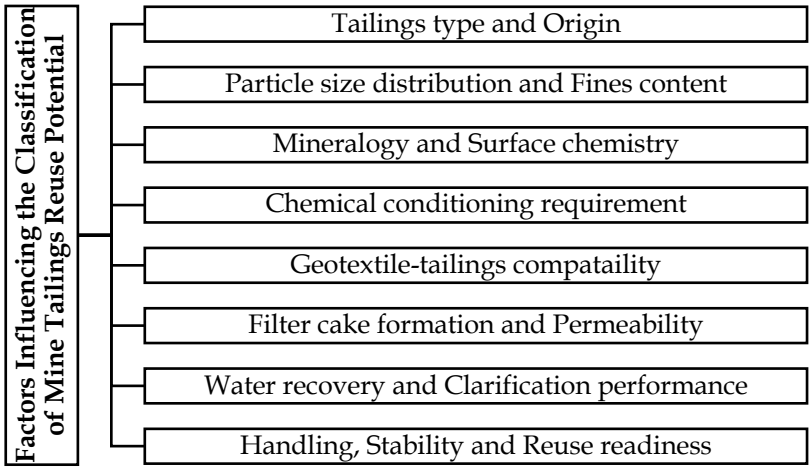


Figure 1. Key Factors Governing the Classification of Tailings Reuse Potential.

THEORETICAL BACKGROUND

Geotextile-based dewatering performance is governed by a set of interrelated factors spanning material characteristics, filtration processes, and post-dewatering outcomes (Aparicio Ardila *et al*., 2020). To establish a coherent theoretical basis for identifying these governing factors, this section synthesises relevant literature across three interconnected themes: the broader context of tailings management, the fundamental mechanisms of filtration-based geotextile dewatering, and the key parameters influencing material behaviour before, during, and after dewatering (Aydilek and Edil, 2002). Figure 2 illustrates the subsections that follow, which categorise existing knowledge into material-controlled, process-controlled, and outcome-based considerations; defining the parameter space that informs the category selection component of this study.

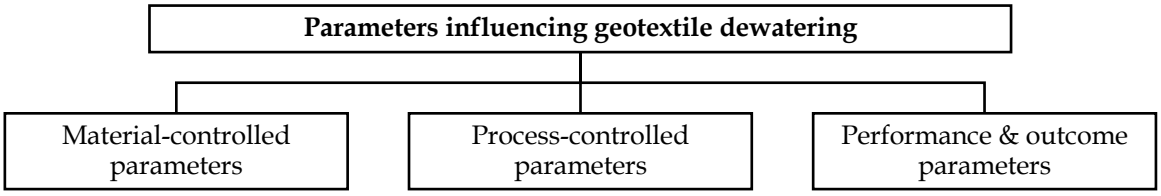


Figure 2. Fundamental parameters of geotextile dewatering.

Linear and Circular Paradigms in Tailings Management

Conventional mine tailings management remains largely governed by a linear waste paradigm, wherein tailings are produced as high-water-content slurries and permanently stored in engineered containment facilities designed primarily for isolation and long-term risk control (Cacciuttolo and Valenzuela, 2022). While this approach prioritises safety and regulatory compliance, it results in extensive land occupation, significant water losses, and long-term environmental liabilities, with limited material recovery or functional reuse (Muthukumaran and Ilamparuthi, 2006).

The magnitude of the tailings challenge is substantial. Globally, mine operations generate approximately 5–7 billion tonnes of tailings annually worldwide, with projections suggesting continued growth as mineral production increases (Araujo *et al*., 2022). In South Africa alone, historic mining has left extensive tailings footprints, with some estimates indicating over 270 historic tailings sites covering more than 400 km² within the Witwatersrand mining belt (Chetty *et al*., 2021). Contemporary surface tailings inventories across the country (including gold, platinum, chrome, and other commodities) are

measured in the hundreds of millions to over a billion tonnes, emphasising the scale of material that remains in legacy systems (*Chetty et al.*, 2021). Circular economy principles seek to address this imbalance by enabling controlled transformation of tailings into secondary resources; however, no single reuse pathway can realistically absorb the full volume of material produced (Pizarro Barraza *et al.*, 2024).

Fundamentals of Geotextile Dewatering

Geotextile dewatering relies on gravity-driven filtration, where water passes through a permeable geotextile while solids are retained, gradually forming a filter cake (Fatema and Bhatia, 2020). Unlike mechanical filtration or thickening processes, geotextile systems operate under low hydraulic gradients and depend on the progressive development of a stable filter cake to sustain drainage (Wang *et al.*, 2022). Dewatering is inherently time-dependent: the volume contained within the geotextile bag increases in cycles as water drains and additional slurry is added, with successive filling and drawdown stages continuing until the material reaches a consolidated state, as illustrated in Figure 3 (Kumar *et al.,* 2006). Performance is influenced by the properties of the filtration medium, as well as the physical, chemical, and interactional characteristics of the tailings (Wang *et al.*, 2025). Key outcomes (including water recovery rate, filtrate clarity, achievable solids content, and the structural stability of the dewatered material) determine the suitability of the system for downstream handling, containment, or reuse (Muthukumaran and Ilamparuthi, 2006).

Material-Controlled Parameters Governing Dewatering Behaviour

Particle size distribution and fines content strongly influence permeability and drainage potential, with fine-grained and ultrafine tailings forming low-permeability structures that restrict water release and prolong consolidation (Fatema and Bhatia, 2020). High proportions of particles smaller than approximately 10 μm increase capillary water retention due to the large specific surface area and pore-scale effects (Otoo *et al.*, 2025a). Tailings origin and processing history further influence dewatering behaviour through their impact on particle morphology and size distribution; for example, mechanically milled or chemically processed tailings typically exhibit finer, more angular particles that reduce permeability and slow drainage (*Chetty et al.*, 2021). Mineralogical composition and surface chemistry also play a critical role in controlling particle interaction and aggregation behaviour. Clay minerals, sulfide phases, and amorphous fines commonly exhibit negatively charged surfaces that promote dispersion and inhibit natural flocculation, resulting in slow settling and reduced filtration efficiency (Otoo *et al.*, 2025a). Conversely, calcium-rich or coarser mineral assemblages may exhibit improved aggregation behaviour and enhanced dewatering potential (Otoo *et al.,* 2025a).

Process-Controlled Parameters During Dewatering

Where material characteristics alone do not permit efficient dewatering, process-controlled parameters become increasingly important. Chemical conditioning through polymer flocculation is widely employed to promote particle aggregation, increase effective particle size, and enhance filter cake permeability (Aparicio Ardila *et al.*, 2020). Over- or under-dosing can result in poor floc structure, restabilisation of fines, or increased operational complexity (Aydilek and Edil, 2002). The interaction between tailings and the geotextile filtration medium further governs dewatering performance (Otoo *et al.*, 2025b). Geotextile properties such as apparent opening size, hydraulic conductivity, and surface texture influence solids retention, drainage rate, and susceptibility to blinding (Gibson *et al.,* 2023). Incompatible tailings–geotextile combinations may lead to excessive solids loss, rapid clogging, or restricted flow, limiting dewatering efficiency (Gibson *et al.*, 2023).

Performance and Outcome Parameters

Beyond initial drainage behaviour, dewatering performance must be assessed in terms of water recovery, filtrate quality, and post-dewatering material characteristics (Wang *et al.*, 2022). Water recovery and clarification performance are increasingly important due to water scarcity, process efficiency requirements, and regulatory constraints (Chetty *et al.*, 2021). Tailings that release water rapidly and produce clarified filtrate are more amenable to filtrate reuse and recirculation within mineral processing systems, while poor clarification increases downstream treatment requirements of the filtrate (Wang *et al.,* 2022). The ultimate dewatering objective is to produce a material that can be

safely handled, transported, and incorporated into engineered containment or infrastructure applications. Achievable moisture content, post-dewatering shear strength, and sensitivity to rewetting govern reuse feasibility (O'Kelly, 2013) . Tailings that remain highly sensitive to moisture changes or exhibit low structural stability after dewatering may present limited reuse potential despite effective water removal (O'Kelly, 2013). Linking dewatering performance to these outcome-based parameters is therefore essential for assessing the potential for tailings reuse.

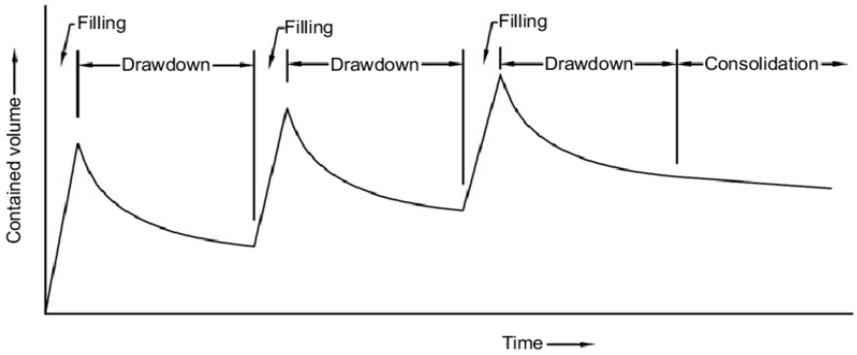


Figure 3. Typical field filling–drainage cycles.

METHODOLOGY

The methodology adopted in this study is conceptual and analytical in nature, aiming to systematically identify and structure the key parameters governing geotextile-based dewatering of mine tailings. The focus is on defining the parameter space to be considered when evaluating tailings dewatering and reuse potential. The scope of the methodology is limited to filtration-driven dewatering using geotextile systems operating under gravity conditions. Mechanical filtration, thickening technologies, and centrifugation-based methods are not considered. Emphasis is placed on parameters that can be assessed at an early stage using readily available material characterisation data, laboratory observations, or bench-scale testing.

Basis for Parameter and Category Identification

Governing parameters were identified through a structured review of published literature on tailings dewatering, filtration theory, geotextile applications, and mine waste management, as illustrated in Figure 2. Parameters were selected based on their consistently reported influence on filtration-driven dewatering performance across different tailings types and operational contexts, with consideration limited to those directly affecting water release, solids retention, filter cake development, and post-dewatering material behaviour. These parameters were structured into three interrelated groups: material-controlled categories, which define inherent drainage limitations before intervention; process-controlled categories, governing filtration effectiveness during dewatering; and outcome-based categories, representing practical performance measures related to handling, containment, and reuse (Figure 2). The inclusion of all three groups ensures that dewatering is evaluated not only as a water removal process, but as a material transformation step with implications for downstream management and reuse.

Defining categories under each parameter

To ensure practical applicability, identified parameters were screened based on their relevance to both laboratory-scale assessment and field-scale geotextile dewatering systems. Parameters requiring site-specific design assumptions or advanced numerical modelling were excluded, as the objective was to support early-stage evaluation rather than detailed system design. The remaining parameters were grouped into eight governing sub-categories that represent the dominant and recurring controls on filtration-driven dewatering behaviour reported in the literature. These categories are examined individually in the results section to evaluate their influence on drainage behaviour, filter cake

development, water recovery, and post-dewatering material performance, thereby providing a structured basis for assessing dewatering and reuse potential. The eight governing categories defined in this study are:

1. Tailings type and origin
2. Particle size distribution and fines content
3. Mineralogy and surface chemistry
4. Chemical conditioning requirement
5. Geotextile–tailings compatibility
6. Filter cake formation and permeability development
7. Water recovery and clarification performance
8. Handling, stability, and reuse readiness

Each category represents a group of related limitations that collectively influence filtration-driven drainage and material behaviour. The categorisation is intended to identify the primary factors controlling geotextile-based dewatering performance while preserving enough detail to reflect the variable and interacting nature of tailings materials.

Methodological Outcome

The primary outcome of this methodology is a structured set of evaluation categories that define the key parameters governing geotextile-based dewatering of mine tailings. These categories provide a conceptual framework for systematically assessing dewatering and reuse potential at an early stage, before detailed testing or system design.

RESULTS

The methodology's outcome is the identification and structuring of eight governing categories that collectively define geotextile-based dewatering behaviour in mine tailings. These categories represent the key material, process, and outcome parameters to consider when evaluating tailings dewatering and reuse potential. Figure 4 shows a longitudinal section of a geotextile tube, illustrating the internal drainage and solids retention mechanisms.

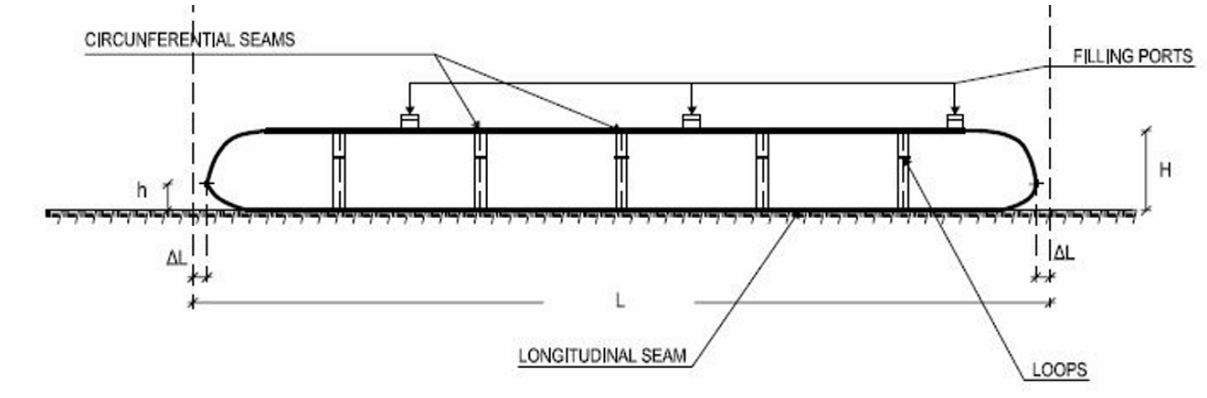


Figure 4. Longitudinal Section of a Geotextile Tube.

Integrated Interpretation of Dewatering Categories

The eight categories collectively describe geotextile-based dewatering as an integrated system rather than a single-process operation. Material-controlled parameters establish baseline constraints, process-controlled parameters govern filtration performance, and outcome-based parameters define practical success. The interdependence of these categories highlights the limitation of evaluating dewatering performance using isolated criteria and reinforces the need for a structured, multi-parameter approach.

Tailings Type and Origin

Mine tailings are highly variable materials whose properties are governed by ore type, mineral processing methods, and degree of grinding during beneficiation (Na *et al.*, 2024). Gold, copper, coal,

platinum group metals (PGM), and iron ore tailings exhibit markedly different particle size distributions, which strongly influence their dewatering behaviour. Coarser tailings, such as coal and iron ore residues, generally exhibit higher permeability and are more amenable to geotextile-based dewatering, often achieving effective drainage with limited or no chemical conditioning. In contrast, fine-grained tailings, including gold and PGM residues, and particularly diamond tailings, are characterised by high fines content and low permeability, resulting in poor natural water release and a greater reliance on polymer conditioning to enable effective filtration (Gibson *et al*., 2023). These differences directly influence settling behaviour, water retention, and the feasibility of dewatering technologies.

Particle Size Distribution and Fines Content

Particle size distribution (PSD) is a primary determinant of tailings dewatering performance, as it directly governs permeability, pore structure, and solids retention during geotextile filtration (Fatema and Bhatia, 2020). Tailings dominated by fine and ultrafine particles tend to form dense, low-permeability filter cakes that restrict water flow and inhibit gravity-driven drainage (Wang *et al.,* 2022). High proportions of particles smaller than 10 μm significantly increase water retention due to elevated specific surface area and capillary forces, resulting in slow consolidation and reduced drainage efficiency (Wang *et al.,* 2022). In geotextile dewatering systems, excessive fines also increase the risk of filter blinding and solids loss, particularly during the initial stages of filtration (Fatema and Bhatia, 2020). As a result, tailings with fine-dominated PSDs commonly exhibit poor untreated dewatering performance and require chemical conditioning or specialised filtration strategies to achieve acceptable water removal (Fatema and Bhatia, 2020).

Mineralogy and Surface Chemistry

Mineralogical composition and surface chemistry exert a critical influence on particle interaction, aggregation, and filtration behaviour in tailings slurries (Otoo *et al*., 2025b). Clay minerals, sulfide phases, and amorphous fines commonly possess negatively charged surfaces that promote particle dispersion and inhibit natural flocculation, resulting in poor settling and limited aggregate formation (Dehmani *et al*., 2026). Low-calcium and siliceous tailings are particularly susceptible to this behaviour due to the absence of naturally occurring binding mechanisms (Otoo *et al*., 2025b). In geotextile dewatering systems, dispersed particles are more likely to migrate through the filtration medium, increasing solids loss and contributing to filter blinding (Fatema and Bhatia, 2020). Surface chemistry, therefore, directly governs the need for chemical conditioning and influences the effectiveness of polymer-assisted aggregation in improving drainage and solids retention (Dehmani *et al.,* 2026).

Chemical Conditioning Requirement

Chemical conditioning using polymeric flocculants is widely employed to improve the settling and filtration performance of fine-grained tailings (Zhang *et al*., 2025). Flocculants promote particle aggregation through mechanisms such as charge neutralisation and polymer bridging, resulting in larger, more permeable floc structures that enhance drainage and solids retention during filtration (Kumar *et al.,* 2006). In geotextile dewatering systems, effective conditioning reduces fine particle migration, mitigates filter blinding, and supports stable filter cake development (Muthukumaran and Ilamparuthi, 2006). However, polymer response is highly material-specific, and inappropriate dosing can lead to floc breakage, restabilisation, or diminished drainage efficiency (Fatema and Bhatia, 2020).

Geotextile-Tailings Compatibility

Filtration-based dewatering systems depend on effective compatibility between the tailings particle size distribution and the selected filtration medium (Fatema and Bhatia, 2020). Key geotextile properties, including apparent opening size, permittivity, and hydraulic conductivity, govern solids retention, drainage capacity, and filter cake development (Muthukumaran and Ilamparuthi, 2006). Where incompatibility exists, fine particles may migrate through the geotextile, leading to excessive solids loss, or accumulate at the interface, resulting in rapid filter blinding and restricted flow. Both mechanisms significantly reduce dewatering efficiency and operational reliability (Fatema and Bhatia, 2020). Evaluating geotextile–tailings interaction is therefore essential for determining whether filtration-based dewatering can achieve stable performance and support tailings reuse objectives.

Water Recovery and Clarification Performance
Water recovery and filtrate clarity are critical performance indicators in tailings management, driven by water scarcity, process efficiency, and regulatory compliance (ICMM *et al.,* 2020). Tailings that release water rapidly and produce clarified filtrate during geotextile dewatering are more amenable to water reuse and recirculation within mineral processing systems (Cacciuttolo and Valenzuela, 2022). In contrast, poor clarification reflects ineffective solids retention, which increases downstream treatment requirements and reduces overall process efficiency. Dewatering performance must consequently be assessed in terms of combined solids consolidation and water quality outcomes when quantifying tailings reuse potential.

Handling, Stability, and Reuse Readiness
The ultimate objective of tailings dewatering is to produce a material that can be safely handled, transported, and incorporated into engineered applications. Achievable moisture content, post-dewatering shear strength, and sensitivity to rewetting are key parameters that govern the feasibility of reuse (Fourie *et al*., 2015). Tailings that retain excessive moisture, exhibit low structural stability, or experience significant strength loss upon rewetting may present limited reuse potential despite effective water removal. Dewatering performance must therefore be interpreted beyond volumetric water reduction and assessed in terms of its influence on material handling, stability, and operational reliability. Linking filtration outcomes to these practical performance indicators is crucial for quantifying the potential for tailings reuse in engineering and operational contexts.

DISCUSSION

This section discusses the implications of the proposed methodology for assessing geotextile-based dewatering of fine industrial residues. The discussion focuses on technical relevance, industry applicability, scalability, commercial value, and sustainability outcomes, demonstrating how structured early-stage assessment can improve dewatering performance and inform tailings reuse decisions.

Understanding Dewatering Behaviour Beyond Material Classification
Dewatering performance cannot be reliably inferred from tailings classification alone. Instead, material characterisation, baseline filtration behaviour, and conditioning response must be evaluated collectively to capture the governing controls on filtration-driven drainage. The methodology addresses this limitation by providing a structured and transparent approach for identifying feasible dewatering pathways without reliance on trial-and-error system design. Figure 5 presents the early-stage recommendations for industry implementation.

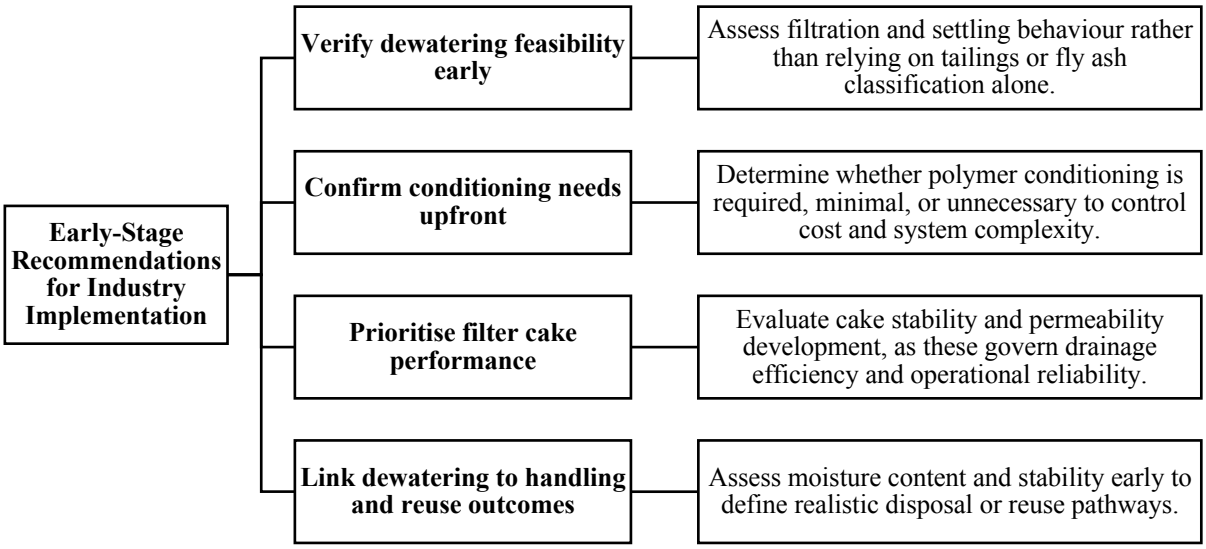


Figure 5: Early-Stage recommendations for industry implementation.

Linking Laboratory Indicators to Scalable Systems

The methodology yields performance indicators that are directly relevant to pilot and field-scale implementation. Observing settling behaviour, floc stability, and filtrate clarity provides insight into expected performance ranges rather than fixed design values, allowing realistic anticipation of drainage behaviour and system response. This screening-based approach aligns with established industry practice, where early-stage laboratory evaluation is used to inform pilot testing, reduce scale-up uncertainty, and guide subsequent system design without premature over-specification.

Commercial and Operational Relevance

The commercial and operational value of the proposed methodology lies in its ability to standardise early-stage dewatering assessment without prescribing site-specific operational parameters. By adopting a performance-based classification approach, the methodology enables comparative evaluation of dewatering options while allowing flexibility for project-specific optimisation. This ensures that key decisions can be made using consistent and transparent criteria, without requiring disclosure of proprietary design details or operational strategies. As a result, the framework supports broad industry applicability and commercial deployment, while maintaining adaptability to diverse materials, operating conditions, and implementation contexts.

Supporting Sustainable Tailings and Fly Ash Management

Improved early-stage assessment of dewatering performance contributes directly to more efficient water recovery, reduced storage volumes, and enhanced handling characteristics of tailings and fly ash. By enabling a shift from disposal-focused management toward reuse-oriented strategies, the methodology supports practical implementation of circular economy principles and encourages the valorisation of industrial residues. These outcomes also align with broader sustainability objectives, including responsible water use and resource efficiency, reflecting the goals of several Sustainable Development Goals (SDGs) while remaining grounded in practical industry application.

Influence of Geotextile Selection on System Performance

Geotextile selection governs solids retention, flow capacity, and susceptibility to clogging during dewatering and must be evaluated in conjunction with the conditioned material behaviour. Properties such as apparent opening size, hydraulic conductivity, and surface texture control the interaction between the filtration medium and the developing filter cake. Mismatched tailings–geotextile combinations can lead to premature blinding, excessive fines loss, or restricted drainage, limiting performance regardless of containment geometry or operating duration. The findings highlight that effective geotextile selection is a system-level decision, dependent on both material characteristics and

conditioning strategy, and is essential for achieving reliable and predictable dewatering outcomes at scale. The typical methods for installing geotextile tube anchors are shown in Figure 6.
.

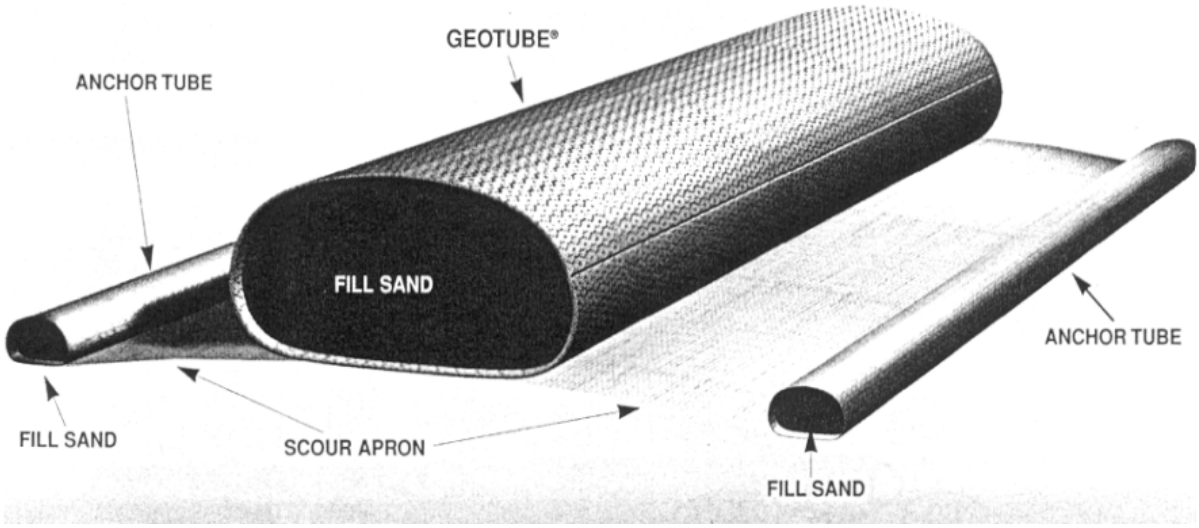


Figure 6. Typical Geotextile Tube Anchor Installation Methods.

CONCLUSIONS

A structured, systematic methodology for evaluating geotextile-based dewatering of fine industrial residues has been presented, highlighting the importance of integrating material characterisation, baseline filtration behaviour, and conditioning requirements. The approach provides a repeatable and transparent framework that reduces reliance on trial-and-error and supports informed early-stage decision-making for project development.

From an industry perspective, the methodology offers practical value by identifying whether conditioning is required, optimising operational efficiency, and enabling scalable implementation across diverse tailings and ash streams. The approach also contributes to sustainable tailings management by supporting water recovery, reducing storage volumes, and enhancing potential for material reuse, aligning with circular economy principles and broader environmental objectives.

REFERENCES

Aparicio Ardila, M.A., Souza, S.T. de, Silva, J.L. da, Valentin, C.A. and Dantas, A.D.B. (2020), "Geotextile Tube Dewatering Performance Assessment: An Experimental Study of Sludge Dewatering Generated at a Water Treatment Plant", *Sustainability*, Vol. 12 No. 19, doi: 10.3390/su12198129.

Araujo, F., Taborda Llano, I., Nunes, E. and Santos, R. (2022), "Recycling and Reuse of Mine Tailings: A Review of Advancements and Their Implications", *Geosciences*, Vol. 12, p. 319, doi: 10.3390/geosciences12090319.

Aydilek, A.H. and Edil, T. (2002), "Filtration Performance of Woven Geotextiles With Wastewater Treatment Sludge", *Geosynthetics International*, Vol. 9, pp. 41–69, doi: 10.1680/gein.9.0210.

Cacciuttolo, C. and Valenzuela, F. (2022), "Efficient Use of Water in Tailings Management: New Technologies and Environmental Strategies for the Future of Mining", *Water*, Vol. 14, p. 1741, doi: 10.3390/w14111741.

Chetty, S., Pillay Letitia and Humphries, M.S. (2021), "Gold mining's toxic legacy: Pollutant transport and accumulation in the Klip River catchment".

Dehmani, Y., Bentahar, I., Lgaz, H., El-Kordy, A., Aldalbahi, A., Alrashdi, A.A., Dehbi, A., *et al.* (2026), "A critical review of natural clay minerals: Structural characterization, textural properties, and adsorption mechanisms for sustainable wastewater treatment", *Materials Today Advances*, Elsevier, Vol. 29, p. 100682, doi: 10.1016/J.MTADV.2025.100682.

Fatema, N. and Bhatia, S. (2020), "Role of geotextiles pore size distribution in dewatering tests", *Geosynthetics International*, pp. 1–15, doi: 10.1680/jgein.20.00029.

Gibson, B.A.K.K., Nwaila, G., Manzi, M., Ghorbani, Y., Ndlovu, S. and Petersen, J. (2023), "The valorisation of platinum group metals from flotation tailings: A review of challenges and opportunities", *Minerals Engineering*, Pergamon, Vol. 201, p. 108216, doi: 10.1016/J.MINENG.2023.108216.

ICMM, UN and PRI. (2020), *GLOBAL INDUSTRY STANDARD ON TAILINGS MANAGEMENT*.

Kumar, S., Bhattacharya, S. and Mandre, N.R. (2006), "Journal of the Southern African Institute of Mining and Metallurgy", *Journal of the Southern African Institute of Mining and Metallurgy*, Southern African Institute of Mining and Metallurgy, Vol. 114 No. 11, pp. 945–949.

Liu, Y., Li, G., Yeoh, J.K.-W. and Hou, J. (2025), "Tailings management in sustainable mining: A production scheduling optimization framework", *Results in Engineering*, Elsevier, Vol. 28, p. 108365, doi: 10.1016/J.RINENG.2025.108365.

Muthukumaran, A. and Ilamparuthi, K. (2006), "Laboratory studies on geotextile filters as used in geotextile tube dewatering", *Geotextiles and Geomembranes - GEOTEXT GEOMEMBRANE*, Vol. 24, pp. 210–219, doi: 10.1016/j.geotexmem.2006.03.002.

Na, H., Eom, Y., Yoo, K. and Diaz Alorro, R. (2024), "A review on the reprocessing of sulfide tailings for resource recovery and AMD prevention using mineral processing methods", *Minerals Engineering*, Pergamon, Vol. 218, p. 109025, doi: 10.1016/J.MINENG.2024.109025.

Nguyen, C., Nguyen, A., Doi, A., Dinh, E., Nguyen, V.T., Ejtemaei, M. and Osborne, D. (2020), "Advanced solid-liquid separation for dewatering fine coal tailings by combining chemical reagents and solid bowl centrifugation", *Separation and Purification Technology*, Vol. 259, p. 118172, doi: 10.1016/j.seppur.2020.118172.

O'Kelly, B. (2013), "Undrained shear strength-water content relationship for sewage sludge", *Proceedings of the Institution of Civil Engineers: Geotechnical Engineering*, Vol. 166, pp. 576–588, doi: 10.1680/geng.11.00016.

Otoo, R., Razavi, M., Abankwa, B., Armah, A., Donkor, S. and Brakohiapa, E. (2025a), "Review of the Combined Effects of Mineralogy and Particle Size on Tailings Dewatering Mechanism", *American Journal of Mining and Metallurgy*, Vol. 8 No. 1, pp. 13–19, doi: 10.12691/ajmm-8-1-2.

Otoo, R., Razavi, M., Abankwa, B., Armah, A., Donkor, S. and Brakohiapa, E. (2025b), "Review of the Combined Effects of Mineralogy and Particle Size on Tailings Dewatering Mechanism", *American Journal of Mining and Metallurgy*, Vol. 8, pp. 13–19, doi: 10.12691/ajmm-8-1-2.

Pirouzi, A., Asrami, M.R. and Sabzehmeidani, M.M. (2024), "Advancement factors in sludge dewatering technology for wastewater treatment from engineering and economic perspectives: A review", *Environmental Functional Materials*, Elsevier, Vol. 3 No. 2, pp. 171–186, doi: 10.1016/J.EFMAT.2025.10.002.

Pizarro Barraza, F., Thiyagarajan, D., Ramadoss, A., Manikandan, V.S., Dhanabalan, S.S., Abarzúa, C.V., Sotomayor Soloaga, P., *et al.* (2024), "Unlocking the potential: Mining tailings as a source of sustainable nanomaterials", *Renewable and Sustainable Energy Reviews*, Pergamon, Vol. 202, p. 114665, doi: 10.1016/J.RSER.2024.114665.

Wang, C., Harbottle, D., Liu, Q. and Xu, Z. (2014), "Current state of fine mineral tailings treatment: A critical review on theory and practice", *Minerals Engineering*, Pergamon, Vol. 58, pp. 113–131, doi: 10.1016/J.MINENG.2014.01.018.

Wang, D., Tao, H., Wang, K., Tan, X. and Liu, Q. (2022), "The filterability of different types of minerals and the role of swelling clays in the filtration of oil sands tailings", *Fuel*, Elsevier, Vol. 316, p. 123395, doi: 10.1016/J.FUEL.2022.123395.

Wang, T., Wang, C., Liu, D., Yang, D., Li, P. and Dong, B. (2025), "Rapid dewatering and discharge of residual water quality through geotextile filtration coupled with flocculant treatment of contaminated dredged mud", *Environmental Research*, Academic Press, Vol. 271, p. 121032, doi: 10.1016/J.ENVRES.2025.121032.

Wu, Y., Gao, M., Zhang, X., Zhang, Y. and Ji, J. (2023), "Effect of initial water content on the dewatering performance of freeze-thaw preconditioned landfill sludge", *Environmental Research*, Academic Press, Vol. 239, p. 117356, doi: 10.1016/J.ENVRES.2023.117356.

Zhang, F., Bournival, G. and Ata, S. (2025), "Overview of fine coal filtration. Part II: Filtration aiding treatments and reagents", *Separation and Purification Technology*, Elsevier, Vol. 353, p. 128584, doi: 10.1016/J.SEPPUR.2024.128584.



Nikhiel Budhai

Civil Engineer
Maccaferri SA

Nikhiel Budhai is a civil engineer, systems thinker, and conscious designer whose work bridges technical innovation with sustainability and purpose. With expertise in geosynthetics, infrastructure resilience, and tailings valorisation, his approach integrates circular economy thinking into practical engineering solutions, particularly in the modelling of passive dewatering systems for mine waste reuse and water recovery. Certified in project management and engaged in postgraduate research in civil and environmental engineering, his work is grounded in both academic rigour and applied impact. His lifestyle, shaped by the principles of balance, clarity, and intentional living, informs a practice of engineering that is as mindful as it is technical.

Nikhiel brings a future-facing perspective to the mining and infrastructure sectors, where sustainability is not just a requirement but a conscious design choice that regenerates environments, strengthens systems, and uplifts the communities they serve.

Assessment and mitigation of slope stability risks for TSF closure

P. Sharma[1], M. Govender[2]

[1]WSP, India
[2]WSP Africa

The closure of a tailings storage facility (TSF) requires a comprehensive slope stability assessment to ensure long-term structural integrity and prevent potential post-closure failures, which can lead to severe environmental and social consequences. Closure planning must align with regulatory requirements, international standards (e.g., ICMM, GISTM), and corporate ESG commitments.

An extreme consequence classification TSF, located in South Africa, and receiving tailings from underground mining operations, is nearing the end of its life and is being planned for closure. To reduce the risks associated with this TSF, the option of partial remining (i.e., harvesting/excavating tailings) is being considered.

The initial slope stability assessment was based on available historical data, however, updated investigations were recommended for improved understanding of geotechnical parameters and pore pressure distribution and to support a more accurate stability analysis.

An updated slope stability assessment was carried out post completion of the recommended updated site investigation work, and for all loading conditions assessed the estimated factors of safety (FoS) values were below recommended targets.

Minimum FoS values were assessed with reference to established international guidelines including ANCOLD, CDA & GISTM guidelines. The two mitigation options were recommended:

- Raise the buttress, or
- Reprofile the downstream (local) slope, between the crest and first step-in/bench.

The assessment considered operational, constructability and freeboard constraints and indicated that either of these mitigation measures would need to be implemented, if feasible, and partial remining by itself is not adequate to reduce the TSF instability.

Keywords: TSF Closure, SLOPE/W, Slope Stability, Remining.

INTRODUCTION

The closure and remining of tailings storage facilities (TSFs) present complex geotechnical, environmental, and operational challenges that require a detailed understanding of both the current (short-term) condition and long-term performance of these structures.

With the growing emphasis on sustainable resource recovery, many legacy and active TSFs are now being evaluated for remining using hybrid approaches, where portions of the facility are reclaimed or reprocessed while other areas are concurrently rehabilitated and progressively closed. Such hybrid strategies not only aim to recover residual metals or critical minerals from previously deposited tailings but also to improve the long-term geotechnical stability and environmental performance of the facility.

As TSFs are typically engineered to remain as permanent landforms, it is essential to ensure that the containment integrity, slope stability, and seepage control remain robust throughout the remining, closure and post-closure phases. Remining activities introduce additional uncertainty in geotechnical parameters and pore pressure behaviour due to tailings removal, redeposition, and changing phreatic conditions. Therefore, an integrated approach that couples geotechnical investigation, numerical analysis, and adaptive closure design is required to maintain both operational safety and long-term stability.

Several recent studies and reviews have highlighted the importance of understanding the long-term hydro-mechanical behaviour of tailings to ensure the physical stability of closed facilities. Rodríguez-Pacheco *et al.*, (2025) emphasised the need for detailed geotechnical and hydrogeological zonation of TSFs to properly define drainage and seepage conditions that govern long-term performance. Similarly, Tunnell and Dippenaar (2024) investigated the mineralogical controls on the compaction behaviour of residual gabbro soils used in platinum TSF construction, noting that mineral composition significantly influences foundation strength and post-closure stability. Comparative design work by multiple researchers demonstrated that slope stability analyses can yield divergent results depending on assumptions regarding phreatic surface position and shear strength, underscoring the uncertainty that closure studies must address.

Long-term stability considerations have also been discussed by Knutsson et *al.,* (2016), who examined slope behaviour and erosion processes in landform design for closed tailings impoundments, and by Singh *et al.,* (2023), which modelled dry closure conditions to evaluate the influence of beach width and phreatic level on FoS. Morales *et al.*, (2021) provided a comprehensive review of tailings hydro-mechanical responses under varying saturation and consolidation conditions, offering practical insight for predicting post-closure performance. Collectively, these studies support the approach adopted in the present work, where updated investigations and numerical analyses were carried out to reduce uncertainty in geotechnical parameters ensuring alignment with international best practice for long-term TSF closure.

During 2024/25, an independent stability and remining readiness review of an extreme classification TSF in South Africa was done. The main objective of the study was to address uncertainties associated with material strength, stratigraphy, phreatic surface behaviour, and consolidation response, all of which are critical for evaluating remining feasibility and closure design. Updated site investigations including in situ testing, sampling, and laboratory characterisation were applied to the slope stability analysis. The approach aligned with the Client's Tailings and Dam Management Standard and complies with international best practices, including the Global Industry Standard on Tailings Management (GISTM) and ICMM guidelines.

SITE DESCRIPTION

The facility is an upstream raised facility, via spigot deposition and comprises of chromium tailings. The footprint area of the facility is 6.5Ha with a basin area of approximately 3.2Ha and fast approaching its end of life. A rock buttress was constructed to increase the slope stability FoS.

The TSF is currently approximately 27 m high, with side slopes of about 1V:2H and containing approximately 2.5 Mt of tailings. This TSF has an Extreme consequence category classification, due to its proximity to the neighbouring communities and its platinum group metals plant.

In August 2024, we conducted an independent stability review of the TSF based on the work completed by reputable consultants. However, due to uncertainties, it was recommended that a Cone Penetration Test (CPTu) campaign be planned and implemented to close the material characteristics data gaps and support a more informed stability assessment. A total of 28 CPTu tests and eight boreholes were used to refine understanding of the stratigraphy of the TSF. Figure 1 presents the location of the CPTu holes on the TSF.

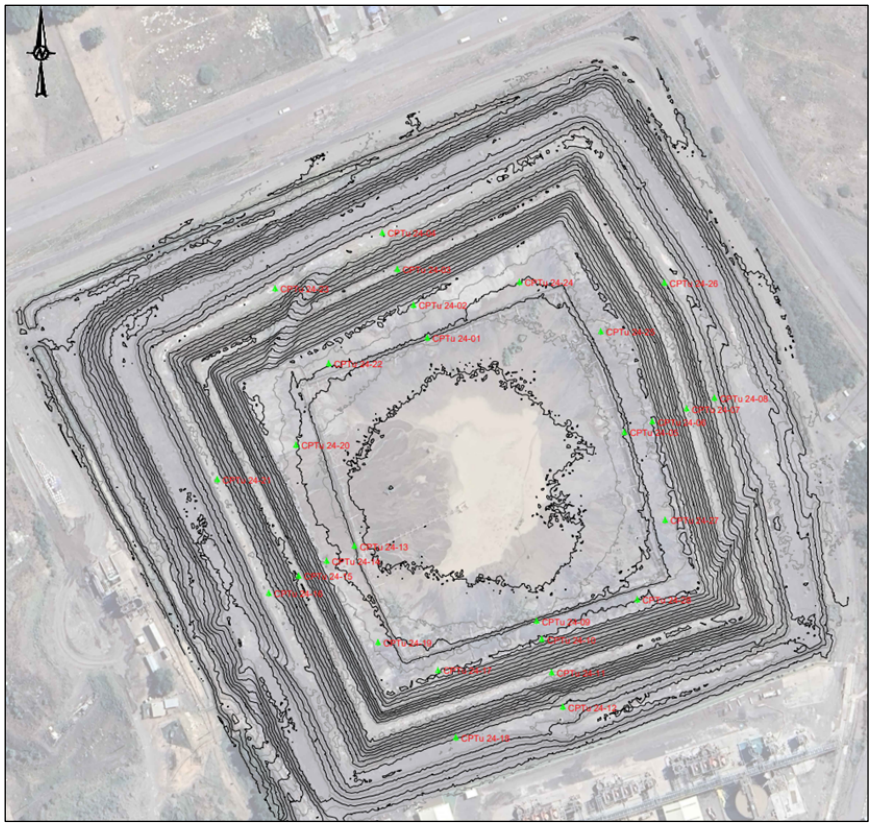


Figure 1. Layout of proposed CPTu investigation on the TSF.

FOUNDATION SOIL AND TAILINGS PROPERTIES

The foundation soil and tailings material properties were assessed using a multi-stage approach comprising data review, site investigation and interpretation. Information reviewed included prior in-situ geotechnical investigations, CPTu test data, laboratory test results and historical stability assessments.

Foundation Indicator testing (grading, hydrometer and Atterberg Limits) was also carried out to characterise the sampled materials in terms of physical characteristics and to augment the tailings characteristics determined from the CPTu tests. The tailings material comprised of an average moisture content of 13%. Consolidated undrained triaxial (CU) tests were performed to determine the shear strength characteristics. The samples were consolidated to confinement stress ranges of 150 kPa, 300 kPa and 600 kPa, respectively.

The tailings material grades from loose to medium dense consistency and contains softer clay zones. The tailings become dense to very dense at the bottom of the TSF. The tailings material is mainly a non-plastic silty fine sand exhibiting generally good drainage.

The borehole data indicates that the TSF is underlain by highly weathered soft rock norite becoming slightly weathered hard rock norite with highly weathered zones to the east of the facility.

Based on the review of the data made available, interpretation of the typical stratigraphy and embankment zoning is illustrated in Figure 2.

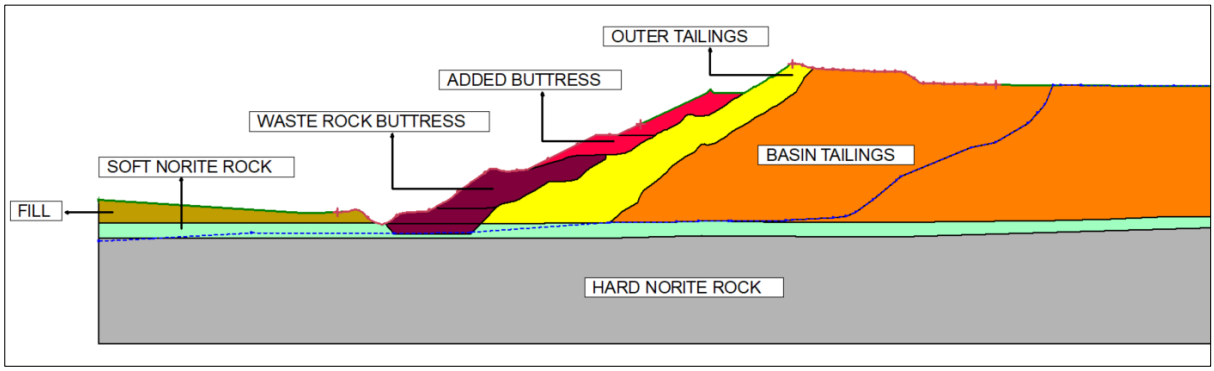


Figure 2. The general stratigraphic profile of the TSF.

Amongst other things, the test results provide critical data for assessing the undrained shear strength parameters and pore pressure response of the TSF tailings under consolidated undrained loading conditions, supporting slope stability and seismic response analyses for the facility. The key geotechnical parameters adopted for modelling are summarised in Table 1. Some key parameters informing the stability assessment were determined based on the CPTu data, laboratory investigations and engineering judgement. These parameters are provided in the material parameter table shown in Table I.

Table I: Geotechnical parameters for modelling

Geotechnical Characteristics				Section	Shear Strength Ratio (su/σ'v)			
					Peak Undrained		Residual Analysis	
Material	**γ (kN/m³)**	**c (kPa)**	**φ (degrees)**		**Tailings above WT**	**Tailings below WT**	**Tailings above WT**	**Tailings below WT**
Fill	18	5	32					
Waste Rock Buttress	23	0.1	35					
Added Buttress	23	0.1	35					
Hard Norite Rock	24	100	50	**S1**	0.4	0.24	0.2	0.06
Soft Norite Rock	23	15	35	**S2**		0.25		0.08
Basin Tailings	19.6	0.1	33	**S3**				
Outer Tailings	19.6	0.1	33	**S4**		0.24		0.06

STABILITY ASSESSMENT

The limit equilibrium slope stability analyses were performed using the GLE/Morgenstern-Price method implemented in SLOPE/W. Both static and dynamic loading scenarios were simulated to evaluate the minimum FoS under drained, undrained, pseudo-static, and post-seismic conditions. The phreatic surface was inferred from standpipe and vibrating wire piezometer (VWP) data, consistent with CPTu derived phreatic surface and topographical surveys conducted at the time of the assessment.

Stability analyses were conducted for five representative cross-sections, approximately mid-flank of each of the four flanks, and an additional section line that presented an area of operational concern (Figure 3). The minimum critical FoS for each section was determined by constraining slip surfaces between the crest and toe.

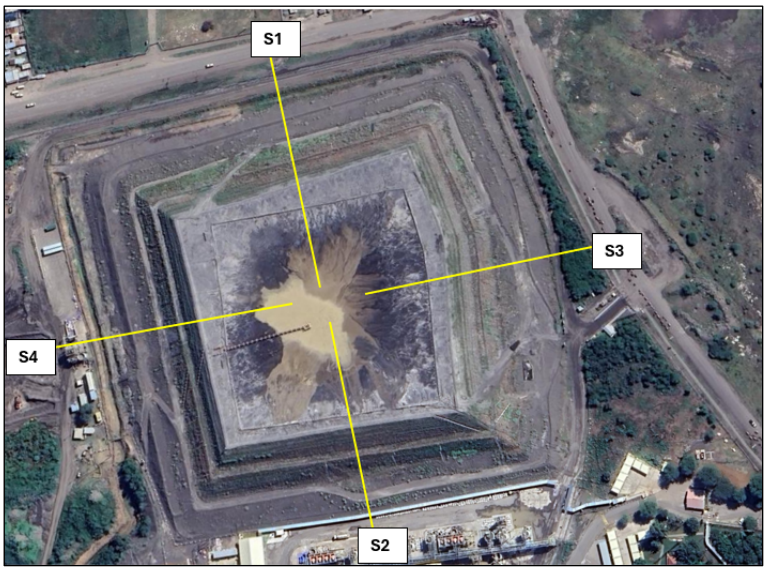


Figure 3. Section lines for stability analysis.

The models were simulated for the optimised and non-optimised slip surfaces. Optimised simulation produces non-linear failure surfaces (a combination of circular and block failures) to provide the statistically lowest FoS for a slope condition, and as such, engineering judgement was applied to exclude surfaces where the solution was deemed kinematically unrealistic. The TSF was assessed for stability under normal load conditions, i.e., no external loads such as construction traffic and/or additional fill stockpiling.

Figure 4 illustrates the stability analysis results for section line S2, for each case. The summary of the results of the stability assessment for all the four section lines is presented in Table II.

The minimum FoS for slope stability analyses shall comply with industry-accepted standards and regulatory guidelines. In general practice, a minimum FoS of 1.5 under static (drained and undrained) conditions and 1.1 under post seismic conditions is considered acceptable to ensure adequate stability of embankments and perimeter slopes.

These values are consistent with recommendations provided in the Canadian Dam Association (CDA, 2022), ANCOLD (2019), and ICOLD Bulletins for TSF design and risk assessment.

Table II: FoS Summary: Current Stability Assessment

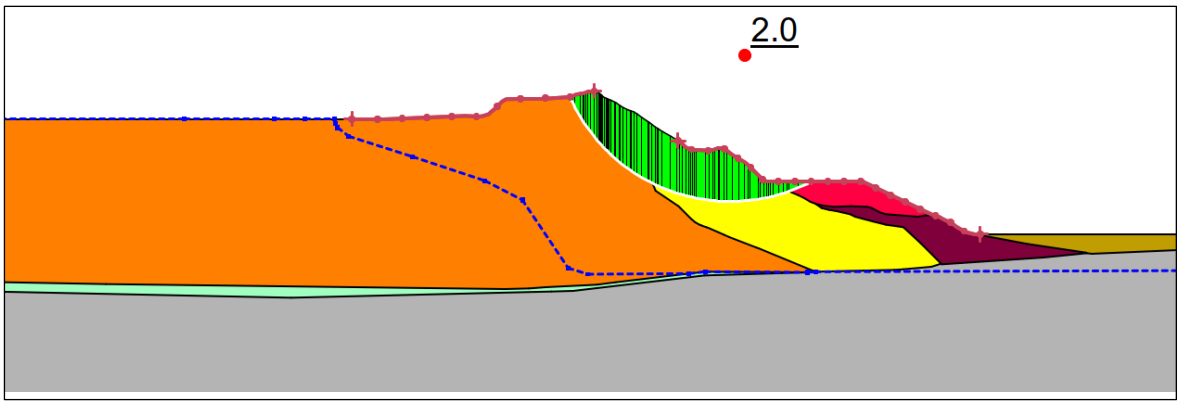
	S1		**S2**		**S3**		**S4**	
Analysis	**FoS**							
Min. slip surface depth (m)	**8**	**20**	**8**	**20**	**8**	**20**	**8**	**20**
Drained Analysis	1.5	2.5	1.5	2.7	1.5	2.7	1.5	2.0
Undrained Analysis	1.4	2.1	1.4	2.0	1.5	2.0	1.4	1.8
Post Seismic Analysis	0.9	1.2	1.0	1.0	0.9	1.0	1.0	1.0

MITIGATION MEASURES

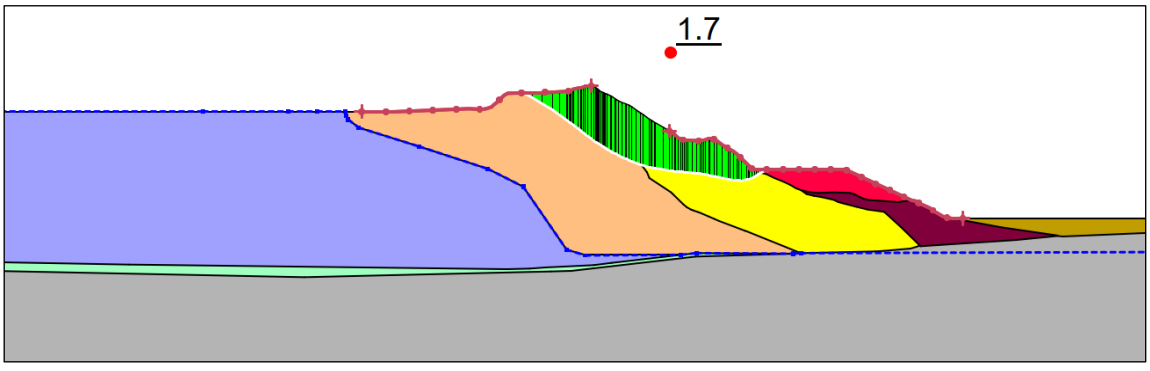
The stability assessment results indicate that the current configuration of the TSF does not meet the minimum required FoS under static and post-seismic conditions without additional mitigation measures. To improve stability, raising the buttress along all the flanks by 3 m was evaluated as a mitigation measure to enhance closure stability. The lowest FoS for each section was associated with a global slip failure, i.e., loss of containment, and was established by confining the failure surface entry limit to the crest of the TSF and the exit limit to the toe of the facility. Shallow and deep-seated failure cases were also considered in the stability analysis. The summary of the stability analysis for all the flanks with raised buttress of 3 m is presented in Table III Figure 4 presents the improvement in FoS (Static Peak Undrained Analysis) with a 3 m buttress raise for S2 section.

Table III: FoS Summary: 3 m Raised Buttress

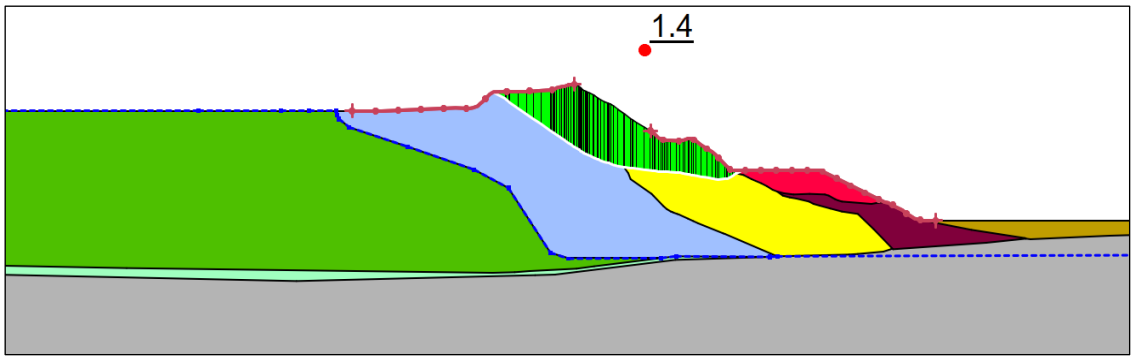
	S1		S2		S3		S4	
Analysis	**FoS**							
Min. slip surface depth (m)	**8**	**20**	**8**	**20**	**8**	**20**	**8**	**20**
Drained Analysis	1.9	2.5	2.0	3.8	1.6	2.0	1.8	4.4
Undrained Analysis	1.8	2.3	1.7	2.5	1.6	1.8	1.6	2.9
Post Seismic Analysis	1.3	1.5	1.4	1.4	1.2	1.2	1.1	1.7



Stability analysis for drained scenario.



Stability analysis for static peak undrained analysis.



Stability analysis for post seismic analysis.

Figure 4. Stability analysis results of S2 section for different cases.

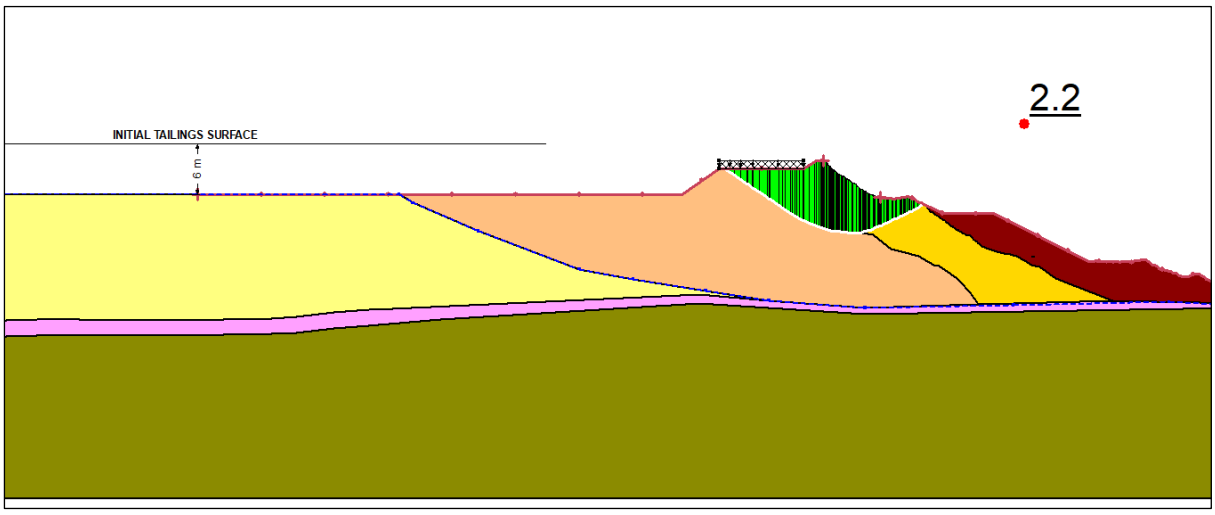
Remining Checks

Various stability scenarios for the remining plan for the TSF, together with the buttress that is currently under construction were reviewed. The objective of this paper is to identify stability risk/s, if any, arising from the proposed remining plan and to verify the stability of the TSF through various stages of the remining operation. The perimeter wall was progressively lowered with each 6 m mining bench drop, maintaining a consistent height difference of approximately 3 m from embankment crest to the top of the mining bench.

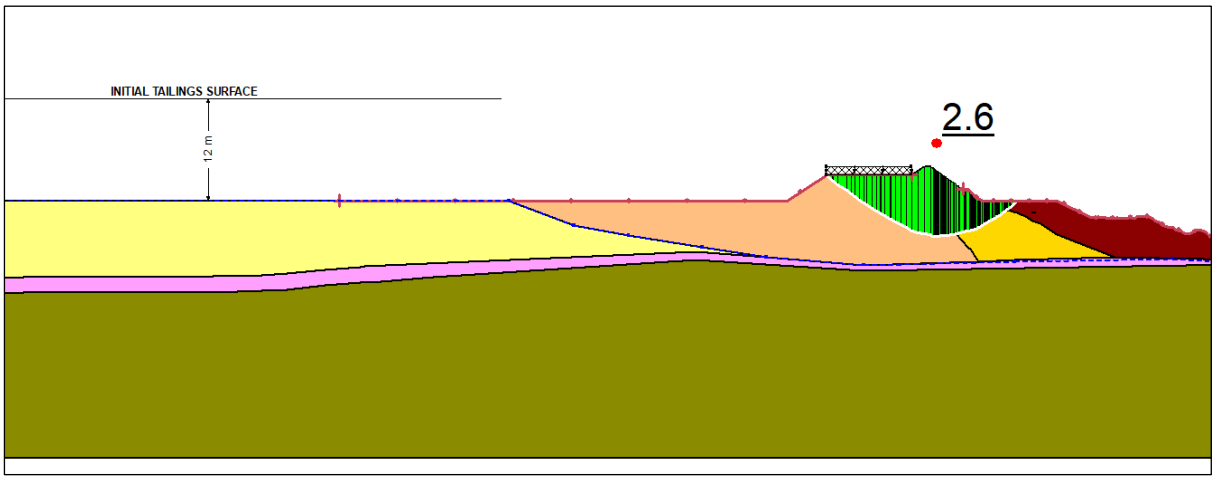
The phreatic surface per section line, for the current condition checks, was based on VWP information, corresponding to the date of the survey. The VWP information was also cross-checked against the CPTu data to confirm phreatic surface adopted for the models. The comparison between the CPTu dissipation profiles and the VWP records showed a consistent pore pressure regime, confirming that the adopted phreatic surface reasonably represents the current field conditions.

Where no positive pore water pressure was measured in the VWPs and in the STPs, the phreatic level was conservatively adopted at the tips of the geotechnical monitoring instrumentation.

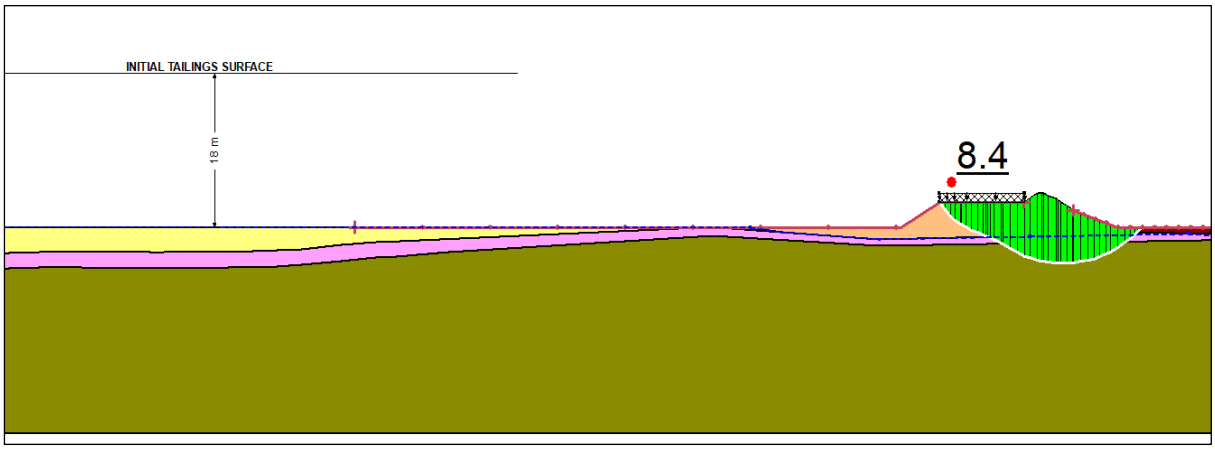
The stability models included a traffic load of 50 kPa applied on the 10 m wide perimeter road (proposed remining methodology) to simulate the loading conditions from trucks and excavators during the remining operations. Figure 5 shows the stability analysis of S3 section line with mining bench drops at 6 m, 12 m and 18 m from the initial tailings surface.



Mining bench drop by 6 m.



Mining bench drop by 12 m.



Mining bench drop by 18 m.

Figure 5. Stability analysis of S3 section performed with mining bench drops at 6m, 12 m and 18 m from the initial tailings surface.

Table III: FoS Summary Remining Stability Assessment

Bench Drop (m)	**6**		**12**		**18**	
Min. slip surface depth (m)	**8**	**20**	**8**	**20**	**8**	**20**
Drained Analysis	2.8	9.9	3.2	10.2	8.6	21.8
Undrained Analysis	2.2	9.8	2.6	10.1	8.4	21.7
Post Seismic Analysis	1.6	9.7	1.8	9.9	8.2	16.8

RESULTS AND DISCUSSION

The paper highlights the importance of updated field investigations and refined modelling to confirm TSF stability at closure. Stability assessment results indicated that the FoS for all flanks were below acceptable limits without mitigation. Consequently, raising the buttress by 3 m is essential to achieve acceptable stability performance for both operational and closure conditions. If adopted, the proposed measures are expected to ensure compliance with required stability criteria and enhance the TSF's long-

term safety and performance during future remining, closure and post-closure phases. Additionally, the stability analysis confirms that the FoS of the remaining TSF improves as the basin and embankment are lowered during remining operation.
The following recommendations are made:

- TSF stability should be reviewed periodically as tailings mining progresses to confirm these outcomes.
- The stability Trigger Action Response Plan (TARP) document is a 'live' document which must be reviewed frequently and revised, as necessary, during the remining operations.
- VWP monitoring instrumentation must remain operational throughout the remining operations.

ACKNOWLEDGEMENTS

The authors acknowledge the contributions of the Client and WSP technical teams for their data, insights, and collaboration during the completion of this assessment.

REFERENCES

Australian National Committee on Large Dams (ANCOLD). (2019). Guidelines on Tailings Dams – Planning, Design, Construction, Operation and Closure. ANCOLD Inc., Sydney, Australia.

Beal (2024). Additional Geotechnical Assessment for TSF.

Canadian Dam Association (CDA). (2022). Technical Bulletin: Application of Dam Safety Guidelines to Mining Dams. Canadian Dam Association, Canada.

GEO-SLOPE International (2012). SLOPE/W for Slope Stability Analysis, User's Guide.

Geotheta Consulting Engineers (2022). SCPTu Testing and Slope Stability Assessment.

Global Industry Standard on Tailings Management (2020). ICMM.

International Commission on Large Dams (ICOLD). (2016). Bulletin 181: Tailings Dams – Risk of Dangerous Occurrences: Lessons Learnt from Practical Experiences. ICOLD, Paris, France.

Jones & Wagener (2019). Geotechnical Investigation Report for TSF.

Klohn Crippen Berger (2024). Stability Assessment Technical Memorandum.

Knutsson, R., Bjelkevik, A., & Knutsson, S. (2016). Slope Stability in Landform Design. In Mine Closure 2016: Proceedings of the 11th International Conference on Mine Closure. Australian Centre for Geomechanics, Perth.

Morales, R., & SRK Consulting. (2021). A Review of the Hydro-Mechanical Behavior of Tailings. SRK News.

Morgenstern, N.R., and Price, V.E. (1965). The analysis of the stability of general slip surfaces. Géotechnique, 15(1), 79–93.

Rodríguez-Pacheco, R., Butlańska, J., & Oliva-González, A. O. (2025). Geotechnical and Hydrogeological Zonation of Tailings Storage Facilities: Importance for Design, Construction, Operation, and Closure. Minerals, 15(2), 105.

SANS 10286 (2017). The Identification and Management of Dams. South African Bureau of Standards.

Singh, A., Sharma, V., & Gupta, P. (2023). Stability Investigation of Embankments of a Tailings Pond for its Dry Closure: An Indian Case Study. Sādhanā – Academy Proceedings in Engineering Sciences, Springer.

Tunnell, J., & Dippenaar, M. A. (2024). Mineralogical Impact on the Compaction of Residual Gabbro Soils in the Construction of Platinum Tailings Storage Facilities. Mining, Metallurgy & Exploration, Springer.



Dr. Priyanka Sharma

Engineer-Tailings
WSP India

Dr. Priyanka Sharma is an accomplished civil engineer specializing in geotechnical and earthquake engineering, with a proven track record in research, design, and technical consultancy. She currently serves as an Engineer-Tailings at WSP India, Noida, where she focuses on geotechnical interpretation, CPTu analysis, and slope stability assessment in tailings and global mine waste management projects.

Dr. Sharma holds a Ph.D. in Soil Dynamics from the prestigious Indian Institute of Technology (IIT) Roorkee, where her research focused on seismic hazard assessment and liquefaction potential in the Indo-Gangetic Plains.

Over the years, she has worked extensively in both academic and industry roles. Her previous role as a Senior Engineer at TechFab India Industries Ltd., New Delhi, saw her leading the design and analysis of reinforced soil structures and rockfall mitigation solutions, while managing client interactions and guiding a team of engineers and draftsmen.

In academia, she served as Faculty at National Institute of Technology (NIT) Jalandhar. She has authored multiple peer-reviewed publications in reputed journals and international conferences. She is a registered Engineer-in-Training (EIT) with the Association of Professional Engineers and Geoscientists of Saskatchewan (APEGS), Canada, further validating her international professional credentials.

With a strong foundation in research, technical expertise, and practical engineering, Dr. Priyanka Sharma continues to contribute meaningfully to advancing safe and resilient infrastructure through innovative geotechnical solutions.

State-dependent undrained strength envelopes for gold tailings from NorSand simulations

J. Swanepoel

Knight Piésold, South Africa

Conventional tailings stability assessment often relies on constant undrained strength ratios (Su/p′) that do not account for spatial or stratigraphic variability in soil state. This paper presents a methodology to develop state-dependent undrained strength envelopes using critical state soil mechanics and the NorSand constitutive model, with application to stability assessment of existing tailings facilities.

Laboratory testing on a representative blended sample of gold tailings established the critical state line from six triaxial tests (consolidated-undrained and consolidated-drained). NorSand was calibrated to match observed stress-strain behaviour, then used to simulate peak and residual undrained strength across a range of state parameters (ψ = -0.05 to +0.30) and confining stresses (100-800 kPa). The resulting state-dependent strength envelope was validated against field conditions at two South African gold tailings facilities using CPT-inferred state parameters from 36 soundings across eight cross-sections.

Field state parameters ranged from ψ = -0.11 to +0.07, with the contractive fine/transitional tailings domain predominantly exhibiting ψ = -0.03 to +0.03. The envelope yields spatially-varying strength ratios of Su/p′ = 0.20 to 0.30 for this range, compared to the constant Su/p′ = 0.25 typically assumed in practice. The methodology provides a transparent, traceable framework for defensible strength assignment in stability assessment, with direct traceability from laboratory testing through field inference. The workflow is reproducible and applicable to stability assessment of any tailings facility where representative sampling and in-situ testing enable state parameter characterisation.

Keywords: Tailings; NorSand; Undrained strength; State parameter; Critical state; CPTu; Triaxial test

INTRODUCTION

Undrained stability assessment of tailings storage facilities (TSF) requires defensible characterisation of undrained shear strength. Conventional practice often assigns constant undrained strength ratios (Su/p′) based on limited laboratory testing or empirical correlations, without explicitly accounting for spatial variability in soil state (dense vs loose) or stratigraphic zonation arising from deposition methods. This approach may obscure real strength gradients and introduce interpretive uncertainty in stability calculations.

Critical state soil mechanics provides a framework to link undrained strength directly to soil state through the state parameter (ψ), defined as the difference between current void ratio and the critical state void ratio at the same mean effective stress (Been & Jefferies, 1985). Denser soils (negative ψ) exhibit higher peak strengths due to dilative tendencies, while looser soils (positive ψ) show lower strengths and strain-softening behaviour. However, translating this framework into practical strength assignment for stability assessment requires integration of laboratory testing, constitutive modelling, and field state inference.

The NorSand constitutive model (Jefferies & Shuttle, 2002) offers a rigorous method to simulate state-dependent undrained behaviour once calibrated to site-specific critical state parameters. By running simulations across a range of states and stress levels, practitioners can develop strength envelopes that explicitly relate Su/p′ to state parameter. When combined with in situ testing methods such as cone penetration testing (CPT), which enables state inference at high spatial resolution, this approach provides a traceable pathway from laboratory characterisation to spatially-varying field strength assignment.

This paper presents a methodology to develop and validate state-dependent undrained strength envelopes for tailings using integrated laboratory testing, NorSand modelling, and CPT interpretation. The approach is demonstrated through application to two South African gold tailings facilities, where 86 MOSTAP samples and 36 CPT soundings provided comprehensive characterisation. The resulting envelopes capture spatial variability from dilative to contractive states, offering a more transparent and defensible alternative to constant strength assumptions. The workflow is reproducible and applicable to stability assessment of existing tailings facilities where field data enables state parameter characterisation.

Literature Review

Advances in the engineering design and safety of mine residue storage facilities have increasingly highlighted the need for methods that move beyond empirical strength estimates and account for the complex, state-dependent behaviour of gold tailings. Historically, the majority of stability assessment practice has relied on constant undrained shear strength ratios—assigning a single value of undrained shear strength to the entire profile of tailings, irrespective of variability introduced by deposition, layering, or stress history (Olson and Stark, 2002). While this approach is simple and familiar, it is increasingly recognised as insufficient for materials whose behaviour depends on density, stress level, and depositional history.

Critical state soil mechanics (CSSM) offers a theoretically sound foundation for characterising undrained strength. Within this framework, the state parameter (ψ) quantifies the relative density of the soil at a given stress level, defined as the difference between the current void ratio and the critical state void ratio at the same mean effective stress (Been and Jefferies, 1985). The state parameter has been shown to correlate strongly with undrained shear strength in sands and tailings, providing a rational basis for strength assignment that reflects actual material state rather than empirical averages (Jefferies and Been, 2016; Olson and Stark, 2002).

Recent research into tailings behaviour has reinforced the importance of considering state-dependent responses, especially in light of high-profile failures where strain-softening and liquefaction have played critical roles (Riveros *et al*., 2020; Liu *et al*., 2024). Studies consistently demonstrate that undrained shear strength can vary by a factor of two or more across a single facility, depending on local density and stress state (Tomasello *et al*., 2024; Silva *et al*., 2022).

Constitutive models such as NorSand, which are based on critical state principles, allow for explicit, site-specific calibration of state-dependent behaviour (Jefferies and Been, 2016; Liu *et al*., 2024). When combined with in situ techniques such as cone penetration testing, which enables state inference at high spatial resolution (Danziger *et al*., 2019; Robertson, 2010), this approach provides a practical pathway for spatially-varying strength assignment in stability assessment.

Despite significant recent progress, gaps remain. Site-specific calibration protocols for gold mine tailings, particularly those with variable mineralogy or fine content, are underrepresented in published work, and there are relatively few studies that combine all steps from laboratory calibration to continuous in situ state mapping and strength assignment for stability assessment of existing facilities. The approach presented in this paper directly addresses this need, offering a comprehensive workflow from laboratory characterisation through field validation to spatially-varying strength assignment for tailings stability assessment.

Materials and Methods

Site Description and Sampling Program

The tailings investigated in this study were sourced from two adjacent gold TSF facilities in South Africa, operational since 1972 and constructed using upstream raising with day-wall deposition methods. The facilities have a current maximum height of approximately 50 m. A comprehensive investigation program comprised 86 MOSTAP samples and 36 CPT soundings distributed across eight cross-sections spanning both facilities. MOSTAP sampling utilised a wide-diameter piston sampler deployed from the CPT rig at representative depths and locations. CPT soundings were advanced through the full tailings profile to foundation contact.

Based on CPT grain size correlation and soil behaviour type classification (Robertson, 2010), three primary stratigraphic units were identified: (1) coarse tailings in the outer embankment shell, (2) transitional tailings in intermediate zones, and (3) fine tailings located predominantly in the pool and subaqueous zones, consistent with day-wall deposition patterns. Statistical analysis of undrained shear strength ratios from CPT interpretation indicated that the transitional and fine tailings exhibit equivalent strength characteristics across both facilities, justifying their combined treatment as a single contractive domain for constitutive modeling. The coarse tailings were characterized separately using effective stress analysis and are outside this study's scope.

Four representative MOSTAP samples from the transitional and fine tailings zones were blended to create a composite sample (CSL1) for critical state characterisation. The particle size distribution envelope and blended sample position are shown in Figure 1. Index properties are summarised in Table I. The tailings comprise predominantly fine, non-plastic silty sands (ML/SP classification) with fines content ranging from 24% to 87% (blended sample: 71%), typical of gold milling operations.

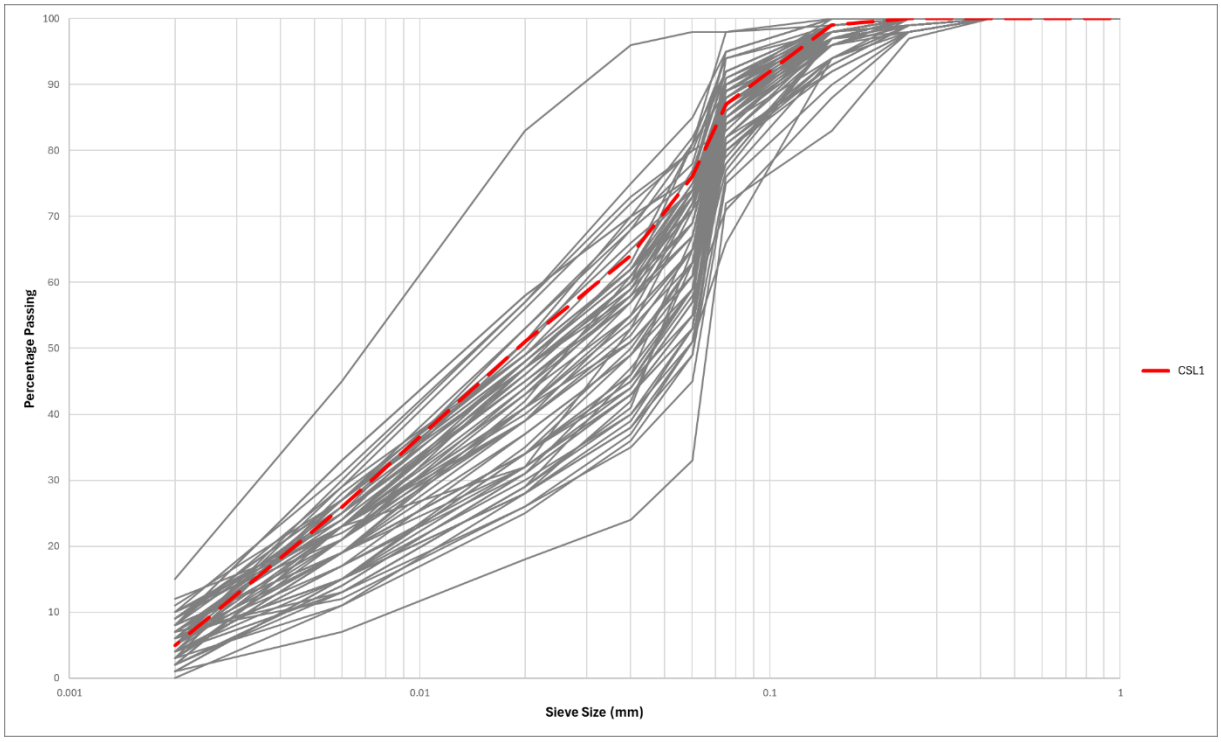


Figure 1: Particle size distribution for 86 MOSTAP samples (grey lines) and blended sample CSL1 (dashed red line).

Table I: Index properties and classification summary for gold tailings across the deposit, including the blended calibration sample (CSL1).

Property	Min	Max	Blended Sample (CSL1)
Specific gravity, Gs	2.68	2.83	2.71
% Passing 0.075 mm	24	87	71
% Sand	2	67	24
% Silt	33	83	71
% Clay	0	15	5
Liquid limit, LL (%)	NP	22	SP
Plasticity index, PI (%)	0	4.5	1
USCS (classification)	ML/SP	-	ML
AASHTO	A-4	A-6	A-4
Grading modulus	0.02	0.34	0.13

Laboratory Testing Program

Critical state testing was conducted on blended sample CSL1 using a computer-controlled triaxial apparatus. The testing program comprised two consolidated-undrained (CU) tests at 200 kPa and 400 kPa, and four consolidated-drained (CD) tests (three at 100 kPa, one at 400 kPa). All specimens were reconstituted using moist tamping to achieve target void ratios spanning the expected field range. Void ratio measurement precision was estimated at ±0.01 to ±0.02. Specimens were saturated (minimum B-value > 0.95) and consolidated before shearing at 0.02 mm/min (CU tests) or 0.002 mm/min CD tests).

Critical state line determination

The critical state line (CSL) was fitted to void ratio and mean effective stress at large axial strain (ε > 15%) where shear stress and void ratio remain constant. The six laboratory tests provided end-state data points spanning contractive and dilative conditions. The fitted CSL parameters shown in Figure 2 are Γ

= 0.8122 and λ = 0.065, with R^2 = 0.44. The moderate correlation coefficient reflects typical scatter in void ratio measurements, particularly for drained tests where continuous volume change complicates end-state determination. The fitted line passes through the central tendency of all test data and is consistent with published gold tailings data. These parameters were used for NorSand calibration and CPT-based state parameter inference.

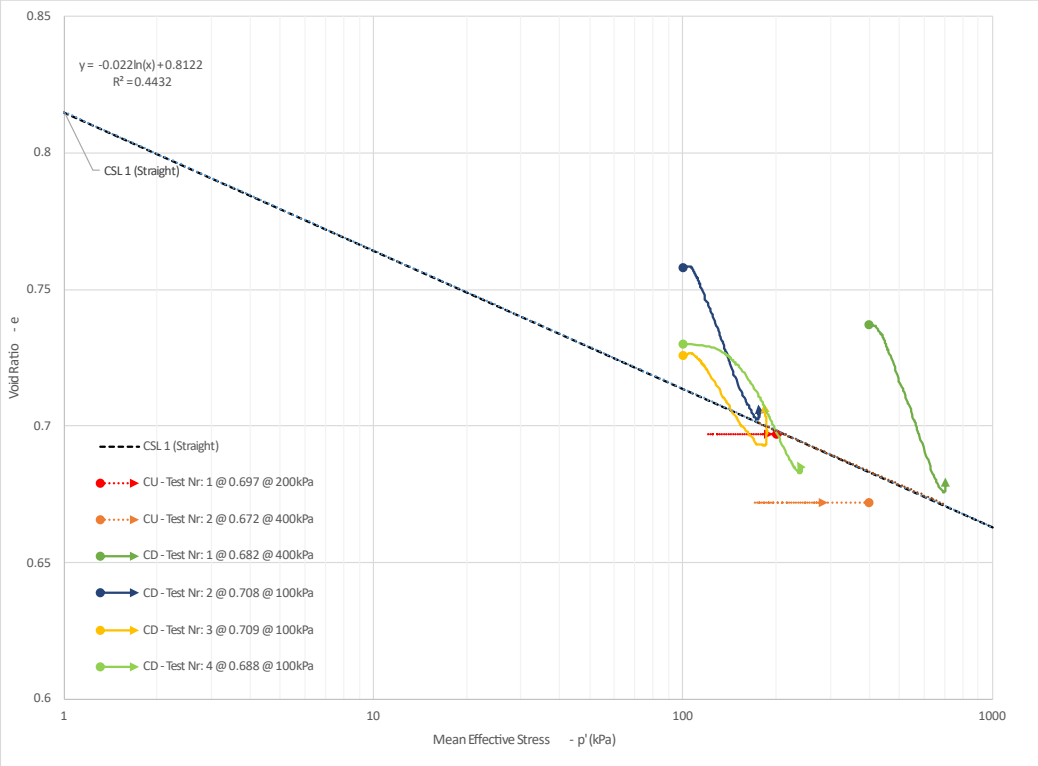


Figure 2: Critical state line fitted to six triaxial tests on blended sample CSL1.

NorSand Constitutive Model Calibration

The NorSand constitutive model (Jefferies and Shuttle, 2002) was calibrated to reproduce observed stress-strain and volumetric behaviour from laboratory tests. NorSand is a critical state-based elastoplastic model that explicitly accounts for state parameter effects on hardening, dilatancy, and peak strength. The model requires seven parameters: three determined directly from the CSL and observed behaviour (λ, Γ, M_tc), and four calibrated by matching peak strength, post-peak softening, and stress-strain stiffness (χ_{tc}, H_0 , H_u, C).

Validation of the calibration is demonstrated in Figure 3 and Figure 4, showing close agreement between NorSand simulations and laboratory data for stress-strain curves and effective stress paths at 400 kPa confining pressure. The model successfully captures contractive behaviour typical of the fine tailings domain, including peak strength mobilisation and strain-softening response. Calibrated parameters are presented in Table II.

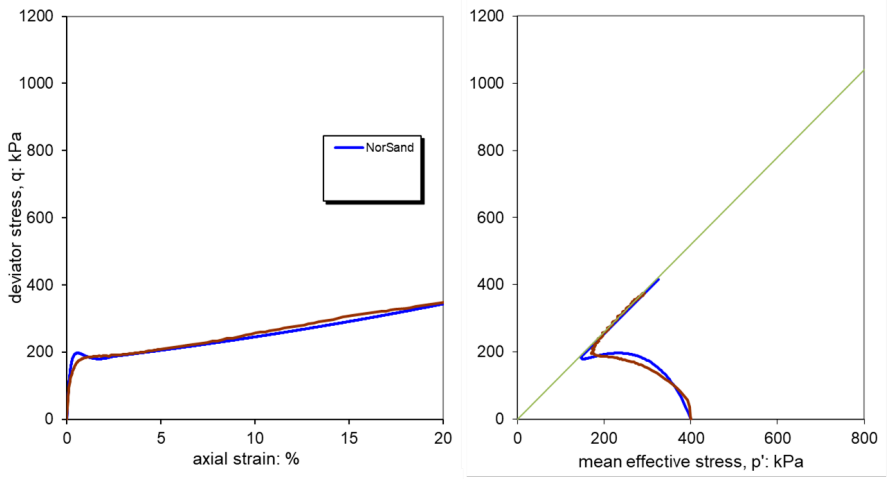


Figure 3: NorSand model validation: simulated undrained response (blue lines) compared to laboratory triaxial tests (brown lines) at 400 kPa.

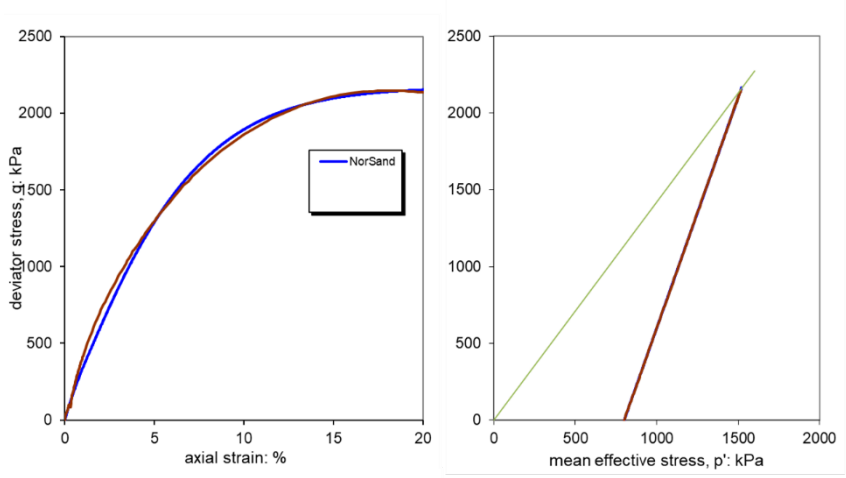


Figure 4: NorSand model validation: simulated drained response (blue lines) compared to laboratory triaxial tests (brown lines) at 800 kPa.

Table II: Fitted NorSand model parameters for the blended calibration sample

Group	Property	Description	Value
CSL	λ	Slope of the critical state line	0.065
	Γ	Void ratio corresponding to a mean pressure equal to 1 kPa	0.8122
	M_{tc}	Friction ratio at critical state in triaxial conditions	1.27
	N	Material parameter controlling the maximum stress ratio as a function of the minimum dilatancy	2.08
Plasticity	χ_{tc}	Material parameter which governs the slope of the minimum dilatancy as a function of the state parameter	0.82
	H_0	Hardening parameter	11.5
	H_u	Hardening parameter	7.0
	C	Fitting parameter for dilatancy function	0.10

Peak and Residual Strength Definition
Peak undrained strength (Su,peak) was identified as the maximum deviatoric stress during undrained shearing. Residual undrained strength (Su,res) represents the post-peak steady-state condition at large strain. For contractive states ($\psi > 0$), residual strength was taken at $\varepsilon \geq 10\%$ where stress has stabilised at the critical state line. For dilative states ($\psi < 0$), residual strength was defined at the post-peak minimum (typically $\varepsilon \approx 0.5$-2.2%) before strain hardening occurs, providing a conservative lower-bound estimate. The identification of peak and residual points across the state parameter range is illustrated in Figure 5.

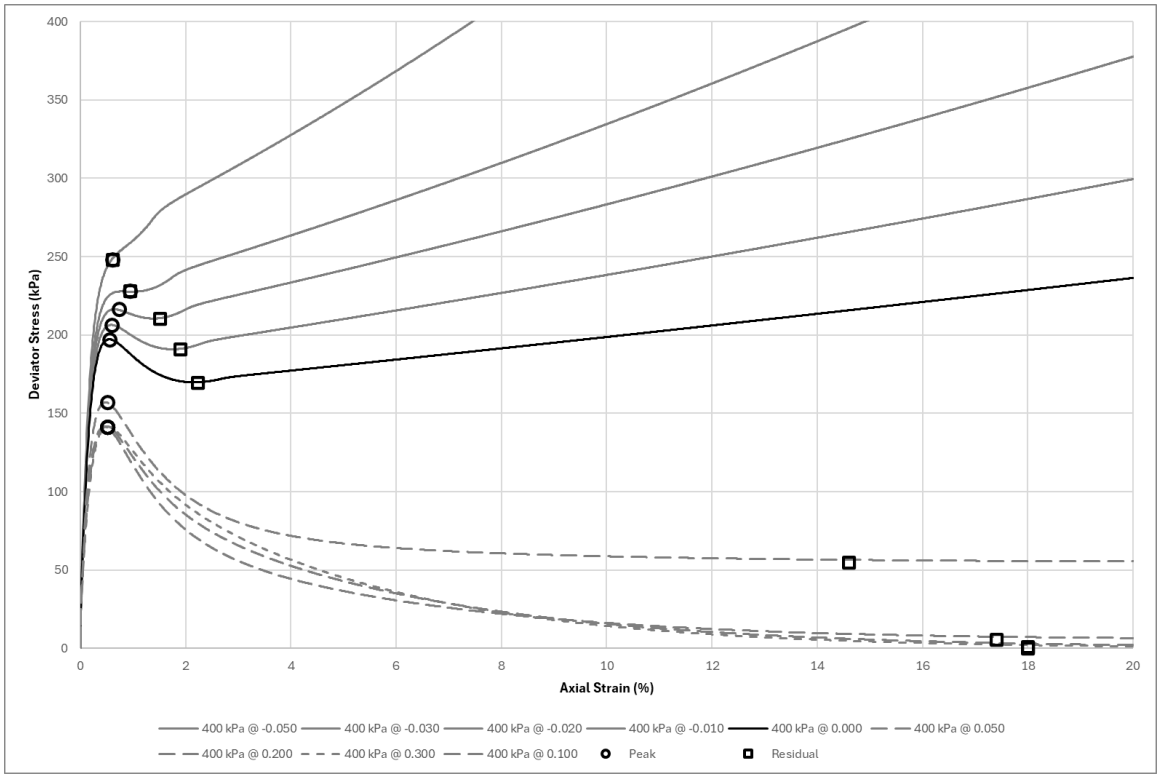


Figure 5: Peak and residual strength identification from NorSand stress-strain simulations at 400 kPa.

Simulation Matrix and Strength Envelope Generation
A parametric simulation matrix was executed across five confining stresses (100, 200, 400, 600, 800 kPa) and state parameter values from $\psi = -0.05$ to $\psi = +0.30$ in 0.01 increments. Each simulation represented an undrained triaxial compression test starting from the specified initial state and confining stress. Peak and residual undrained strength ratios (Su/p') were extracted from each simulation according to the definitions above.

The complete strength envelopes are presented in Figure 6, plotting Su/p' vs state parameter for both peak and residual conditions across all confining stresses. The envelopes capture the full spectrum of state-dependent behaviour: high peak strengths ($Su/p' > 0.40$) with limited softening for dilative states ($\psi < -0.03$), transitioning to lower peak strengths ($Su/p' \approx 0.20$-0.25) with significant strain-softening for contractive states ($\psi > +0.05$). The convergence of peak and residual envelopes for dilative conditions reflects strain-hardening behaviour. These envelopes provide a direct look-up relationship for assigning spatially-varying undrained strength-based on field-inferred state parameter.

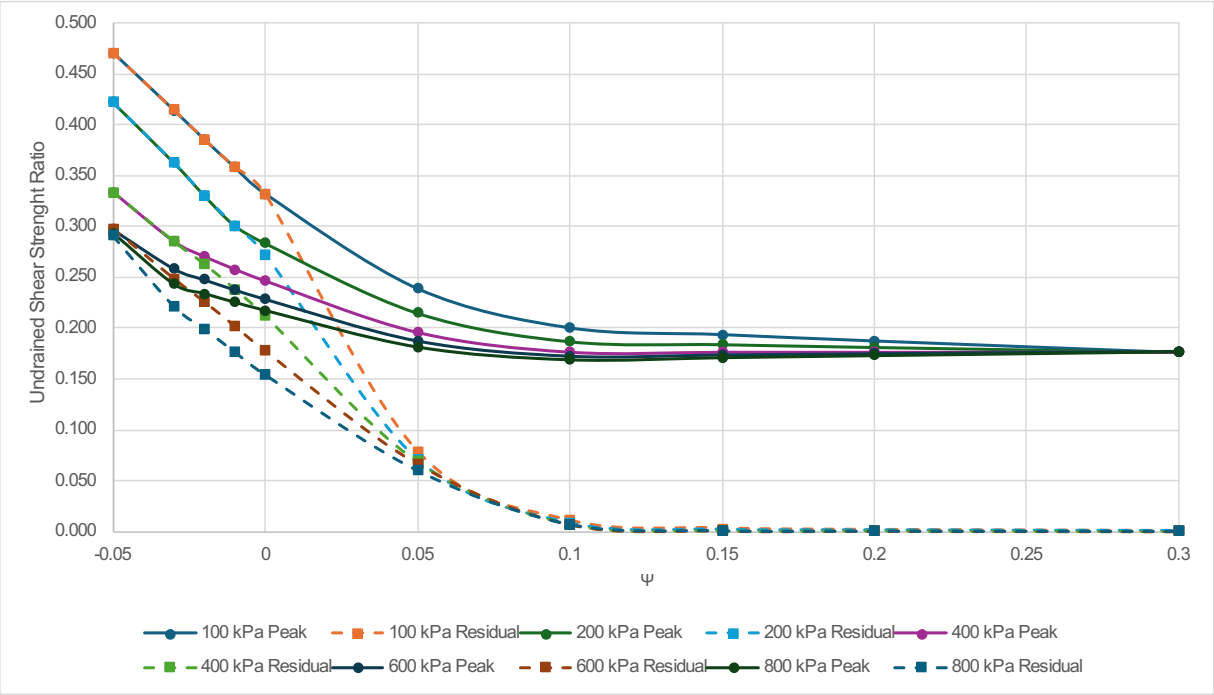


Figure 6: State-dependent undrained strength ratio (Su/p') as a function of state parameter for gold tailings, based on NorSand simulations.

CPT-Based State Parameter Inference

State parameter at each CPT sounding was inferred using three published methods: Widget (Been and Jefferies, 2004), Plewes *et al.,* (1992), and Robertson (2010). All three methods were applied at 0.02 m depth increments to assess consistency and variability. Comparison of results for representative CPT soundings is shown in Figure 7. All three methods identify similar stratigraphic trends and layer boundaries, though absolute state parameter values differ due to inherent differences in calibration databases and normalisation approaches. The Widget method was selected for final strength assessment because it directly incorporates the site-specific CSL parameters determined from laboratory testing, providing the most defensible linkage between field inference and laboratory characterisation. State parameter profiles were generated using the Widget method for all 36 CPT locations.

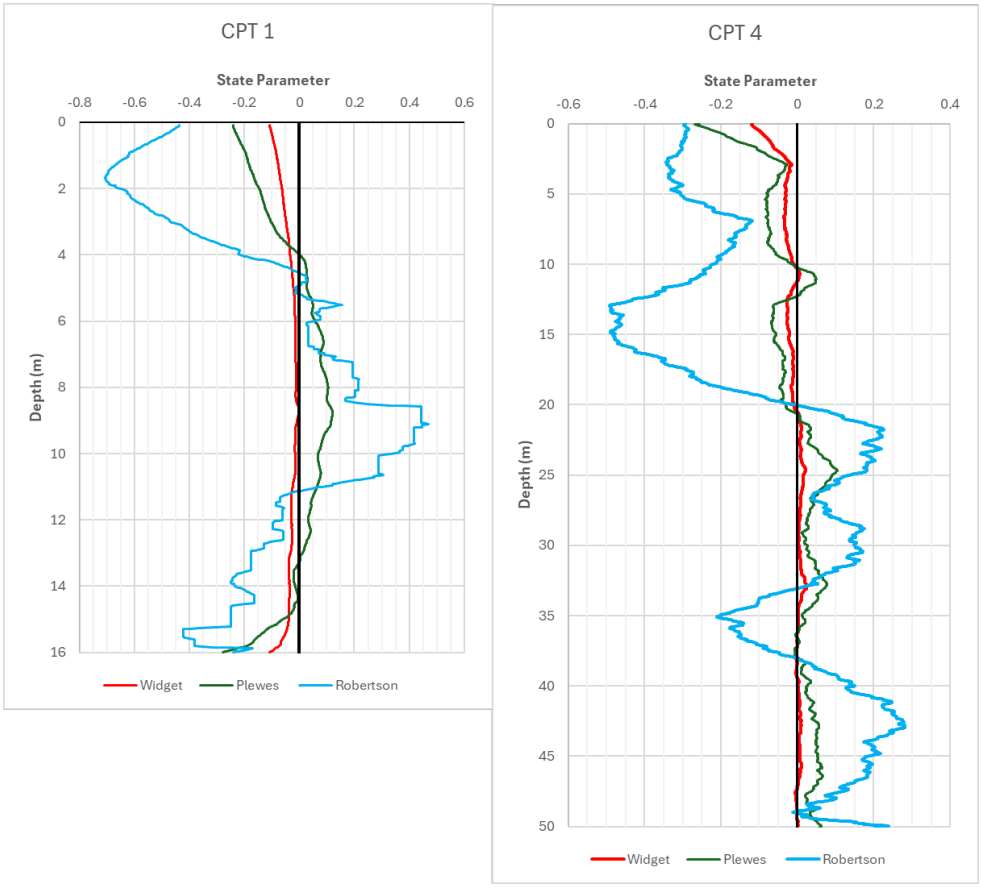


Figure 7: State parameter versus depth at selected CPT locations, by Widget (red), Plewes (green), and Robertson (blue) methods.

Spatial Distribution and Statistical Analysis

Raw state parameter profiles exhibit high-frequency variability due to measurement noise and micro-scale heterogeneity. A moving average filter was applied to each CPT profile to extract stratigraphically meaningful trends while preserving layer boundaries. The window size was selected to smooth measurement noise while capturing the distinct coarse/transitional/fine layering observed in the deposit.

The spatial distribution of state parameter across a representative cross-section is shown in Figure 8, demonstrating stratigraphic zonation and lateral variability typical of day-wall deposition. The moving average profiles reveal systematic trends: slightly dilative to neutral conditions ($\psi \approx -0.05$ to 0) dominate the upper and mid-profile zones, transitioning to slightly contractive conditions ($\psi \approx 0$ to $+0.03$) in deeper subaqueous tailings.

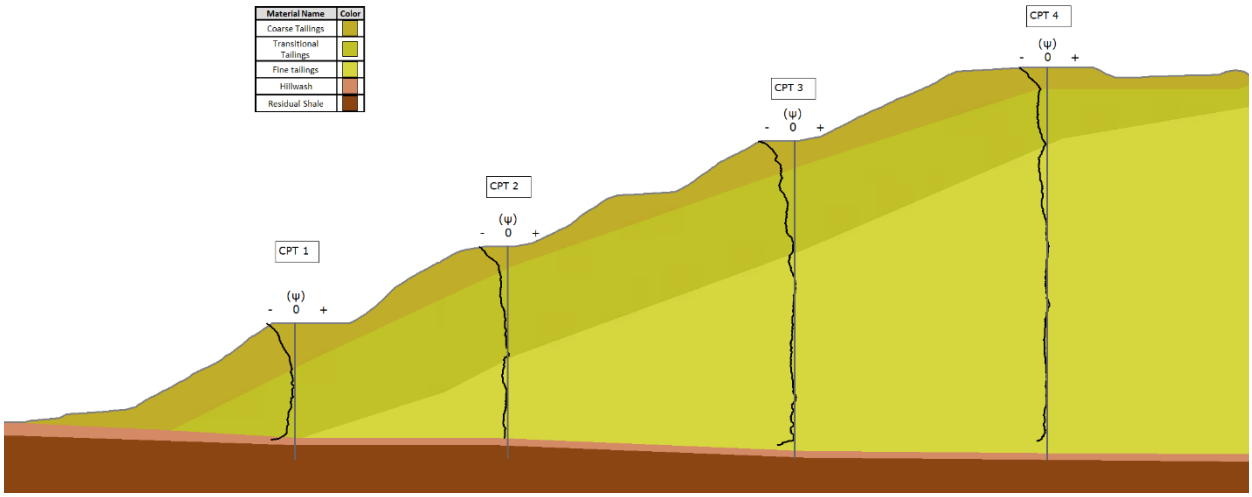


Figure 8: Cross-section showing state parameter distribution (moving average) at CPT locations. Stratigraphic layers indicated by colour; markers show dilative (−), critical (0), and contractive (+) zones.

Statistical analysis of all state parameter values across the contractive tailings domain is presented in Figure 9. The facility predominantly exhibits slightly dilative to neutral conditions, centred at ψ ≈ -0.02 to 0, with range extending from ψ ≈ -0.11 to ψ ≈ +0.07. This distribution validates that the minimum and maximum values reported for individual CPT locations represent the actual range of field conditions rather than isolated outliers. The majority of the contractive tailings domain falls within ψ = -0.04 to +0.02, corresponding to predominantly near-critical to slightly dilative behaviour.

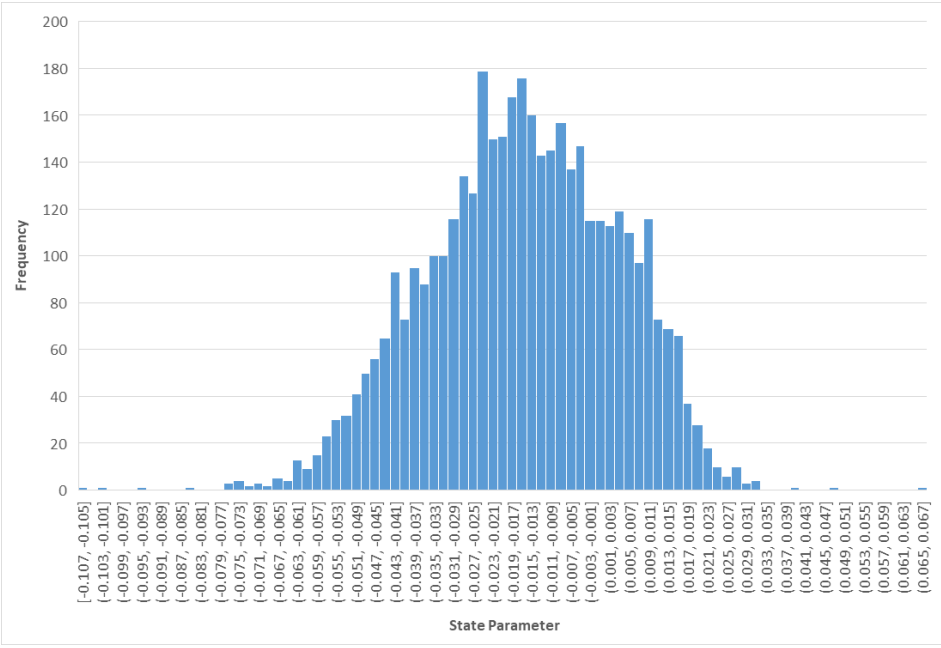


Figure 9: Distribution of state parameter values across all CPT soundings in the contractive tailings domain

RESULTS

The parametric NorSand simulation matrix generated comprehensive state-dependent undrained strength envelopes presented in Figure 6. Peak undrained strength ratio ranges from $Su/p' = 0.45$ at $\psi = -0.05$ (dilative) to $Su/p' = 0.20$ at $\psi = +0.05$ (contractive) at 200 kPa confining stress. The envelopes capture the full spectrum of state-dependent behavior: high peak strengths with minimal softening for dilative states ($\psi < -0.03$), transitioning to lower peak strengths with significant strain-softening for contractive states ($\psi > 0$). The convergence of peak and residual envelopes for dilative conditions reflects strain-hardening behavior where both values approach the critical state from below. Peak and residual strength identification across the state parameter range is illustrated in Figure 5.

Application of the Widget method to 36 CPT soundings across eight cross-sections reveals systematic spatial variability in state parameter consistent with day-wall deposition patterns. The spatial distribution shown in Figure 8 demonstrates stratigraphic zonation and lateral variability: slightly dilative to neutral conditions ($\psi \approx -0.05$ to 0) dominate upper and mid-profile zones, transitioning to slightly contractive conditions ($\psi \approx 0$ to +0.03) in deeper subaqueous tailings. Comparison of three CPT interpretation methods presented in Figure 7 shows consistent stratigraphic trends despite differences in absolute values, with the Widget method selected for its direct incorporation of site-specific CSL parameters.

Statistical analysis of all state parameter values across the contractive tailings domain is presented in Figure 9, showing the facility predominantly exhibits slightly dilative to neutral conditions centred at $\psi \approx -0.02$ to 0, with range extending from $\psi = -0.11$ (dense, dilative) to $\psi = +0.07$ (loose, contractive). This distribution validates that the minimum and maximum values reported for individual CPT locations represent actual field conditions rather than isolated outliers. The majority of the contractive tailings domain falls within the state parameter range $\psi = -0.04$ to +0.02.

Mapping field-inferred state parameters to the strength envelopes provides spatially-varying strength assignment that reflects actual stratigraphic conditions. For the four representative CPT locations analysed in detail, state parameters ranged from $\psi = -0.052$ to +0.029, corresponding to peak strength ratios $Su/p' = 0.20$ to 0.45. These ranges reflect actual stratigraphic variability, with denser zones yielding higher strengths and looser zones yielding lower strengths, in contrast to a constant strength assumption which obscures this spatial variability.

DISCUSSION

The strength envelopes presented in Figure 6 provide a validated, site-specific framework for state-dependent strength assignment anchored to laboratory-derived critical state parameters and constitutive modelling. Field application at 36 CPT locations demonstrates the practical applicability of the methodology, with the resulting state parameter distribution (Figure 9) consistent with expected depositional patterns for subaqueous gold tailings: predominantly near-critical to slightly dilative conditions reflecting the high relative density typical of day-wall deposition.

Conventional stability assessment practice often assigns a single undrained strength ratio (e.g., $Su/p' = 0.25$) to the entire tailings profile, ignoring spatial variability in density state. This study demonstrates that state parameter varies systematically across the facility ($\psi = -0.11$ to +0.07), corresponding to strength ratios ranging from $Su/p' = 0.20$ to 0.35. Applying a constant value obscures this variability and may result in unconservative assessment of loose zones or overly conservative treatment of dense zones. The state-dependent approach captures beneficial strength gradients: higher strengths in dilative embankment zones where slope stability is governed, and realistic lower strengths in contractive pool zones where liquefaction potential is assessed. This spatial differentiation provides more realistic input for stability analysis and supports defensible factor of safety calculations.

A key advantage of the workflow is complete traceability from laboratory characterisation through field application. The critical state line is determined from site-specific triaxial testing (Figure 2); NorSand parameters are calibrated to match observed behaviour (Figure 3 and 4, Table II), strength envelopes are generated through systematic simulation (Figure 6), and field state is inferred using CPT methods that incorporate the site-specific CSL (Figure 7). This chain of evidence provides transparency for regulatory review, peer scrutiny, and major hazard reporting requirements. The approach also allows ongoing refinement as additional data become available, supporting risk-informed, data-driven management of tailings facilities throughout operational life and closure.

For practitioners applying this methodology, the workflow comprises five steps: (1) obtain representative samples from the contractive tailings domain; (2) conduct triaxial testing to define the critical state line; (3) calibrate NorSand and generate state-dependent strength envelopes; (4) infer state parameter profiles from CPT or other in situ testing; and (5) assign spatially-varying strengths by mapping field state to the envelopes. The resulting strength distribution can be implemented in slope stability analysis using standard limit equilibrium or finite element methods.

Several limitations should be acknowledged. First, this study uses a single blended critical state line to represent the combined fine/transitional tailings domain. Statistical analysis demonstrated that these layers exhibit equivalent strength-state behaviour across both facilities, justifying this simplification. However, deposits with greater stratigraphic complexity or distinct material sources may require multiple CSLs for different domains. Second, CPT-based state parameter inference carries method-dependent uncertainty, typically ±0.02 to ±0.05 in state parameter. The comparison of three methods (Figure 7) provides insight into this variability, with the Widget method selected to minimise uncertainty through direct incorporation of site-specific CSL parameters. Parametric stability analyses spanning the inferred state range can quantify sensitivity of factors of safety to this uncertainty.

The methodology is applicable to stability assessment of any tailings facility where representative sampling enables critical state characterisation and in situ testing allows state parameter inference. It is particularly valuable for high-consequence facilities under regulatory scrutiny, where transparent, defensible strength assignment is essential. While demonstrated here for gold tailings, the framework is applicable to other mine residues (copper, iron ore, oil sands) provided that representative critical state behaviour can be established through laboratory testing.

CONCLUSIONS

This paper developed and validated a methodology for state-dependent undrained strength assessment of tailings using integrated laboratory testing, NorSand constitutive modelling, and CPT-based field inference. Application to two South African gold tailings facilities (86 MOSTAP samples and 36 CPT soundings across eight cross-sections) generated comprehensive strength envelopes relating S_u/p' directly to field-measured state parameter.

Field state parameter ranged from $\psi = -0.11$ to $+0.07$, centred at slightly dilative to neutral conditions ($\psi \approx -0.02$ to 0), corresponding to strength ratios $S_u/p' = 0.20$ to 0.45. This demonstrates significant spatial variability obscured by traditional constant strength assumptions (e.g., uniform $S_u/p' = 0.25$). The state-dependent approach captures beneficial strength gradients while providing complete traceability from laboratory characterisation through field application, supporting transparent, defensible strength assignment for regulatory review and major hazard reporting.

Key advantages include explicit quantification of spatial variability reflecting actual density state, differentiation of peak and residual strength for post-peak deformation assessment, and capture of realistic strength distributions where denser zones exhibit higher strengths. Limitations include reliance on a single representative critical state line (justified by statistical equivalence of transitional and fine layers across both facilities), CPT inference uncertainty (±0.02-0.05), and applicability to existing facilities with field data rather than predictive design of future facilities.

The workflow is reproducible and applicable to stability assessment of any tailings facility where representative sampling enables critical state characterisation and in situ testing allows state parameter inference, particularly valuable for high-consequence facilities requiring defensible strength assignment under regulatory scrutiny.

REFERENCES

Been, K. and Jefferies, M.G. (1985). A state parameter for sands. Géotechnique, 35(2), 99–112.

Danziger, F.A.B., Coop, M.R., Azevedo, R.F., Fonseca, A.V. and Rodrigues, R.A. (2019). In situ undrained shear strength by CPT and Vane in iron ore tailings. Proceedings of Tailings and Mine Waste 2019, Vancouver, Canada, 244–256.

Jefferies, M.G. (2016). NorSand: A comprehensive critical state model for sand and tailings. Canadian Geotechnical Journal, 53(9), 1419–1431. https://doi.org/10.1139/cgj-2015-0540

Jefferies, M.G. and Been, K. (2016). Soil liquefaction: A critical state approach. 2nd Edition, CRC Press, Boca Raton, FL. https://doi.org/10.1201/9781315368609

Liu, H., Wang, F., Li, X. and Chang, Y. (2024). Considerations for using critical state soil mechanics based constitutive models for capturing static liquefaction failure of tailings dams. Computers and Geotechnics, 163, 105498. https://doi.org/10.1016/j.compgeo.2024.105498

Olson, S.M. and Stark, T.D. (2002). Liquefied strength ratio from liquefaction flow failure case histories. Canadian Geotechnical Journal, 39(3), 629–647. https://doi.org/10.1139/t02-028

Riveros, G., Bonelli, S., Évrard, H. and Lino, M. (2020). Static liquefaction behaviour of gold mine tailings. Canadian Geotechnical Journal, 57(12), 1962–1974. https://doi.org/10.1139/cgj-2019-0528

Robertson, P.K. (2010). Soil behaviour type from the CPT: an update. Proceedings of CPT'10, Huntington Beach, CA, USA, 7–9 May 2010. Paper #4.

Silva, J.P., Danziger, F.A.B., Fonseca, A.V. and Coop, M.R. (2022). Behavioural analysis of iron ore tailings through critical state soil mechanics. Soils and Rocks, 45(3), e20220177. https://doi.org/10.28927/SR.2022.077222

Tomasello, G., da Fonseca, A.V., Danziger, F.A.B. and Coop, M.R. (2024). Assessment of undrained cyclic resistance of sand with non-plastic fines under sustained shear stress using a critical state interpretation. Bulletin of Engineering Geology and the Environment, 83(1), 37. https://doi.org/10.1007/s10064-023-03549-7



Juan Swanepoel

Geotechnical Engineer
Knight Piésold (Pty) Ltd

Juan Swanepoel is a Geotechnical Engineer at Knight Piésold specialising in tailings dam stability assessment and advanced in situ testing. His expertise includes cone penetration testing (CPT) with seismic and resistivity modules, critical state soil mechanics, NorSand constitutive modelling, and laboratory testing programs for mine waste characterisation. His work encompasses CPT data interpretation, state parameter inference, development of critical state lines for tailings materials, slope stability analysis, and geotechnical reporting for high-consequence facilities. He has presented technical findings to Independent Tailings Review Boards and contributes to stability assessments of operating tailings storage facilities across southern Africa.

Cross-calibrated in-situ shear strength of gold tailings from CPTU, Vane Shear, and Norsand modeling

J. Swanepoel

Knight Piésold, South Africa

Reliable undrained shear strength (Su) characterization is essential for stability assessment of tailings storage facilities. This paper presents a tri-method validation approach for deriving site-specific cone penetration test (CPT) undrained strength calibration in gold tailings, integrating field vane shear testing (VST), CPT interpretation, and laboratory-based NorSand constitutive modelling.

CPT testing at 36 locations and VST at 21 depths were conducted at two South African gold tailings facilities. Quality screening of 31 VST tests identified 16 exhibiting clear undrained response suitable for calibration (Group A), with the remainder excluded due to blade damage or drained conditions. Back-calculation from Group A measurements yielded site-specific cone bearing factor Nkt ranging from 8.8 to 46.8 (mean = 24.7, median = 21.4). After statistical screening, regression analysis established Nkt = 23.1 for CPT-based strength derivation.

Tri-method validation demonstrates convergence of three independent approaches. At average state parameter ψ = 0.01, VST yields Su/p' = 0.27, CPT with calibrated Nkt = 23.1 yields Su/p' = 0.24, and NorSand modelling (Paper 1) predicts Su/p' = 0.25. This agreement, all methods within 12%, validates the site-specific calibration. In contrast, CPT with default Nkt = 15 yields Su/p' = 0.37, overestimating strength by 48%.

The calibrated approach narrows the Su/p' distribution significantly (standard deviation reduced 47%). The workflow, comprising systematic VST quality grouping, CPT-VST back-calibration, and validation against constitutive modelling, offers a reproducible framework for site-specific strength calibration with quantified confidence through multi-method triangulation.

Gold tailings; undrained shear strength; CPTu; Vane shear; Nkt calibration; NorSand

INTRODUCTION

Undrained shear strength (Su) is a critical parameter for stability assessment of tailings storage facilities, governing both static slope stability and liquefaction potential under monotonic or seismic loading. Accurate characterization of Su profiles is essential for defensible factor of safety calculations and risk management, particularly given increased regulatory scrutiny following recent tailings dam failures worldwide. Cone penetration testing (CPT) offers high-resolution in situ profiling of strength and stratigraphy, but derivation of Su from CPT tip resistance requires a cone bearing factor (Nkt) defined by Su = (qt - σv)/Nkt, where qt is corrected tip resistance and σv is total vertical stress (Lunne et al., 1997). Nkt is determined empirically, usually by correlation to reference tests, and typically ranges between 10 and 18, with an average of 14 for clays.

For tailings, particularly the fine-grained, non-plastic materials typical of gold milling operations, published Nkt values span a wide range, and application of generic correlations developed for natural clays may introduce significant bias. Default Nkt values (typically 10-15) are commonly applied without site-specific validation, potentially leading to unconservative or overly variable strength estimates that obscure real spatial trends. Site-specific calibration of Nkt with laboratory reference values or field benchmark tests such as vane shear is the best approach, though this requires considerable extra time and funding to accomplish (Mayne and Peuchen, 2018).

Field vane shear testing (VST) provides an indication of in situ undrained shear strength of saturated fine-grained soils and mine tailings (ASTM D2573-18). However, VST in tailings presents challenges: the predominantly silty sand composition, potential for partial drainage at standard test rates, blade refusal in dense zones, and mechanical damage in coarse materials can compromise test reliability. Recent research has highlighted limitations of ASTM D2573 when applied to nonplastic or permeable mine tailings, necessitating equipment and procedural modifications for reliable results, with particular attention to rotation rates to achieve undrained conditions. Despite these recognised challenges, VST remains valuable for CPT calibration when appropriate quality control protocols are applied.

Laboratory-based constitutive modelling using critical state frameworks offers a third, independent method for Su characterisation. NorSand modelling, calibrated to site-specific critical state parameters from triaxial testing, can predict state-dependent undrained strength as a function of soil state and stress level (Jefferies and Been, 2016). When combined with CPT-inferred state parameters, NorSand provides a theoretical reference envelope for validating field-measured strengths. Few studies have demonstrated triangulation between CPT, VST, and constitutive modelling to cross-validate Su interpretation in tailings.

This paper presents a comprehensive approach for deriving and validating site-specific CPT-based undrained strength in gold tailings through triangulation of three independent methods: CPT with back-calibrated Nkt, quality-screened VST measurements, and laboratory-based NorSand modelling (companion Paper 1). The study is based on 36 CPT soundings and 31 VST tests across two South African gold tailings facilities. Rigorous quality screening identified reliable VST measurements suitable for Nkt back-calculation. Validation through comparison of CPT-derived strength, VST measurements, and NorSand predictions demonstrates convergence of all three independent methods, providing robust confidence in the calibrated strength profiles. The site-specific Nkt was found to be significantly higher than default values typically applied in practice. The workflow offers practitioners a reproducible framework for site-specific Nkt calibration with quantified validation through multi-method triangulation.

Literature Review

The characterisation of undrained shear strength in mine tailings has become a central focus of geotechnical research and practice, driven by recognition that tailings behaviour differs substantially from natural soils and that strength variability significantly influences stability assessment outcomes. Whilst CPT offers high-resolution in situ profiling, published Nkt values for tailings are limited, and application of generic correlations developed for natural clays may introduce significant bias. Site-specific calibration of Nkt with laboratory reference values or field benchmark tests such as vane shear is the best approach, though this requires considerable extra time and funding to accomplish (Mayne and Peuchen, 2018). Recent studies on bauxite and iron ore tailings have demonstrated that material-specific calibration can yield Nkt values significantly different from clay-based defaults, with important implications for stability assessment (Danziger et al., 2019).

Field vane shear testing (VST) provides direct measurement of in situ undrained strength and is frequently employed in accordance with ASTM D2573/D2573M-18. However, ASTM D2573 is intended specifically for saturated natural fine-grained silts and clays, excluding materials that are sandy or nonplastic, yet the test is frequently used in mine tailings where zones may be nonplastic or highly permeable, and partial drainage may occur during testing (Hogan et al., 2025). Recent research has highlighted limitations of the standard when applied to silty tailings, necessitating equipment and

procedural modifications, particularly faster rotation rates to achieve undrained conditions (Reid, 2016; Hogan et al., 2025).

Time factor analysis provides a framework for assessing whether undrained conditions were achieved during testing. For contractive mine tailings exhibiting higher strengths in drained than undrained condition, VST performed in accordance with the ASTM standard will result in measured strengths that overestimate actual undrained strength due to drainage effects (Blight, 1968; Reid, 2016). Despite these recognised challenges, VST remains valuable for CPT calibration as it is the only direct measurement of in situ undrained strength.

Laboratory-based NorSand modelling (Jefferies and Been, 2016) offers a third, independent validation method by predicting state-dependent undrained strength from critical state parameters, enabling comparison with field-measured values.

Despite growing recognition of the importance of site-specific calibration and multi-method validation, comprehensive triangulation of CPT, VST, and laboratory-based modelling for tailings facilities remains underrepresented in published case studies. This paper addresses this gap by presenting systematic cross-validation across all three methods, with explicit treatment of VST quality screening and statistical analysis for a well-characterised gold tailings site.

Materials and Methods

Site Description and Investigation Programme

The investigation was conducted at two adjacent gold tailings storage facilities in South Africa, operational since 1972 and constructed using upstream raising with day-wall deposition methods. The facilities have a current maximum height of approximately 50 m and comprise predominantly non-plastic silty sand tailings with characteristic stratigraphic zonation from coarse outer shell to fine pool deposits.

The field investigation programme comprised 36 cone penetration test (CPT) soundings with pore pressure measurement (CPTu) and 31 field vane shear tests (VST) distributed across eight cross-sections spanning both facilities. CPT soundings were advanced through the full tailings profile to foundation contact, with measurements recorded at 20 mm depth increments. VST locations were selected to characterize the contractive fine and transitional tailings zones governing undrained stability behaviour, with tests performed at depths ranging from 4 to 25 m.

VST Testing and Equipment

Field vane shear testing was conducted following ASTM D2573/D2573M-18 using a four-bladed rectangular vane manufactured by AP van den Berg, with 40 mm diameter and 100 mm height. The vane was advanced to target depth and rotated at 0.1°/s (6°/min) to measure peak undrained shear strength. Following peak failure, the vane was rotated rapidly at 4-6°/s to measure remoulded strength. Test durations to peak failure ranged from 2 to 5 minutes. Undrained shear strength was calculated from measured torque using standard vane shear equations. No additional corrections for rod friction or anisotropy were applied.

Quality assessment was performed using time factor analysis to verify undrained test conditions. Time factor (T) was calculated as $T = cvt/D^2$, where cv is the coefficient of consolidation (estimated from CPT dissipation tests), t is time to failure, and D is vane diameter. Tests with $T < 0.02$ were classified as undrained following Blight (1968) criteria. Post-test inspection documented blade condition and test completion status.

VST Quality Assessment and Grouping Criteria

All 31 VST measurements were classified into three groups based on time factor analysis, post-test blade inspection, and test completion status:

Group A (reliable, undrained): Tests completed successfully with T < 0.02, showing clear undrained response and no visible blade deformation. These tests (n=16) exhibited consistent torque-rotation curves characteristic of undrained shearing and were retained for Nkt calibration.

Group B (blade damage): Tests completed but with evidence of blade bending or deformation identified during post-test inspection (n=4). These tests were excluded from calibration due to uncertain strength mobilisation but retained for transparency.

Group C (refused or drained): Tests incomplete due to mechanical refusal, drained response (T > 0.02), or incomplete rotation (n=11). These tests were excluded from calibration but documented for reproducibility.

This quality grouping protocol aligns with recent guidance emphasising systematic screening of in situ test data prior to strength calibration and recognition that achieving undrained conditions in silty, permeable tailings requires careful attention to test rate and drainage conditions (Hogan et al., 2025; Reid, 2016).

NorSand Reference Envelope

Laboratory-based NorSand constitutive modelling was performed on representative blended tailings samples as detailed in companion Paper 1. Six triaxial tests (consolidated-undrained and consolidated-drained) established the critical state line (λ = 0.065, Γ = 0.8122), and NorSand was calibrated to reproduce observed stress-strain behaviour. Parametric simulations generated state-dependent undrained strength envelopes relating Su/p' to state parameter (ψ) across confining stresses of 100-800 kPa. These envelopes provide an independent, laboratory-derived reference for validating field-measured strengths. State parameters at VST and CPT measurement depths were inferred from CPT data using the Widget method (Been and Jefferies, 2004) with site-specific critical state line parameters.

Nkt Back-Calculation Methodology

Site-specific cone bearing factor (Nkt) was back-calculated from Group A VST measurements by comparing measured Su with CPT net cone resistance at matched depths and locations. For each of the 16 Group A tests, Nkt was calculated as:

$$Nkt = (qt - \sigma v) / Su(VST) \quad [1]$$

where qt is CPT corrected tip resistance, σv is total vertical stress, and Su(VST) is the vane-measured undrained strength at the corresponding depth. The back-calculation was performed only at the specific VST test depths by pairing VST-measured Su with CPT measurements at corresponding depths and locations. The calibrated Nkt value was subsequently applied to all CPT data across the 36 soundings to generate continuous Su profiles for stability assessment.

Statistical Screening and Calibration Approach

Back-calculated Nkt values were subjected to statistical screening to identify outliers. Values exceeding Nkt > 100 were excluded as non-representative based on deviation from physically reasonable ranges reported in published tailings studies (typically Nkt = 15-35). Following screening, linear regression of VST-measured Su versus CPT net cone resistance was performed on the remaining Group A dataset to determine the final calibrated Nkt. CPT-based undrained strength was then calculated for all soundings using:

$$Su(CPT) = (qt - \sigma v) / Nkt(calibrated) \quad [2]$$

Strength ratios (Su/p') were calculated as Su(CPT) / σ'v, where vertical effective stress σ'v was determined from unit weight profiles and pore pressure measurements. Mean effective stress p' was approximated as σ'v, assuming Ko ≈ 0.5 typical for normally consolidated recent deposits.

RESULTS

VST Quality Distribution and Group A Dataset

A total of 31 field vane shear tests were performed across the two facilities. Following rigorous quality screening based on time factor analysis ($T < 0.02$), post-test blade inspection, and test completion assessment, 16 tests exhibited clear undrained response suitable for calibration (Group A), 4 tests showed blade damage (Group B), and 11 were incomplete or exhibited drained response (Group C).

Group A test results used for Nkt back-calculation are presented in Table I, showing VST-measured Su, vertical effective stress (σ'v), CPT-derived Su using default Nkt = 15, and back-calculated Nkt for each matched-depth measurement. Tests span depths from 4.5 m to 24.1 m and encompass both the fine and transitional tailings zones. Vertical effective stress ranges from 80 kPa to 440 kPa, representing the typical stress conditions within the contractive tailings domain. Group B and Group C test outcomes are not presented in tabular form but are included in statistical summaries for transparency.

Table I: Group A VST test results and back-calculated Nkt values used for CPT calibration

Test ID	Depth (m)	VST Su (kPa)	σ'v (kPa)	Nkt	CPT Su (kPa)
VST-01	14.5	91.1	257.9	17.4	106.1
VST-02	16.3	100.9	285.8	12.0	80.0
VST-03	21.3	65.0	381.8	22.5	99.8
VST-04	23.7	9.6	423.0	134.8	89.1
VST-05	24.1	30.0	435.6	46.7	83.9
VST-06	18.5	79.4	351.6	21.1	134.0
VST-7	23.3	36.0	440.1	46.0	111.9
VST-08	12.7	18.8	208.2	135.7	79.0
VST-09	13.6	18.0	222.6	215.8	75.1
VST-10	15.5	4.8	229.7	302.5	91.1
VST-11	21.3	65.0	368.7	30.9	103.4
VST-12	21.8	77.3	377.5	18.6	101.2
VST-13	24	62.9	398.9	29.7	122.8
VST-14	12.5	71.0	227.6	8.7	41.5
VST-15	4.5	43.4	80.5	21.3	52.1
VST-16	5.5	43.4	100.9	21.3	76.4

Nkt Statistical Distribution and Screening

Back-calculated Nkt values from the 16 Group A tests ranged from 8.8 to 302.5, exhibiting substantial variability. Four values exceeded Nkt > 100 (specifically 135.7, 215.8, 302.5, and 134.8), representing potential measurement anomalies or localised drainage effects. Following exclusion of these outliers based on the Nkt > 100 threshold, the remaining Group A dataset (n=12) yielded mean Nkt = 24.7, median Nkt = 21.4, and standard deviation = 11.9.

Statistical distributions of back-calculated Nkt values for all three quality groups are shown in Figure 1. Group A (after outlier exclusion) exhibits a central tendency in the range Nkt = 18-30, with median = 21.4. Groups B and C show lower median values (Nkt = 22.8 and 8.1 respectively) and generally wider scatter, consistent with their compromised test quality. The box plot demonstrates that quality screening effectively isolates a defensible Nkt distribution from Group A data, while Groups B and C would introduce unacceptable uncertainty if included in calibration.

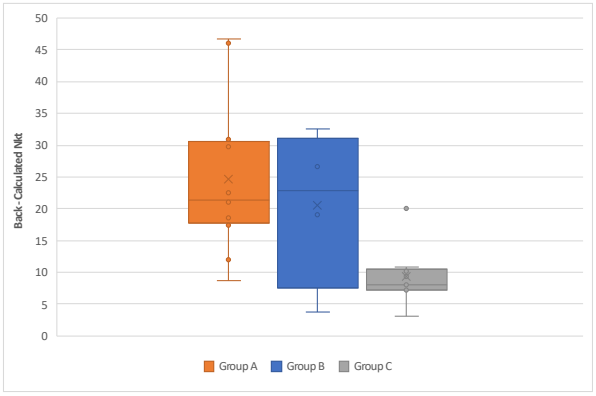


Figure 1: Box and whisker plot of back-calculated Nkt values by VST quality group

Regression Calibration of Nkt

Linear regression of VST-measured Su versus CPT-derived Su for the screened Group A dataset (n=12) is shown in Figure 2. The regression analysis yields a calibrated cone bearing factor Nkt = 23.1 (R^2 = 0.86), representing the best-fit relationship between the two measurement methods. This value is 54% higher than the default Nkt = 15 commonly applied in practice, indicating that default calibration significantly underestimates Nkt and consequently overestimates undrained strength for the subject gold tailings.

Figure 2 also presents the regression relationships for Groups B and C for comparison. Group B yields Nkt = 27.4 (R^2 = 0.78) and Group C yields Nkt = 9.29 (R^2 = 0.82), with the latter showing essentially no correlation due to the prevalence of drained or refused tests. The close agreement between Group A and Group B calibrations (Nkt = 23.1 vs 27.4) suggests that whilst blade damage affects individual measurements, the overall trend remains similar. However, the small sample size and uncertain test mechanics of Group B justify its exclusion from the final calibration

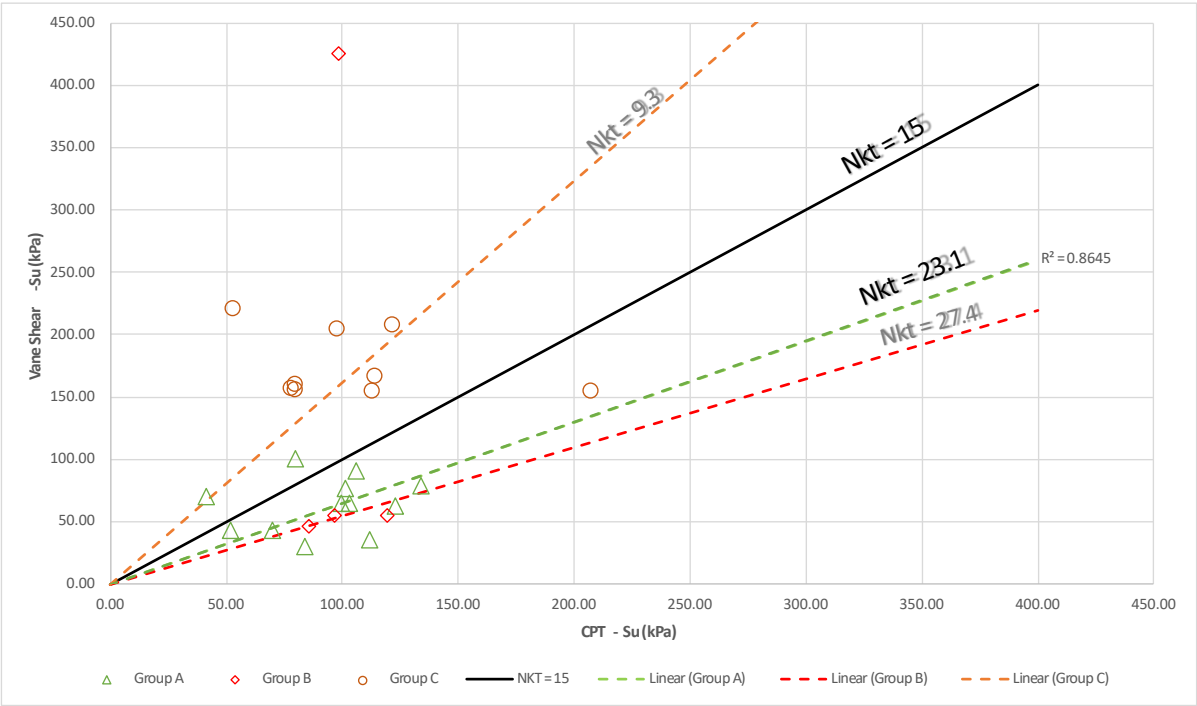


Figure 2: Regression calibration of Nkt from VST measurements by quality group. Group A yields Nkt = 23.1 (R^2 = 0.81). Default Nkt = 15 shown for comparison.

The calibrated Nkt = 23.1 was applied to all CPT data across the 36 soundings to derive continuous undrained strength profiles for stability assessment.

Tri-Method Validation: VST, CPT, and NorSand Convergence

Triangulation of undrained strength from three independent methods is presented in Figure 3, plotting Su/p' versus state parameter (ψ) for VST measurements (Group A), CPT-derived values using both calibrated Nkt = 23.1 and default Nkt = 15, and the NorSand peak strength envelopes from companion Paper 1. This comparison enables direct assessment of whether the calibrated Nkt yields CPT-Su values consistent with both direct field measurement (VST) and independent laboratory-based constitutive modelling (NorSand).

Visual inspection of Figure 3 demonstrates clear convergence of the three methods. VST measurements (green triangles) plot on or near the NorSand peak strength envelopes across the observed state parameter range, validating the laboratory-based model against field measurements. CPT-derived values using calibrated Nkt = 23.1 (red circles) cluster closely with VST data and also plot near the NorSand envelopes, demonstrating that the calibration successfully brings CPT interpretation into agreement with both VST and constitutive predictions. In contrast, CPT values using default Nkt = 15 (blue squares) plot consistently above both VST measurements and NorSand predictions across the full state parameter range, demonstrating systematic overestimation of undrained strength.

Quantitative comparison of average Su/p' from the three methods is presented in Table II. For the contractive tailings domain (ψ = 0 to +0.05, n=10 matched pairs), VST measurements yield average Su/p' = 0.27, CPT with calibrated Nkt = 23.1 yields average Su/p' = 0.24, and the NorSand envelope predicts Su/p' = 0.25 at the average state parameter ψ = 0.01. This convergence—with all three independent methods agreeing within 12%—provides robust validation of the site-specific Nkt = 23.1 calibration. Individual data points exhibit scatter around the central tendency (Su/p' ranging from 0.12 to 0.54), reflecting natural variability in field measurements, state parameter inference uncertainty (±0.02-0.05), and stress-level effects. In contrast, CPT interpretation using default Nkt = 15 yields average Su/p' = 0.37, overestimating strength by 48% relative to the triangulated value.

Table II: Average Su/p' from three independent methods at state parameter ψ = 0.01

Method	n	Average Su/p'	Deviation from Triangulated Mean
VST (Group A)	10	0.27	+8%
CPT (Nkt = 23.1, calibrated)	10	0.24	-4%
NorSand Envelope (200-800 kPa)	-	0.25	0%
Triangulated Average		**0.25**	**±12%**
CPT (Nkt = 15, default)	10	0.37	+48%

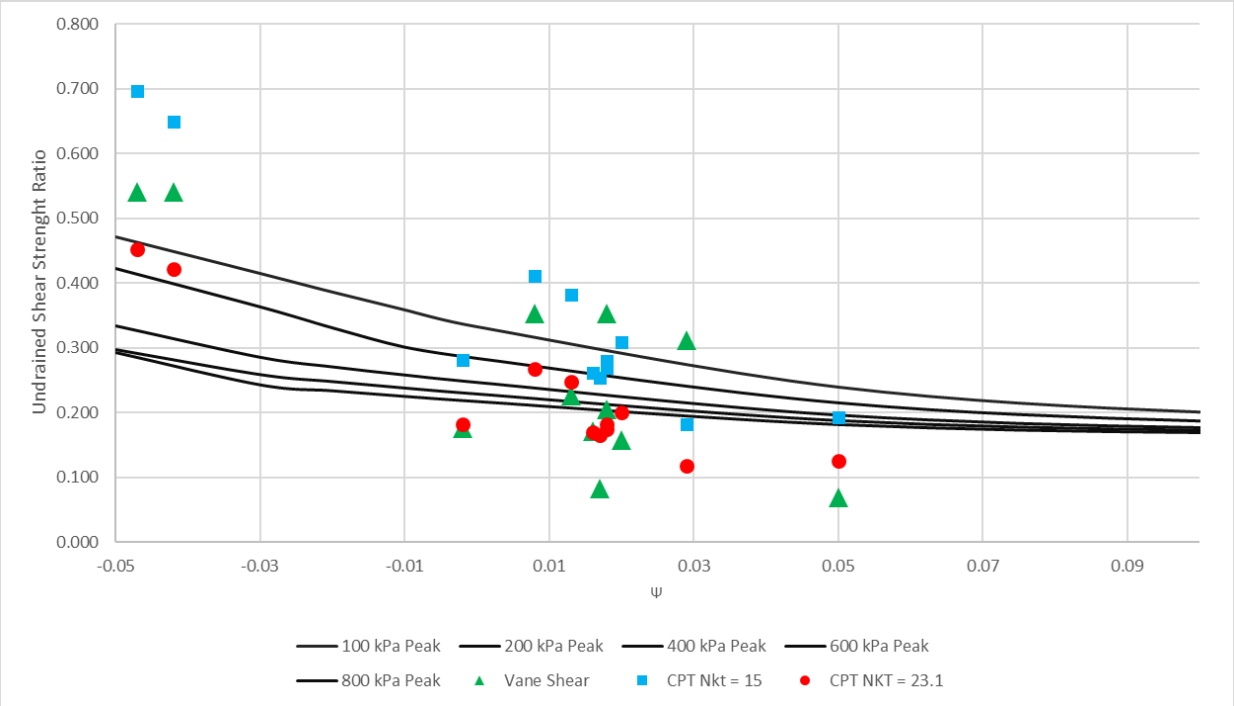


Figure 3: Triangulation of Su/p' versus state parameter from VST, CPT, and NorSand modelling

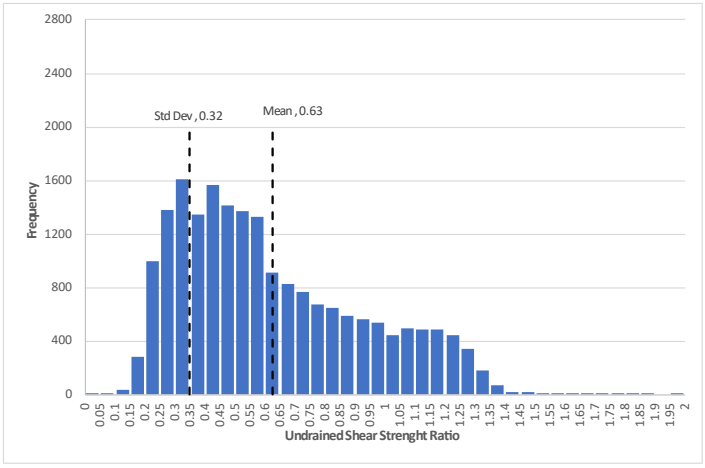
Two VST measurements at shallow depths (4.5-5.6 m) in dilative zones ($\psi \approx -0.04$) yielded higher Su/p' = 0.54, plotting above the NorSand envelope prediction of approximately 0.40 at this state. These measurements correspond to low confining stress conditions ($\sigma'v \approx 80$ kPa) in the coarse outer shell tailings and may reflect strain-rate effects, partial saturation, or vane performance limitations in dense, dilative materials. These data points are retained for completeness but did not influence the calibration, which focused on the contractive domain ($\psi > -0.02$) where the majority of tailings are located and where liquefaction risk is highest.

Impact of Calibration on Su/p' Distribution

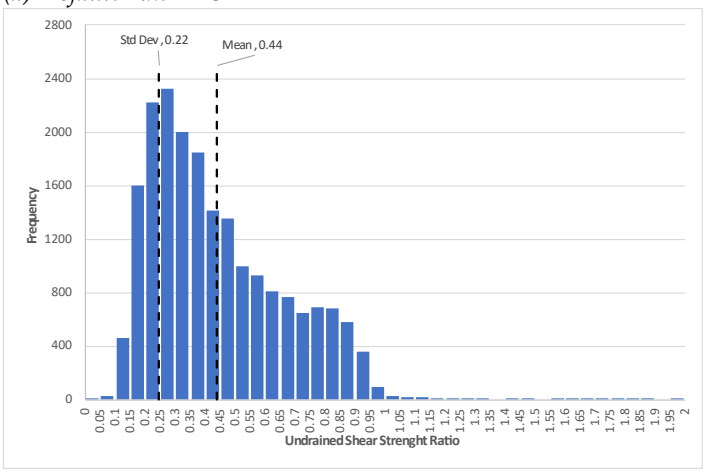
The effect of site-specific Nkt calibration on the overall undrained strength distribution is shown in Figure 4, comparing Su/p' histograms derived from the complete CPT dataset across all 36 soundings using default Nkt = 15 versus calibrated Nkt = 23.1.

Using default Nkt = 15 (Figure 4a), the Su/p' distribution is broad and right-skewed, with mean = 0.63, median = 0.35, and standard deviation = 0.32. The distribution extends to Su/p' > 1.0, representing an unacceptably wide range for design strength assignment. In contrast, using calibrated Nkt = 23.1 (Figure 4b), the distribution shifts to lower values and narrows significantly, with mean = 0.44, median = 0.25, and standard deviation = 0.22. This represents a 31% reduction in standard deviation and a 30% reduction in mean value, providing a tighter distribution centered near the triangulated value (Su/p' ≈ 0.25) validated by VST and NorSand.

The calibrated distribution aligns with both VST measurements and NorSand predictions, whereas the default distribution systematically overestimates strength across the facility. This narrowing directly improves confidence in stability assessment and enables more reliable strength assignment.



(a) Default Nkt = 15



(b) Calibrated Nkt = 23.1

Figure 4: Comparison of Su/p' distributions from complete CPT dataset using (a) default Nkt = 15, and (b) calibrated Nkt = 23.1

DISCUSSION

Tri-Method Validation and Significance

The triangulation presented in Figure 3 and quantified in Table II provides compelling validation of the site-specific Nkt = 23.1 through convergence of three independent methods. Laboratory-based NorSand modelling (Paper 1), direct VST field measurement, and calibrated CPT interpretation all yield Su/p' = 0.24-0.27 for the predominant state parameter range (ψ = 0 to +0.03) characterising the contractive tailings domain. This multi-method agreement—spanning laboratory constitutive modelling, direct field testing, and in situ interpretation—significantly strengthens confidence in the assigned strengths for stability assessment and addresses the inherent uncertainties of relying on any single method.

The convergence is particularly noteworthy given that the three methods are fundamentally independent. NorSand predictions derive from laboratory triaxial testing and critical state theory, with no input from field strength measurements. VST provides direct measurement of in situ undrained strength through an independent mechanism (rotational shearing) at discrete depths. CPT interpretation relies on continuous penetration resistance measurements calibrated through back-calculation from VST. The fact that all three methods converge within 12% at the same state parameter validates not only the Nkt calibration, but also the underlying NorSand model, the VST measurement quality, and the state parameter inference approach. This triangulation provides a level of confidence unattainable from any single method alone.

Implications of Site-Specific Versus Default Nkt
The calibrated Nkt = 23.1 differs substantially from the default Nkt = 15 commonly applied in practice, with direct implications for stability assessment. Default Nkt = 15 yields average Su/p' = 0.37, whilst the triangulated value is Su/p' = 0.25—a 48% overestimation of undrained strength ratio. For a typical section with 30 m height and average vertical effective stress of 250 kPa, this difference translates to Su = 93 kPa (default) versus Su = 63 kPa (calibrated)—a 30 kPa (48%) overestimation.

This systematic overestimation of strength is unconservative for stability assessment. Higher assigned strengths result in higher calculated factors of safety, potentially masking marginal stability conditions or liquefaction susceptibility. The calibrated approach, validated by both VST and NorSand, provides more realistic strength values and therefore more defensible stability assessments. The narrow distribution (Figure 4) also reduces uncertainty, enabling clearer decision-making and more transparent communication with regulators and stakeholders.

Importance of VST Quality Screening
The quality screening protocol proved essential for obtaining reliable calibration. Of the 31 VST tests performed, only 16 (52%) exhibited clear undrained response suitable for calibration, with the remainder excluded due to blade damage (n=4) or drained/incomplete response (n=11). This high exclusion rate is consistent with published experience in tailings, where achieving undrained conditions in silty, permeable materials presents challenges (Hogan et al., 2025; Reid, 2016).

Furthermore, even within Group A (nominally undrained tests), four back-calculated Nkt values exceeded 100, indicating measurement anomalies or local drainage effects. Inclusion of these outliers would inflate the calibrated Nkt and obscure the defensible central tendency (mean = 24.7, median = 21.4 after screening). The box plot analysis (Figure 1) demonstrates that systematic screening effectively isolates a robust calibration dataset from artefact-prone measurements.

This experience underscores that VST in tailings requires not only appropriate equipment and procedures, but also rigorous post-test quality assessment and statistical screening. Time factor analysis, blade inspection, and outlier detection are not optional quality checks but essential components of defensible calibration.

Practical Implementation
For practitioners applying this methodology, the workflow comprises five steps: (1) conduct VST at representative depths spanning the tailings stratigraphy; (2) apply rigorous quality screening using time factor analysis and post-test inspection to identify reliable undrained tests; (3) back-calculate Nkt from quality-screened VST measurements at matched CPT depths; (4) perform statistical screening to exclude outliers and determine calibrated Nkt through regression analysis; and (5) apply the calibrated Nkt to the complete CPT dataset to generate continuous Su profiles.

The triangulation with NorSand modelling provides an additional validation step that significantly strengthens confidence in the calibrated Nkt. If site-specific laboratory testing enables critical state characterisation and NorSand calibration (as detailed in Paper 1), the resulting state-dependent strength envelope offers an independent check on field-derived values. Convergence of CPT, VST, and NorSand, as demonstrated here, confirms that the assigned strengths are consistent across laboratory and field scales and across different measurement mechanisms.

Limitations and Uncertainties
Several limitations should be acknowledged. First, VST in tailings carries inherent uncertainties related to drainage effects, blade-soil interaction, and equipment limitations. Whilst time factor analysis and quality grouping mitigate these concerns, the 52% exclusion rate demonstrates the challenges of obtaining reliable VST measurements in silty tailings. The calibration is therefore dependent on the quality and representativeness of the Group A dataset.

Second, CPT-based state parameter inference carries method-dependent uncertainty (±0.02-0.05 in ψ), which propagates into the triangulation analysis. The scatter observed in Figure 3 (Su/p' ranging from 0.12 to 0.54 at similar state parameters) reflects combined uncertainties from VST measurement, CPT interpretation, and state inference. Despite this scatter, the average convergence (0.24-0.27) provides confidence in the central tendency.

Third, the calibrated Nkt = 23.1 represents the best-fit relationship for the specific gold tailings characterised in this study. Extrapolation to other tailings facilities or different depositional units should be undertaken with caution. Material-specific factors including fines content, mineralogy, stress history, and deposition method may influence Nkt. The methodology is applicable to other sites, but site-specific calibration is recommended rather than direct adoption of Nkt = 23.1.

Finally, this study focuses on peak undrained strength. The relationship between peak and residual strength, critical for post-liquefaction stability assessment, is addressed through the NorSand framework (Paper 1) but is not directly validated by VST in this study.

Broader Applicability and Connection to Companion Study

The methodology presented here is complementary to the state-dependent strength envelope approach detailed in Paper 1. Together, the two studies provide comprehensive characterisation of undrained strength for the subject facilities: Paper 1 develops the theoretical framework and state-dependent relationships from laboratory testing, whilst this paper validates the field application through tri-method convergence. The combined workflow—laboratory CSL and NorSand calibration, CPT-based state inference, VST validation, and triangulation—offers a robust, transparent pathway for defensible strength assignment in tailings stability assessment.

Whilst demonstrated here for gold tailings, the triangulation framework is applicable to any tailings facility where representative sampling enables laboratory characterisation and where in situ testing programmes include both CPT and direct strength measurements. The approach is particularly valuable for high-consequence facilities under regulatory scrutiny, where multi-method validation provides defensible evidence of strength characterisation quality.

CONCLUSIONS

This study presents a comprehensive approach for deriving and validating site-specific CPT-based undrained strength in gold tailings through triangulation of three independent methods: quality-screened VST measurements, calibrated CPT interpretation, and laboratory-based NorSand constitutive modelling. Applied to two South African gold tailings facilities (36 CPT soundings, 31 VST tests), the methodology demonstrates robust convergence across all three approaches.

Rigorous quality screening of VST data identified 16 of 31 tests exhibiting reliable undrained response (Group A), with the remainder excluded due to blade damage or drained conditions. Back-calculation from Group A measurements yielded site-specific Nkt ranging from 8.8 to 46.8 (mean = 24.7, median = 21.4 after outlier exclusion). Regression analysis established Nkt = 23.1 as the calibrated cone bearing factor, 54% higher than the default Nkt = 15 commonly applied without validation.

Tri-method validation demonstrates that VST measurements (Su/p' = 0.27), CPT with calibrated Nkt = 23.1 (Su/p' = 0.24), and NorSand modelling (Su/p' = 0.25) converge within 12% at average state parameter ψ = 0.01. This triangulation provides robust confidence that the calibrated strengths are correct, validated through independent laboratory and field approaches. In contrast, CPT with default Nkt = 15 overestimates strength by 48% (Su/p' = 0.37), demonstrating the critical importance of site-specific calibration for defensible tailings assessment.

Application of the calibrated Nkt = 23.1 to the complete CPT dataset narrows the Su/p' distribution significantly (mean reduced 30%, standard deviation reduced 31%), providing tighter, more defensible

strength profiles aligned with independent validation methods. The workflow—comprising systematic VST quality grouping, CPT-VST back-calibration, statistical screening, and triangulation with constitutive modelling—offers practitioners a reproducible framework for site-specific Nkt calibration with quantified validation. Combined with the state-dependent NorSand envelope approach (Paper 1), this provides comprehensive, multi-method characterisation of undrained strength for stability assessment of tailings facilities.

REFERENCES

ASTM D2573/D2573M-18 (2018). Standard Test Method for Field Vane Shear Test in Saturated Fine-Grained Soils. ASTM International, West Conshohocken, PA.

ASTM D5778-20 (2020). Standard Test Method for Electronic Friction Cone and Piezocone Penetration Testing of Soils. ASTM International, West Conshohocken, PA.

Been, K. and Jefferies, M.G. (1985). A state parameter for sands. Géotechnique, 35(2), 99–112.

Been, K. and Jefferies, M.G. (2004). Stress-dilatancy in very loose sand. Canadian Geotechnical Journal, 41(5), 972–989.

Blight, G.E. (1968). A note on field vane testing of silty soils. Canadian Geotechnical Journal, 5(3), 142–149.

Danziger, F.A.B., Coop, M.R., Azevedo, R.F., Fonseca, A.V. and Rodrigues, R.A. (2019). In situ undrained shear strength by CPT and Vane in iron ore tailings. Tailings and Mine Waste 2019, Vancouver, Canada, 244–256.

Hogan, A.A., Kelly, S.A., Sharp, J.T. and DeJong, J.T. (2025). A comprehensive review of field vane shear testing in mine tailings and recommendations for tailored standards. Geotechnical Testing Journal, 48(1), 80–91.

ICOLD (2022). Tailings Dam Safety. Bulletin 194. International Commission on Large Dams, Paris.

Jefferies, M.G. and Been, K. (2016). Soil Liquefaction: A Critical State Approach. 2nd Edition. CRC Press, Boca Raton.

Jefferies, M.G. and Shuttle, D.A. (2002). Dilatancy in general Cambridge-type models. Géotechnique, 52(9), 625–638.

Lunne, T., Robertson, P.K. and Powell, J.J.M. (1997). Cone Penetration Testing in Geotechnical Practice. Blackie Academic & Professional, London.

Mayne, P.W. and Peuchen, J. (2018). Evaluation of CPTU Nkt cone factor for undrained strength of clays. Cone Penetration Testing 2018. CRC Press, 415–420.

Reid, D. (2016). Effect of rotation rate on shear vane results in a silty tailings. Geotechnical and Geophysical Site Characterisation 5. Australian Geomechanics Society, Sydney, 1145–1150.

Robertson, P.K. (2010). Soil behaviour type from the CPT: an update. 2nd International Symposium on Cone Penetration Testing, Huntington Beach, CA.

Robertson, P.K. and Cabal, K.L. (2015). Guide to Cone Penetration Testing for Geotechnical Engineering. 6th Edition. Gregg Drilling & Testing, Inc., Signal Hill, CA.



Juan Swanepoel

Geotechnical Engineer
Knight Piésold (Pty) Ltd

Juan Swanepoel is a Geotechnical Engineer at Knight Piésold specialising in tailings dam stability assessment and advanced in situ testing. His expertise includes cone penetration testing (CPT) with seismic and resistivity modules, critical state soil mechanics, NorSand constitutive modelling, and laboratory testing programs for mine waste characterisation. His work encompasses CPT data interpretation, state parameter inference, development of critical state lines for tailings materials, slope stability analysis, and geotechnical reporting for high-consequence facilities. He has presented technical findings to Independent Tailings Review Boards and contributes to stability assessments of operating tailings storage facilities across southern Africa.

Undrained shear strength selection within a critical state framework

L.H. Kirsten, H.A. Brandão, F.D. Walsh, L. Murray

Klohn Crippen Berger, Australia

Reliable evaluation of shear strength for tailings storage facility design requires consistent interpretation of stress history and consolidation state. This paper presents a method for selecting representative peak undrained shear strength ratio for uncompacted bauxite residue within a critical state–based, SHANSEP framework. Laboratory and field data are interpreted through yield stress ratio and state parameter (ψ), which together describe consolidation and density state. Bayesian updating is applied to combine multiple datasets and refine representative strength estimates. The approach results in peak undrained strength ratio that is consistent across consolidation domains and supported by both theoretical and empirical evidence.

Keywords: undrained shear strength, critical state soil mechanics, SHANSEP, tailings storage facility, consolidation state, Bayesian updating

INTRODUCTION

The undrained strength of bauxite residue depends on its stress history and in-situ consolidation state, which determine whether shearing causes contraction or dilation. In the first part of this paper, a method for defining a representative peak undrained shear strength function for uncompacted bauxite residue is presented. The approach uses yield stress ratio (YSR) and state parameter (ψ) to describe apparent consolidation and state and combines laboratory and field data using Bayesian updating. The theoretical background applicable to the proposed method follows in the second part of the paper. The third part demonstrates application of the proposed method on an operating tailings storage facility (TSF) dataset, showing its practical benefit for the determination of representative peak undrained strength and the definition of a representative shear strength function for design. The method supports transparent, defensible strength selection for TSF design using laboratory and field data.

PROPOSED METHOD

The key steps proposed herein for structured, critical state-based derivation of representative peak undrained shear strength from laboratory and field data include:

- Select critical state and constitutive model parameters
- Predict undrained shear strength
- Evaluate laboratory consolidation and strength testing
- Calibrate and filter field data (including drainage condition and YSR filtering)
- Evaluate field consolidation state within the laboratory consolidation framework
- Compare predicted, laboratory and field-derived peak undrained strengths
- Select a representative peak undrained strength distribution using Bayesian inference
- Define the peak undrained strength function

THEORETICAL BACKGROUND

This section outlines the key theoretical concepts for interpreting stress history and consolidation state and deriving representative undrained shear strength for fine-grained soils.

Consolidation stress history

Consolidation of fine-grained soils involves precompression up to the preconsolidation stress, followed by normal compression, rebound, and recompression if unloading and reloading occur. The overconsolidation ratio (OCR) is the ratio of the maximum past effective stress to the current effective stress after rebound. Materials subjected to compaction, i.e., densified, may also exhibit apparent OCR.

For hydraulically deposited tailings, significant unloading rarely occurs, aside from transient matric suction dissipation within the vadose zone. Consolidation therefore progresses toward the yield stress (YS) and ultimately approaches a normally consolidated (NC) state. The YSR, defined as the ratio of yield stress to current effective stress, serves as a proxy for the degree of consolidation along a stress path referenced to yield. At the intersection of a consolidation path and the critical state line (CSL) the YSR is denoted as the YSR_{CSL}. Figure 1 illustrates these concepts in semi-logarithmic e–ln p′ space for isotropic consolidation.

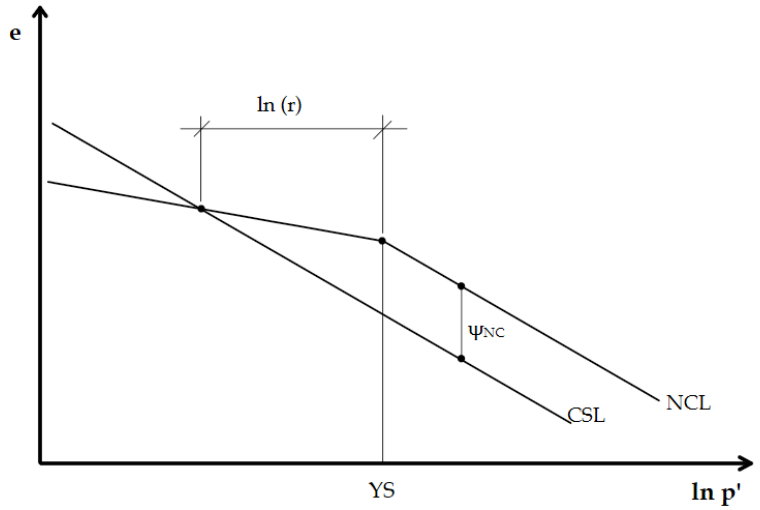


Figure 1. Conceptual framework of isotropic consolidation.

The state parameter (ψ) is the void ratio difference between the current state and the critical state at the same mean effective stress (Jefferies & Been, 2016). If the normal consolidation line (NCL) is parallel to the CSL, the difference between them, ψ_{NC}, is constant. Depending on initial density, numerous consolidation paths are possible, and it remains uncertain whether these converge or remain parallel to the CSL within the effective stress ranges typical of TSFs.

Undrained strength

Wroth (1984) established that the normalised undrained strength (s_u/p'_0), or strength ratio, depends on the critical friction ratio (M_{tc}) in triaxial compression, OCR, and the spacing ratio (r) shown in Figure 1. Substituting YSR for OCR in Wroth's original formulation results in:

$$\left(\frac{s_u}{p'_0}\right) = \left(\frac{M_{tc}}{2}\right)\left(\frac{YSR}{r}\right)^{\Lambda} \quad [1]$$

Or, if s_u is normalisated with respect to vertical effective stress,

$$\left(\frac{s_u}{\sigma'_{v0}}\right) = \left(\frac{1+2K_0}{3}\right)\left(\frac{M_{tc}}{2}\right)\left(\frac{YSR}{r}\right)^{\Lambda} \quad [2a]$$

where M_{tc} is defined by:

$$M_{tc} = \frac{6\sin\varphi'_c}{3-\sin\varphi'_c}; \quad \varphi'_c = arcsin\left(\frac{3\eta_c}{6+\eta_c}\right); \quad \eta_c = \frac{q_c}{p'_c} \quad [3]$$

and K_0 is the at-rest lateral stress coefficient, φ_c is the friction angle at the critical state and η_c is the limiting stress ratio at large strain in terms of deviatoric and mean effective stress at the critical state (q_c, p'_c). Wroth defined the plastic volumetric strain ratio (Λ) as:

$$\Lambda = 1 - \frac{\kappa}{\lambda_{10}} \approx 1 - \frac{C_s}{C_c} \quad [4]$$

The spacing ratio r is equal to YSR_{CSL}. The isotropic compression and swelling indices are respectively λ_{10} and κ. The terms c_s and c_c are their one-dimensional equivalents.

Equations (1) are commonly taken to describe normalised 'peak' undrained strength ratio. For monotonic loading, the shear strength response is characterised by an initial increase to a yield (or peak) value, followed by either strain softening (strength decreases with strain), strain hardening (strength increases beyond yield), or ideal plasticity (strength is constant with strain). This paper distinguishes between yield strength (also referred to as peak in strain-softening behaviour); strain-hardened residual strength beyond yield; and strain-softened residual strength beyond yield (commonly referred to as residual).

The softened normalised residual undrained strength ratio (s_r/p'_0) is usually expressed in terms of the initial state parameter (ψ_0) and the CSL slope (λ_e) in semi-logarithmic space (Jefferies & Been, 2016).

$$\left(\frac{s_r}{p'_0}\right) = \left(\frac{M_{tc}}{2}\right)e^{-\left(\psi_0/\lambda_e\right)} \quad [5]$$

Or, normalised in terms of vertical effective stress,

$$\left(\frac{s_r}{\sigma'_{v0}}\right) = \left(\frac{1+2K_0}{3}\right)\left(\frac{M_{tc}}{2}\right)e^{-\left(\psi_0/\lambda_e\right)} \quad [6a]$$

The negative signs preceding the exponents in Equations (4) signify a downward positive convention for the CSL slope. In the NC state, YSR = 1, and r may be obtained by equating Equations (1) and (4) and simplifying:

$$r = YSR_{NCL} = e^{\left(\psi_{NC}/(\lambda_e \Lambda)\right)} \quad [7]$$

Notably, Equations (1) and (4) represent equivalent stress–strength relationships through alternative state descriptors (ψ and YSR). For several isotropic consolidation paths relative to a CSL as in Figure 2, their numerical equivalence is shown in Table I. In all cases, M_{tc} = 1.4.

Integration of the undrained strength-, consolidation- and critical state domains

Taylor (1948) linked stress history to the drained and undrained strength behaviour in cohesive soils, showing that lightly overconsolidated (LOC) and NC or loose soils tend to contract during shearing, generating positive pore pressures and undrained strengths equal to or lower than their drained strengths at comparable effective stress. In contrast, heavily overconsolidated (HOC) or dense soils dilate during shearing, generating negative pore pressures and undrained strengths exceeding drained strengths.

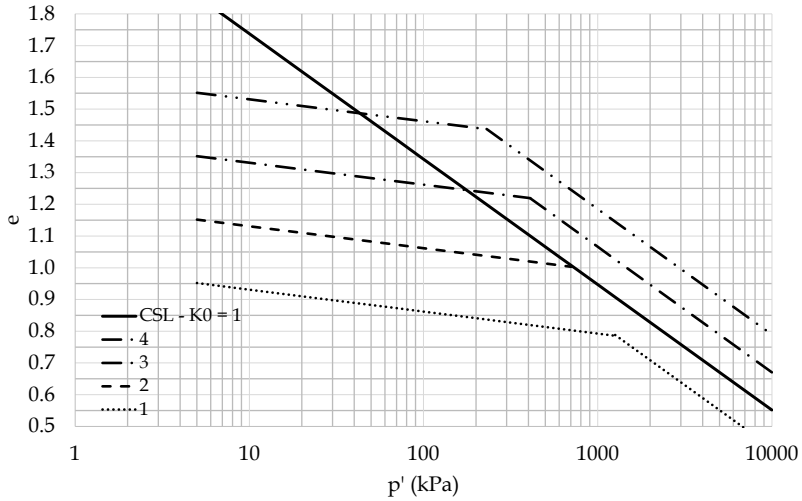


Figure 2. Various isotropic consolidation paths for different initial void ratios.

Table I. Computed undrained shear strength ratios for points along the isotropic consolidation paths in Figure 2

Consolidation path	Coordinate points		YSR	r = YSR_{CSL}	Ψ	$\frac{s_u}{p'_0}$ [1]	$\frac{s_r}{p'_0}$ [2]
	p' (kPa)	e					
4	5	1.55	46	5.35	-0.3	4.13	4.13
	43	1.49	5.35		0	0.70	0.70
	230	1.44	1		0.24	0.18	0.18
3	5	1.35	82	2.32	-0.5	13.25	13.25
	176.4	1.24	2.32		0	0.70	0.70
	410	1.22	1		0.12	0.35	0.35
2	5	1.15	141	1	-0.7	42.5	42.5
	724	1.00	1		0	0.70	0.70
	705	1.00	1		0	0.72	0.72
1	5	0.95	252	0.42	-0.9	136.1	136.1
	2968	0.76	0.42		0.0	0.70	0.70
	1260	0.79	1		-0.12	1.42	1.42

Ladd & Foott (1974) restated Taylor's stress-history concept in empirical form by normalising undrained strength with respect to the maximum past vertical effective consolidation stress in the SHANSEP approach as represented by:

$$\frac{s_u}{\sigma'_v} = S_{NC}\,(OCR)^m \qquad [8]$$

where s_u is the undrained shear strength, σ'_v is vertical effective stress, S_{NC} is the undrained strength ratio in an NC state, and m is the empirical exponent. Equation (6) has the same form as Equations (1) and (4); however, it is independent of the spacing and critical friction ratios.

Schofield and Wroth (1968) showed within the critical state framework that plastic shear deformation in saturated soils evolves toward unique combinations of mean effective stress and void ratio on the CSL. Building on this, Shewbridge (2019) integrated the Taylor, Ladd and Foott, and Schofield and Wroth frameworks to relate undrained shear strength to consolidation history and proximity to the critical state. For undrained shearing, states above the CSL are contractive, generating positive pore pressures and strength loss, while states below the CSL are dilative, producing negative pore pressures and strength gain; states at the CSL exhibit equal drained and undrained strength. The resulting strength function (Figure 3) is consistent with the ICOLD (2025) capped-SHANSEP framework and provides a rational basis for selecting representative strength functions consistent with integrated

critical-state and undrained strength models.

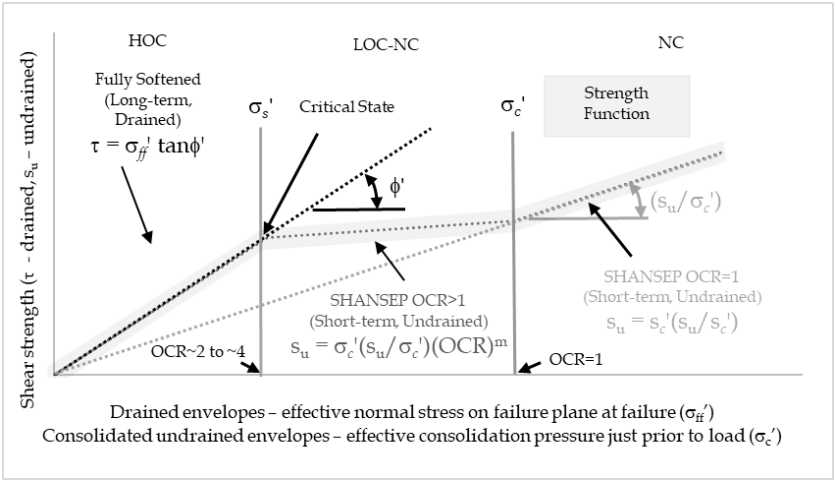


Figure 3. Overlay of SHANSEP and critical state reference points on Taylor's Mohr envelopes for the drained and consolidated-undrained cases (Shewbridge, 2019).

Strength selection by Bayesian inference

Bayesian analysis provides a consistent framework for combining new or updated information with existing knowledge (Straub & Papaioannou, 2014) and is commonly used to estimate parameters derived from multiple laboratory and field datasets. In strength characterisation, parameters are treated as random variables with probability distributions representing uncertainty. Additional measurements update these distributions through Bayesian inference, combining prior information with observations to produce posterior distributions reflecting the updated state of knowledge. This process can be expressed as:

$$Pr(F|Z) = \frac{Pr(Z|F)\,.Pr(F)}{Pr(Z)} \quad [9]$$

where Pr(F) is the prior probability; Pr(Z | F) is the likelihood of Z given F; Pr(Z) is the probability of observation Z, and Pr(F | Z) is the posterior probability. For continuous strength parameter distributions this relationship may be expressed in terms of probability density functions (PDFs):

$$f_x''(x) = a\,.L(x)\,.f_x'(x) \quad [10]$$

where $f_x'(x)$ and $f_x''(x)$ are the prior and posterior PDFs of strength respectively such that $f_x''(x) = f_{(x|Z)}$ and L(x) is the likelihood function. The normalising constant is:

$$a = \frac{1}{\int_{-\infty}^{+\infty} L(x)\,.f_x'(x)} \quad [11]$$

Posterior PDFs typically fall between the prior and likelihood PDFs and, in many cases, are dominated by the measurements.

DEMONSTRATION OF UNDRAINED STRENGTH SELECTION WITH CONSIDERATION OF CONSOLIDATION STATE

This section demonstrates application of the proposed method to derive a representative peak undrained shear strength function using laboratory and field data from a bauxite residue TSF. The same procedure applies to residual undrained strength selection.

General characterisation

The bauxite residue is a silt-like to elastic silt material, comprising 60–70% silt and 30–40% clay-sized

fractions respectively, with a mean fines content of 94%. The particle size distribution is poorly graded (C_u = 29, C_c = 0.96) but internally stable. The specific gravity (G_s) ranges from 2.66 to 3.58. The consistency limits indicate medium plasticity (LL = 40–79%, PI = 9–21%). The plastic limit ranges from 28% to 38%, and the shrinkage limit varies from 6% to 13%. From mineralogical analysis, the residue primarily comprises hematite (iron oxide, Fe_2O_3), aluminium oxide (Al_2O_3), and silica (SiO_2).

Critical state- and constitutive model parameters
Critical state parameters were derived from isotropically consolidated triaxial (CIU) tests on slurry-deposited samples. The NorSand parameter set was established following Jefferies & Been (2016) and comprises:

- CSL: slope on a natural logarithmic scale λ_e = 0.17; intercept Γ = 2.13 at 1 kPa
- Plasticity: M_{tc} = 1.4; hardening moduli H_0 = 81.7 and H_ψ = 150; Nova's volumetric coupling coefficient N = 0.1; state dilatancy scaling factor χ_{tc} = 5.6
- Elasticity: reference shear modulus (G_{ref}) = 22.9 × 10^3 kPa (from bender element testing); elastic exponent n_G = 0.68; Poisson's ratio v = 0.1
- Initial consolidation state: OCR = 1.07

Predicted undrained shear strength
Prediction of undrained strength involved simulations with the SoilTest tool in PLAXIS 2D using the NorSand parameter set. K_0 was varied between 1.0, 0.8, and 0.6. In all cases of strain hardening, the onset of yield was defined as the undrained strength corresponding to zero volumetric strain rate.

Figure 4 shows the undrained strength normalised by vertical effective stress (s_u/σ'_v and s_r/σ'_v) plotted against initial state parameter (ψ_0). Solid lines represent residual strength (hardened or softened) obtained using Equation (4b), while dashed lines represent simulated yield strength; both are referenced to ψ_0. Values of ψ_0 were limited to less than 0.55, beyond which the ratio of plastic to elastic stiffness (H/I_r) becomes negative for the parameter set, precluding simulation convergence.

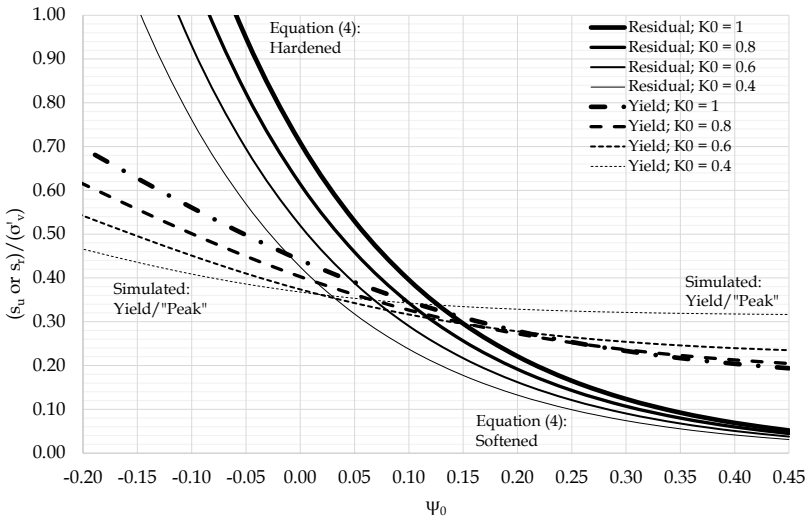


Figure 4. Normalised undrained shear strength (s_u/σ'_v and s_r/σ'_v) versus ψ_0 for selected K_0 .

The intercept of ∽0.7 (0.66) on the vertical axis at ψ_0 = 0 corresponds to φ'_c = 33.3° from Equation (2) where drained strength ≈ hardened residual undrained strength. For uncompacted residue and K_0 ≈ 0.6, a representative normalised yield strength of ∽0.35 would limit the influence of negative pore pressures under stress dilation. This cap effectively bounds the hardened residual undrained strength at 0.35. On the contractive side, selection of peak (or yield) normalised undrained strength should not exceed ∽0.35, with residual strengths no less than about 0.1 for the credible range of positive ψ_0.

Laboratory test evaluations

Consolidation

The background plots in Figure 5 represent oedometer tests on undisturbed and remoulded (slurry deposition or light tamping) samples while the back-extended NC limbs of these are shown in the foreground. The unload/reload lines in the background are nearly horizontal, indicating low elastic rebound. The YS or transition from precompression to normal compression, ranges from 30 kPa to 111 kPa (mean = 71 kPa). In semi-natural logarithmic space, the average compression index $C_c \approx 0.172$, and is equal to λ_e. The offset (ψ_{NC}) between the back-extended NCLs and CSL ranges from 0.09 to 0.43.

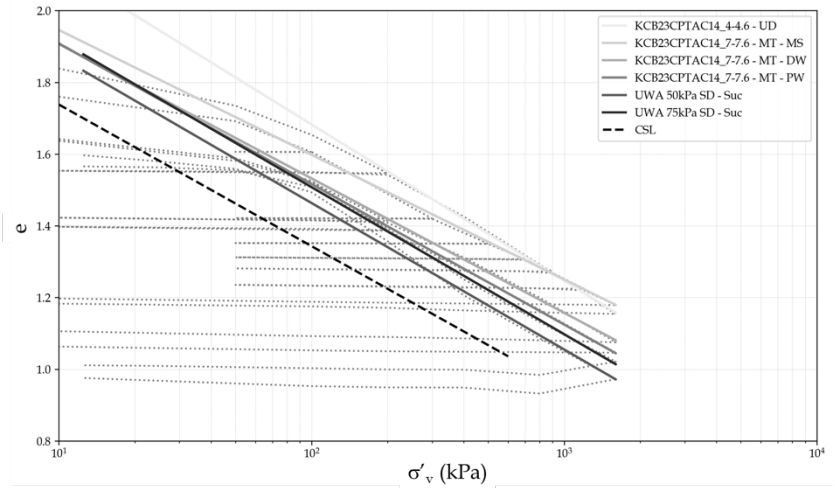


Figure 5. Normal consolidation paths (background) and limiting compression range ψ_{NC} (foreground).

The maximum ψ_{NC} offset of 0.43 may be taken to delineate a limiting compression zone (LCC), corresponding to $\psi_{NC,max}$, which represents the likely lower-density bound for the deposition and consolidation regimes at the subject TSF: that is, higher offsets are likely not physically attainable without microstructure development. An infinite number of NCLs – depending on the initial void ratio for any normal consolidation path – would be bounded by this LCC.

Strength

Laboratory strength tests included monotonic simple shear (MSS), MSS after completion of cyclic simple shear (CSS), and CIU tests. The peak normalised undrained strength distribution parameters for these (assuming normality) are summarised in Table II. The mean values occurred at axial strains of 5% or greater. The tests all showed moderately ductile post-peak behaviour.

Table II. Peak (or yield) normalised undrained laboratory strength by test type

Test type	Preparation	Number of tests	Initial void ratio (post consolidation)	Mean $(s_u/\sigma'_c)^1$ or $(\tau/\sigma'_c)^2$	Standard deviation
MSS	Undisturbed	7	1.24 – 3.18	0.33	0.06
CSS	Undisturbed & remoulded	7	1.1 – 3.47	0.27	0.05
CIU	Undisturbed	3	1 to 1.7	0.33	0.03

1 – triaxial; 2 – simple shear

Field test evaluations

CPTu calibration and strength derivation

In-situ stress was estimated using the bulk density inversion proposed by Conetec (2023), calibrated against bulk density measurements at CPTu locations. Vertical effective stress (σ'_v) was calculated from total stress and equilibrium pore pressure, calibrated using dissipation tests. Undrained shear strength

(s_u) was obtained from cone tip resistance (q_t) using Equation (10), with the net cone factor N_{kt} calibrated against vane shear tests (VST) following Brandão *et al*., (2025), giving N_{kt} = 13.

$$s_u = \frac{q_t - \sigma_v}{N_{kt}} \quad [10]$$

The resulting undrained strength data was filtered for drainage condition following Schneider *et al*., (2008) and normalised with respect to σ'_v.

Field consolidation stage and density state

The consolidation state was assessed through YSR (ratio of σ'_p to σ'_v) for the CPTu data following Mayne and Sharp (2022). The preconsolidation pressure (σ'_p) or YS was obtained from CPTu data using Equation (11), where $q_{net} = q_t - \sigma'_v$ and m'_p follows from the Robertson (2009) material index:

$$\sigma'_p = 0.33(q_{net})^{m'_p} \quad [11]$$

$$m'_p = 1 - \frac{0.28}{1 + \left(\frac{I_{c,RW}}{2.65}\right)^{25}} \quad [12]$$

Cumulative distribution and probability density plots for the full dataset, and for data filtered to YSR ≤ 1, are shown in Figure 6. The differences in summary statistics highlight the importance of accounting for consolidation state when comparing laboratory and field data; for example, the 5% fractile and mean shift from 0.19 and 0.3 (all data) to 0.22 and 0.24 for the NC-filtered dataset.

The in situ state (ψ) was assessed according to Jefferies and Been (2016), as per Equation (13) with $\lambda_{10} = 2.33\lambda_e$ and $M_{tc} = 1.4$. Q'_p is the effective penetration resistance normalised by mean effective stress, and B_q is the normalised excess pore water pressure parameter. K_0 was derived from CPTu data using YSR and dilatometer (DMT) data. The representative mean K_0 value of 0.64 from CPTu data closely coresponds to the DMT dataset mean of 0.56.

$$\psi = \frac{1}{(11.9 - 13.3\,\lambda_{10})}\, ln\left(\frac{Q'_p\,(1 - B_q) + 1}{M_{tc}\left(3 + \frac{0.85}{\lambda_{10}}\right)}\right) \quad [13]$$

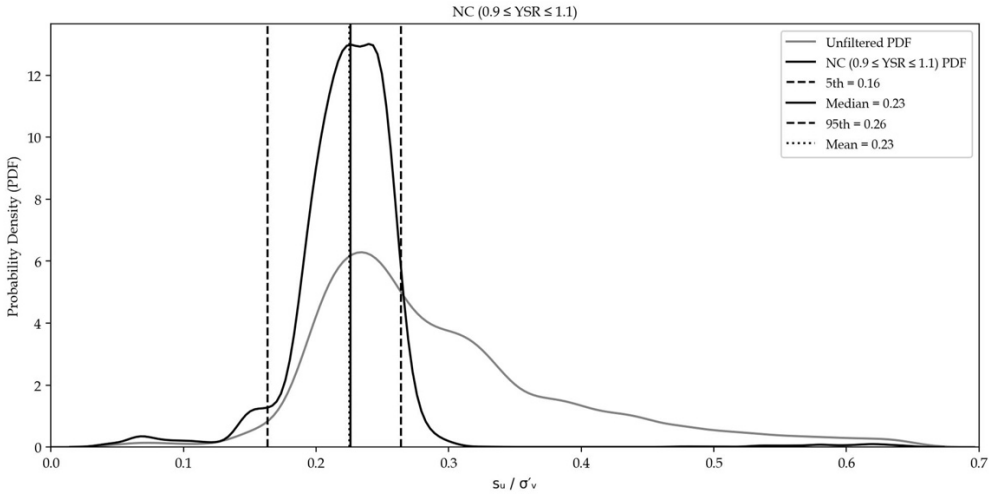


Figure 6. s_u/σ'_v distribution from CPTu – all consolidation states and NC-filtered states.

Field peak undrained shear strength

Peak field undrained shear strength (s_u) was derived from CPTu (after N_{kt} calibration), DMT, seismic CPTu (SCPTu), and VST testing. The DMT strengths were based on the horizontal stress index K_D and σ'_v prior to insertion, while SCPTu derived strengths were estimated from shear wave velocity using

correlations from anisotropically consolidated undrained triaxial test databases. No additional calibrations were applied to the DMT or SCPTu datasets. YSR, and hence consolidation state for VST, DMT and SCPTu were taken from collocated CPTu profiles and filtered for the NC state (defined as 0.9 < YSR < 1.1). Representative distributions of NC peak (or yield) normalised undrained strength were filtered by YSR. As shown in Table III, the mean normalised peak strengths ranged from ∽0.22-0.42. The SCPTu derived distribution is considered outlying due to its markedly higher mean and standard deviation compared to the other test types.

Table III. Field-determined normalised peak (or yield) undrained strength

Test type	**Sample size**	**Mean $(s_u/\sigma'_v)_{NC}$ 0.9 < YSR < 1.1**	**Standard deviation**
CPTu-derived (N_{kt}=13)	3745	0.24	0.17
DMT	60	0.22	0.07
SCPTu	27	0.42	0.31
VST	5	0.22	0.09

Comparison of field and laboratory consolidation states

The field consolidation state was found to be consistent with the laboratory one by overlaying the e_{CPT}–p'_0 coordinates from the CPTu probings onto the extended NCLs from the oedometer tests (Figure 7). In situ void ratio (e_{CPT}) was derived from state parameter (ψ) by subtracting the estimated in-situ critical state (e_c) void ratio from the state parameter (ψ) at corresponding mean effective stress. The LCC at $\psi_{NC,max}$ = 0.43 is an upper bound to points except NC filtered data at very low mean effective stress which may reflect the density state under near-zero effective stress adjacent to the supernatant pond and where subaqueous migration could facilitate approach to the upper-bound loosest state within the compression envelope.

CPTu-derived YS for the NC-filtered, uncompacted residue ranged from 11 kPa to 151 kPa, compared with 30 kPa to 111 kPa from the oedometer tests. Yield generally initiated at mean effective stress of ∽100 kPa for both datasets, consistent with the laboratory YS mean of 71 kPa.

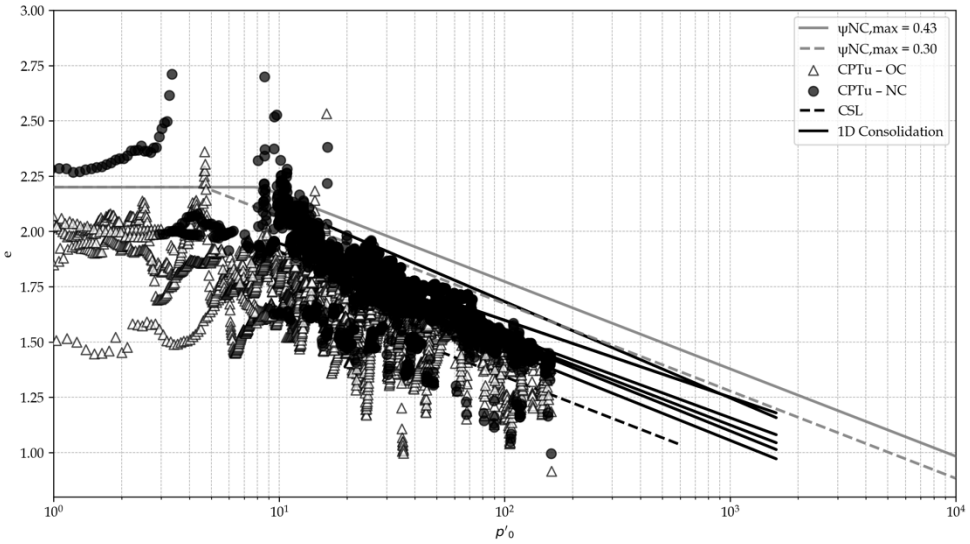


Figure 7. Field-derived consolidation history superimposed onto 1-D consolidation history.

Comparison of field-, laboratory-, and predicted undrained strengths

Figure 8 compares predicted normalised yield and residual strengths for K_0 = 0.6 with field- and laboratory-derived undrained strengths. Three strength domains are evident: HOC (YSR > 4), LOC-NC (2–4 > YSR ≥ 1) and NC (YSR ≤ 1). Across these domains, the data follows the expected inverse relation between s_r/σ'_v and ψ_0, consistent with Equation (4b).

For $\psi_0 < 0.15$ the field data exceeds the predicted peak/yield curve (i.e., hardened residual strength). As ψ_0 increases beyond 0.15, the field data falls a little below the predicted curve ($0.2 \leq s_u/\sigma'_v \leq 0.25$) – indicative of somewhat softened residual strength. The cluster of field data centred on $s_u/\sigma'_v \approx 0.3$, $\psi_0 \approx 0.15$ indicates the profile is largely in a lightly contractive state. The majority of NC data clusters between $\sim 0.1 < \psi_0 < 0.35$ which aligns with the range of oedometer-derived NCL offsets from the CSL in Figure 5. A normalised yield strength of ~ 0.35 would credibly bound dilative hardening while peak/yield strengths of ~ 0.2 – 0.25 are representative for contractive conditions. The scatter of CPTu data is consistent with variability in K_0 and consolidation history.

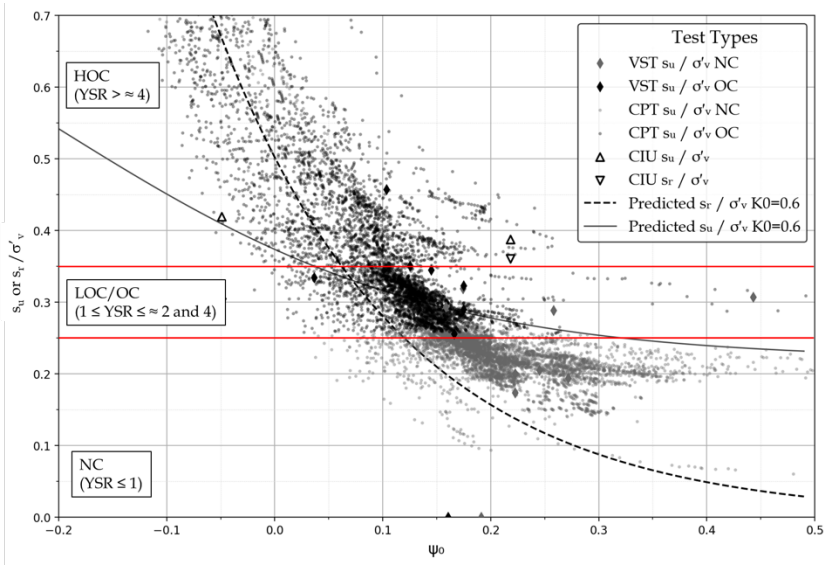


Figure 8. s_u/σ'_v against ψ_0 for CIU, MSS, CSS, CPTu, DMT, SCPTu and VST data.

Selection of strength distribution by Bayesian inference

Figure 9 illustrates Bayesian updating applied to the laboratory and field undrained strength datasets:

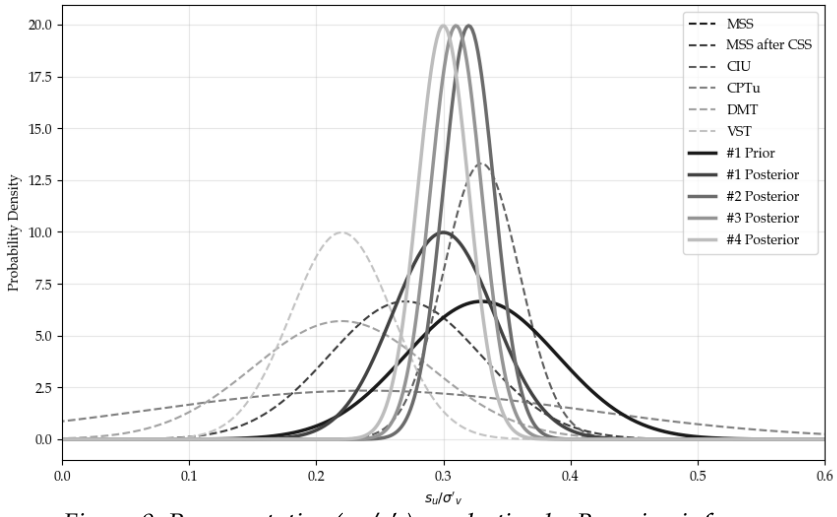


Figure 9. Representative $(s_u/\sigma'_v)_{NC}$ selection by Bayesian inference

For this demonstration all datasets are weighted equally and the outlying SCPTu dataset is omitted to avoid undue influence on the posterior, consistent with the intent to demonstrate the proposed procedure rather than assess dataset weighting or outlier treatment strategies.

The initial prior is taken as the MSS dataset which, given the upper bound of ~ 0.35, provides a credible estimate of normalised peak undrained strength before incorporating additional evidence. The first

update applies the MSS-after-CSS dataset as the likelihood, producing a refined posterior with reduced uncertainty. Subsequent updates sequentially incorporate the CIU, CPTu, DMT, and VST datasets, with each posterior serving as the prior for the next update. After five iterations, the posterior converges to $\backsim N(\mu = 0.30, \sigma = 0.02)$. Convergence of the mean indicates mutual consistency between the datasets, while the progressive reduction and stabilisation of the standard deviation reflect decreasing epistemic uncertainty.

The final posterior distribution provides a credible estimate of representative normalised peak (yield) undrained strength, integrating laboratory and field evidence. The stability of the posterior mean ($\mu \approx 0.30$) and narrow standard deviation ($\sigma \approx 0.02$) demonstrate the robustness of the Bayesian updating procedure for representative strength selection. Any appropriate fractile of the final posterior distribution may be adopted as characteristic value, consistent with Eurocode 7 (EN 1997). In this paper, the mean is used to define the strength function; however, this does not imply that the mean is the most appropriate characteristic value in all applications.

Selection of representative peak strength design function

The peak strength function in Figure 10 is derived using the method described in this paper. In the HOC (YSR > 4) domain, strength increases following the $\varphi_c = 33.3^0$ envelope which defines the drained reference separating contractive and dilative responses. The capped formulation here limits undrained strength to values corresponding to the onset of dilation, constraining the function in the dilative range. In the LOC-NC domain (2-4 > YSR ≥ 1) the transition from the dilative to a fully contractive response is represented by a horizontal relationship bounded below by a minimum undrained strength of $s_{u,min}$ = 20 kPa, determined empirically from the MSS and CIU tests at low effective confining stress. In the NC domain (YSR ≤ 1) the normalised undrained strength is taken as $(s_u/\sigma'_v)_{NC} = 0.3$, obtained through Bayesian updating.

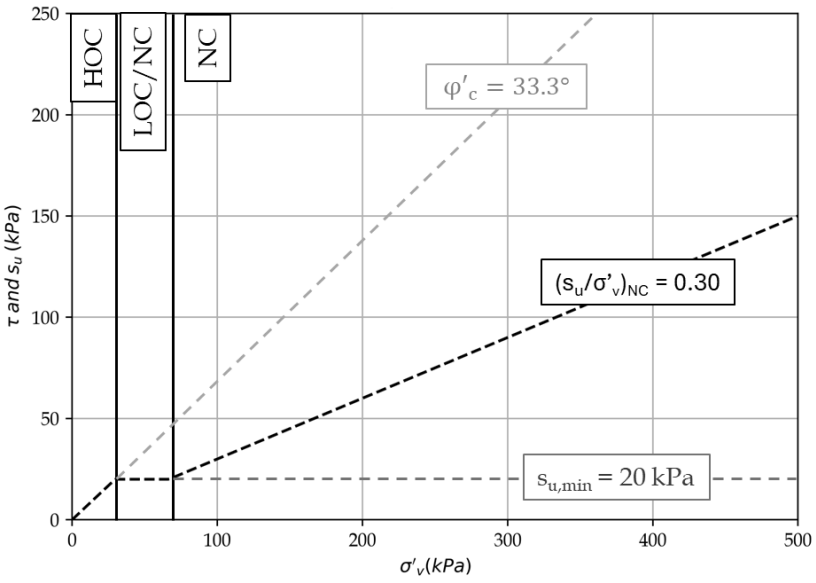


Figure 10. Representative peak undrained strength design function.

DISCUSSION

The demonstration confirms that integrating critical state concepts with undrained strength selection in a capped SHANSEP framework provides a consistent basis for interpreting and comparing undrained shear strength across consolidation states. Agreement between predicted, laboratory and field strengths indicates that consolidation history and state govern the observed strength response. Use of ψ and YSR enables consistent description across NC and OC domains, replacing OCR as state descriptor –

particularly relevant for hydraulically deposited tailings where unloading is limited and yield stress defines the effective reference state.

Bayesian updating provides a quantitative check on dataset consistency. Convergence of the posterior mean and reduction in standard deviation indicate compatibility of the available datasets and stability of the representative strength estimate under further testing. In this demonstration, datasets are equally weighted and the outlying SCPTu dataset is excluded to avoid undue influence; alternative weighting schemes and Eurocode 7-consistent characteristic value selection are beyond the scope of this paper.

By referencing consolidation state directly, the proposed method reduces potential bias associated with simple averaging or arbitrary distribution-based selection. The derived representative peak undrained strength function is bounded by credible physical limits – cautious under dilative conditions and realistic under contractive ones – providing a defensible basis for TSF embankment assessment. The same procedure may be applied to derive a residual undrained strength function, noting that the critical state expressions for residual and peak strength ratios are equivalent and should be applied consistently for YSR filtering and state description.

CONCLUSION

A practical method is presented for deriving a representative undrained shear strength function for uncompacted bauxite residue within an integrated critical state–SHANSEP framework. The approach reconciles laboratory and field data through state-based filtering and Bayesian updating, yielding a peak undrained shear strength function that is consistent across consolidation domains and supported by both theoretical and empirical evidence.

ACKNOWLEDGEMENTS

The support and committed effort by the Klohn Crippen Berger project team are sincerely appreciated.

AUTHOR CONTRIBUTIONS

LK: Conceptualisation, Methodology, Analysis, Writing, Supervision; HB: Conceptualisation, Methodology, Analysis, Writing, Supervision; FD-W: Conceptualisation, Writing; LM: Supervision.

REFERENCES

Brandão, H., Kirsten, L.H. and Campello, I., (2025). Bauxite residue: a data-driven approach to strength characterisation. *Proceedings of the 9th International Symposium for Geotechnical Safety and Risk* (ISGSR). Research Publishing, Singapore.

Conetec, (2023). *The Cone Penetration Test: Better Information, Better Decisions. A CPT Design Parameter Manual*. 1st ed., Rev.1.1. Conetec, February 2023.

International Commission on Large Dams (ICOLD). (2025). *Tailings Dam Safety / Sécurité des Barrages de Stériles*. Bulletin 194, 1st Edition. CRC Press.

Jefferies, M. & Been, K., (2016). *Soil Liquefaction: A Critical State Approach*. 2nd edn. CRC Press, Taylor & Francis Group, Boca Raton.

Mayne and Sharp (2022). Screening for flow liquefaction for tailings and natural soils by CPTu. *Proceedings of the 20th International Conference on Soil Mechanics and Geotechnical Engineering*. Sydney, Australia.

Orr, T., Sorgatz, T., Estaire, J., Prästings, J., D'Ignazio, M., Andries, J., Ene, A., & Polo Lopez, C. S. (2025). *Determination of representative values from derived values for verification with limit states with EN 1997 - Guidelines for the application of the 2nd generation of Eurocode 7: Geotechnical design*. Joint Research Centre. https://doi.org/10.2760/0980105.

Shewbridge, S.E. (2019). Undrained strengths and long-term stability of slopes. *Journal of Geotechnical and Geoenvironmental Engineering*, ASCE, 145 (11), 02519002.

Schneider, J.A., Randolph, M.F., Mayne, P.W. and Ramsey, N.R. (2008). Analysis of factors influencing soil classification using normalized piezocone tip resistance and pore pressure parameters. *Journal of Geotechnical and Geoenvironmental Engineering*, 134 (11). pp.1569–1586.

Straub, D. and Papaioannou, I. (2015). Bayesian analysis for learning and updating geotechnical parameters and models with measurements. *Risk and reliability in geotechnical engineering*. Phoon, K.K. and Ching, J. (eds.). CRC Press, Taylor & Francis Group, Boca Raton. pp. 221–264.

Taylor, D.W. (1948). *Fundamentals of Soil Mechanics*. Wiley, New York.

Wroth, C.P., (1984). The interpretation of in-situ soil tests. *Géotechnique*, 34(4), pp.449–489.



Louis Hendrik Kirsten

Senior Geotechnical Engineer, Associate
Klohn Crippen Berger

Louis Kirsten is a senior civil and geotechnical engineer with experience across the resources, infrastructure, and public sectors. His work spans research, consulting, and project delivery, from concept through closure, including dispute resolution. He has led projects across Australia, Africa, Canada, and the Middle East, with a focus on tailing storage facilities and water management, dam safety, closure engineering, and foundation and slope stability. He applies practical soil and rock mechanics, deformation analysis, and reliability-based design. Louis has served as Engineer of Record on extreme consequence facilities and has provided expert opinion in forensic investigations. His approach is evidence-based, technically disciplined, and focused on sound engineering judgment.

Installation of an advanced monitoring network for a Tailings Storage Facility

A. Hertenberger[1], E.C. Lukombo[2], K.L. Morton[3], M. Msitsini[3], T.M. Namane[3]

[1]Tecwise Africa, South Africa
[2]Catoca Mining Society, Angloa
[3]KLM Consulting Services Pty Ltd, South Africa

Catoca diamond mine is a 26-year-old open pit diamond mine in North-Eastern Angola. It has a very large active tailings storage facility (TSF) and two smaller dormant TSFs. Over three years, a bespoke monitoring network has been installed that is fully automated and linked to a detailed dashboard. The network comprises suspended vibrating wire piezometers (VWPs), sealed VWPs, water level monitoring sensors, weather stations and inclinometers.

The monitoring network is state of the art for modern TSF monitoring in line with the principles of the Global Industrial Standard for Tailings Management (GISTM). The network integrates monitoring of water levels, beach lengths, pore pressures, slope movement and weather information and is linked to an early warning system that not only addresses movement but also addresses the causes of movement of a TSF.

The paper describes the drilling techniques used and the protocols followed for the installation of each type of equipment. The installation took over a year to install and the project management and installation sequences are given in detail.

The installation is an excellent example of collaboration of engineering, geotechnical interpretation, instrumentation design and software connectivity. It is an example of African initiative and innovation leading the world.

Keywords: Angola, Tailings Storage Facilities, Monitoring, VWPs, inclinometers, water levels, risk management.

INTRODUCTION

Catoca diamond mine is a 26-year-old open pit diamond mine in North-Eastern Angola. It has a very large active tailings storage facility (TSF) and two smaller dormant TSFs. Over three years, a bespoke monitoring network has been designed and installed that is fully automated and linked to a detailed dashboard. The network comprises suspended vibrating wire piezometers (VWPs), sealed VWPs, water level monitoring sensors, weather stations and inclinometers.

Figure 1 shows the location of Catoca and the three TSFs.

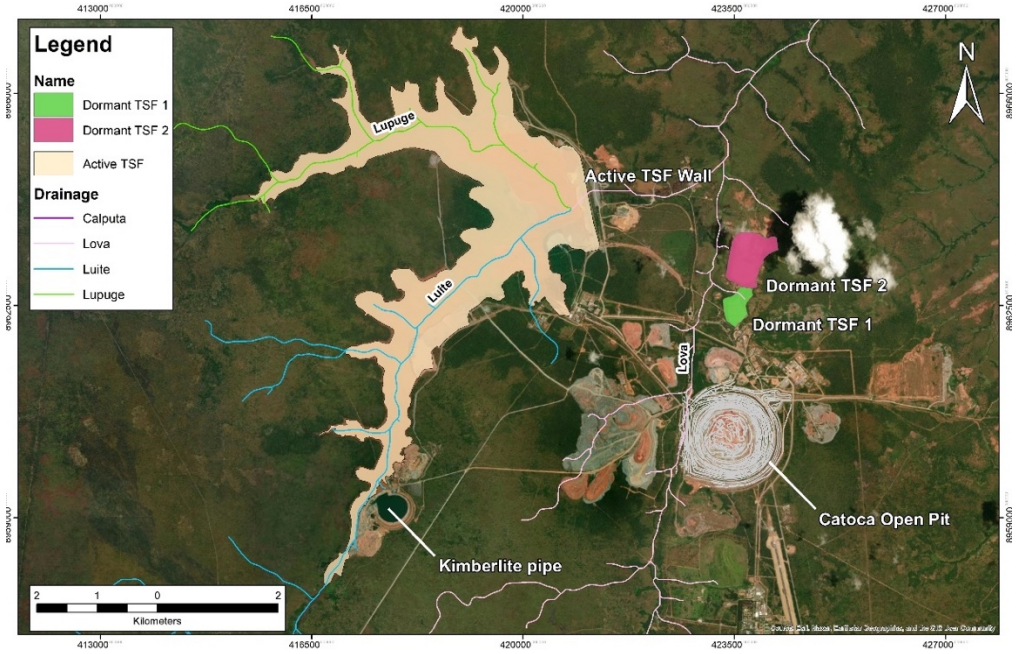


Figure 1. Location of Catoca mine.

The installation was done by a team comprising:

- Catoca management
- Catoca TSF department
- Hydrogeologists
- Hydrologists
- Geotechnical engineers
- TSF designers
- Geologists
- Instrument technicians
- Drilling company
- Catoca surveyors
- CAD GIS
- IT technical installers
- Satellite communications experts
- Dashboard architects

Work took one year to complete through two rainy seasons.

Instrumentation

The monitoring network is state of the art for modern TSF monitoring in line with the principles (2,3,7 and 13) of the Global Industrial standard for Tailings Management (GISTM). The network integrates monitoring of water levels, beach lengths, pore pressures, slope movement and weather information and is linked to an early warning system that not only addresses movement but also addresses the causes of movement of a TSF.

Equipment was sourced from Italy, Spain, South Africa, Sweden and France. The equipment installed included:

- Weather stations
- VWPs
- Inclinometers
- Kiosks

Weather stations.
Three weather stations were installed.
Figure 2 shows a weather station and Figure 3 shows an installation. The weather station was set to measure rainfall, temperature, air pressure and humidity. The Vaisala WTX353 can take readings as frequently as every second, but the actual interval is configurable—you can set it anywhere from 1 second up to 3600 seconds (1 hour) depending on your requirements. The data is uploaded to the gateway every half an hour.



Figure 2. Vaisala WTX 535 weather station.



Figure 3. Vaisala WTX 535 weather station.

Water level measurements
Water level measurements are required for the pond levels and the flumes being installed on the streams and rivers. Figure 4 is a photograph of the sensor.



Figure 4. Pond level sensor.

Vibrating wire piezometers
VWPs were installed to measure water pressure in the upstream country rock, the TSF embankments, within the dormant TSFs and in the downstream areas below the TSF embankments.
Two types of installation were used: sealed and open hole. The sealed VWPs were used in the TSF embankment and the body of the dormant TSFs.

The holes were drilled at 72 mm diameter using core drilling to typical depths of ~40 m.

Figure 5 shows a typical drilling log indicating the geology, construction and location of the VWP.

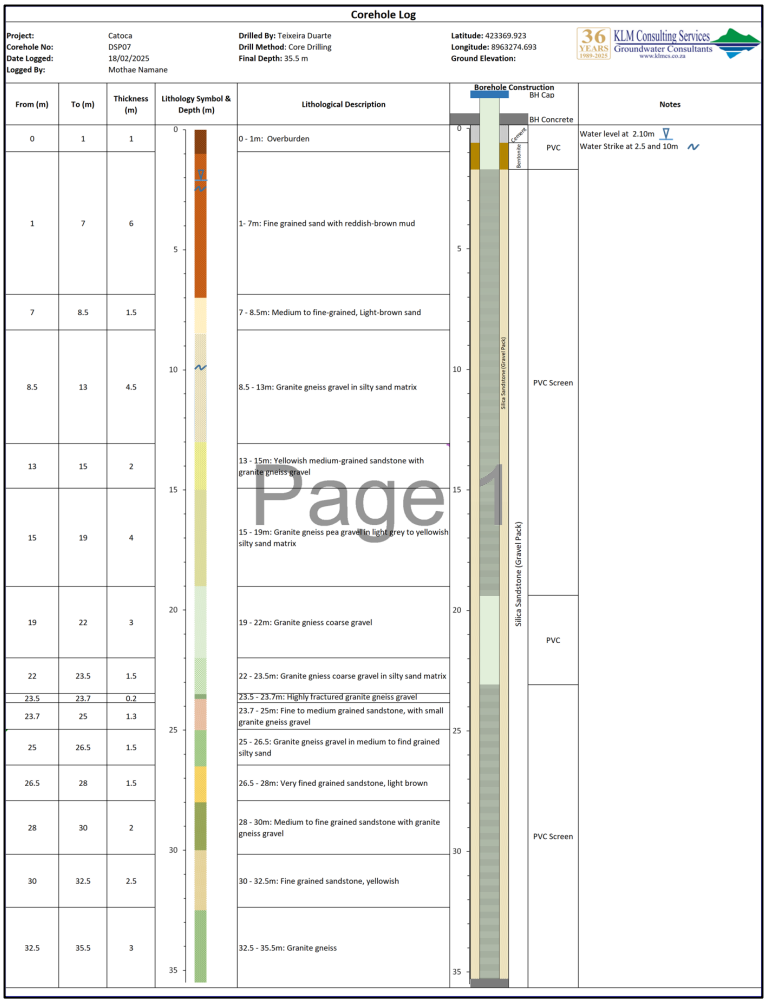


Figure 5. Drilling log showing the geology and construction.

Inclinometers

The Sisgeo BH-Profile is a borehole in-place inclinometer system designed for continuous remote monitoring of soil or structural movements, particularly in casings affected by active ground displacement. It consists of a chain of MEMS-based inclinometer probes connected by carbon fibre extension rods, forming a modular string that is installed inside an inclinometer casing. Each probe measures tilt relative to gravity, enabling accurate profiling of borehole deformation over time. Installation involves assembling the chain by connecting the probes and rods, lowering it into the inclinometer casing, and securing the terminal wheel assembly at the top. The system is then connected to a datalogger such as the wireless node via RS-485 or Modbus protocol for real-time data acquisition and remote management. This design ensures high accuracy, quick installation, and compatibility with standard Sisgeo casings for applications like landslide monitoring, deep excavations, and dam safety. The inclinometer installation is shown in Figure 6.



Figure 6. Inclinometer installation method.

Kiosks
The control centre acts as the central hub for monitoring, analysis, and decision-making for the tailings dam. It integrates IoT sensors, wireless gateways, and cloud-based analytics to ensure real-time visibility, predictive insights, and automated alerts for dam safety and operational efficiency.

Insight Terra Platform
This is the part of the system that collects the data, creates information and presents knowledge as a digital dashboard viewed on individual devices and in the main control room. Figure 7 shows the control room. The platform comprises:

- Data Ingestion: Raw sensor data is uploaded from Worldsensing gateways to the cloud.
- Data Processing: Automated algorithms clean, validate, and structure data.
- Analytics & Visualisation:
    - Real-time dashboards showing dam health indicators.
    - Predictive models for failure risk and trend analysis.
    - Heatmaps and time-series graphs for pore pressure, displacement, and water levels.
- Alerts & Notifications:
    - Threshold-based alarms for critical parameters.
    - SMS/email notifications to engineers and operators.

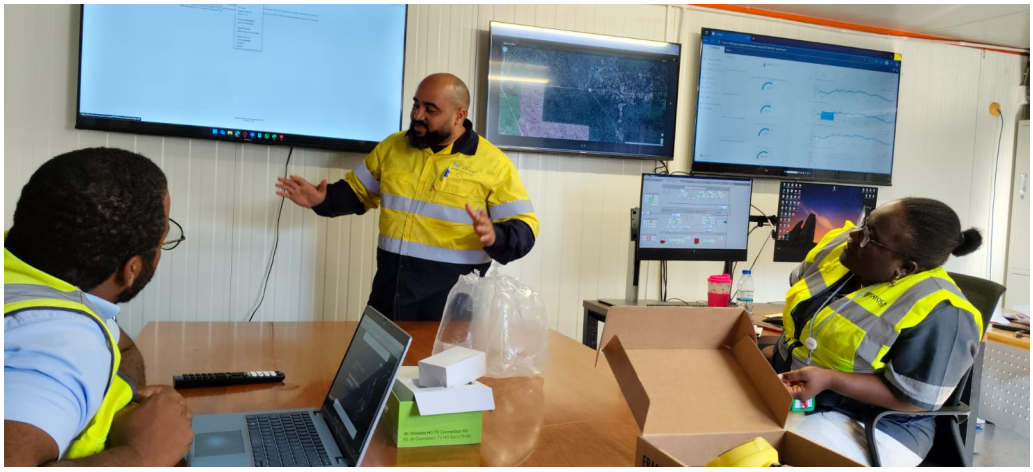


Figure 7. Control centre in operation.

Overall layout
Figure 9 shows the overall layout of the monitoring points.

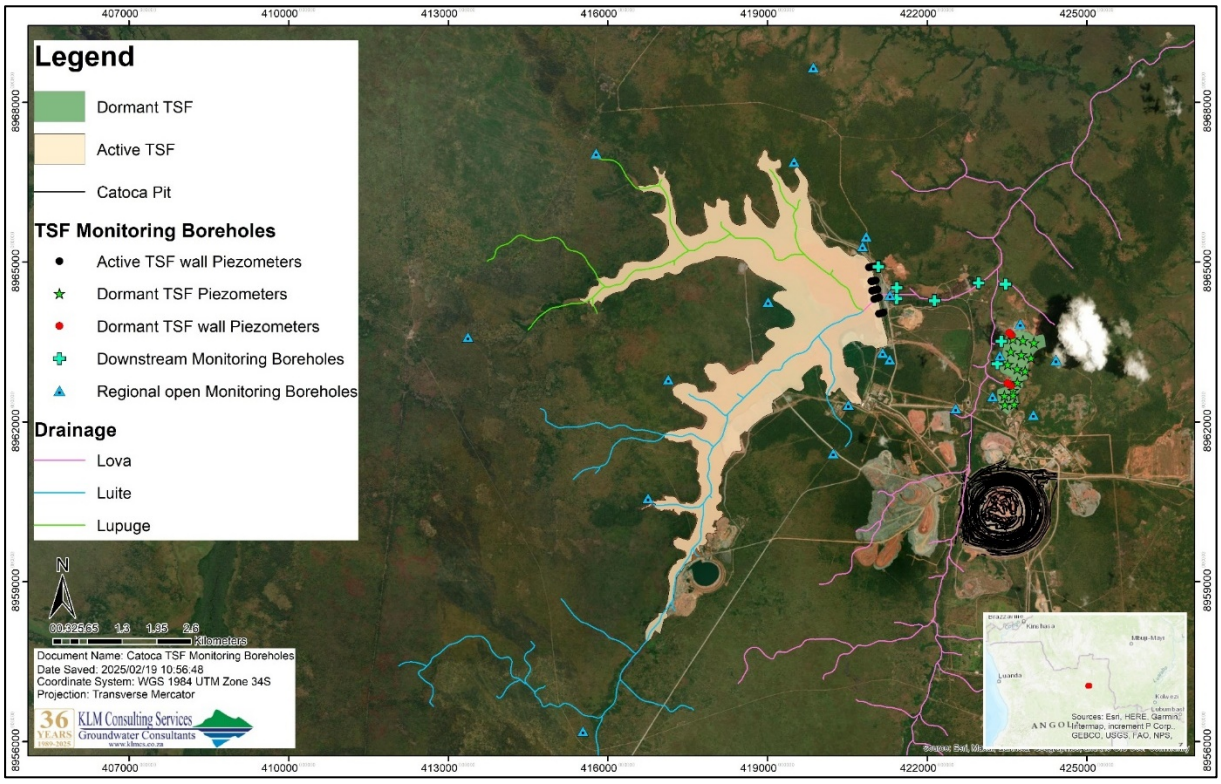


Figure 9. Location of monitoring equipment.

The instruments were connected using Worldsensing gateway system. A Worldsensing gateway is a central device that collects data from wireless monitoring sensors and transmits it to a cloud or local server, while Worldsensing loggers are field units that record measurements from geotechnical or structural sensors and send the data wirelessly to the gateway for remote access and analysis. The data is then transmitted to a dashboard in real time. Some data is still collected manually.

CONCLUSION

The installation required work from hydrogeologists, hydrologists, civil engineers, geotechnical engineers, drillers, software engineers, instrument technicians and the logistical support of the mine operating in a remote area. Challenges were heavy rainfall over the three years that the installation took and theft of some of the components in the early stages of installation. A robust security system had to be designed to protect all the equipment. The installation is an excellent example of collaboration of engineering, geotechnical interpretation, instrumentation design and software connectivity. The system has been described by an external international reviewer as one of the most advanced tailings monitoring systems in the world. It is an example of African initiative and innovation leading the world.

REFERENCES

Vigario et al 2026. Catoca Diamond Mine – implementation of an advanced monitoring network for a Tailings Storage Facility (TSF).

Vigario et al 2025. Catoca Diamond Mine – implementation of an advanced monitoring network for a Tailings Storage Facility (TSF). International Mine Water Association conference Braga Portugal 2025



Anton Hertenberger

CEO Africa
Tecwise Africa

Anton Hertenberger is a seasoned business leader with a strong passion for developing and commercialising advanced technical and engineering solutions across the African continent. His career spans senior development and leadership roles within globally recognised industrial brands, including PowerTeam Ernest Lowe, Donaldson Filtration, and his current role as CEO of TecWise Africa.

Throughout his career, Anton has played a pivotal role in growing and positioning leading technology brands such as Sisgeo, Worldsensing, Norgren, Donaldson, and Nederman. Under his guidance, these brands have achieved exceptional market growth, consistently outperforming industry benchmarks and expanding their footprint across Africa.

Anton combines deep engineering insight with strong commercial acumen. He holds an MBA and a Postgraduate Diploma in Business Administration from the Gordon Institute of Business Science (GIBS), equipping him with strategic and managerial expertise that complements his technical background.

The application of remote sensing techniques in mapping abandoned tailings storage facilities in the West Rand, Gauteng, South Africa

L. Nqasha[1], M. Mpanza[2]

[1]University of the Witwatersrand, South Africa
[2]University of Johannesburg, South Africa

The tailings storage facilities (TSFs) associated with abandoned mine sites are characterised by sparse vegetation, erosion features, deposition, and are surrounded by contaminated water. The TSFs' abandonment results from the poor management of mine sites, which can occur due to sudden or temporary mine closures. The TSFs associated with abandoned mine sites tend to lack the development of flora owing to the toxicity of their metal content. These TSFs tend to cause environmental impacts, such as soil, water, and air pollution. The contamination of soil, water, and air can result in damage to aquatic life, animals, plants, and threaten human health. It is not clear what the quantity of abandoned TSFs is in the Gauteng Province of South Africa. It is for this reason that it remains challenging to estimate the extent of the hazard posed by the abandoned TSFs. This study aims to identify and quantify the number of abandoned TSFs in the Gauteng Province. The study used remote sensing techniques to understand the TSFs' spatial features and classify them. Sentinel 2A and B satellite imagery were used to classify the reflected TSF spatial features and understand their distribution. The Google Earth Engine (GEE) was used to process and analyse satellite data and allowed users to access and analyse remotely sensed imagery without the need to download the data onto local computers. The GEE computing programme was utilised to perform machine learning (ML) supervised classification to classify Land Use and Land Cover (LULC), intending to identify the different types of TSFs. Three types of TSFs were identified: active, dormant, and abandoned TSFs. The active TSFs are marked by ongoing deposition and growing plantations, while the dormant TSFs have no active deposition from mining operations and feature mature plantations. They were found using coordinates and characteristics. The abandoned TSFs typically exhibit sparse vegetation, polluted water sources, and pronounced erosion gullies. This paper shows how the integration of ML and satellite imagery data can assist in mapping and categorising TSFs in the West Rand of the Gauteng Province. The detection of active, dormant, and abandoned TSFs with outstanding spatial accuracy was made possible by the combination of Sentinel-2 MSI data and ML algorithms (RF and SVM). Using short-wave infrared (SWIR) and NIR bands, the abandoned TSFs are often obscured by partial vegetation or misclassified due to spectral similarities, which were effectively identified, revealing their environmental impact and proximity to at-risk communities. In terms of overall accuracy, the RF model performed better than the SVM, especially when it came to differentiating between the various types of surrounding land cover and different TSFs. The significance of scalable, data-driven methods for environmental monitoring, adherence to regulations, and rehabilitation priority is highlighted by these findings. This paper helps create a more open and proactive structure for handling South Africa's mining heritage in accordance with global tailings governance standards.

Keywords: Tailings storage facilities, abandoned, active, dormant, remote sensing techniques

INTRODUCTION

Gold mine tailings storage facilities (TSFs) are distinctively constructed and engineered buildings that have been utilised to store mining material byproducts, many of which remain abandoned and environmentally hazardous. The history of gold mining activities in South Africa has left an enormous footprint from abandoned TSFs, especially in areas such as the West, Central, and East Rand of Gauteng Province. This is particularly so in the West and East Rands, where the TSFs produce hazards due to their toxic metal content, physical instability, and the lack of rehabilitation. Since they are characterised by sparse vegetation, erosion gullies and contaminated water bodies, abandoned TSFs contribute to air, soil and water pollution, threatening both ecological integrity and public health.

These TSFs produce dust contamination (Mpanza *et al.*, 2020), acid mine drainage, and illicit mining operations. These structures present hazards to the natural environment, human health, and public safety. Despite their occurrence, the exact number and spatial extent of these gold TSFs remain poorly documented and neglected, complicating efforts to assess and mitigate their environmental impact. This paper uses remote sensing methods, specifically satellite Sentinel-2 imagery and machine learning (ML) integrated with Google Earth Engine (GEE), where the classifiers, including Random Forest (RF) and Support Vector Machines (SVM) algorithms, were used to identify, classify, and map the abandoned TSFs. A strong set of instruments for locating, monitoring, and overseeing these facilities is provided by temporal satellite imagery, particularly in areas with hazardous or restricted ground access.

The rest of the paper is organised as follows: Section 2 comprises the literature review. Section 3 presents the research methodology, outlining the process and steps undertaken to collect and analyse the data. Sections 4 and 5 are dedicated to the presentation of the results as well as the discussion of the findings. Lastly, Section 6 provides the conclusion of the study, summarising the key insights and implications drawn from the research.

LITERATURE REVIEW

Since the latter part of the 19th century, the gold mining sector has been a major activity in the Witwatersrand region, which includes the West, Central, and East Rands (Mabaso, 2023), situated in the Gauteng Province. Many TSFs remained unrehabilitated when mining operations ceased or were transferred to smaller enterprises. Very fine-grained gold tailing materials are exposed to the atmosphere where the abandoned TSFs have not been properly rehabilitated (Mabaso, 2023; Mpanza *et al.*, 2024). Dry seasons make these loose surfaces more vulnerable to erosion by wind (Mpanza *et al.*, 2020). The ensuing dust, which is carried by the wind, comprises radioactive chemicals and metallic particles that can travel many kilometres and land in urban areas (Mine Dust Network, 2022). Asthma, irritation to the eyes, and respiratory problems are common complaints from the communities surrounding these places (Nwaila, 2021; Mabaso, 2023), such as Krugersdorp, as well as Springs. The absence of containment buildings and vegetation cover exacerbates this issue, making TSFs enduring sources of pollutants in the air (Mpanza *et al.*, 2020).

Acid rock drainage (ARD), which happens when sulfuric acid minerals in gold tailings oxidise when exposed to air (Mpanza *et al.*, 2020), and water pollution are also other environmental issues. Heavy metals found in tailings are released into adjacent water bodies through water runoff that contains sulfuric acid, which is created by this chemical process. The Blesbokspruit as well as the Klip River systems in Gauteng have been reported to have ARD, where tainted runoff from TSFs has harmed the aquatic environments and made the water unfit for agricultural and residential usage. Rainfall exacerbates the issue since surface water releases acidic leachates entering streams and groundwater, posing long-term hazards to the environment.

Remote Sensing Techniques for TSF Mapping

Large-scale, economical mapping of TSFs utilising satellite and aerial photography is made possible by remote sensing. Thus, in areas including the West Rand, where the legacy of mining has produced a

large number of abandoned sites, remote sensing offers an innovative approach for mapping gold TSFs. Researchers may identify TSFs using satellite observatories such as Sentinel-2 and Landsat because of their distinct spectral signatures, which are frequently characterized by low vegetation indices and high reflectance in the SWIR (Transon *et al*., 2018). Based on the spectral fingerprints of TSF material, multispectral data from Sentinel-2, as well as Landsat satellites, are frequently utilised to identify TSFs. SWIR spectral bands are especially useful for determining moisture content as well as mineral residues. Even in isolated or difficult-to-reach places, analysts can detect TSFs using multispectral datasets, which provide reliable, consistent observations across wide regions. By offering high-resolution images that record fine-scale phenomena like erosion ravines and structural cracks, aerial imaging enhances satellite data.

ML and Geospatial Analysis

The mapping, tracking, and evaluation of TSFs has been completely transformed and revolutionised by the integration of ML and geospatial analysis. Satellite-provided spectral data is used to train ML algorithms, such as RF, SVM, and Convolutional Neural Networks (CNNs), which are used to assess mineral content, detect TSFs, and classify LULC (Lou *et al.*, 2025). By recognising trends in values of reflectance throughout multispectral bands (such as SWIR, NIR, and Red Edge) that are suggestive of TSF material, these models acquire information from labelled datasets. After training, the models can be used to automatically identify TSFs, such as those that have not been catalogued across wide geographic regions. For instance, Mpanza *et al*., (2024) showed the efficacy of deep learning in LULC mapping by using Mask Region-based Convolutional Neural Network (R-CNN) and Faster RCNN to detect TSFs with great precision.

ML enhances geospatial analysis by providing spatial context, visual representation, and decision-making support. Users can integrate model outputs with terrain, hydrological features, physical structures, and demographic information through platforms such as ArcGIS Pro and GEE. Through spatial reporting, this convergence improves regulatory compliance and facilitates risk assessment, including the identification of TSFs close to towns or water bodies. Agard (2023) used ML to forecast residual gold values in the East Rand's gold TSFs and used geographic information systems (GIS) to show the findings, emphasising locations with potential for profitable reprocessing. In line with international norms, including the Global Industry Standard on Tailings Management (GISTM), the combination of ML and spatial techniques enables scalable, data-based management of TSFs, promoting sustainable after-mining land use.

METHODS

Data collection and processing

The GEE computing program was primarily used to acquire satellite data via JavaScript code. Geospatial data were primarily accessed using the JavaScript code performed using GEE. GEE is a powerful cloud computing platform for gathering and analysing data. GEE provides free access to different datasets in Copernicus sources, including access to satellite imagery. The satellite imagery was obtained using a computing code from GEE with a link: Ee. ImageCollection ("COPERNICUS/S2_SR_HARMONIZED"), which allowed a selection of specific times that matched the purpose of the data. When the satellite was imported, the Gauteng shapefile was imported to clip and focus on the West Rand area. The satellite used was Sentinel-2 imagery, a harmonised multispectral image (MSI) with 13 spectral bands used to monitor LULC or environmental changes, and has a temporal resolution for detecting the latest terrain features for LULC classification. GEE cloud computing platform interfaces with Sentinel-2, providing high-quality images with both temporal and spatial resolutions. MSI and High-Resolution Sensor (HSR) collected real data about the Earth's surface, useful for surveying, monitoring, and detecting LULC, including vegetation, water indices, and contamination levels.

When the imagery was clipped, the main step for processing involved applying red-green-blue (RGB) values for high-quality satellite images. This improved natural colour, enhanced spatial detail with

spectral radiometric features, and prepared the data for classification. The spectral bands' features boost image quality for spectral signature (natural colour) identification by using bands like Red, Green, and Blue (RGB: B4, B3, B2). This step was crucial for increasing image resolution and differentiating similar pixels. Spatial land feature labelling and collection were based on observable LULC to assign classification classes for data collection. Gamma was reduced by 1% to manage noise from spatial features, and cloud cover was limited to 5% or less to remove clouds, which improved terrain feature visibility. The chosen period was from 2025-04-01 to 2025-06-30 to access the satellite imagery. This period helped the classification for providing results rather than providing issues. This process also involved integrating geospatial modelling and ML by selecting training points for labelling classes for the LULC classification. Training points are digitised to classify different classes.

To perform the supervised classification of satellite imagery, a code was applied to run automatically in GEE. In GEE, the code for JavaScript automates LULC supervised classification by collecting satellite images, choosing appropriate spectral bands, and applying an ML algorithm (e.g., RF or SVM) to label training data. Following that, it assesses algorithm performance using criteria such as confusion matrices, allowing for quick, repeatable mapping of land cover with no operator involvement. To prevent code errors, ML algorithms were integrated with GEE code to detect the classified features under RF and SVM algorithms. Additionally, for classifying the terrain features, the best spectral bands were included for proper classification to differentiate similar reflectance of the classes. These bands were included in the classification: B2, B8, B11, and B12. It is a good combination LULC classification because it combines visible, NIR, and shortwave infrared wavelengths that improve spectral contrast between moisture content, plants, and mineralised surfaces, reducing misclassification and enhancing class separability.

When the imagery processing was completed, training points data were collected by creating digitising points representing dissimilar terrain cover classes, including active TSFs, dormant TSFs, abandoned TSFs, vegetation, water, and built-up areas. These training points of data were then utilised to train both RF and SVM classifiers in the GEE code. In the West Rand area, 548 training feature points were collected for all classes for the classification. These feature points were collected through geometrical selection of the classes and digitised. RF was used because of the ensemble learning technique that combines numerous decision trees to advance the accuracy as well as robustness of the supervised classification, while SVM is also a supervised learning classifier that aims to discover the best hyperplane that splits the LULC classes.

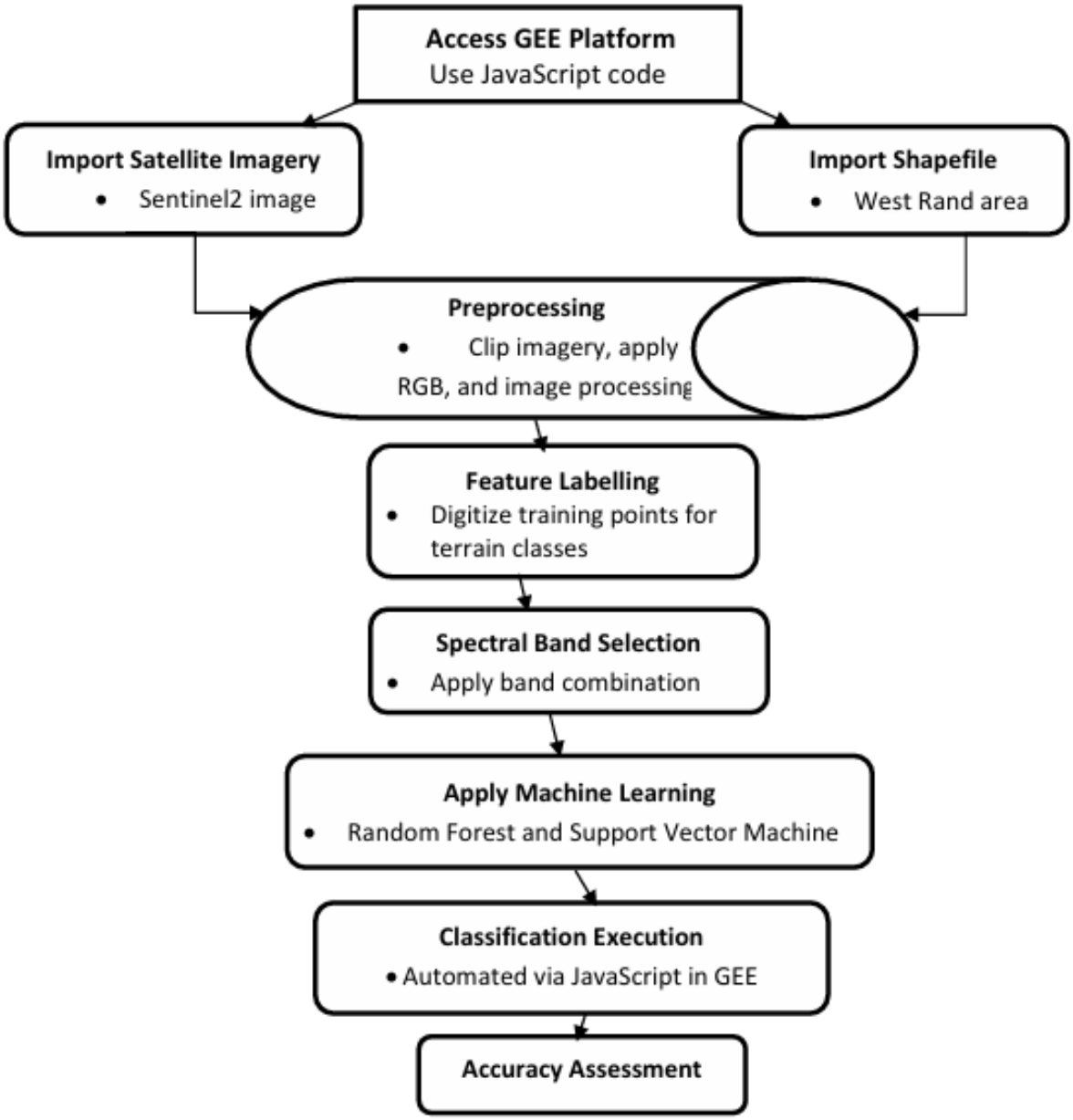


Figure 1: A study methods flow chart.

Data analysis

When the RF and SVM algorithms were trained on the digitised features with 586 training points of data (geometry imports) for classifying different classes, these training points were used to classify the satellite imagery to produce the classified LULC in the study areas. The outputs of classified LULC were exported as a Tag Image File Format (TIFF) and imported into ArcGIS Pro to produce classified maps to analyse the identification patterns and land cover changes. To assess the classification accuracy of each algorithm's results, metrics were evaluated to gauge and assess the classification precision, including overall accuracy, kappa statistics, and confusion matrices were calculated. Moreover, the classified maps reveal valuable information, including land cover extents and landscape metrics.

The GEE results analysis was performed using ArcGIS Pro for mapping, and Excel was used for filtering

data to present the results graphically. Furthermore, spatial analysis was employed to visualise the LULC maps, while filtering was used to identify the locations of specific classes. Reducing was applied to calculate statistics for classification accuracy and validation metrics for these classified maps. However, identifying the TSFs was crucial for environmental management authorities to be aware of all abandoned TSFs without licences.

Model Validation

The accuracy of ML classification was validated using field-verified TSF coordinates obtained from the Department of Mineral and Petroleum Resources (DMPR). These DMPR data points, which identify the true locations and operational status of active, dormant, and abandoned TSFs across the West Rand, were overlaid onto the RF and SVM classification outputs to assess spatial agreement.

RESULTS

RF TSF Classification

These results were produced through geospatial analysis integrated with ML algorithms to map and differentiate active, dormant, and abandoned TSFs. The West Rand area of the Gauteng Province is dominated by grassland, trees, agricultural land, and shrubs. Residential (built-up) areas are scattered across this area. In the southern and eastern parts of the West Rand, active and abandoned TSFs are dominant in the area. In Figure 1, active TSFs were classified using the RF algorithm and are presented in red colour for clear visibility. This shows that there are many ongoing mining activities around the area.

Furthermore, the abandoned TSFs are also dominant in the area shown in yellow (see Figure 2). Some of the abandoned TSFs were not clearly demonstrated by the satellite imagery because some of their parts are covered by vegetation, which makes their visibility a challenge. The abandoned TSFs are mostly towards the west, and very few are on the eastern side of the West Rand area. The dormant TSFs are very few, as shown in an orange colour (Figure 2), and a misclassification is noticed between the abandoned and dormant TSFs, caused by similar reflectance between dormant and abandoned TSFs at various places. In most cases, dormant/inactive TSFs with owners are characterised by proper management, with evidence of vegetation growth.

West Rand Random Forest LULC Map

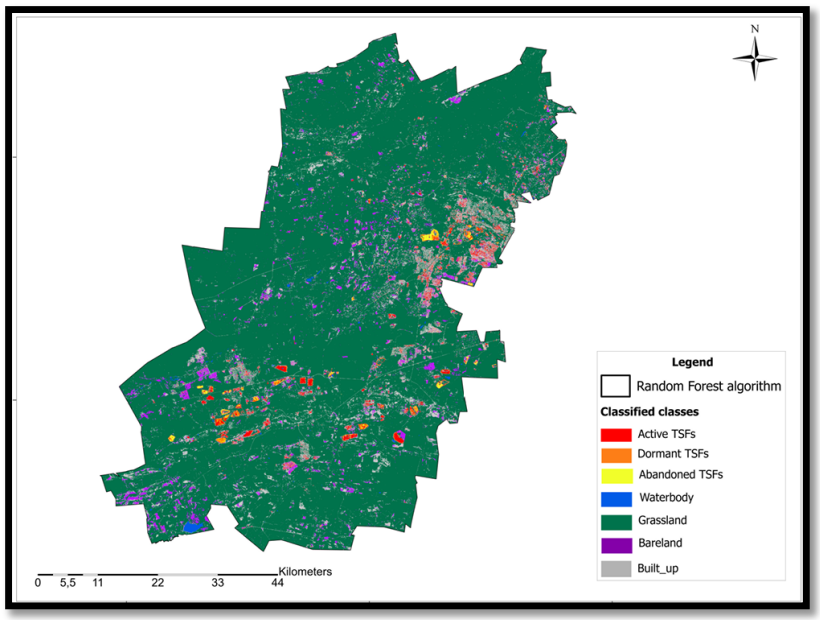


Figure 2: RF algorithm TSF classification in the West Rand.

SVM TSF Classification

The results presented in Figure 3 show the SVM classification map, with a clear distinction of the classified TSFs. In this classification, the results show that grassland is dominant, followed by built-up areas, which are more prolific in the eastern side and sparsely found in the southern parts of the map. Based on the results from the SVM map, built-up areas were built very close to the TSFs or mining areas; for instance, in Krugersdorp, an area where this class is found close to the mines. Houses are built near TSFs because of illegal mining opportunities, fragmented or poorly enforced by housing departments (McCarthy, 2011). Vegetation cover and growth are shown to cover dormant TSFs that are shown in an orange colour.

Some of these TSFs were also covered by built-up areas that were built on top of them. The vegetation covered a few parts of abandoned TSFs, which are characterised by very large erosion trenches. The abandoned TSFs are more dominant and found on the eastern side of the SVM map, which is known as Krugersdorp. The abandoned TSFs are vast in area and resulted from large historical mining operations and have attracted illegal mining and encroachment of housing, thereby creating informal settlements (McCarthy, 2011). Active mine operations prevail in the southern parts of the map, although some TSFs were misclassified as active while they are abandoned because of the texture. The built-up areas were similarly classified by RF in the same area where SVM classified built-up areas. Many water bodies were mapped and classified by SVM, and a similar observation was made in the RF classification map.

West Rand Support Vector Machine LULC map

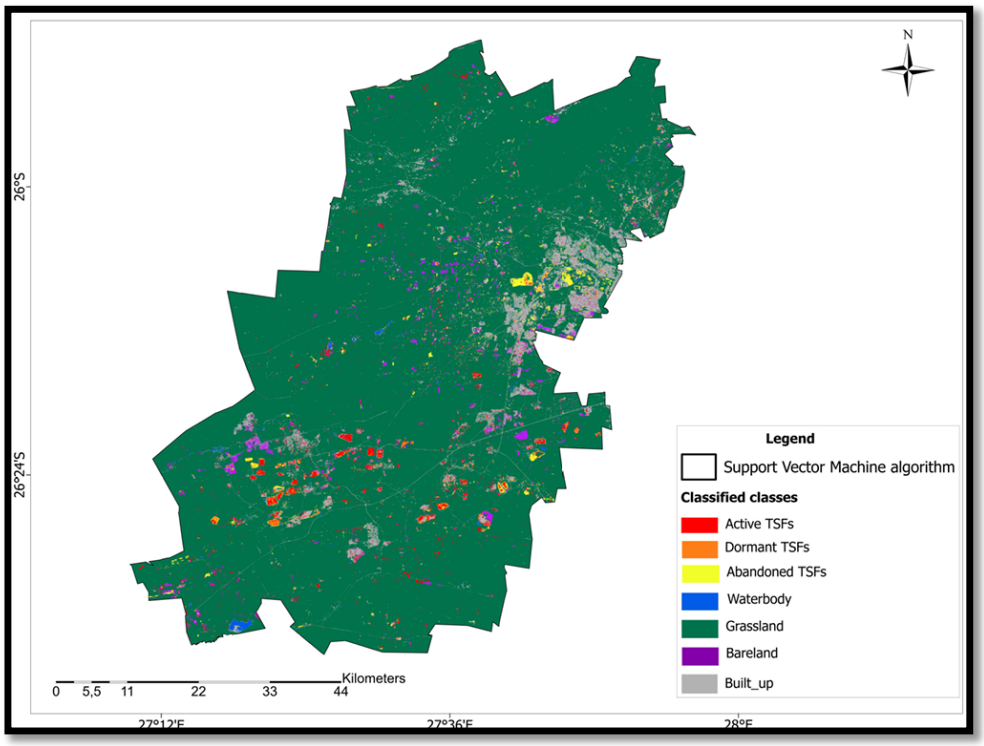


Figure 3: Support Vector Machine TSF classification in the West Rand.

Supervised Classification accuracy

RF confusion matrix

In Table 1, across seven different classes, the RF classification findings for these TSFs and surrounding LULC types show a very accurate performance of the model. All 92 training points were correctly digitised for active TSFs that were precisely classified according to the presented confusion matrix, resulting in a Producer's Accuracy (PA) showing 100% and a User's Accuracy (UA) of 98.92%. There was little uncertainty among these operational stages, as evidenced by the single pixel that was incorrectly identified as an abandoned TSF. The incorrect classification could be an issue of pixels with the same colour or similar features.

The non-TSF land cover classes also showed strong classification performance. Waterbodies, bare-land, and built-up areas were nearly perfectly classified, with waterbodies and bare-land achieving 100% PA and UA. Built-up areas had a PA of 98.6% and a UA of 100%, with one grassland pixel misclassified as built-up, which is likely due to sparse vegetation or proximity to urban features. The grasslands were correctly classified in most cases, with a PA of 100% and a UA of 97.3%, again showing minor confusion with built-up areas. Overall, the model classified 417 out of 420 training points correctly, resulting in an impressive overall accuracy (OA) of approximately 99.29%. Given the minimal off-diagonal confusion, the Kappa coefficient is expected to exceed 0.98, indicating near-perfect agreement beyond chance. These results affirm the robustness of the RF classifier in mapping TSFs and surrounding land cover types. These findings suggest that the RF model is well-calibrated for TSF mapping. To further refine classification between active and abandoned TSFs, feature importance analysis could help identify which spectral bands or indices contribute most to class separability.

Table 1 shows the distribution of trained points for the RF algorithm in the confusion matrix, where accurately trained points have a green background and are bolded in the middle of the table. These numbers are also represented by misclassification.

Table 1. Random Forest confusion matrix for West Rand

Class Names	Active TSF 1	Abandoned TSF 2	Dormant TSF 3	Waterbody 4	Grasslands 5	Bare-land 6	Built-up 7	Row total	PA%
Active TSF	**92**	0	0	0	0	0	0	92	100
Abandoned TSF	1	**33**	1	0	0	0	0	35	94,3
Dormant TSF	0	0	**128**	0	0	0	0	128	100
Waterbody	0	0	0	**13**	0	0	0	13	100
Grasslands	0	0	0	0	**36**	0	0	36	100
Bare land	0	0	0	0	0	**46**	0	46	100
Built-up	0	0	0	0	1	0	**69**	70	98,6
Column Total	93	33	129	13	37	46	69		
UA%	98,92	100	99,2	100	97,3	100	100		

SVM confusion matrix

Table II presents an SVM result showing that only 70 out of 92 training points in active TSF classes were correctly identified, indicating significant confusion. The classification class's Producer's Accuracy (PA) was 76.1%, while its User's Accuracy (UA) was 80.5%. A total of 13 training points were misclassified as built-up, seven as dormant TSFs, and two as abandoned TSFs. This implies that SVM experienced challenges in differentiating active, transitory TSFs and residential features because of similar spectral signatures discovered in the geographic area.

The performance of abandoned TSFs is superior; 32 of 35 training points were successfully identified (PA = 91.4%, UA = 94.1%). Given the changing status of these places, there is some misunderstanding with active TSFs, which is to be expected. The four training points were incorrectly identified as active TSFs, but 124 out of the 128 training points were accurately identified (PA = 96.9%), demonstrating the good classification of dormant TSFs. This highlights structural or spectral similarity among TSFs, which creates doubt on the SVM's boundaries-based classification methodology.

Waterbody, grasslands, bare land, and built-up areas are non-TSF LULC classes that are typically accurately classified. With immaculate PA and UA ratings of 100%, Waterbody, pastures, and bare-land

all demonstrate distinct spectral separation and reliable model performance. Nevertheless, 10 training points were incorrectly labelled with active TSF, indicating a moderate level of misclassification in built-up areas. This yields a PA of 85.7% along with a UA of 82.2%, indicating that certain urban features, particularly in after-mining landscapes, may have textures or reflectance similar to that of TSFs.

With an overall accuracy of almost 95.0%, the SVM algorithm successfully identified 399 out of the 420 points. Although SVM identified the 399 training points, the performance of the RF classifier is noticeably better. The ML classification of active TSFs exhibited the greatest decline in accuracy, with the SVM model struggling to distinguish this class effectively compared to others. Although the dormant TSF class achieved a high recall, its user's accuracy (UA) was exceptionally low at 5.3%, indicating overprediction and poor precision. The low classification was influenced by sharing spectral characteristics with other bright or disturbed surfaces (covered by vegetation), causing the classifier to mislabel many non-TSF pixels as dormant TSF and drastically lowering the user's accuracy. The inconsistent spectral patterns further prevent the model from learning a distinct class boundary, leading to broad and extensive false positives. This discrepancy branches from the large number of predicted dormant TSFs (131), which only slightly exceeded the actual correct matches (124), highlighting the model's tendency to misclassify.

According to these findings, SVM may need more feature engineering, high-resolution images from the satellite, and kernel tuning to enhance TSF condition discrimination, even though it can work well for LULC types. It may be possible to reduce misclassification between TSF classes as well as urban regions by including contextual characteristics, spatial filters, and ensemble approaches. Furthermore, object-based modification and after-classification smoothing may improve border delineation and lessen noise at the pixel level. In the confusion matrix, Table 2 displays the distribution of trained points for the RF method. Accurately trained points are in bold in the centre of the table and have a green backdrop. Additionally, these figures can show misclassification numbers with no colour in the background.

Table II. SVM confusion matrix for West Rand

Class Names	Active TSF 1	Abandoned TSF 2	Dormant TSF 3	Waterbody 4	Grasslands 5	Bare-land 6	Built-up 7	Row total	PA%
Active TSF	**70**	2	7	0	0	0	13	92	76,1
Abandoned TSF	3	**32**	0	0	0	0	0	35	91,4
Dormant TSF	4	0	**124**	0	0	0	0	128	96,9
Waterbody	0	0	0	**13**	0	0	0	13	100
Grasslands	0	0	0	0	**36**	0	0	36	100
Bare land	0	0	0	0	0	**46**	0	46	100
Built-up	10	0	0	0	0	0	**60**	70	85,7
Column Total	87	34	131	13	36	46	73		
UA%	80,5	94,1	5,3	100	100	100	82,2		

Model and Field Observation

These TSFs are concentrated in Krugersdorp, Westonaria, Fochville, and Carletonville areas of the study area, particularly around Krugersdorp and Randfontein, as visualised in Figure 4. A total of 29 abandoned TSFs were identified in the West Rand, where many TSFs are prominent in Krugersdorp and Carletonville. The area covering the TSFs is approximately 7240.0 ha in Krugersdorp and Westonaria, Fochville, and Carletonville, which covers approximately 66 286.00, which makes 73 526.00 ha in total. However, Figure 4 shows the field observation conducted by the DMPR and provides the data coordinates of the different TSFs. Consequently, the abandoned TSFs are the yellow points, the active are red points, and the dormant are blue points on the map. This depicts that the abandoned TSFs

are dominant in Krugersdorp and fewer in Carletonville, which corresponds with the classified map.

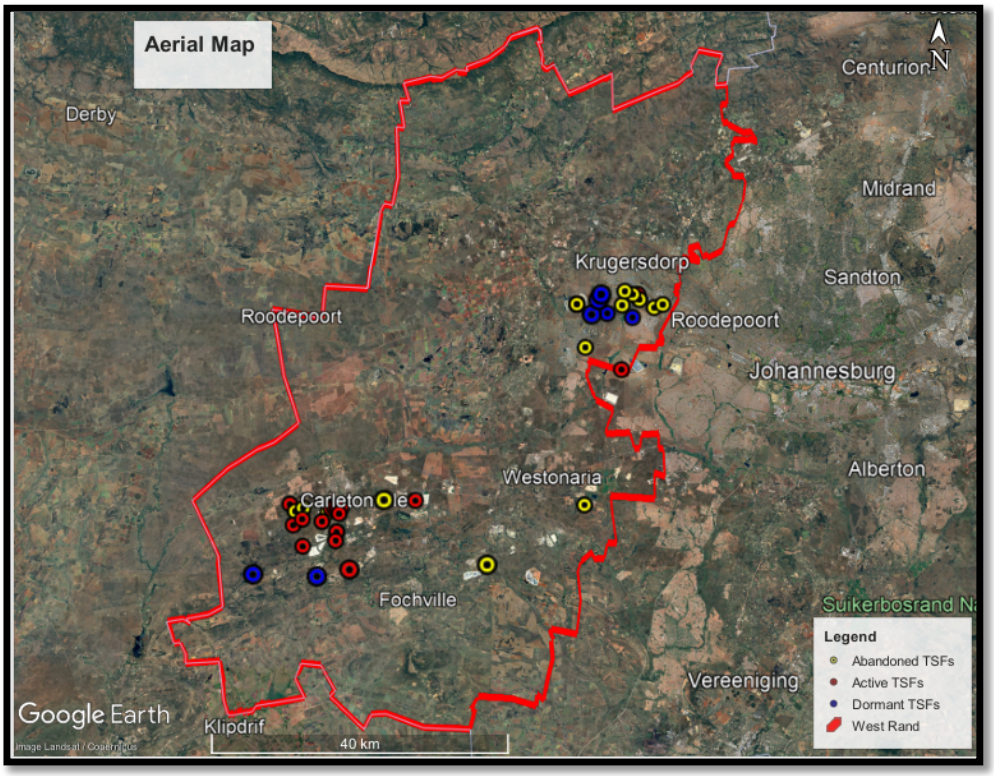


Figure 4: shows the validity of different TSFs in the West Rand.

Figures 2 and 3, together with the field-validated TSF locations (Figure 4) provided by the DMPR, show strong spatial agreement between the ML classifications and the actual distribution of TSFs across the West Rand. The mapped clusters of active, dormant, and abandoned TSFs in Krugersdorp, Randfontein, Westonaria, Fochville, and Carletonville correspond closely with the DMPR-verified sites visible in the reference image, confirming that both the RF and SVM outputs correctly captured the major TSF footprints. Although some misclassification occurred, particularly between dormant and abandoned TSFs, the overall spatial patterns align with the DMPR field data, demonstrating that the classification models reliably identified the true TSF locations and their status across the mining belt. Thus, there is an ongoing waste application for the reclamation and rehabilitation of the TSFs; some might be reclaimed to lessen environmental pollution (water and air pollution). The number of reclaimed TSFs should now be confirmed by the DMPR.

Comparison of the ML Model and Field Observation

The classification outputs from the RF and SVM models were validated against field-verified TSF location data provided by the DMPR. The DMPR dataset contained georeferenced coordinates of active, dormant, and abandoned TSFs across the West Rand, enabling a direct spatial comparison between the ML predictions and real-world TSF positions. When the classified maps (Figures 2 and 3) were overlaid with the DMPR field points (Figure 4), there was strong spatial agreement across all three TSF categories, with the highest correspondence observed in the dense mining belts of Krugersdorp, Randfontein, Westonaria, Fochville, and Carletonville.

The clusters of abandoned TSFs identified by the models aligned closely with the DMPR-verified sites, confirming that the spectral-based classification successfully captured the true distribution of legacy mining features. Although some misclassification occurred —particularly between dormant and abandoned TSFs due to similar reflectance patterns and partial vegetation cover — the overall spatial coherence between the model outputs and DMPR field observations demonstrates that the classification approach reliably mapped TSF footprints and their operational status. This validation step confirms

that the integrated remote sensing and ML workflow provides an accurate and defensible representation of TSF conditions in the West Rand.

The outputs of this paper support environmental regulators, mine closure practitioners, and municipal planners by providing spatially explicit inventories of abandoned TSFs. These maps can guide compliance monitoring, prioritise rehabilitation, identify high-risk TSFs near communities affected by the effects of the TSFs, Department of Water and Sanitation monitoring the state of water, DMPR to consider the number of companies applying for waste reclamation, and support enforcement of the National Environmental Management Act and the Global Industry Standard on Tailings Management.

CONCLUSION

This paper shows how the integration of ML and satellite imagery data can assist in mapping and categorising TSFs in the West Rand. The detection of active, dormant, and abandoned TSFs with outstanding spatial accuracy was made possible by the combination of Sentinel-2 MSI data and ML algorithms (RF and SVM). Using SWIR and NIR bands, the abandoned TSFs are often obscured by partial vegetation or misclassified due to spectral similarities, which were effectively identified, revealing their environmental impact and proximity to at-risk communities. In terms of overall accuracy, the RF model performed better than the SVM, especially when it came to differentiating between the various types of surrounding land cover and different TSFs. The significance of scalable, data-driven methods for environmental monitoring, adherence to regulations, and rehabilitation priority is highlighted by these findings. This paper helps create a more open and proactive structure for handling South Africa's mining heritage in accordance with international tailings governance guidelines.

STUDY LIMITATIONS

1. Short period of the imagery acquisition and classification.
2. Satellite image resolution and inability to classify TSFs covered by vegetation.

REFERENCES

Agard, S. (2023). In-situ gold resource estimation using satellite remote sensing and machine learning in defunct tailings storage facilities (South Africa). MSc Thesis, Uppsala University. Available at: https://www.diva-portal.org/smash/record.jsf?pid=diva2:1734994 [Accessed 12 Oct. 2025].

Ballard, M. (2021). Geospatial technology helps improve tailings management. Esri Industries Blog. Available at: https://www.esri.com/en-us/industries/blog/articles/geospatial-technology-helps-improve-tailings-management [Accessed 12 Oct. 2025].

Crous, P.A. and Jacobsz, S.W. (2023). Geotechnical centrifuge modelling of undrained triggers of tailings dam instability. Tailings 2023 Conference, Southern African Institute of Mining and Metallurgy. Available at: https://www.saimm.co.za/Conferences/files/tailings-2023/01%20577_Crous.pdf [Accessed 12 Oct. 2025].

Department of Water and Sanitation (DWS) (2025). Acid Mine Drainage: Long-Term Solution for the Witwatersrand. Available at: https://www.dws.gov.za/iwrp/AMDFSLTS/default.aspx [Accessed 12 Oct. 2025].

Grant-Stuart, D. (2021). Advances in ensuring tailings dam safety. SANCOLD Sediment Workshop. Knight Piésold. Available at: https://www.knightpiesold.com/sites/en/assets/File/SANCOLD%202021%20-%20Advances%20in%20Ensuring%20Tailings%20Dam%20Safety.pdf [Accessed 12 Oct. 2025].

Hobbs, P.J. and Cobbing, J.E. (2007). A hydrogeological assessment of acid mine drainage impacts in the West Rand Basin, Gauteng Province. CSIR Report No. CSIR/NRE/WR/ER/2007/0097/C. Pretoria: CSIR. Available at: https://researchspace.csir.co.za/server/api/core/bitstreams/e432d2f5-60c1-40d2-a953-3c1908c28bf2/content [Accessed 12 Oct. 2025].

Khanyile, S. (2024). Renaturing Gauteng's mining wastescapes? Gauteng City-Region Observatory (GCRO). Available at: https://www.gcro.ac.za/outputs/map-of-the-month/detail/renaturing-gautengs-mining-wastescapes/ [Accessed 12 Oct. 2025].

Lieferink, M. (2023). Air quality risks pertaining to tailings storage facilities within the Witwatersrand Goldfields. *Clean Air Journal*, 33(1), pp.12–18. Available at: https://scielo.org.za/pdf/caj/v33n1/02.pdf [Accessed 12 Oct. 2025].

Lou, C., Al-qaness, M.A., AL-Alimi, D., Dahou, A., Abd Elaziz, M., Abualigah, L. and Ewees, A.A., 2025. Land use/land cover (LULC) classification using hyperspectral images: a review. *Geo-spatial information Science*, 28(2), pp.345-386.

Mabaso, S.M. (2023). Legacy gold mine sites and dumps in the Witwatersrand: Challenges and required action. *Natural Resources*, 14, pp.65-77. Available at: https://vahlengweadvisory.co.za/wp-content/uploads/2023/05/nr_2023050913502000.pdf [Accessed 12 Oct. 2025].

McCarthy, T.S., 2011. The impact of acid mine drainage in South Africa. *South African Journal of Science*, *107*(5), pp.1-7.

Mine Dust Network, 2022. West Rand Tailings Storage Facilities – ArcGIS StoryMap. Available at: https://storymaps.arcgis.com/stories/27b9e5ced2164fa78c5eac06b73f9682 [Accessed 12 Oct. 2025].

Mpanza, M., Adam, E. and Moolla, R. (2020). Dust deposition impacts at a liquidated gold mine village: Gauteng province in South Africa. *International Journal of Environmental Research and Public Health*, 17(14), p.4929. Available at: https://www.mdpi.com/1660-4601/17/14/4929 [Accessed 12 Oct. 2025].

Mpanza, M., Wistockk, J. and Rupprecht, S. (2024). Mapping tailings storage facilities associated with abandoned mine sites. In: Proceedings of the 2024 International Conference on Mine Closure. Australian Centre for Geomechanics. Available at: https://papers.acg.uwa.edu.au/d/2415_44_Mpanza/44_Mpanza.pdf [Accessed 12 Oct. 2025].

Mpanza, M., Wistockk, J. and Rupprecht, S. (2024). Mapping tailings storage facilities associated with abandoned mine sites. Proceedings of the 2024 International Conference on Mine Closure. Australian Centre for Geomechanics. Available at: https://papers.acg.uwa.edu.au/d/2415_44_Mpanza/44_Mpanza.pdf [Accessed 12 Oct. 2025].

Nwaila, M. (2021). Impacts and conflicts associated with defunct gold TSFs in South Africa. MSc Thesis, University of Cape Town. Available at: https://open.uct.ac.za/handle/11427/33936 [Accessed 12 Oct. 2025].

O'Donovan, A. (2023). Use of multispectral satellite imagery to monitor the decant pond of tailings dams. MSc Thesis, University of the Witwatersrand. Available at: https://wiredspace.wits.ac.za/bitstreams/758d5344-ceb5-41d1-82d0-8eb26592d6f0/download [Accessed 12 Oct. 2025].

O'Donovan, A., Adam, M. and Torres-Cruz, L.A., 2022. Remote sensing of the decant pond of tailings dams: insights from a South African case study. *Journal of the Southern African Institute of Mining and Metallurgy*, 122(4), pp.197–204. Available at: https://scielo.org.za/scielo.php?script=sci_arttext&pid=S2225-62532022000400003 [Accessed 12 Oct. 2025].

Swift Geospatial, (2025). Tailings dam monitoring – satellite technology in South Africa. Swift Geospatial Blog, 10 April. Available at: https://swiftgeospatial.solutions/2025/04/10/why-tailings-storage-facility-monitoring-matters/ [Accessed 12 Oct. 2025].

Transon, J., d'Andrimont, R., Maugnard, A. and Defourny, P., 2018. Survey of hyperspectral earth observation applications from space in the sentinel-2 context. *Remote Sensing*, 10(2), p.157.



Nqasha Lusizo

Senior GIS and EIA Consultant
University of Witwatersrand and Vahlengwe Mining Advisory and Consulting

Nqasha Lusizo is a dedicated Geoscientist and Environmental Specialist whose work integrates environmental management in water quality and waste management, geospatial science, and sustainable development. Lusizo holds a Master of Science in Geography from the University of the Witwatersrand, grounding his work in strong academic and scientific principles. His multidisciplinary exposure has strengthened his ability to interpret environmental dynamics, assess ecological risks, and contribute to mitigation strategies aligned with national legislation and industry best practice. With advanced expertise in Environmental Management, GIS, and Remote Sensing, he has built a solid foundation in environmental consulting, particularly in mining rehabilitation and natural resource management. His professional experience includes environmental impact assessments, environmental auditing, and the use of geospatial technologies to support evidence-based environmental decision-making. As a Senior GIS and EIA Consultant at Vahlengwe Mining Advisory and Consulting, Lusizo plays a key role in MPRDA and NEMA regulatory processes that guide responsible resource use. He leads advanced geospatial workflows, applying machine learning, CNN modelling, and geospatial programming to tasks such as land use/land cover classification, environmental change detection, and spatial data integration for environmental reporting. His technical capabilities are complemented by practical experience in environmental health and safety, water quality assessment, waste management, and field-based ecological surveys. Driven by a commitment to environmental sustainability and scientific rigor, he continues to advance his professional profile through research, technical development, and active engagement in environmental consulting, with a long-term vision of contributing to more sustainable and scientifically informed environmental governance in South Africa and beyond.

Combining real-time and scheduled monitoring of upstream raised TSFs and a filter stack – why both are required

D. Johns, J. Olivier

Klohn Crippen Berger, Australia

The paper presents examples of risk-informed dam safety decisions based on real-time and traditional monitoring systems at an Australian site with several upstream-raised tailings storage facilities (TSFs) and a filtered tailings stack. The real-time monitoring system is described, including vibrating wire piezometers, shape arrays, GNSS surface displacement, and slope monitoring radar. Other monitoring at the site includes manual inclinometers and prisms, InSAR surveys, high-resolution photogrammetric surveys and frequent drone photography. The most recent data is available at all times via a website maintained by the owner. In the first example, a combination of monitoring methods and historical construction records allowed the rapid analysis of a potential dam safety concern related to displacement of the TSF slope. The analysis concluded that the movement was due to consolidation settlement. In the second example, real-time pore pressure monitoring of the filter stack alerted the dam safety team to a potential concern during construction of a buttress. The multi-year monitoring record allowed the team to determine that the observed large pore pressure increase was a typical response to wet season rainfall. This information informed a decision to continue with buttress construction. Construction induced pore pressures are examined in a third example. The paper concludes that both real-time and scheduled or 'traditional' non-real time monitoring methods provide value. Access to drone aerial imagery and photogrammetric construction progress are also valuable, as well as a full record of all monitoring data. Instantly available data facilitated rapid decision making; this is often needed where the safety of TSFs is concerned.

Keywords: real-time monitoring, risk-informed decision making, dam safety, automatic trigger alerts, filtered tailings.

INTRODUCTION

Examples of the complementary use of real-time and scheduled (non real-time) monitoring of tailings storage facilities (TSFs) are discussed in this paper. The subject site is an example in which many different monitoring types are used, ranging from the low-tech e.g., survey monuments, to 'best available technology' e.g., shape array inclinometers, InSAR and Global Navigation Satellite System (GNSS) prisms.

The site and its monitoring system

General characteristics

The subject site comprises several active upstream raised TSFs receiving waste material generated from bauxite processed at an alumina refinery using a conventional Bayer process. The refinery produces a waste stream consisting of a coarse sand fraction and a fine silt-sized mud fraction, typically in a 1:1 weight ratio.

These fractions are hydraulically separated, with the fine fraction (<0.15 mm) directed to a thickener and the coarse sand, also referred to as *residue sand*, pumped as a slurry to designated stockpile areas, primarily for embankment and underdrain construction. The fine fraction is thickened into a high-density slurry, which is deposited via droppers into the TSFs as a *residue mud* and subsequently mud-farmed and solar dried.

The TSFs typically comprise of an initial starter embankment, a clay basal liner system, and in some cases, a geomembrane liner. Starter embankments for these TSFs were typically constructed by compacting sand sourced from excavations within the facility footprint. Subsequent upstream raises were executed by constructing perimeter embankments using the *residue sand* placed hydraulically or mechanically. Most of the TSFs have a complex interlayering of *residue sand* and *residue mud* within the impoundment.

Monitoring system

The TSFs are equipped with a suite of real-time and manual monitoring instruments primarily installed along 59 embankment sections. These instruments monitor pore pressure, deformation, pond levels, underdrain sump levels and precipitation. The instruments at the site are summarised in Table I.

The real-time instruments, such as vibrating wire piezometers and GNSS receivers record data at 30 minute intervals. Instrument data loggers transmit the data to Vista Data Vision (VDV) which is a web-based software platform designed for instrumentation data management and visualisation. VDV provides a wide range of tools for interpreting complex datasets, including interactive graphs and dashboards. The monitoring data is downloadable from VDV in comma separated variable or text formats, allowing for further analysis and data processing such as statistical evaluation, maximum and minimum levels, rates of change etc. Custom alerts are configured within VDV for each instrument based on predefined trigger level thresholds.

Table I. Monitoring instrumentation and survey inventory

Instrument Type	Real-time / Scheduled	Purpose	Number	Frequency
Vibrating Wire Piezometers (VWPs)	Real-time	Pore water pressure	359	30 minutes
Manual Inclinometers	Scheduled	Deformation	42	Fortnightly
Magnetic Extensometers	Scheduled	Displacement	30	Fortnightly
Prisms	Scheduled	Displacement	43	Monthly
GNSS Prisms	Real-time	Displacement	4	30 minutes
Shape Array Inclinometer	Real-time	Deformation and displacement	1	30 minutes
Slope Monitoring Radar	Real-time	Deformation	1	10 minutes
Underdrain sump levels using VWPs	Real-time	Liquor level in sumps	28	30 minutes
Pond water levels	Scheduled	Liquor pond levels	15	Weekly
Interferometric Synthetic Aperture Radar (InSAR)	Scheduled	Displacement	-	11-day satellite flyovers, reported monthly
High resolution photogrammetry survey	Scheduled	Deposition monitoring, construction progress	-	Fortnightly or as required
Drone photography	Scheduled	Visual assessment	-	Monthly

Example 1: Slope deformation

The site's VDV automatic email and text message alert system issued an alert that an inclinometer on the slope of an upstream raised TSF had exceeded its predetermined trigger level. Although this type of inclinometer is recorded manually by a field technician, the VDV alert was triggered when the readings were entered into VDV. The inclinometer had reached a cumulative displacement of 21.5 mm at a depth of 16 m, exceeding the alarm threshold level of 20 mm. The dam safety team immediately commenced a review of the inclinometer's deformation as well as conducting visual inspections of the slope, as per the actions defined in the trigger action response plan. The review extended to three other nearby inclinometers and the piezometers on the embankment section.

The inclinometer cumulative displacement and incremental displacement plots are provided in Figure 1 compared to the baseline of April 2022. The cumulative plot is superimposed on the embankment cross-section as shown in Figure 2. The triggering displacement occurred at a depth of 16 m, although the displacement at the surface of the TSF was much larger, around 100 mm. Note that the figure is plotted with the downstream (downslope) direction on the right; the correct orientation is shown on the embankment cross-section figure.

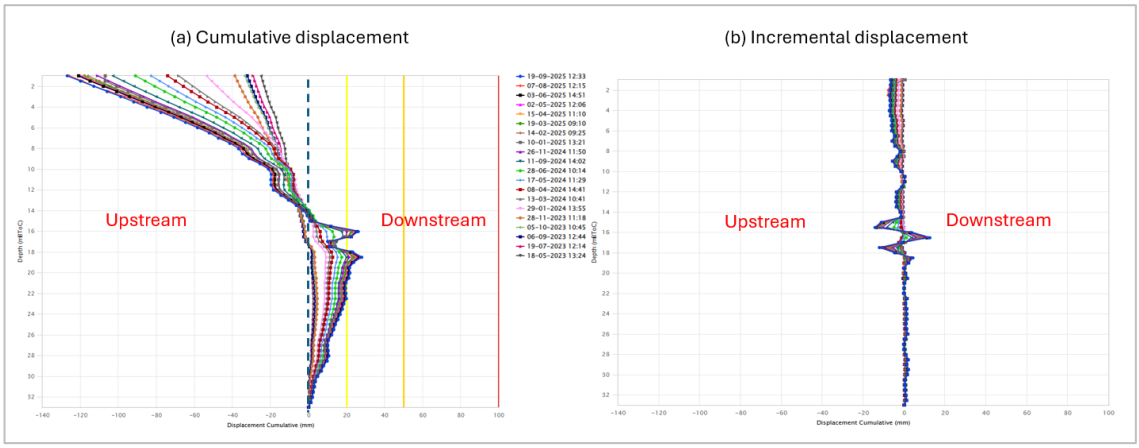


Figure 1. Cumulative and incremental inclinometer displacements.

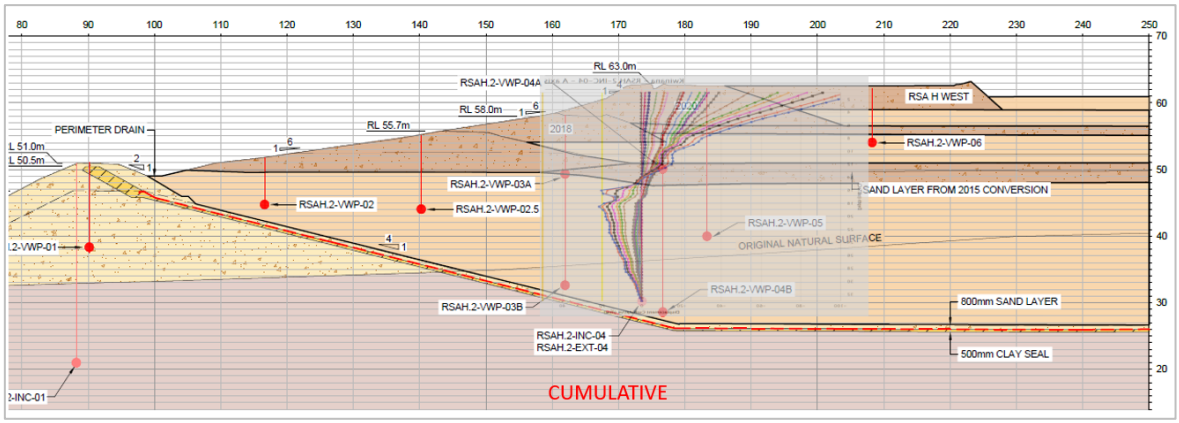


Figure 2. Inclinometer cumulative displacement superimposed on embankment cross-section (the inclinometer plot is at an exaggerated scale).

Inclinometer review

The objective of the review was to determine whether the displacement was 'real', and whether it indicated a zone of shear displacement consistent with a rotational or sliding slope failure, with its

associated potential for strain softening of the tailings. It is important to note that the inclinometers are not anchored in firm foundations, which somewhat reduces the reliability of the analysis.

The inclinometer plot on the embankment cross-section suggests that the slope has undergone a gradual overall rotational movement. However, review of InSAR, survey monuments (prisms) and visual observations found no evidence at the ground surface to support this. Also, no zone of incipient shear is discernible in the inclinometer plots. On the other hand, the incremental displacement plot presents a clearer picture of displacement in both the upstream and downstream directions over a narrow depth range of 14 m to 18 m, suggesting a 'buckling' behaviour of the inclinometer casing at the interface of sand and mud tailings. All inclinometers along about 300 m of embankment showed a similar displacement, as do others on this site.

The inclinometer displacement-depth data was downloaded from VDV and processed in a spreadsheet to develop time-series plots of the displacement of a zone along the inclinometer at depths of interest i.e., at the surface (0 to 1 m) and at depth of 16.5 m (the location of the upper buckling deformation).

The photogrammetry surveys available on the Trimble Propeller platform were also consulted. These surveys, taken at intervals of approximately one month, accurately captured the progress of construction of the most recent upstream embankment raise. A cross-section of the slope was extracted from Propeller showing the progress of the embankment raise construction. The surveys made it possible to estimate the start and finish dates of construction. The inclinometer is directly beneath the embankment raise.

The time-series plots show that the inclinometer's rate of displacement underwent a change. At the ground surface, the initial displacement rate increased at a time coinciding with the start embankment raise construction and reduced again following the end of construction (see Figure 3), indicated on the figure by tangent lines. This was validated by the similar behaviour of a nearby inclinometer in which its increased displacement rate coincided with the construction of a sand stockpile nearby. The reduction in rate is consistent with decreasing rate of consolidation. At the greater depth of 16 m, the increased and decreased displacement rates lagged those at the TSF surface, which is consistent with consolidation at that depth due to a longer drainage path length.

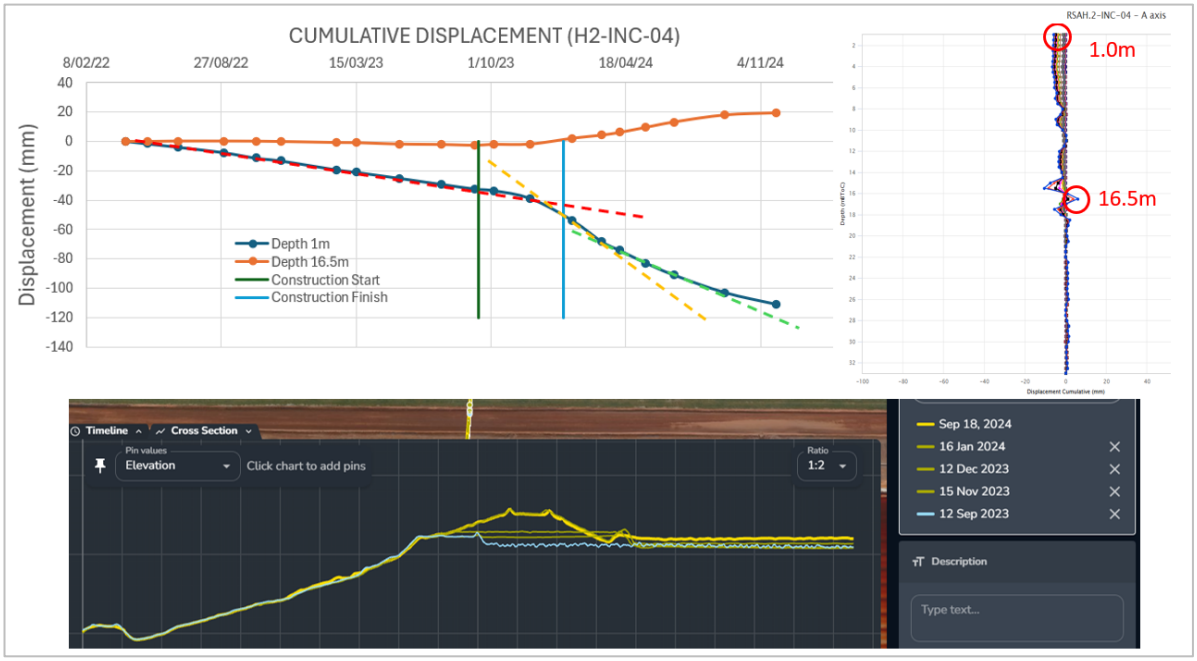


Figure 3. Inclinometer displacements versus embankment raise construction history.

InSAR and survey prisms

The survey monuments (prisms) and the InSAR survey was reviewed to see if these indicated surface displacements consistent with a potential incipient sliding or rotational slope failure. It should be appreciated that displacement in the north-south direction can not currently be resolved by InSAR surveys i.e., the downslope direction in this case. However, vertical displacements are reasonably reliable. The surveys showed no evidence of uplift or heaving at or near the toe of the embankment, which would be an indicator of slope rotation. The InSAR, prism and inclinometer vertical movement rates all approximately correspond being 0.1 mm/day (InSAR vertical and inclinometer lateral), and 0.06 mm/day for the prism nearest the dam crest. Neither InSAR nor prisms indicated an acceleration of the displacement (Figure 4).

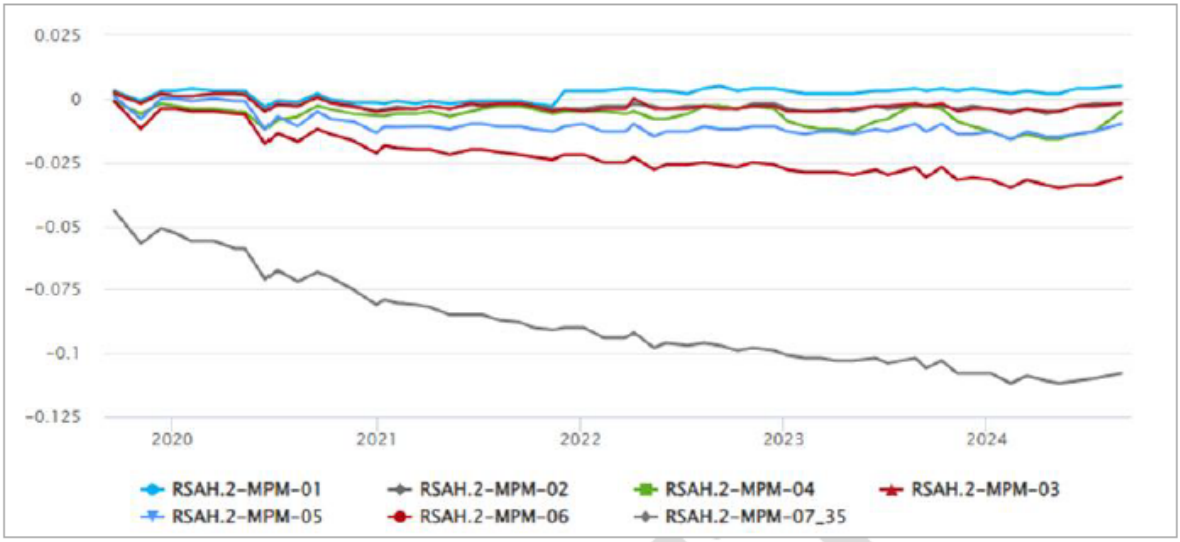


Figure 4. Prisms vertical displacement along embankment transect H.2.

Example 1 conclusion

The complementary monitoring techniques of InSAR, photogrammetric surveys and prism records, and the slowing rate of displacement provided the dam safety team with increased confidence that the inclinometer displacements were unlikely to be indicative of an incipient slope failure. The predominant displacement of the embankment is vertical settlement of the tailings as it consolidates. The displacement indicated by the inclinometer is theorised to be buckling of the inclinometer casing due to down drag of the consolidating tailings in response to the construction of the embankment raise. This explains why the inclinometer deflects in both the upstream and downstream directions on its A-axis, while also showing this displacement along its B-axis.

The analysis would not have been possible without access to frequent inclinometer and construction surveys (in this case photogrammetry), InSAR and complementary surface displacement monitoring by survey prisms, and the ability to download the raw data for further interpretation.

Example 2: Filtered tailings stack response to seasonal rainfall

Real-time pore pressure monitoring of the filter stack alerted the dam safety team to a potential concern during construction of a stabilising buttress. An earlier construction campaign identified that buttress fill placement generated excess pore pressures in the foundation of the buttress (a hydraulically placed tailings) i.e., construction-induced pore pressures. Furthermore, it was understood that the excess pore pressures could be transmitted to areas remote from the fill placement and thereby potentially temporarily reduce the safety margin for slope stability at those locations. This risk was mitigated by the installation of a piezometer network which was monitored twice daily against construction trigger

levels. This monitoring found that some piezometers located a considerable distance upstream and at a higher elevation than the buttress indicated large, sudden increases in pore pressure of up to 5 m, which could not reasonably be explained by the buttress construction. An example is shown in

Figure .

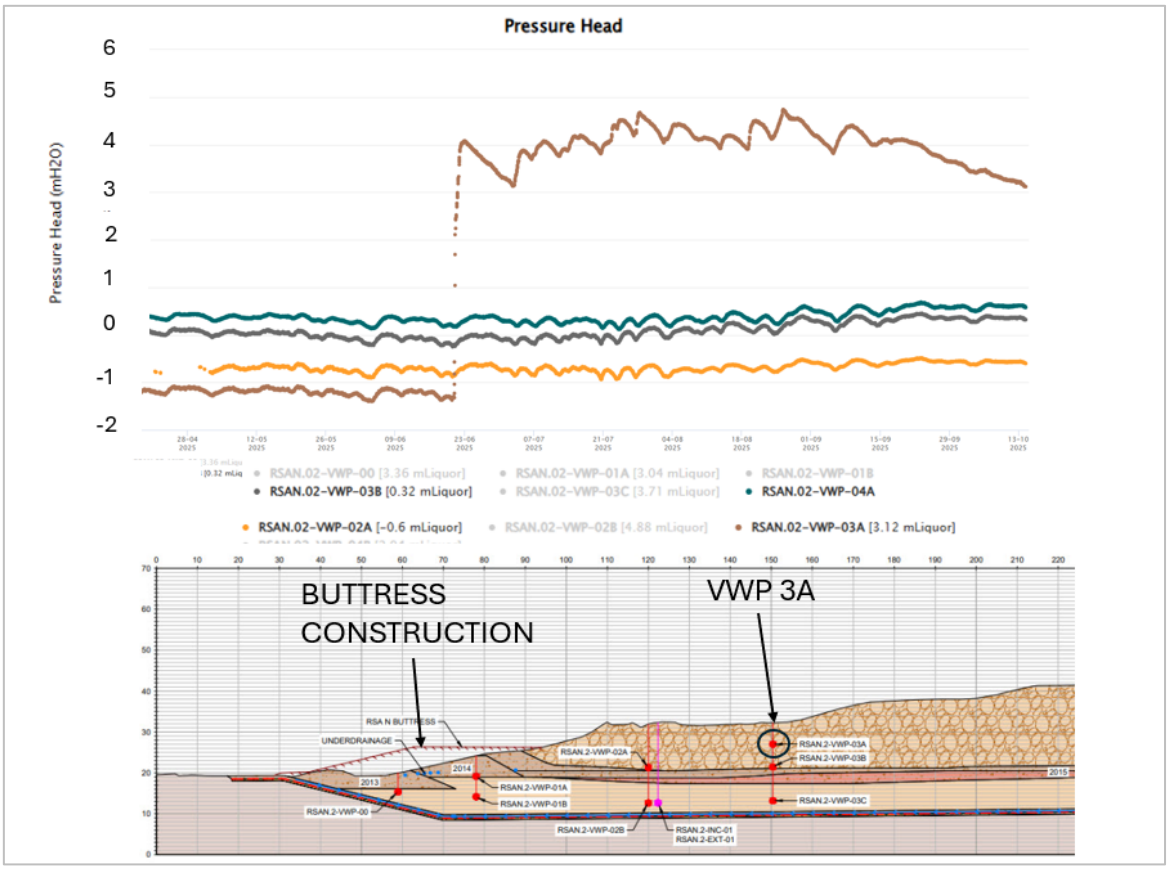


Figure 5. Pore pressure increase of VWP-03A in one day and location of the VWP.

The multi-year monitoring record allowed the team to visualise the pore pressure over a period of the previous four years. When plotted over the time scale of years rather than weeks it became evident that the observed large pore pressure increase was a typical response to wet season rainfall, as shown in Figure 6. This figure is a typical example of piezometers in the upper part of the filter stack; the piezometer transitions suddenly from an unsaturated condition in summer to positive pore pressure starting in May each year, coinciding with the start of the rainfall season, and reversing the trend in October each year. The main rainfall period at the site is May to September as shown in Figure 7. The rainfall over this period is approximately 590 mm of the annual 844 mm.

The cause is likely due to cracking of the filter cake; rain-water infiltrates the cracks to several metres below the surface causing pore pressures to rapidly increase locally but not necessarily throughout the filter stack and not within zones which control the stability. Deeper piezometers do not show a response to rainfall.

Once the dam safety team understood that the filter stack had experienced sudden increases and high pore pressures in the past without obvious detriment to the filter stack, and that the cause is probably due to rainfall, the team decided to continue with the buttress construction.

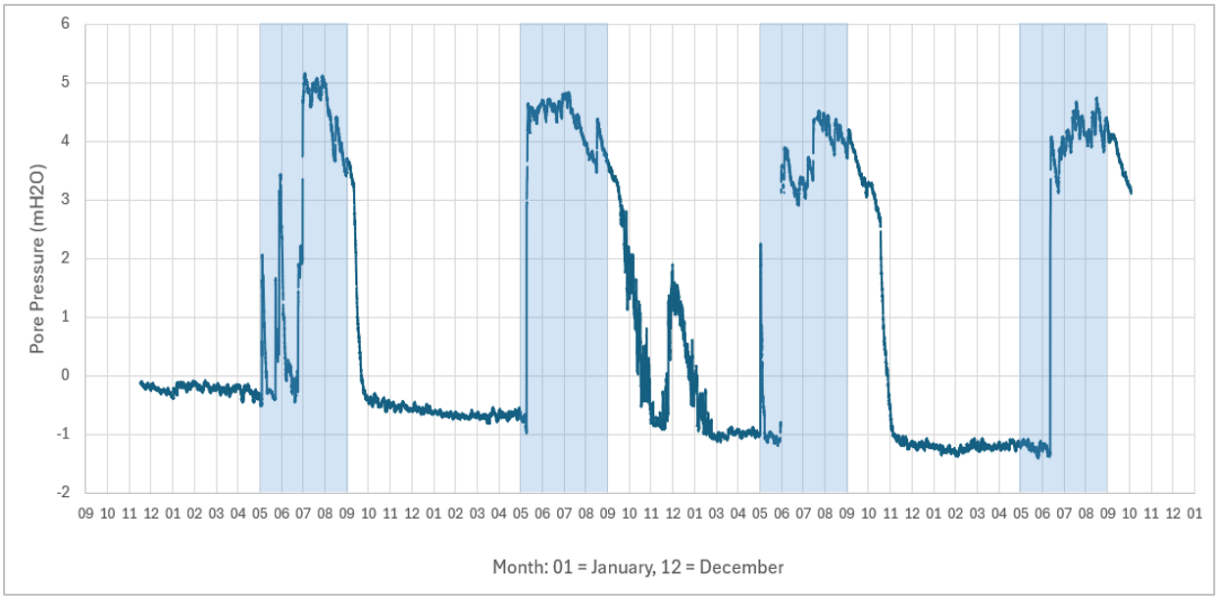


Figure 6. Pressure head of VWP3A over a four-year period indicating response to wet season rainfall, indicated by the shaded regions (May to September each year).

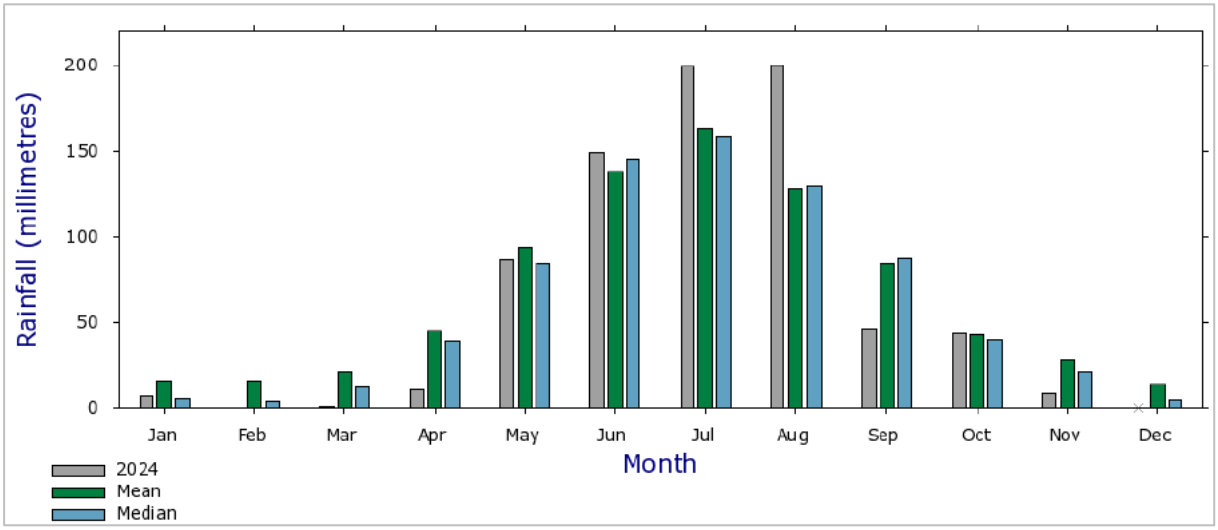


Figure 7. Annual rainfall distribution at the site.

Example 3: Construction-induced pore pressure

Construction-induced pore pressures were monitored for the construction of an upstream embankment raise at one of the TSFs. Pore pressures were automatically recorded at 30-minute intervals which provided assurance that construction was proceeding without detriment to the safety of both facilities.

Each construction lift of the embankment generated pore pressure in the tailings forming the raise foundation. The arrangement of the VWPs and the embankment raise is shown in Figure 8. A typical pore pressure time series during construction is shown in Figure 9, in which it can be seen that the pore pressure increased instantly with the loading of each construction lift, followed by very slow dissipation. This behaviour is expected for the low-permeability silt tailings at the site.

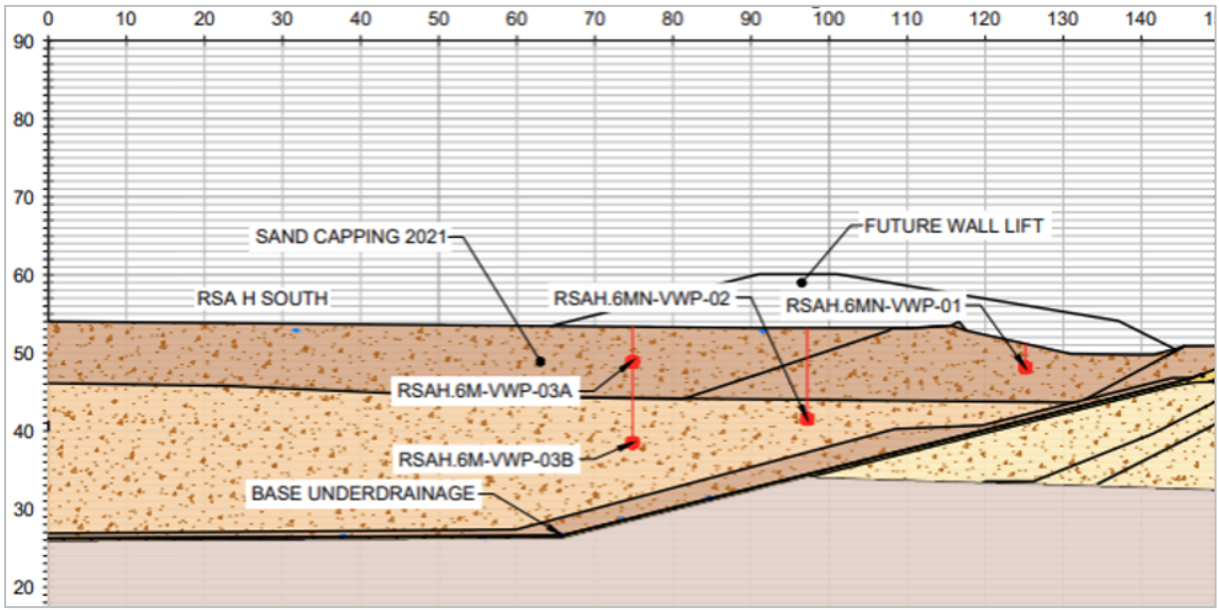


Figure 8. Arrangement of VWPs in the tailings below the raise embankment ('Future Wall Lift').

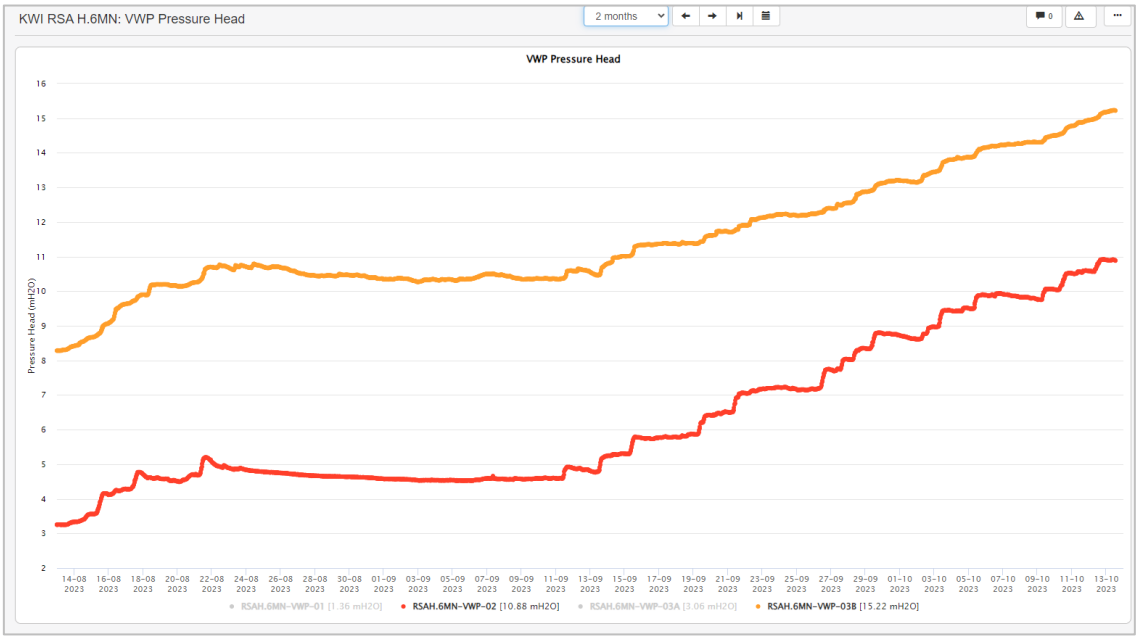


Figure 9. Pore pressure time series for VWP-02 and VWP-03B during construction of the upstream raise of the embankment.

B-Bar

The 'B-bar' parameter is a pore-water coefficient related to the major principal stress, commonly applied in limit equilibrium (LE) modelling. The definition is per Equation 1, in which Δu is the change in pore pressure and $\Delta\sigma_1$ is the change in the major principal stress usually assumed to be the overburden stress.

$$\bar{B} = \frac{\Delta u}{\Delta \sigma_1} \qquad [1]$$

As for Example 1, the monthly photogrammetric surveys allowed for accurate tracking of the construction progress. The cumulative and incremental fill elevations at the time of interest was

available for conversion to an equivalent total vertical stress which could be compared to the pore pressure increases available on the VDV monitoring website to calculate the B-bar parameter.

The B-bar calculation for the tailings under the raise, at the position of piezometer VWP02, is given in Table II. The value of 0.73 is within an expected average value for these tailings over the time period, and generally agrees with estimates made with a finite difference spreadsheet method. The measured B-bar value has been used as an assumption in subsequent design and stability calculations for construction planning. For example, if VWPs during construction indicate a B-bar above a certain threshold that has been pre-determined by LE modelling, then the construction rate should be slowed or paused to allow pore pressures to dissipate.

Table II. B-Bar Calculation for VWP02

Parameter	**Value**
Starting fill elevation	55.25 m
Finishing fill elevation	60.00 m
Fill thickness	4.75 m
Starting pore pressure head	4.59 m
Ending pore pressure head	10.88 m
Change in pore pressure, Δu	6.29 m or 63 kPa
Change in overburden stress, $\Delta\sigma$	4.75 m * 18 kN/m^3 = 86 kPa
B-Bar, $\Delta u/\Delta\sigma$	=63/86 = 0.73

Rate of Consolidation

The dissipation of the construction excess pore pressure took approximately 470 days, (see Figure 10). Estimations of one-dimensional consolidation with time developed by Terzaghi (Terzaghi, 1926) were plotted for the mean, lower and upper values of the estimated coefficient of consolidation cv (100 m^2/year, 70 m^2/year, and 200 m^2/year, respectively). These values were estimated from 14 CPTu dissipation tests in the tailings. The adopted drainage distance of 8 m was based on the stratigraphy of the TSF at the VWP location. The analysis is presented in Figure 11, which shows good agreement with the mean c_v value.

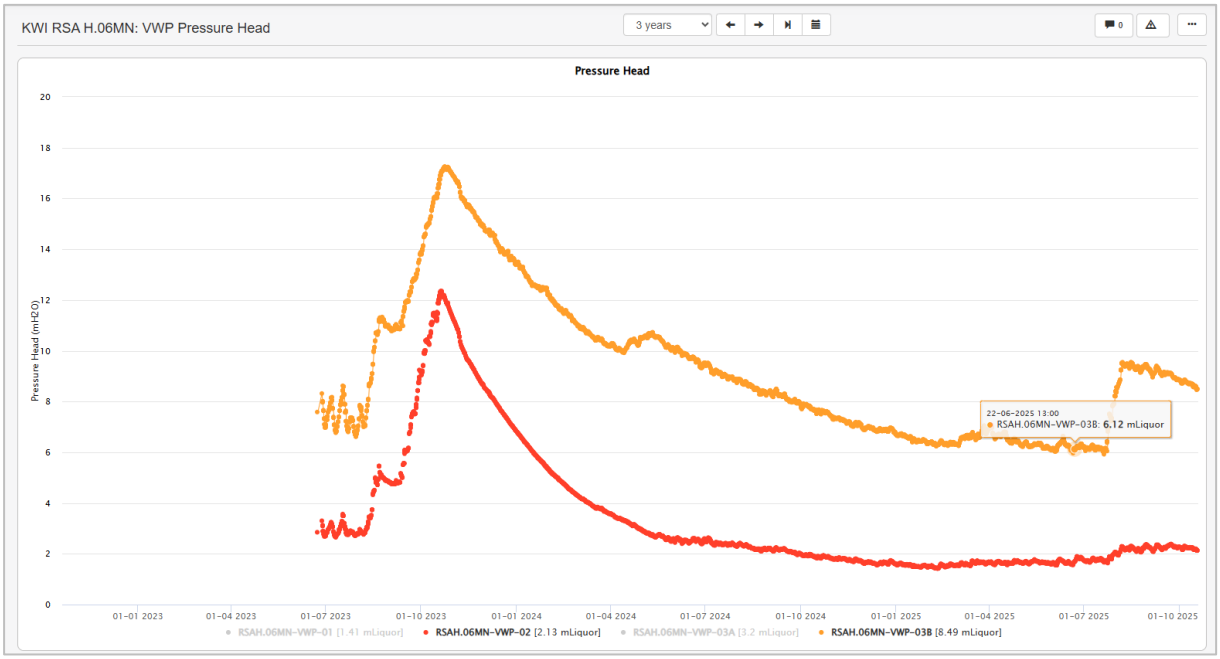


Figure 10. Pore pressure time series showing consolidation after the end of construction. The time from the peak pressure to 100% consolidation is approximately 470 days.

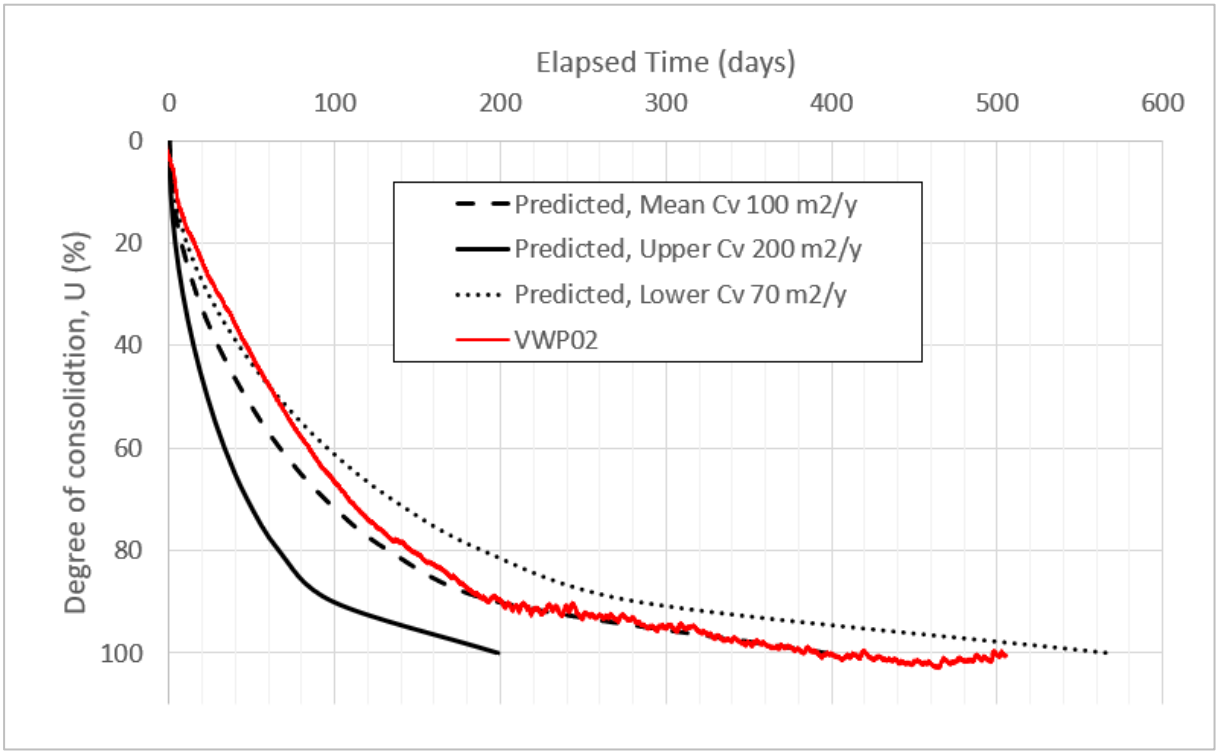


Figure 11. Actual versus predicted consolidation for different values of c_v.

The analyses described in this example allow validation of design parameters for forward analysis (in this case the coefficient of consolidation and B-bar coefficient). The analyses were greatly aided by the comprehensive data history of the VWPs due to the frequent reading intervals and storage of all historic data, as well as non-automated monitoring data (progress surveys in this case).

Example 4: Monitoring of slope displacement
One of the TSFs has a slope that exhibited signs of historic downslope movement, accompanied by mid-slope seepage expressions. Limit equilibrium stability assessments indicate a low factor of safety. While buttressing was initially considered as a stabilisation measure, this option was rejected due to the presence of a critical water storage facility located immediately downstream of the slope toe, where the buttress would have been founded. Given the importance of this water storage facility to site-wide water management, alternative stabilisation approaches were required. A revised option is currently being developed to achieve the necessary stability by cutting back the slope.

While an alternative stabilisation measure is being developed, the slope is actively monitored using a suite of instrumentation to track displacement and pore water pressure. This includes multiple real-time GNSS sensors, in-place inclinometers, and numerous VWPs. All instruments are integrated into the VDV platform for continuous real-time monitoring with data recorded every 30 minutes. Since monitoring commenced, no slope movement at the area of concern has been observed.

CONCLUSIONS

This paper has presented examples of real-time and scheduled (i.e., non real-time) monitoring of TSFs for evaluating dam safety conditions during operations and construction. Both types provide value and indeed often complement each other. The frequent data acquisition of the real-time monitoring has enabled and aided validation of design assumptions e.g., the B-bar pore pressure parameter and the coefficient of consolidation, which is useful in forward analysis for future designs and construction.

A lesson drawn from our experience at this site is the importance of having access to not only real-time data, but also historical construction records, aerial imagery, and the full record of all monitoring data. Instantly available data has facilitated rapid, risk-informed decision making; this is often needed where the safety of TSFs is concerned. Finally, the real time monitoring and surveillance, and frequent drone survey of the site is an example of how a high level of surveillance is possible even for physically very remote sites.

REFERENCES

Terzaghi (1926) "Principles of Soil Mechanics. Reprint of eight articles published Nov.-Dec. 1925 in Engineering News Record, Vol. 25. McGraw-Hill, New York."



David Johns

Senior Geotechnical Engineer, Associate
Klohn Crippen Berger (KCB)

David is a consulting geotechnical dam engineer with 20+ years' experience in tailings management, with a focus on design and operation of upstream tailings dams, filtered tailings, embankment dams (tailings and water) and waste rock dumps in Australia, Southern Africa, South America and PNG covering diverse geologic, seismic and climatic conditions.

David is a Chartered Professional Engineer with Engineers Australia and a Registered Professional Engineer of Queensland.
David is an Engineer of Record for major tailings dams in Australia. He has been lead designer or senior reviewer for many of KCB's dam projects and has completed design and dam safety reviews in Australia, Africa, and South America. Recently David led the construction and commissioning of two major upstream tailings dams for Rio Tinto and BHP.

His interests include the application of geosynthetics in mining, quantitative risk assessments of embankment dam failure modes, advanced soil laboratory testing, and critical state soil mechanics in the assessment of soil liquefaction. Construction monitoring of major embankment dams in PNG and Australia introduced David to the challenges of construction in very high rainfall and tropical environments, where he also gained experienced with tropical residual and lateritic dam foundations.